# Stratigraphy, structure and metamorphism of Archean rocks, Clan Lake, N.W.T.

by

E.J. Hurdle

A thesis
presented to the University of Ottawa
in partial fulfillment of the
requirements for the degree of
M.Sc.
in
Geology

OTTAWA, Ontario, 1985

UNIVERSITÉ D'OTTAWA
UNIVERSITY OF OTTAWA

The University of Ottawa requires the signatures of all persons using or photocopying this thesis. Please sign below, and give address and date.

## ABSTRACT

The Clan Lake area, Slave Structural Province, consists of a volcanic and sedimentary sequence that during the late Archean was polydeformed, metamorphosed (from green schist to lower amphibolite grade) and intruded by gabbroic and granitic bodies.

Deposition of the volcanic pile was within a turbidite sedimentary basin and included: 1) subaqueous extrusion of mafic lava, 2) buildup of an andesitic to dacitic volcanic cone into a volcanic island which culminated in a dacite dome complex, 3) subaerial erosion of the volcanic island and redeposition as alluvial deposits, 4) subaerial felsic pyroclastic activity. Extrusion of mafic lava on the submerged eastern flank of the volcanic cone was concurrent with the felsic volcanism.

Regional deformation of the sedimentary and volcanic rocks produced a succession of structures grouped as D1 to D4. Included are D1 , NE and NW trending macroscopic isoclinal folds unaccompanied by obvious rock fabrics; D2, a steep NW striking foliation commonly overprinted and transposed by later structures but preserved in the main body of the volcanic rocks; D3, a variably N striking, steeply east

dipping foliation and steeply plunging mesoscopic folds; D4, a NNE striking, steep foliation which, with associated mesoscopic folds, is confined to the sedimentary rocks.

Granitic plutons emplaced during D3 influenced development of D3 structures. For example, S3 foliation deflects and flattens in inclination around plutons.

The turbidite sedimentary rocks are subdivided into progressive metamorphic zones by biotite and cordierite isograds that lie on each side of a lower greenschist zone extending northeastward. Metamorphism began during D2 deformation, progressed until it peaked with the growth of cordierite and andalusite in the higher grade rocks during and just after D4. As part of the metamorphic progression, biotite crystals changed in growth habit from subequant during preD3 deformation to markedly elongate laths during D3, to shorter laths during D4.

CONTENTS

Appendix page

## LIST OF FIGURES

# Chapter I

# INTRODUCTION

The Clan Lake map area is in the southwestern part of the Archean Slave Structural Province of the Canadian Shield (Figure 1-1). Centred at Clan Lake, it includes 15 km2 covering part of Quyta Lake topographic sheet (N.T.S. 85J16), and lies between latitudes 62 54'N and 63 00'N and longitudes 114 05'W and 114 21'W. The nearest city is Yellowknife, 50 km to the south. Access is by light aircraft or winter road from Yellowknife.

The terrain is moderately rugged with a local relief attaining 50 m. Rock exposures are generally good and many are stripped of plant growth due to recent forest fires. The region was heavily glaciated during the Pleistocene, when sediments were deposited, including lucustrine clays upon which Clan Lake is situated. The lake is one of a number along the Yellowknife River, a major river system that flows southward through the map area.

Jolliffe (1939,1940) included the area in a preliminary map at a scale of 1 in=0.5 mi accompanied by a geological report. Fortier (1946) prepared a preliminary map of the Yellowknife-Beaulieu Region at a scale of 1 in=4 mi and

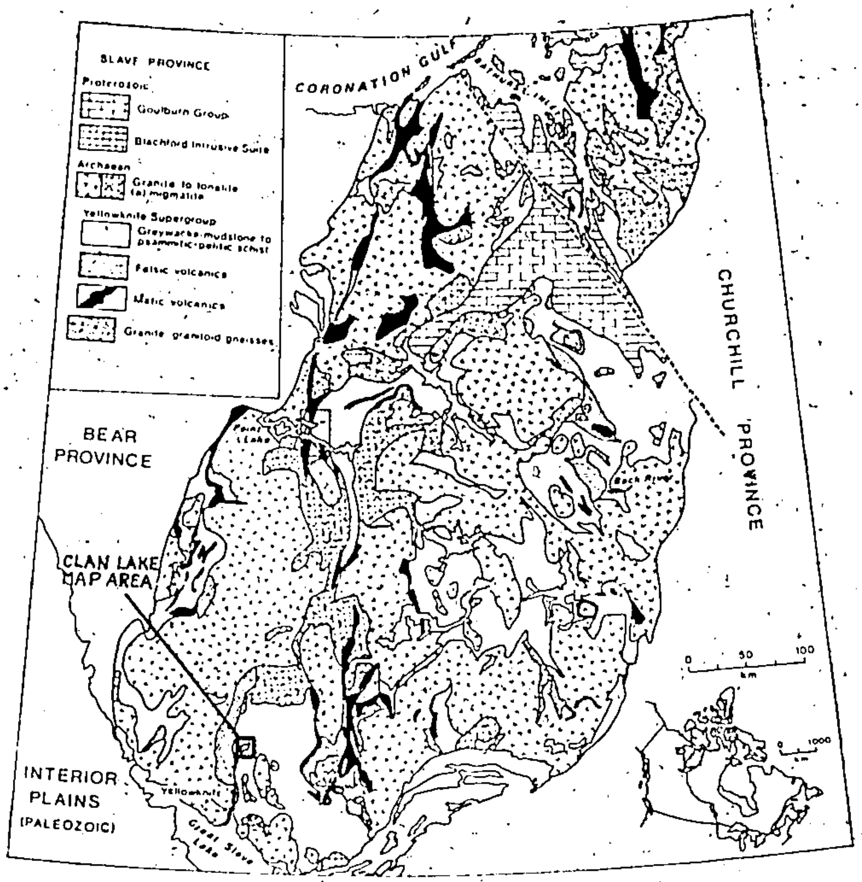


FIGURE 1-1:

Location of Clan Lake map area within the Slave Structural Province (after Henderson, 1981).

Henderson (1976) compiled a 1:250,000 geological map of the Yellowknife map area (85J), both of which include the Clan Lake map area.

This thesis study was undertaken with the following objectives:

1. map the geology of the Clan Lake area at a scale of 1:10,000.
2. describe lithologic variations and determine the stratigraphic succession of the volcanic rocks.
3. describe the structural geometry and determine the deformational history.
4. describe the metamorphic rocks and determine the metamorphic history and conditions.
5. provide a paleoenvironmental interpretation for formation of the rocks during Archean time.

Field mapping was carried out during the summers of 1981 and 1982 using air photo enlargements at a scale of 1:5000. The geological data obtained was transferred to 1:10,000 photomosaics and published by D.I.A.N.D. (map sheets A, B & C, in pocket; Hurdle, 1983). Rock samples were collected and thin sections examined.

W.K. Fyson provided valuable discussion and constructive criticism while supervising the thesis, R. Kretz and M. Lambert critically reviewed parts of the manuscript and L.B. Aspler edited parts. W.A. Padgham, D.I.A.N.D., gave logistic and monetary support during the field seasons and initially proposed the study of this area. N. Labenek and L.B. Aspler provided field assistance in 1981 and M.K. Fyson in 1982.

# Chapter II

# STRATIGRAPHY

## 2.1 INTRODUCTION

The Clan Lake area consists of a volcanic pile surrounded by predominantly younger sedimentary rocks which are intruded by gabbroic and granitic bodies, all crosscut by Proterozoic diabase dykes (Figure 2-1). The sedimentary and volcanic rocks are of the Yellowknife Supergroup of Archean age (Henderson, 1970). The stratigraphic order shown in Figure 2-2 can only be generalised, especially for the volcanic rock units, as they commonly interfinger with and are lateral equivalents of one another. The thicknesses given for the volcanic units are only approximate estimates as these rocks have been deformed and therefore flattened or shortened. A lack of reliable stratigraphic top determinations makes it difficult to determine whether a section of rocks represents a true stratigraphic section or repeated sections of a unit due to folding.

The paleogeographic setting is interpreted as a subaerial volcanic dome complex surrounded by subaqueous volcanic and sedimentary deposits.

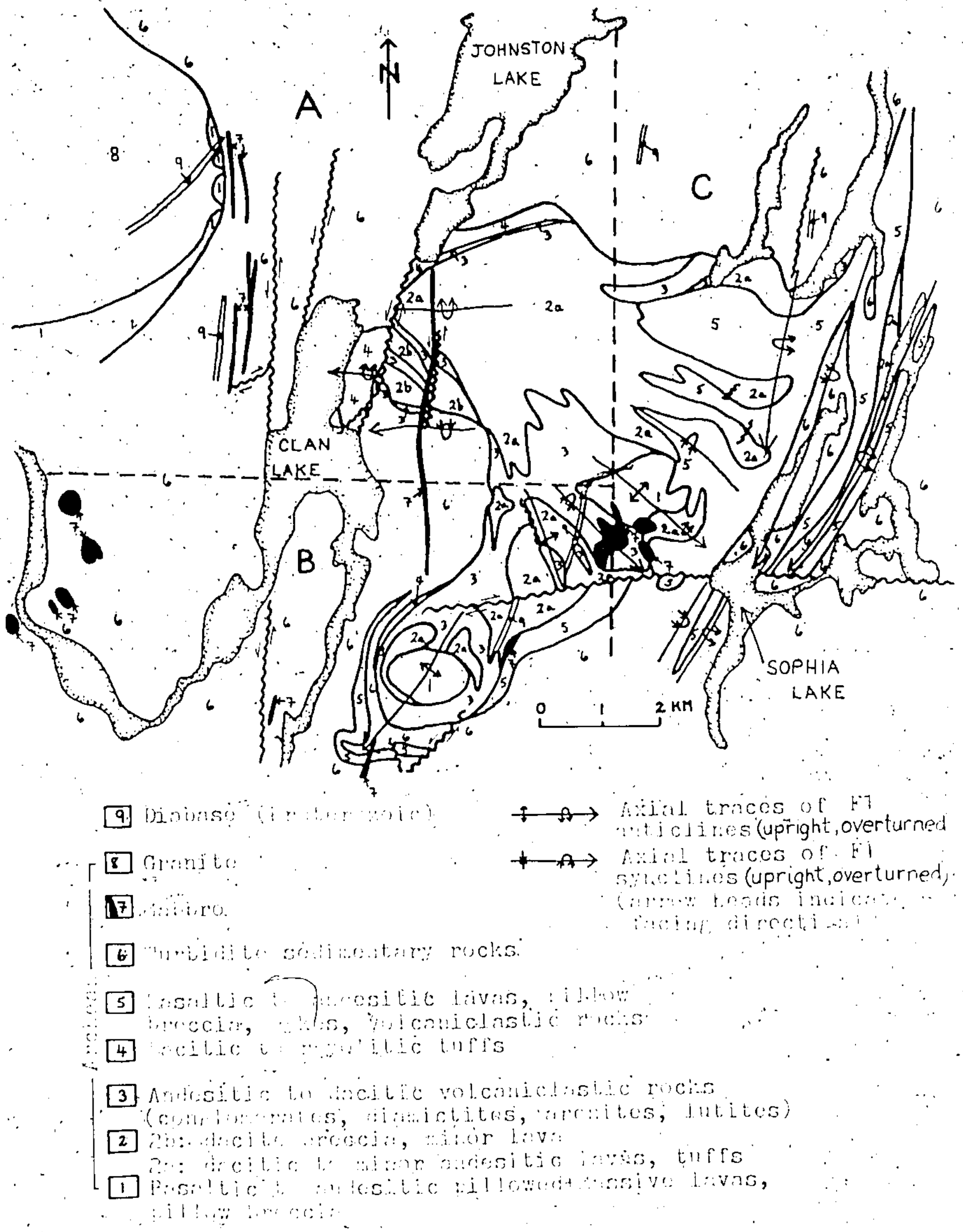


FIGURE 2-1:

Geological sketch map of Clan Lake area.

| | Unit number | | | Lithology | Estimated thickness (metres) |
|---|---|---|---|---|---|
| Proterozoic | 9 | | | Diabase | 1-50 |
| | | | | intrusive contact | |
| | 8 | | | Granite | - |
| | | | | intrusive contact | |
| | 7 | | | Gabbro | Dykes: 50-75 |
| | | | | intrusive contact | |
| ARCHEAN | 6 | YELLOWKNIFE SUPERGROUP | | Turbidites sedimentary rocks | - |
| ARCHEAN | 5 | YELLOWKNIFE SUPERGROUP | Volcanic rocks | Basaltic to andesitic lavas, pillow breccias, dykes, volcaniclastic rocks | 100-300 |
| ARCHEAN | 4 | YELLOWKNIFE SUPERGROUP | Volcanic rocks | Dacitic to rhyolitic tuffs | 200-600 |
| ARCHEAN | 3 | YELLOWKNIFE SUPERGROUP | Volcanic rocks | Andesitic to dacitic volcaniclastic rocks (diamictite, arenite, conglomerate, lutite) | 100-500 |
| ARCHEAN | 2 | YELLOWKNIFE SUPERGROUP | Volcanic rocks | Dacite breccia, minor lava (2b)<br>Dacitic to andesitic tuffs, lavas (2a) | 2b 500<br>2a 100-500 |
| ARCHEAN | 1 | YELLOWKNIFE SUPERGROUP | Volcanic rocks | Basaltic to andesitic pillowed and massive lavas, pillow breccia | 250 |

FIGURE 2-2:

Generalised stratigraphic chart of Clan Lake lithologic units. Units 1 - 6 interfinger and are, in part, stratigraphically equivalent (see Figure 2-3).

Figure 2-3 is a fence diagram illustrating the interelationships of the volcanic and sedimentary rocks units and Figure 2-18 is the paleogeographic interpretation.

Each volcanic unit description includes extent, thickness, lateral and vertical variability, relationships to other units, and field and petrographic descriptions.

2.1.1 volcanic rocks

The volcanic pile is divided into five major lithologic units (Figure 2-2). The units are generalised and as mapped (map sheets A,B,C; in pocket) may include some lithologic variation resulting from interfingering relationships: each unit may contain minor amounts of rocks typical of other units. Unit 1, the oldest rock unit of the pile, includes basaltic to andesitic lavas and pillow breccias with minor dacite; unit 2 is dacitic breccia, lava and tuff with minor andesite; unit 3 includes andesitic to dacitic volcaniclastic rocks; unit 4 is dacitic to rhyolitic tuffs; and unit 5 is basaltic to andesitic pillow lava and breccia, massive lava, massive to layered dykes and volcaniclastic rocks.

To determine composition of the rocks, specific gravities ( from 2.8 to 3.15 for basalt, 2.75 to 2.85 for andesite and 2.68 to 2.76 for rhyolite to dacite, Lambert, 1975) were used in conjunction with colour and hardness. Because of alteration (particularly of the mafic volcanic rocks) these were not always reliable indicators of composition and

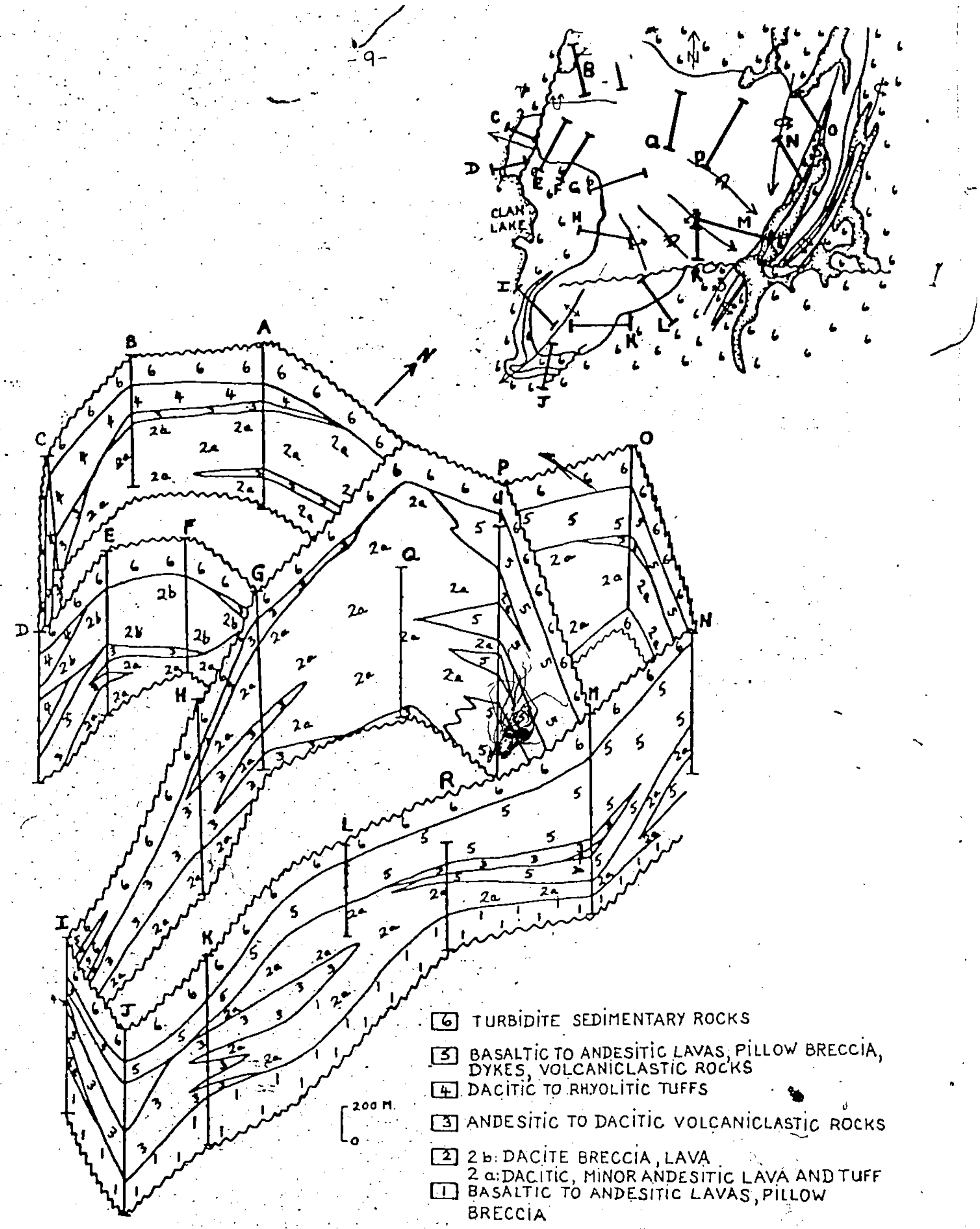


FIGURE 2-3:

Schematic fence diagram showing stratigraphic relations of volcanic and sedimentary units. Distortion, which affects position and orientation of sections, due to folding is not accounted for. Inset map shows locations of sections and major folds.

therefore other aspects such as matrix mineralogy, phenocryst types and primary features and textures similar to rocks of known composition were used. XRF analyses of 16 samples from rock units 1, 2 and 5 (Appendix II) generally support the compositions determined by these methods. The only exceptions are analyses for unit 1 which are more siliceous than field interpretations, probably due to abundant micro-quartz amygdules in the rock samples taken.

The terminology for volcanic rocks follows Carlisle (1963) for subaqueous mafic deposits; Fisher (1966) and Schmincke (1974) for pyroclastic deposits; and MacDonald (1972) for volcanic deposits in general.

2.1.1.1 unit 1

Unit 1 comprises basaltic to andesitic lavas and pillow breccias. The unit is of limited extent, being exposed at the cores of two major anticlines in the southwest and east-central parts of the volcanic pile (Figure 2-1). The estimated minimum thickness is 250 meters. This unit is in sharp, conformable contact and interbedded with dacite of unit 2 (Figure 2-4a) and volcaniclastic rocks of unit 3. It also contains minor interbeds of turbidite sedimentary rocks of unit 6.

Unit 1 becomes less mafic up stratigraphic section, changing from minor basaltic lavas to andesitic lavas and

FIGURE 2-4: ANDESITIC LAVAS AND BRECCIAS OF UNIT 1.

A) andesite lava (dark) in contact with and intruded by dacite lava (light) of unit 2. Andesite has a dark altered contact. Pen is 1 cm thick. B) pillowed andesite. The pillows are generally larger than basaltic ones. Field book is 19 cm long. C) polygonal cooling joints and primary layering in andesite lava. D) closeup of andesite pillows. The pillows contain abundant quartz amygdules, particularly near margins. Note the larger amygdules concentrated at the upper margin. Stratigraphic top is up photo. E) isolated pillow breccia. A pillow (at right of photo) floats in a hyaloclastite matrix of lapilli-size angular fragments. Lense cap is 5 cm.

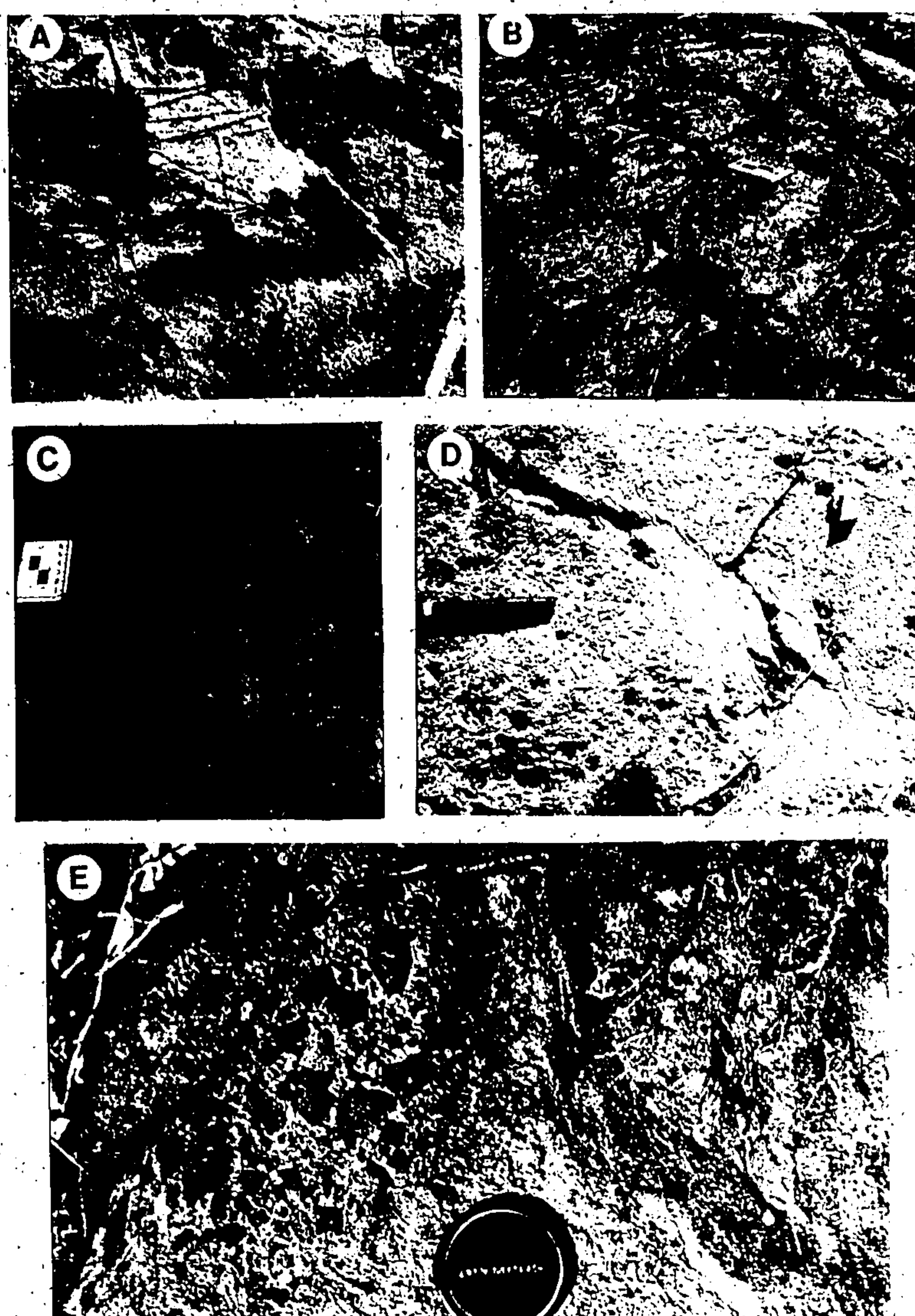
A
B
C
D
E

pillow breccias. The basalt is blackish-green and aphyric, contains a few millimeter-sized amygdules, and is massive to, a minor extent, pillowed. The andesite is dark to medium grey, weathering to rusty grey; generally contains 10 to 20% plagioclase phenocrysts ; and has abundant vesicles and quartz amygdules ranging from < 1 mm to > 1 cm. The andesitic lavas are massive (Figure 2-4a), pillowed (Figure 2-4b) or layered (Figure 2-4c). At one locality the andesite repeatedly grades from layered lava to vesicular, massive lava to pillowed lava to pillow breccia, with each cycle 2 to 3 meters thick. The massive lavas have vesicles and amygdules that are evenly dispersed or concentrated in pockets or at their margins. At one locality massive andesite lava has 1 to 3 cm thick , greenish-grey alteration bands.

The pillowed lavas contain pillows that are generally large (0.5 to 2 meters long, Figure 2-4b) compared to those that are basaltic. Pillows display dark, 2 to 3 cm thick selvages, locally yellow-green, epidotised cores and commonly hyaloclastite interstices. They also have abundant vesicles and amygdules, usually concentrated near their margins, with the larger ones at their upper margins (Figure 2-4d), or concentrically concentrated in zones.

The pillow breccias are mainly of the isolated pillow type within a hyaloclastite matrix containing angular, lapilli-sized fragments (Figure 2-4e).

The layered lavas have centimeter thick layers, parallel to their contacts with pillowed lavas and defined by changes in mafic mineral to plagioclase content. In one locality a layered lava contains cooling joints (Figure 2-4c).

The environmental interpretation is that rocks of unit 1 were deposited as lava flows in a predominantly subaqueous environment (Figure 2-18a) as evidenced by the presence of pillow lava and pillow breccia and interbeds of turbidite sedimentary rocks of unit 6. The abundance and size of vesicles and amygdules and the cyclic repetition of layered to vesicular to pillowed flows to pillow breccias suggest shallow water conditions (c.f. Jones 1969, Cousineau & Dimroth 1982).

2.1.1.2 unit 2

Unit 2 is subdivided into dacitic and minor andesitic lava and tuff (subunit 2a) and a dacite breccia (subunit 2b).

Subunit 2a ranges from 100 to 500 meters in thickness and makes up the bulk of the northwestern quarter of the pile. It interfingers with mafic volcaniclastic rocks of unit 5 to the east and dacitic conglomerates and diamictites of unit 3 to the south. Lenses of volcaniclastic rocks of unit 3 are found throughout unit 2a. The southern parts and stratigraphically lower parts of unit 2a contain beds of massive and pillowed andesite and turbidite sedimentary rocks of unit 6. The upper parts contain lenses of volcaniclastic rocks of unit 3 identifiable as alluvial deposits, such as diamictites, conglomerates and cross-bedded sandstones.

Subunit 2b dacite breccia is confined to a spectacular, steep-sided hill in the northwest corner of the volcanic pile (Figure 2-6a). The breccia forms a lense about 1 km in length with an estimated thickness of 500 m. It is fringed by and has an irregular, sharp to gradational contact with monolithic (dacitic) conglomerates, diamictites and cross-bedded sandstones of unit 3.

Subunit 2a consists of dacitic to minor andesitic lava, tuff breccia, lapilli tuff and stratified tuff. The dacite lava is an aphanitic to finely crystalline rock that is aphyric to 20 to 30% plagioclase phyric or quartz- plagioclase phyric (Figure 2-5a). It is medium grey to pinkish grey on fresh surfaces and light grey and rust brown on weathered surfaces. It is generally massive, except where vesicular at its margins (Figure 2-5b). It locally protrudes into (Figure 2-5b) and alters adjacent rock types (Figure 2-4a). It rarely contains polygonal joints (Figure 2-5c) and mafic clasts (Figure 2-5a). The tuff breccia and lapilli tuff (Figure 2-5d) are up to 15 m thick and have no internal stratification. They contain rare to abundant

FIGURE 2-5: DACITIC AND MINOR ANDESITIC LAVAS AND TUFFS OF UNIT 2A.

A) plagioclase phyric dacite. A rare mafic clast is present in the lower right hand corner. B) dacite lava protruding into volcarenite of unit 3. The dacite lava is vesicular at its margin (arrow). C) plagioclase phyric dacite containing polygonal cooling joints. D) tuff breccia. Plagioclase phyric clasts are floating in an aphyric, more felsic matrix. E) stratified dacitic tuff. Note waviness of stratification. F) dacitic tuff lobe (L) truncating stratified tuff. The lobe contains floating andesitic to dacitic clasts (dark areas) up to 15 cm across.

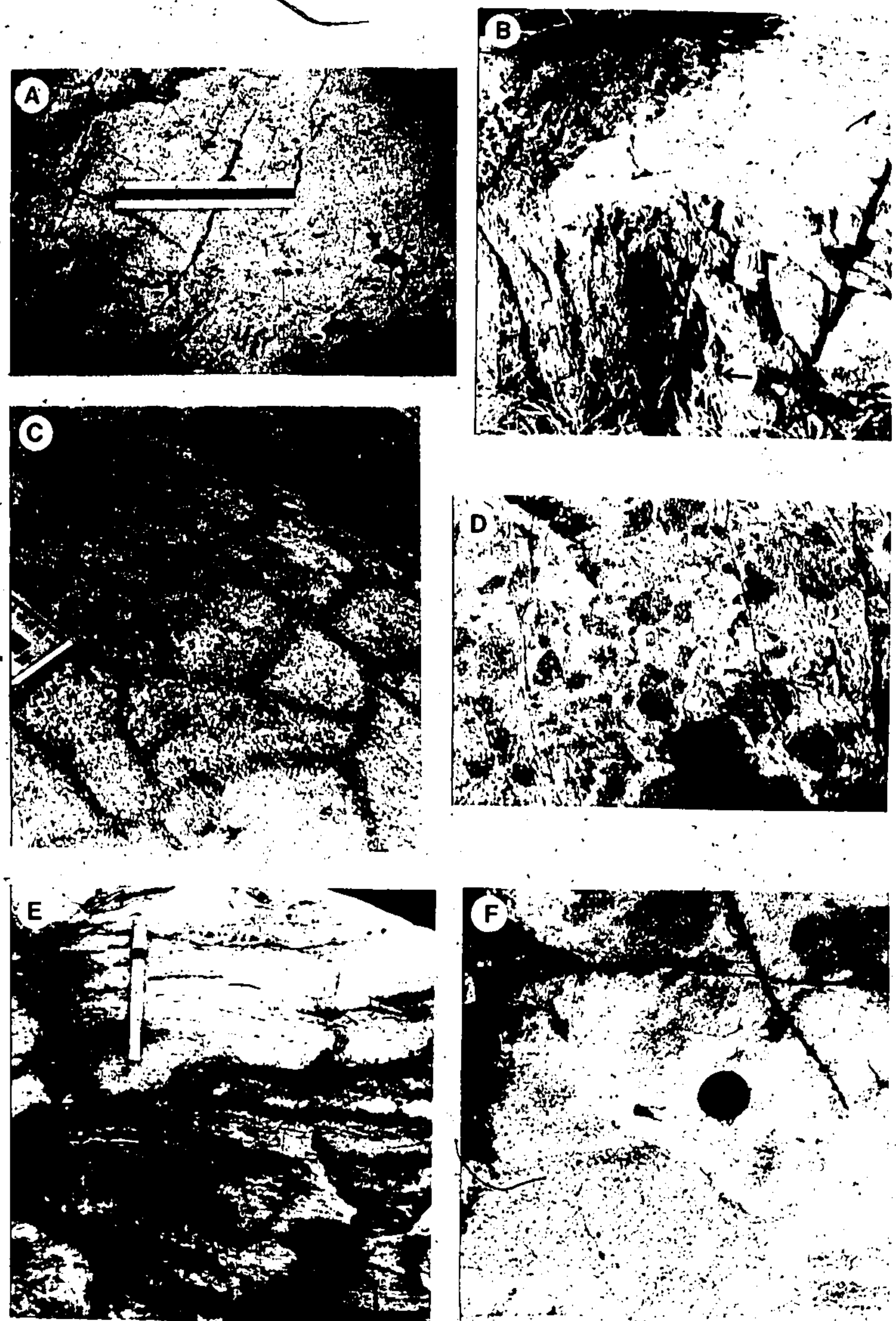
A
B
C
D
E
F

plagioclase phyric clasts in a dacitic, aphyric to plagioclase phyric, clastic matrix. The clasts (where abundant) are poorly sorted, rarely graded, angular to subrounded, usually no larger than 15 centimeters in size and are monolithic, being mainly andesite or dacite. Where dacitic, the clasts are obscured by the dacitic matrix. These tuffs locally have centimeter sized vesicles in the matrix at their upper contact and a thin, reversely graded basal layer. Also lobes of dacitic tuff are present within stratified tuffs of unit 2a (Figure 2-5f) and volcaniclastic rocks of unit 3 at two localities. The stratified tuffs (Figure 2-5e) range from 0.5 to 2 meters in thickness and are interbedded with lapilli tuffs and tuff breccias. They have millimeter to centimeter thick laminations which, at two localities, are truncated by tuff breccia. At another locality a stratified tuff interbedded with tuff breccia contains wavy bedding (Figure 2-5e).

The andesite component of subunit 2a is similar to unit 1, being plagioclase phyric, vesicular and/or amygdaloidal, dark grey and locally pillowed. At one locality a dacite lava containing andesite clasts lies on top of a massive andesite layer.

The dacite breccia of subunit 2b, is poorly sorted, has crude layering due to change in clast size, and contains minor massive dacite portions (Figure 2-6b). Clasts are angular, monolithic and closely packed (Figure 2-6e); range from

FIGURE 2-6: DACITE BRECCIA AND LAVA OF UNIT 2B (DOME COMPLEX).

A) dacite breccia confined to a steep-sided hill in the northwest corner of the volcanic pile. B) dacite breccia containing a minor massive dacite layer (to right). C) massive dacite grading into dacite breccia. From left to right, dacite with incipient fractures grades into breccia with large clasts (up to 30 cm long) and little matrix into breccia with smaller clasts within a matrix of fine clasts (< 3 cm). D) massive dacite containing cooling? joints filled with tuffaceous sediment. E) typical outcrop of dacite breccia.

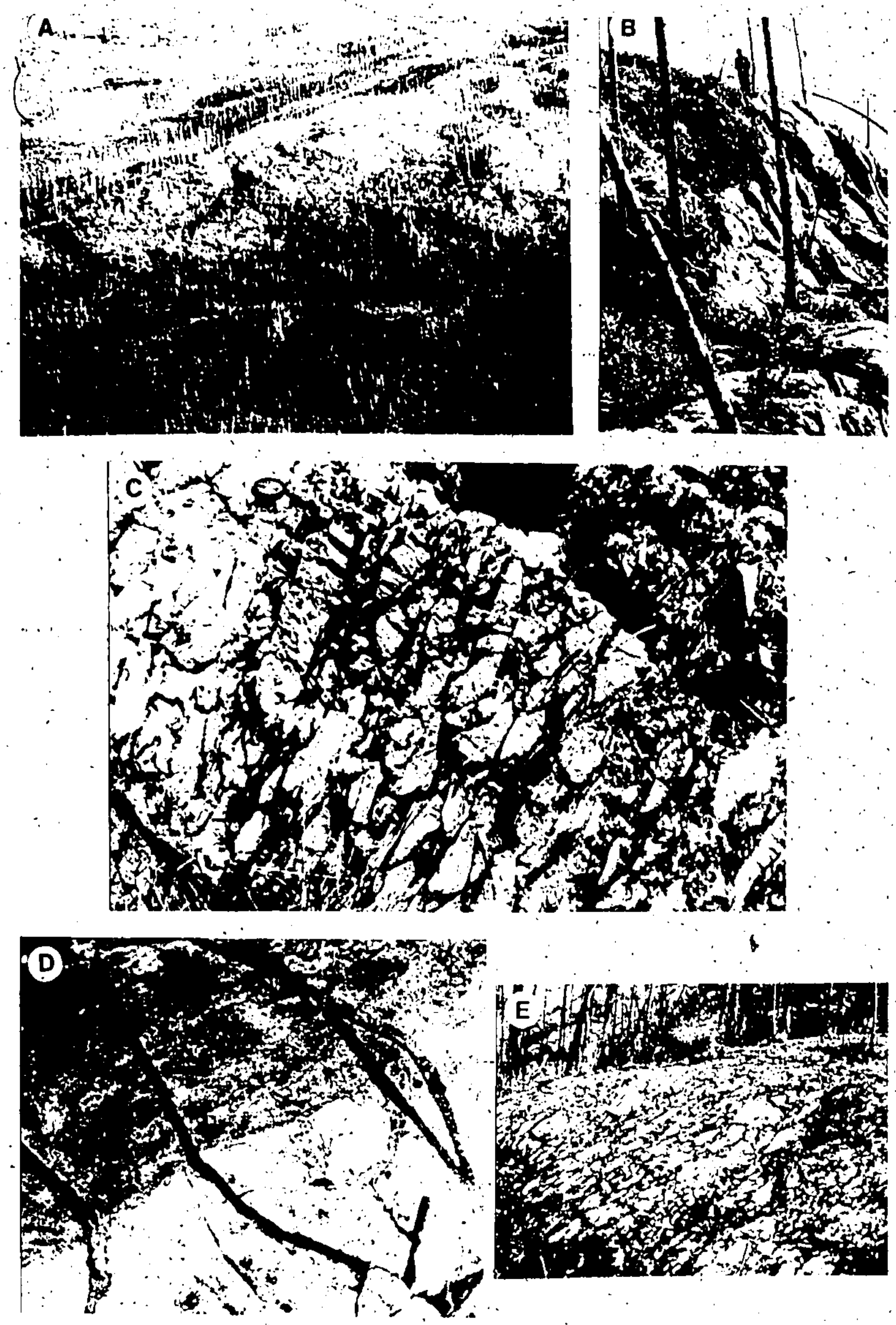
A
B
C
D
E

a few centimeters to more than a meter in size; and are within a matrix of small fragments (up to 1 cm) of the same material, cemented by carbonate. The dacite is plagioclase-quartz phyric in the western part of subunit 2b and aphyric to the east. The massive dacite is contained by and in sharp to gradational contact with the breccia. At one place the massive dacite grades into a dacite with incipient fractures to a coarse breccia with little to no matrix to a breccia with smaller clasts within a matrix of finer material (Figure 2-6c). At another place massive dacite contains joints filled with fine-grained tuffaceous material (Figure 2-6d).

Petrographically, the dacite of unit 2a&b consists mainly of recrystallised quartzo-feldspathic material, with or without phenocrysts of plagioclase and minor quartz, biotite and/or amphibole, opaques, carbonate and less commonly chlorite, epidote, muscovite and garnet (Figure 2-7a&b). In addition, the aphyric dacite lava contains in a few localities biotite/quartz ovoids that are possibly amygdules (Figure 2-7c) and the dacite tuffs have broken phenocrysts and flattened dark fragments that possibly are pumice (Figure 2-7d).

2.1.1.3 interpretation

Because of a lack of discernible primary features, such

FIGURE 2-7: PHOTOMICROGRAPHS OF DACITE OF UNIT 2.

A) Plagioclase phyric dacite of unit 2b dacite breccia. The matrix is mainly biotite, amphibole and opaque minerals in a quartzofeldspathic groundmass. Field of view is 10 cm. B) plagioclase phyric dacite of unit 2a lava. Matrix is similar to Figure 2-7a. a is amphibole. Field of view is 10 cm. C) aphyric dacite of unit 2a containing a spheroid of quartz and biotite, possibly an amygdule. The matrix is mainly biotite, opaques and quartzofeldspathic material. Field of view is 2 mm. D) aphyric dacite tuff of unit 2a containing flattened, dark fragments, possibly pumice. The quartzofeldspathic matrix contains biotite and garnet (g). Field of view is 8 cm.

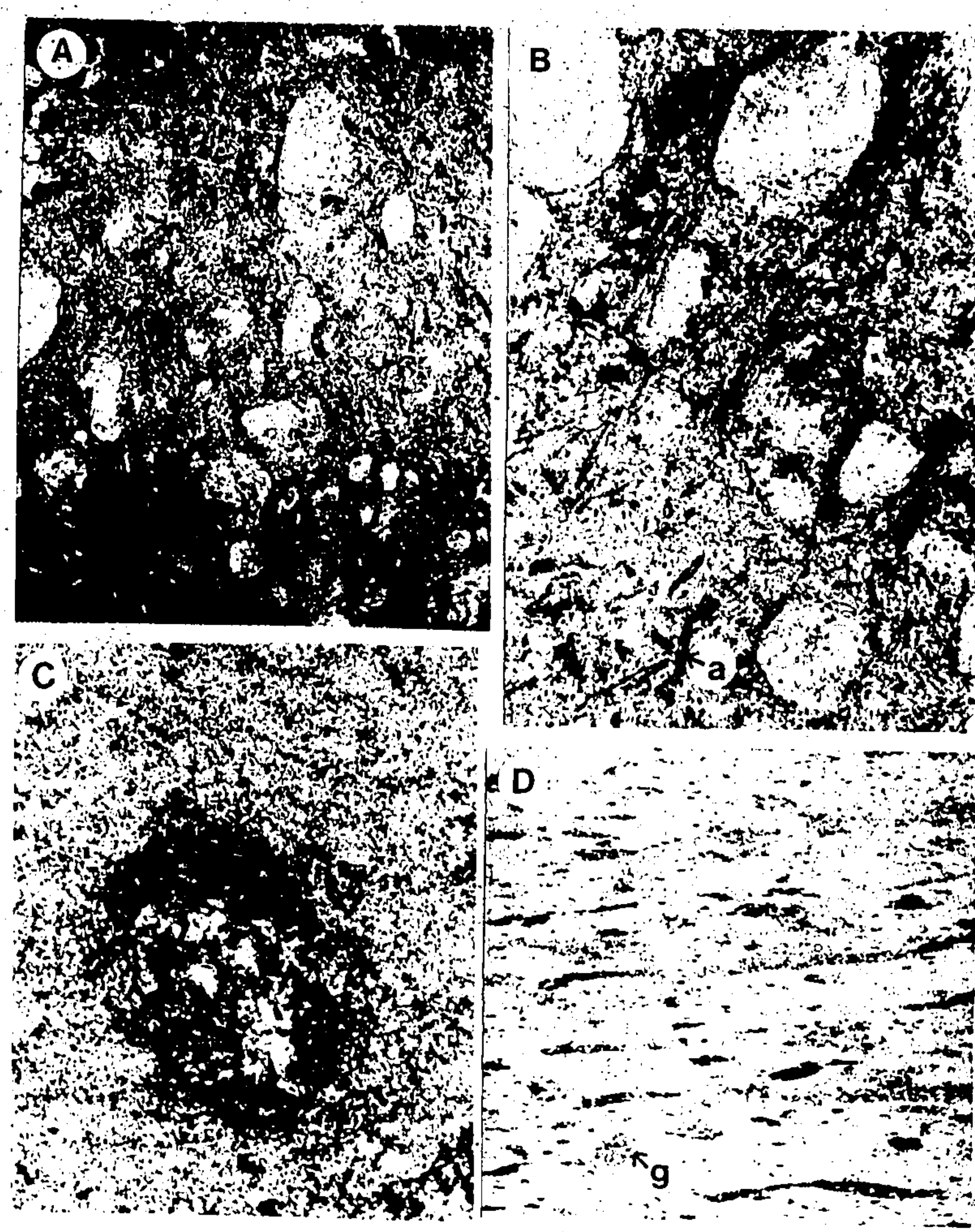
A
B
a
C
D
g

as glass shards and pumice fragments, due to recrystallization, the environmental setting in which rocks of subunit 2a were formed is difficult to interpret. This subunit includes a number of different types of deposits such as 1) massive lava flow/flow breccia: the massive dacite lava represents lava flow deposits, being crystalline and vesicular (particularly at its margins) (c.f. Self,1982) and intrusive into and altering other rock types. The massive andesite layer topped by dacite containing andesite clasts could be an andesite lava flow with flow top breccia injected by a dacite lava flow. 2) pyroclastic deposits: the dacite tuffs, microscopically containing broken phenocrysts and flattened pumice fragments, are thought to represent pyroclastic deposits (c.f. Fisher and Schmincke, 1984). Tuff breccias and lapilli tuffs could represent pyroclastic flow deposits because they are poorly sorted and lack internal stratification except for a thin basal layer with reverse grading (c.f. Fisher, 1982; Wright et al, 1980). They also are generally monolithic (c.f. Lajoie, 1979). Also at two localities the presence of flow lobes of dacite tuff within volcaniclastic rocks of unit 3 characterise pyroclastic flow deposits. Tuff breccias and lapilli tuffs are commonly overlain and underlain by stratified tuffs which could be pyroclastic fall and/or surge deposits. The fact that these stratified tuffs are well-sorted and well-bedded (c.f. Wright et al, 1980) and at one locality contain wavy laminations (c.f. Crowe and Fisher, 1973) are in accord with such deposits.

The presence of local interbeds of pillowed andesite and turbidite sedimentary rocks in subunit 2a, particularly in the lower part of the unit and distal parts with respect to the dome complex (subunit 2b), indicates that this subunit to some extent was deposited under subaqueous conditions. Other parts of the unit lack pillowed forms in lava flows and contain interbeds of fluvial deposits (unit 3) and thus appear to have been deposited subaerially (not deposited under a standing body of water).

Subunit 2b could represent a dome complex, the dacite breccia representing crumble breccia and the massive dacite being unbrecciated interiors and/or minor lava flows. This interpretation is based on: 1) the physical characteristics of the breccia (unsorted, monolithic and containing angular clasts within a matrix of the same composition as the clasts) being unique to crumble breccias (c.f. Rose, 1972; Parsons, 1969; and McDonald, 1972). 2) the limited extent of the dacite breccia, being confined to one locality, (Parsons, 1969) and 3) the breccia setting, notably the surrounding monolithic conglomerates and diamictites of unit 3, which could represent unstable debris from the dome that was subsequently reworked by fluvial processes and/or mass movement (c.f. Lambert, 1982; Self, 1982).

Tectonic shearing is not considered as the primary cause of the breccia. The rock is siliceous and if originally massive, it would not have readily brecciated in comparison with the surrounding rock types, some of which are much less competent but not brecciated to the same extent. However, there is evidence for local tectonic shearing. Breccia with small, angular clasts that are strongly aligned is immediately next and in sharp contrast to an unsheared breccia with larger, unaligned clasts.

2.1.1.4 unit 3

Unit 3 consists of dacitic to andesitic volcaniclastic rocks including diamictites (Flint et al., 1960), conglomerates, arenites and lutites.

Lateral changes within the unit are marked. At the dome complex formed by the dacite breccia (unit 2b), volcaniclastic rocks of unit 3 form two 100 m thick lenses stratigraphically below the breccia, each extending laterally about 800 m, as well as a 50 m by 100 m lense above the breccia. These lenses have irregular, sharp to gradational contacts with the dacite breccia. They contain, primarily, interlayered monolithic conglomerates and diamictites, which grade into one another, planar- to cross-bedded arenites, lutites, and thin interbedded arenites and lutites containing dacitic dropstones. Minor dacite tuff (petrographically similar to tuffs of unit 2a) is interbedded (Figure 2-9b) as flow lobes.

Southward in a separate outcrop area, away from the dome complex, unit 3 thickens to 500 m and is mainly composed of heterolithic diamictites, conglomerates and minor arenites and lutites. These rocks interfinger and are in sharp, conformable contact with dacite lavas and tuffs of unit 2a. They are conformably overlain by turbidite sedimentary rocks of unit 6. Individual beds of unit 3 range from 1 meter to several meters in thickness.

Unit 3 thins to about 250 meters farther south (in the SW corner of the volcanic pile, Figure 2-1) and to less than 100 meters to the north of the dome complex. These distal facies (with respect to the dome complex) lie below and are in sharp, conformable contact with felsic tuffs of unit 4. They are also in sharp, conformable contact and interfinger with lavas of units 1 and 2. The distal facies consists of well-bedded (generally 15 to 50 cm thick beds), conglomerates, arenites, lutites and minor diamictites. The arenite beds are more common in the distal facies than in the proximal and clasts in the minor diamictite beds are generally better rounded and sorted, and smaller than those within the proximal facies.

Eastward, away from the dome complex, unit 3 appears to thin stratigraphically and disappear. Mafic volcaniclastic rocks of unit 5 predominate in the eastern part of the volcanic pile and may be, to some extent, lateral equivalents of unit 3.

The diamictites (Figures 2-8a,b&c) are poorly sorted to unsorted, framework-disrupted, and locally are crudely layered due to change in grain-to -matrix ratio and clast size (Figure 2-8d). They commonly have a 2 to 4 cm basal layer devoid of clasts and rarely display crude normal grading. The diamictites are heterolithic (Figure 2-8b&c) to locally monolithic (dacitic) near the dome complex (Figure 2-8a&d) and have a sandy to muddy matrix. At two localities clasts of underlying lavas are included within the base of diamictites (Figure 2-8e). Clasts are dacitic, andesitic and less commonly rhyolitic and basaltic in composition and rarely turbidite sedimentary rocks. Locally they have rims wholly to partially altered (weathered?) white (Figure 2-8c), or black. Clasts are angular to subrounded, range from less than a centimeter to greater than a meter across and rarely show autobrecciation. The mafic clasts are smaller and more angular than the felsic clasts.

The conglomerates are generally monolithic (dacitic) near the dome complex (Figure 2-9a) and heterolithic away from the dome (Figure 2-9b), are poorly to well sorted and have

FIGURE 2-8: DIAMICTITES OF UNIT 3.

A) monolithic (dacitic) diamictite with a pelitic matrix. Clasts are 5 cm to >1 m long. B) heterolithic diamictite with felsic to mafic volcanic clasts within a sandy matrix. Clasts are up to 20 cm across. C) heterolithic diamictite with clasts that are angular to rounded. Note the single dacite clast with a white alteration rim (arrow). Clasts are up to 30 cm long. D) monolithic diamictite with rare crude layering due to change in grain-to-matrix ratio and clast size. Pen is 13 cm long. E) diamictite containing clasts (C) picked up from underlying dacite lava of unit 2.

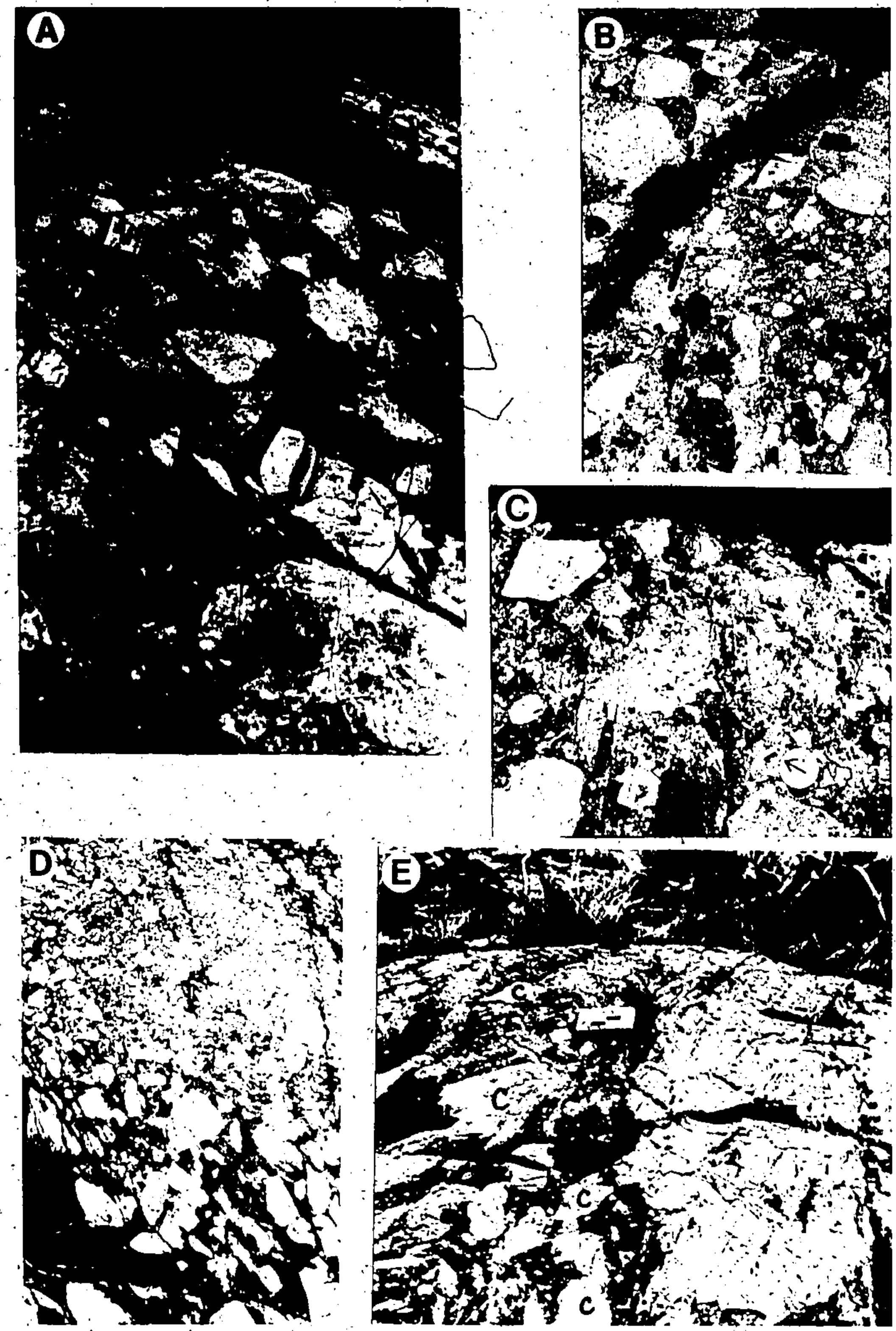
A
B
C
D
E
C
C
C
C

a sandy to gritty matrix. Clasts are subrounded, range from 2 to 15 cm across and are slightly disrupted to closely packed. Conglomerates near the dome complex are thicker bedded than conglomerates in distal parts of unit 3. The distal conglomeratic beds are interbedded with arenite and lutite, the bedding ranging from 15 cm to 1 m in thickness. One 0.25 m conglomeratic bed shows reverse and normal grading of dacite clasts and reverse grading of dark, possibly pumice fragments (Figure 2-9f).

The arenites have a coarse salt and pepper appearance due to the presence of amphibole and plagioclase crystals (Figure 2-10a&b) or are a uniform, medium grey to green. They vary from massive to well-bedded, the massive units (up to 1 m thick) in places repetedly grading into the well-bedded ones (up to 1 m thick) (Figure 2-10c). The well-bedded arenites are planar to cross-bedded (Figure 2-10a&b) and locally have rippled (Figure 2-10a) and convoluted beds.

The lutites are thinly bedded to massive (up to 1 m thick), generally brown, green or dark grey, and are soft and recessive (Figure 2-9g). Lutites and arenites contain, in a few places, dacitic blocks which disrupt internal bedding (Figure 2-10d).

FIGURE 2-9: CONGLOMERATES OF UNIT 3.

A) monolithic conglomerate near the dome complex. Clasts are plagioclase phyric dacite and range from 1 to 13 cm across. B) heterolithic conglomerate in distal part of unit 3 with respect to the dome complex. Clasts are mafic to felsic, with andesitic to dacitic clasts predominating. C) monolithic (dacitic) conglomerate interbedded with a massive dacite flow lobe of unit 2a. The massive dacite is 1.5 m wide. D) interbedded conglomerate and massive arenite in distal part of unit 3. E) photomicrograph of matrix to conglomerate in Figure 2-9d. Field of view is 1 cm. F) conglomeratic bed showing rare reverse grading of lithic fragments (light coloured) near bottom and normal grading towards top of bed (stratigraphic top). Pumice fragments (dark coloured) are reversely graded near top of bed. Pen is 13 cm long. G) conglomerate (right), interbedded lutite and arenite, and diamictite (left). Field book is 19 cm long.

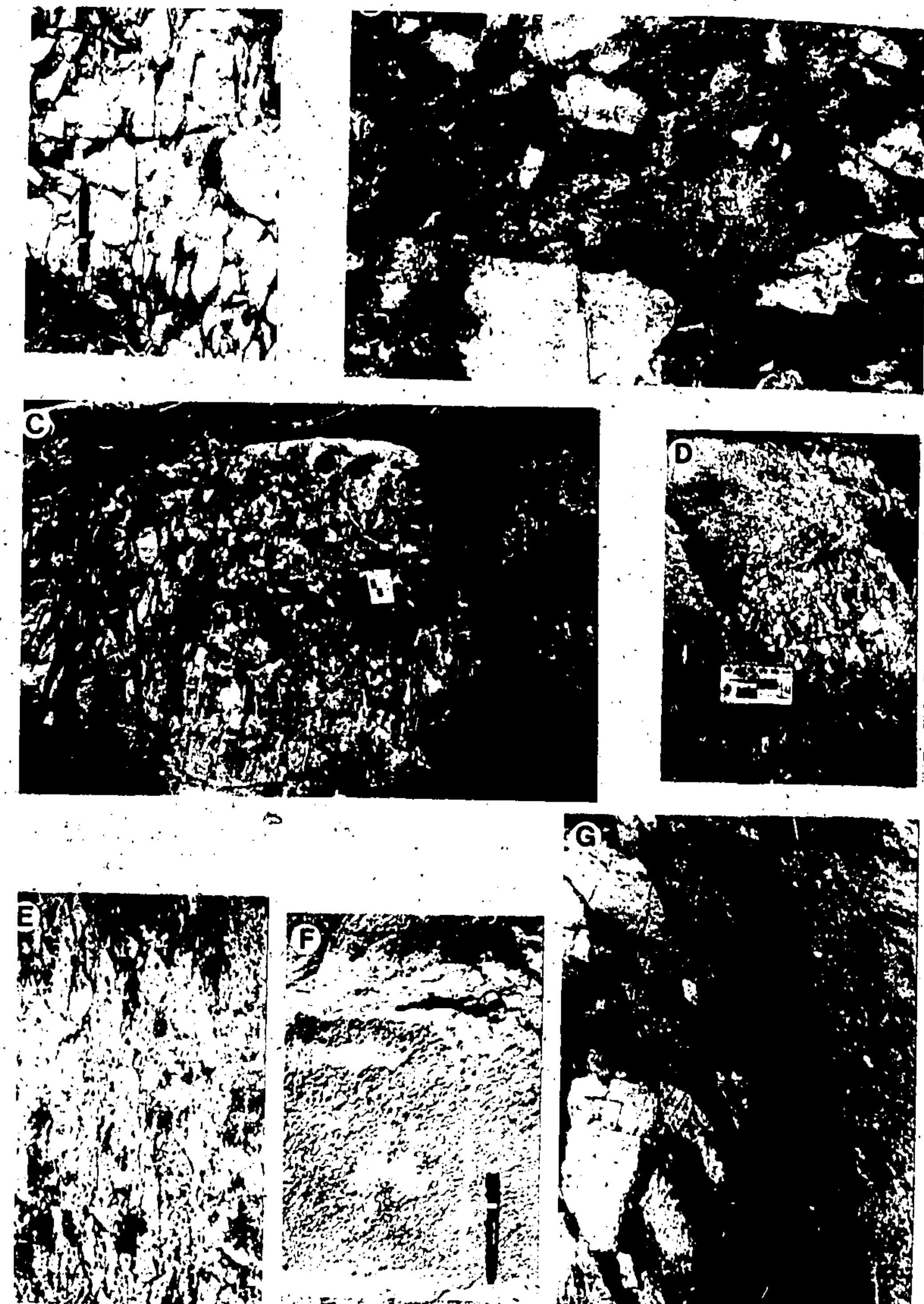
C
D
E
F
G

FIGURE 2-10: VOLCANIC ARENITES AND LUTITES OF UNIT 3.

A) thinly bedded volcarenite with cross-bedding (x) and possible starved ripples (r). Sedimentary tops are upward. Edge of field book is 11 cm. B) Arenite with trough cross bedding. Lense cap is 5 cm. C) massive arenite grading upward into thinly bedded arenite. D) dacite blocks from unit 2b that puncture and distort thinly bedded arenites and lutites. Pen is 13 cm long.

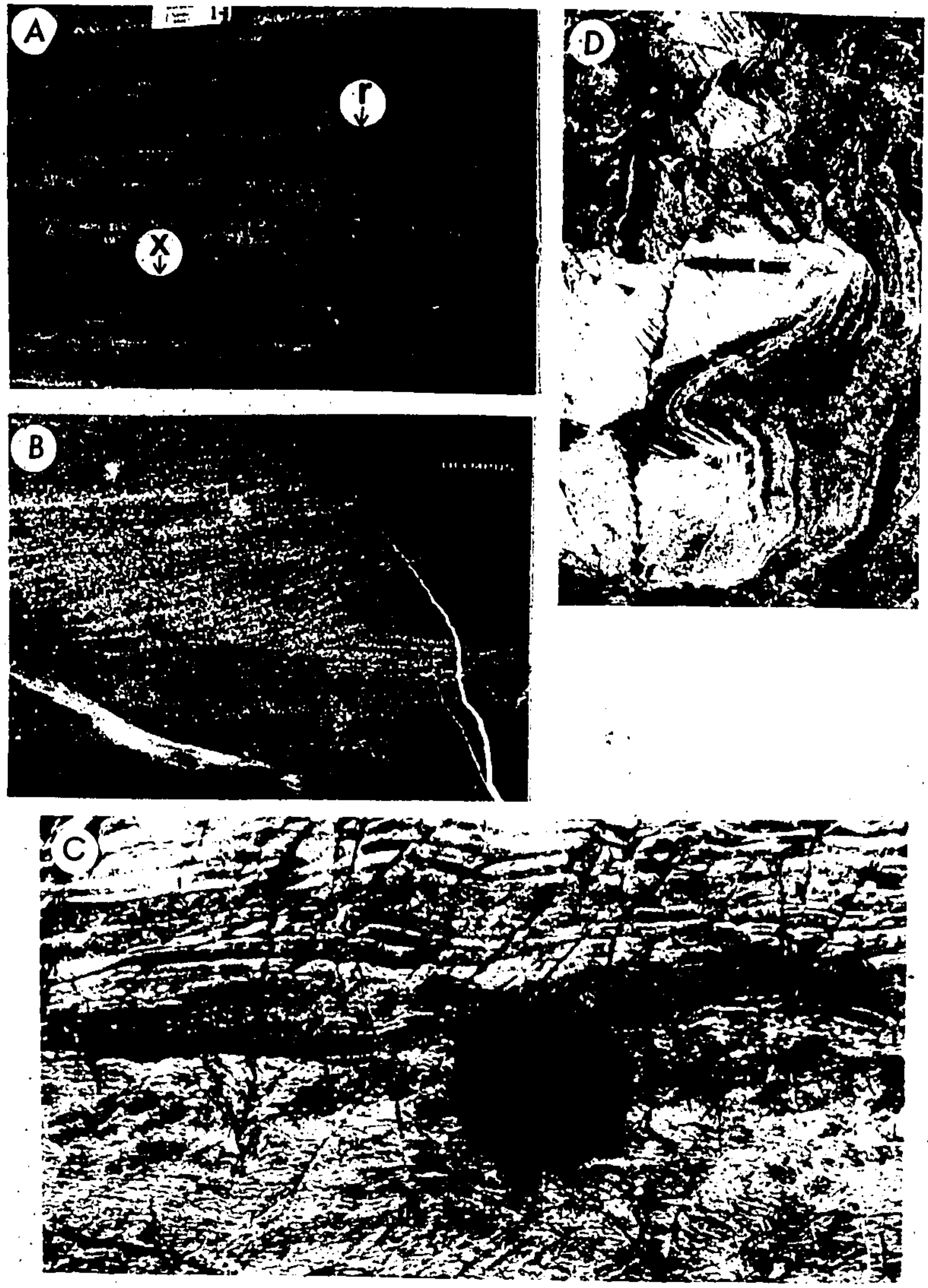
A
B
C
D

2.1.1.5 interpretation

The diamictites are characteristic of debris flow deposits. This interpretation is based on a number of features as no single one is unique to lahars. These features include extremely poor sorting, boulders exceeding 1 meter in size, heterolithic clasts, vertical grading, debris from underlying deposits and lack of pumice fragments (c.f. Fisher, 1960, 1982; Fisher and Schmincke, 1984; Parsons, 1969; and Mullineaux and Crandell, 1962).

The conglomerates and rippled and cross-bedded sandstones characterise fluvial deposits , such as sheet flood and stream channel deposits (c.f. Reading, 1978). The fluvial deposits and diamictites (lahars) together are characteristic of alluvial fan deposits. The interbedded conglomerates, massive to well-bedded arenites and lutites are possibly a combination of sedimentary deposits (reworked volcanic deposits), distal parts of lahars, and, to a minor extent, pyroclastic deposits. Many of these interbedded clastic rocks cannot be readily identified as pyroclastic because distinguishing features such as glass shards and pumice fragments may have been destroyed by recrystallization and deformation. One has been readily identified such as a conglomeratic bed (Figure 2-9f) with reversely graded lithic clasts at the bottom and normally graded lithic clasts and reversely graded pumice fragments at the top, features that characterize a pyroclastic deposit (c.f. Sparks, 1976; Wright et al, 1980; Walter and Croasdale, 1971; Parsons, 1969).

Dacitic blocks in arenites and lutites close to the dacite breccia of the dome complex may represent debris from the complex, which contains similar fragments. The blocks may have rolled or dropped onto and punctured soft, unconsolidated sedimentary beds. The minor dacite tuff lobes interfingering with the conglomerates and diamictites near the complex could be pyroclastic flow lobes of unit 2a that came from the same vent as the dome complex.

In summary, mainly diamictites, conglomerates and cross-bedded and rippled sandstones may represent a mixture of debris flow and fluvially reworked volcanic deposits ie. alluvial fan deposits. The material for the deposits possibly came from unstable volcanic material of the dome complex. With increase in distance from the dome complex, the deposits of unit 3 become thinner and more clearly bedded and generally contain better rounded, sorted and, to some extent, smaller sized clasts due to a change from proximal to distal parts of debris flow deposits.

Unit 3 was , to some extent, subaerially deposited as seen by the fluvial deposits.

2.1.1.6 unit 4

Unit 4 comprises dacitic to rhyolitic tuffs which include varieties that are crystal-rich, pumice-lithic-rich, deformed and/or welded, laminated and massive. Also included is minor massive to brecciated dacite.

The tuffs of unit 4 are preserved as a 200 to 600 m thick body in the northwest corner of the volcanic pile, disrupted by a left lateral fault. They are also present as a thin 70 m sliver in the southwest corner. In each case the tuffs have a conformable upper contact with turbidite sedimentary rocks (unit 6) and a lower conformable contact with the volcaniclastic rocks of unit 3. At the upper contact, cobbles of tuff commonly form a conglomerate within the base of the sedimentary rocks of unit 6. The thickest section of tuffs is west of the dome complex, in the southern faulted part of the main body. Undeformed to deformed and/or welded pumice-lithic tuffs occupy the bottom of the section whereas interbedded crystal tuffs and pumice-lithic tuffs lie at the top, separated by a 100 m by 300 m wedge of massive to brecciated dacite. The crystal and pumice-lithic tuffs taper along strike northeastward away from the dome complex into laminated and massive tuffs. The tuffs in the southwest sliver are massive and laminated tuffs grading upward into lapilli-sized lithic tuffs.

The crystal tuffs (Figure 2-11a) are fine-grained, well-sorted clastic rocks that are light to medium grey, weathering to light greenish-grey and brownish-grey. They are massive to rarely, faintly stratified (Figure 2-11b), 1 to 2 meter thick beds. Where stratified, the internal beds are 1 mm to 1 cm thick and defined by change in colour or phenocryst content. The tuffs generally contain 20 to 25 % broken plagioclase and embayed quartz phenocrysts which range from 0.25mm to 3.0mm in size. Rarely the phenocrysts are graded (Figure 2-11b). In places, <1 to 2 mm sized, lenticular pumice fragments are present. The matrix is recrystallised quartzofeldspathic material with chlorite, muscovite, carbonate, minor biotite and amphibole. Glass shards were not identified, probably because of recrystallisation.

Pumice-lithic tuff beds, 2 to 5 m thick, (Figure 2-11c&e) are light to medium grey and generally include < 10% plagioclase phenocrysts and < 2% quartz phenocrysts. Poorly sorted fragments of pumice and plagioclase phyric dacite range from < 1 cm to > 4 cm across and lie within a disrupted framework. The pumice fragments, commonly dark brown to grey, are vesicular with ragged ends (Figure 2-11d).

FIGURE 2-11: FELSIC CRYSTAL AND PUMICE-LITHIC TUFFS OF UNIT 4.

A) crystal tuff with broken phenocrysts of plagioclase. B) crystal tuff showing plagioclase phenocrysts and massive crystal tuff grading upward (towards stratigraphic top) into faintly stratified tuff (s). C) pumice-lithic tuff containing mainly dark, lenticular to ragged fragments of pumice. Field of view is 15 cm. D) closeup of pumice fragment showing vesicles and ragged ends. Field of view is 15 cm. E) photomicrograph of matrix to pumice-lithic tuff of Figure 2-11c. The matrix contains welded pumice fragments. Field of view is 8 mm.

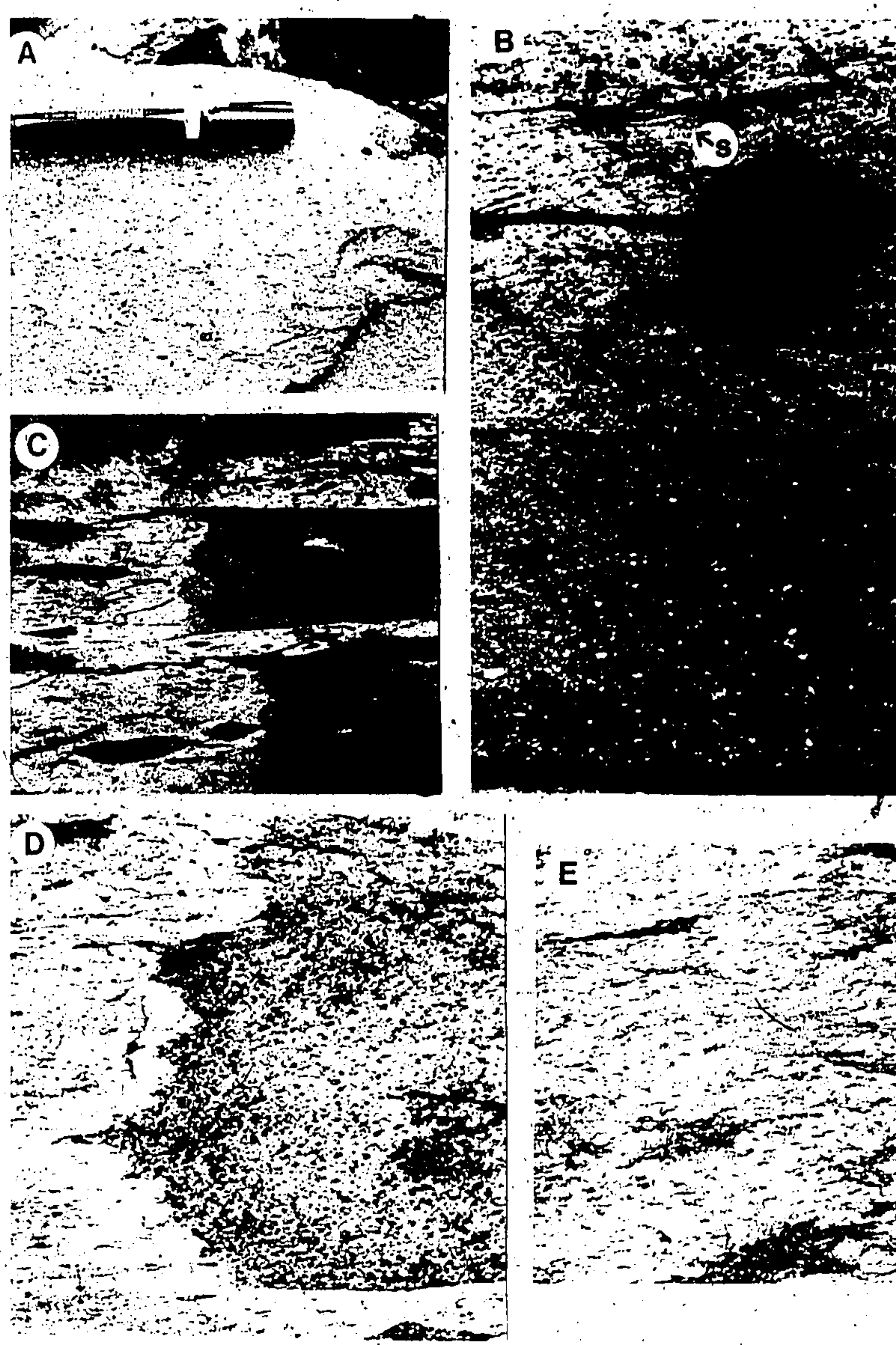
A
B
S
C
D
E

Deformed and/or welded tuffs are similar to the pumice-lithic tuffs in colour but contain dark grey, 1 to 10 cm sized, lenticular bodies with wispy ends (Figure 2-12a&b). The fragments also form dark, discontinuous, 1 mm to 15 cm bands alternating with a light grey tuffaceous matrix (Figure 2-12c). Outlines of the fragments may not be discernible, but along strike the bands change into dark, vesicular fragments of possibly pumice (Figure 2-12d). It is difficult to determine whether the banding represents fragments that are deformed and flattened or welded.

Laminated tuffs (Figure 2-12e&f), which are cream white to olive yellow, are aphanitic clastic rocks composed of alternating muscovite-rich and quartzofeldspathic-rich beds varying from < 1 mm to several cm in thickness (Figure 2-12g). The muscovite-rich beds contain embayed quartz crystals and flattened, dark pumice? fragments (Figure 2-12h).

Massive tuffs, white to light grey in colour, are fine to medium grained and contain 0% to 10 % plagioclase phenocrysts and locally patches of recessive and brownish-grey spheroids 0.25 to 4.0 cm in size. In thin section the plagioclase phenocrysts are broken crystals in a quartz- carbonate-sericite matrix.

The massive to brecciated dacite is medium to light grey weathering to pale greenish-grey. It contains a few quartz and plagioclase phenocrysts. Brecciated parts are similar to

FIGURE 2-12: DEFORMED AND/OR WELDED FELSIC TUFF AND LAMINATED FELSIC TUFF OF UNIT 4.

A) tuff with dark, welded or deformed pumice? fragments. B) tuff with dark, lenticular fragments of pumice. C) tuff with dark bands alternating with light grey tuffaceous matrix. D) tuff with dark pumice? fragments along strike from Figure 2-12c. Clasts are up to 20 cm long. E) laminated tuff. Laminae are defined by alternating muscovite-rich and quartzofeldspathic-rich zones. Small, dark pumice fragments are seen in upper right-hand corner. F) laminated tuff strongly crenulated. G) photomicrograph of crenulated, laminated tuff. Quartzofeldspathic beds alternate with muscovite-rich beds. Field of view is 8 mm. H) photomicrograph of laminated tuff with an embayed quartz crystal which deflects a flattened pumice? fragment. Field of view is 2 mm.

the breccia of unit 2b, being poorly sorted, having coarsely packed angular fragments (2 to 15 cm across), and having little matrix cemented by carbonate.

2.1.1.7 interpretation

The pumice-lithic tuffs have characteristics of pyroclastic flow deposits such as pumice and lithic fragments, broken plagioclase phenocrysts and dark lenticular bodies and zones which could be welded fragments and/or welded portions of a tuffaceous matrix. Additionally they are poorly sorted, lack internal stratification, and are framework disrupted (c.f. Ross and Smith, 1961; Frisch,1973; Sparks, 1976; Cas, 1978; Wright et al, 1980; Fisher, 1982; and Fisher and Schmincke, 1984). The massive tuffs could be eroded pyroclastic flow deposits as seen by their pocked mark appearance (Ross and Smith, 1961).

The crystal tuffs and laminated tuffs are good candidates for pyroclastic fall deposits, being clastic rocks that are well sorted, in places well bedded and containing pumice fragments and broken plagioclase phenocrysts. The change along strike away from the dome complex from massive crystal tuff to thinnly bedded tuffs is also characteristic of air-fall deposits (c.f. Self, 1982).

The massive and brecciated dacite within the tuffs could be a displaced part of the dome complex of unit 2b.

Unit 4 was probably deposited in a subaerial environment because it is restricted to the northwest corner of the volcanic pile, stratigraphically above the fluvial deposits of unit 3. Elsewhere airfall deposits probably were reworked because of subaqueous conditions.

2.1.1.8 unit 5

Rocks of unit 5 are basaltic to andesitic in composition and consist mainly of massive lava, pillow lava, pillow breccia, volcaniclastic rocks and massive to layered dykes.

Unit 5 comprises most of the eastern portion of the volcanic pile (Figure 2-1), having a maximum thickness of about 1300 m. The unit thins to the northeast, where it is isoclinally folded, and to the southwest to about 100 to 200 m. The bottom of the thickest section of this unit consists of predominantly pillow lava, pillow breccia, dykes and minor volcaniclastic beds. The middle part consists of mainly volcaniclastic rocks with minor pillow lava, pillow breccia and dykes, interfingering and in sharp contact with massive dacite of unit 2a. At the top of the section there are primarily massive and pillowed lava and minor pillow breccia. The extremities of unit 5 are along strike from and similar to the uppermost parts of the main body, consisting of pillow lava and breccia. These extremities also include thin interbeds of gossanous turbidite pelites which, in places, are cherty. They are surrounded by turbidite sedimentary rocks which are stratigraphically above the felsic volcanic pile.

In general, the rocks are aphanitic to finely crystalline and dark grey to dark green, though also light grey and white where altered to carbonate, sericite, epidote and /or silica (Figure 2-13c&f).

The volcaniclastic portions of unit 5 consist of 0.25-2.0 m clastic beds, the layering defined by changes in grain- matrix ratio, clast size, and matrix type (sandy to pelitic) (Figure 2-13a&b). Some of these beds display normal grading (Figure 2-13b&c). The rocks range from poorly to well sorted and from matrix- to clast-supported. Most clasts are 1 to 10 cm across (with a few larger), monolithic, and angular to well-rounded. They are commonly vesicular, the vesicles being evenly dispersed (Figure 2-13c) or arranged in zones (Figure 2-13e). Some clasts have white, altered rims, though more commonly they are completely altered white to light grey by carbonate, epidote and sericite, in contrast to a dark grey matrix. Interbeds of pillow lava, pillow breccia and hyaloclastites grade vertically and laterally into the volcaniclastic rocks (Figure 2-15b). Two lobes of volcaniclastic rocks contain matrix-supported, rounded clasts in a pelitic matrix (Figure 2-13d).

FIGURE 2-13: MAFIC VOLCANICLASTIC ROCKS OF UNIT 5.

A) basaltic volcaniclastic beds with layering defined by change in grain-to-matrix ratio, clast size and matrix type. Thin pelitic beds with a few floating clasts alternate with thick beds of packed clasts. Field book is 19 cm long. B) mafic volcaniclastic beds defined by change in grain-to-matrix ratio and clast size. Clasts may be slightly graded. C) mafic volcaniclastic beds separated by a garnetiferous, pelitic bed. The vesicular clasts are altered white by sericite and carbonate. The upper clastic bed is normally graded by a change in clast size and grain-to- matrix ratio. D) flow lobe of pelitic, matrix-supported volcaniclastic bed (dark colour) between pillow breccia beds. E) closeup of vesicular clasts within a volcaniclastic bed (pillow breccia?). Some of the clasts show zoning of vesicles; the largest (26 cm across) displays concentric zoning. F) microphotograph of a vesicular clast. The mafic clast is altered to carbonate, sericite and quartz, with vesicles filled with quartz and carbonate. The clast has little biotite and amphibole compared to the matrix on left side of photo. Field of view is 1 cm.

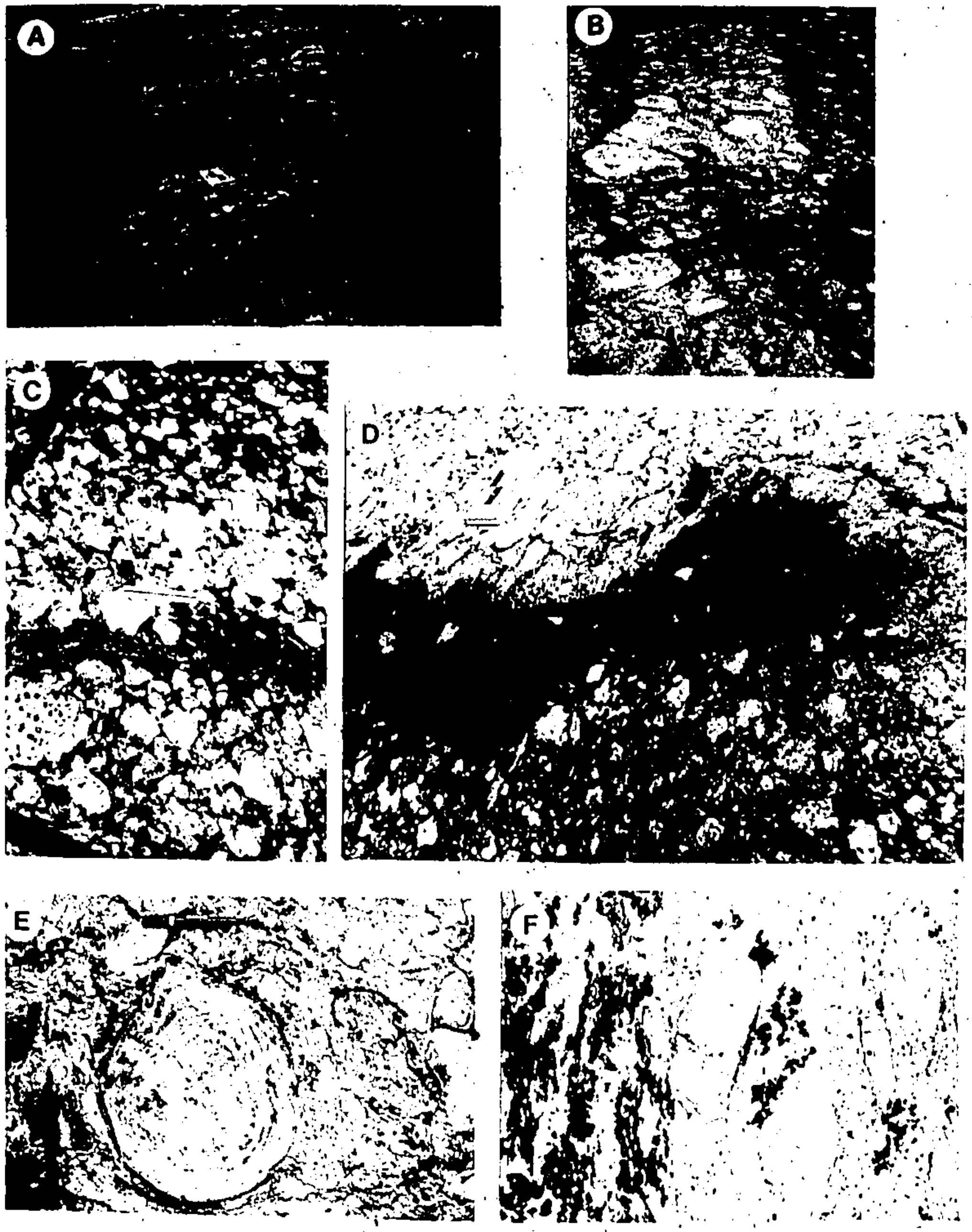
A
B
C
D
E
F

The pillow lava (Figure 2-14a,b&c) has pillows that range from 20 cm to 1 m in longest exposed dimension, and vary from being uniformly vesicular to concentrically vesicular (Figure 2-14d) to radially vesicular (Figure 2-14e) to non-vesicular. Rarely the pillows are variolitic (Figure 2-14f). Locally the pillows grade upward from small, non-vesicular to larger and vesicular ones (Figure 2-14g). However, overall the pillows decrease in size and vesicularity upsection through the unit. Pillow lava locally grades upward and laterally into pillow breccia and hyaloclastite (Figure 2-14h) and in two localities grades laterally into small globules, possibly pillow breccia, (Figure 2-15a), similar in appearance to clasts of some of the volcaniclastic beds.

Pillow breccia has centimeter to meter sized clasts that range from packed, angular fragments (broken pillow breccia) (Figure 2-15b) to amoeboid-shaped clasts floating in a hyaloclastite matrix (isolated pillow breccia) (Figure 2-15c). At one locality pillow breccia is separated from overlying and underlying pillow lavas by 2 to 3 cm thick lava beds or dyklets (Figure 2-15d). At another, pillow breccia (between pillow lava) has subangular to subrounded clasts similar to clasts in some of the volcaniclastic rocks (Figure 2-15f).

Hyaloclastite consists of small, angular fragments ranging from less than a millimeter to greater than a centimeter in size that form as a matrix to pillow breccia (Figure

FIGURE 2-14: MAFIC PILLOW LAVA OF UNIT 5.

A) basaltic pillow lava showing budding pillow (p). Stratigraphic top, determined from adjacent sediments, is to the right. Field book is 19 cm long. B) pillow lava with uniform vesicularity. The interstices are hyaloclastite. C) pillow lava with mafic pillows that are light grey to white due to sericitisation and carbonatisation. D) pillows with concentric, compositional zoning. E) pillows with radially aligned amygdules. Edge of field book is 11 cm. F) variolitic pillow. Felsic varioles are present in a basaltic matrix. G) pillows grading, from left to right, from small and vesicular-poor to large and vesicular-rich. H) pillow lava grading stratigraphically upward (down photo) into pillow breccia and hyaloclastite within the volcaniclastic rocks of unit 5.

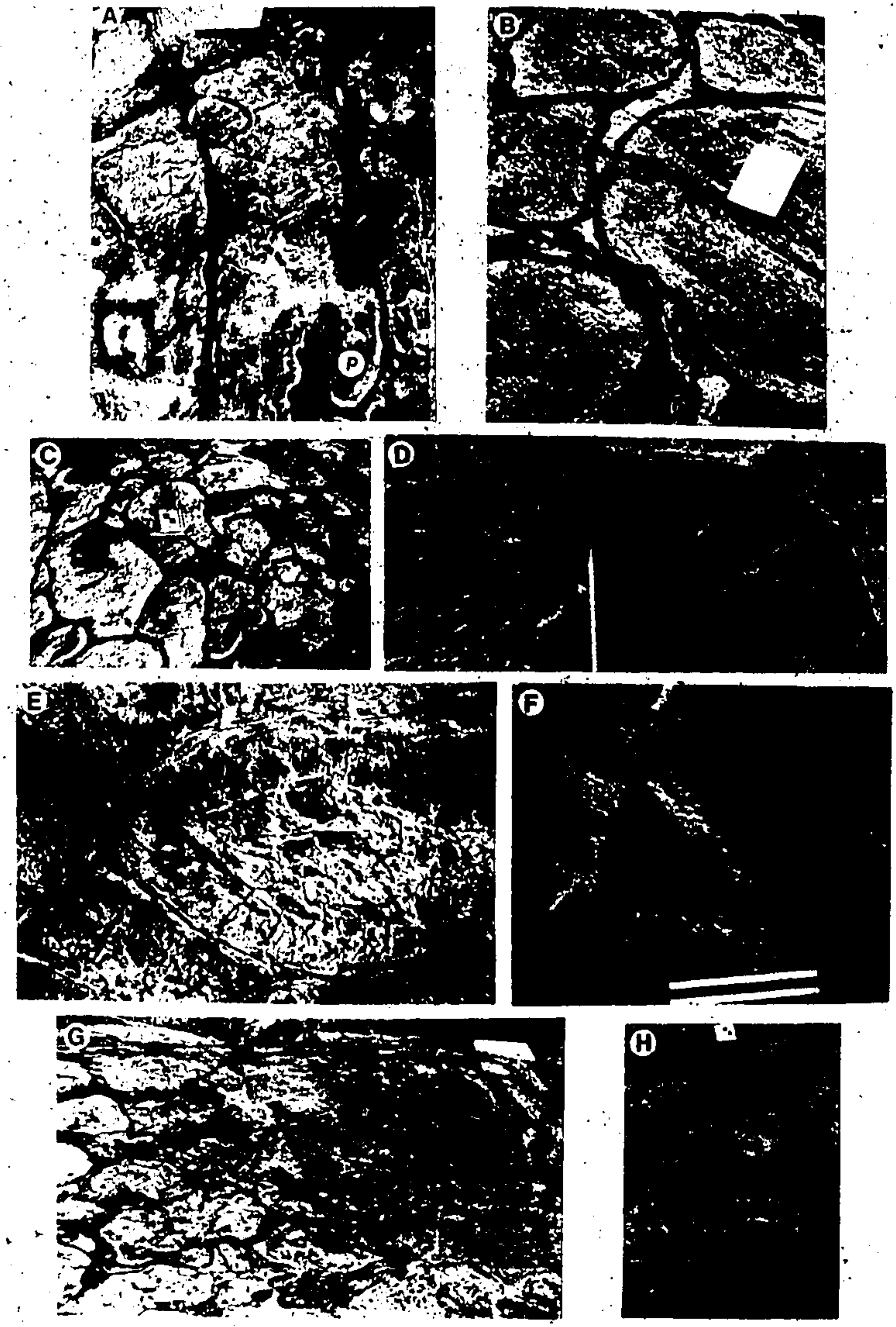
A
B
P
C
D
E
F
G
H

FIGURE 2-15: MAFIC PILLOW BRECCIA OF UNIT 5.

A) mafic globules, one type of pillow breccia, grading along strike (to right) into pillows. Bedding is defined by a thin, garnetiferous pelite. B) broken pillow breccia. Pillow fragments are packed within a hyaloclastite matrix. C) isolated pillow breccia. Large amoeboid-shaped pillows (up to 0.5 m across) float in a hyaloclastite matrix. D) pillow breccia (b) separated from pillow lava (p) by thin layers of lava (dyklets?). E) pillow breccia (b) in contact with pillowed lava (p).

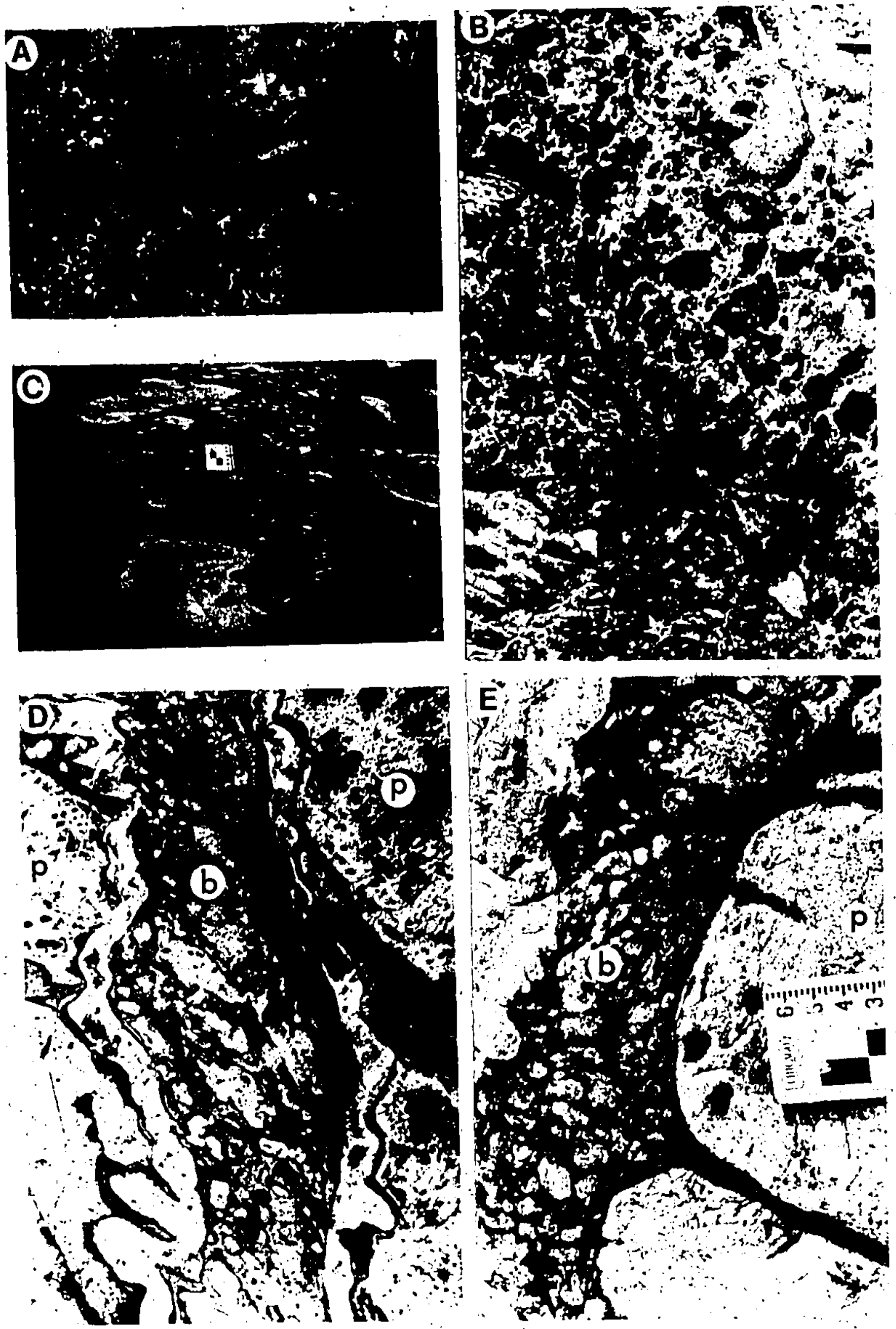
A
B
C
D
p
b
p
E
b
p
6 5 4 3

2-15c), interstices to pillows (Figure 2-14c), or massive beds, commonly grading into pillow breccia (Figure 2-14h).

Massive lava is mainly present in the upper portion of unit 5, interbedded with and grading up into pillowed lava, minor pillow breccia and gossanous turbidite mudstones of unit 6. The massive lava generally has poor vesicularity.

In the lower and, to a minor extent, middle parts of unit 5, pillow lava and pillow breccia include 1 to 2 meter thick massive to layered dykes (and possibly sills) (Figure 2-16). These dykes have sharp, irregular contacts (Figure 2-16d&e) that are almost parallel to bedding. Locally, the contacts truncate pillows and pillow fragments and in others protrude into, and seem to be contributing to the pillow lava or breccia (Figure 2-16f,g&h). The dykes vary from being completely unlayered (Figure 2-16e) to having massive interiors and layered margins (Figure 2-16b) to being completely layered throughout (Figure 2-16a). One dyke changes outward from massive at the center to thickly layered (5 cms) to thinnly layered (2 cms) at the margins (Figure 2-16b). Also the dykes commonly are finely crystalline at their margins to coarser crystalline at their centers. The dykes, in places, peeter out; at one locality a dyke ends as a lobe in which the layers are folded around and where there are more vesicles than farther back along the dyke. Also along strike, in front of this lobe, is a pillow similar to the lobe, being concentrically layered and vesicular.

FIGURE 2-16: MASSIVE TO LAYERED MAFIC DYKES OF UNIT 5.

A) layered dyke with graded units folded in the centre. Graded units are defined by change in plagioclase-to- mafic mineral ratio. B) dyke with massive centre (right) changing into thick (5 cm) graded units and then thin (2 cm) graded units at margin (left). C) closeup of a graded unit. Plagioclase-rich zone (light coloured) grades upward into mafic mineral rich zone (dark coloured). D) layered dykes intruding pillow breccia. Note the irregular, sharp contacts. E) dyke with extremely irregular contacts with pillow lava (to left and right). The central part of the dyke, in foreground, is brecciated, similar to pillow breccia. F) massive dyke (in foreground) with irregular contact with pillow lava. One irregular protrusion of the dyke ressembles a pillow bud (p). G) layered dyke contributing clasts to a breccia. Protrusions of the dyke are seen at (p). H) layered dyke protruding into pillow breccia. The layers grade from 5 cm thick ones at centre of dyke to <1 cm thick ones at margin.

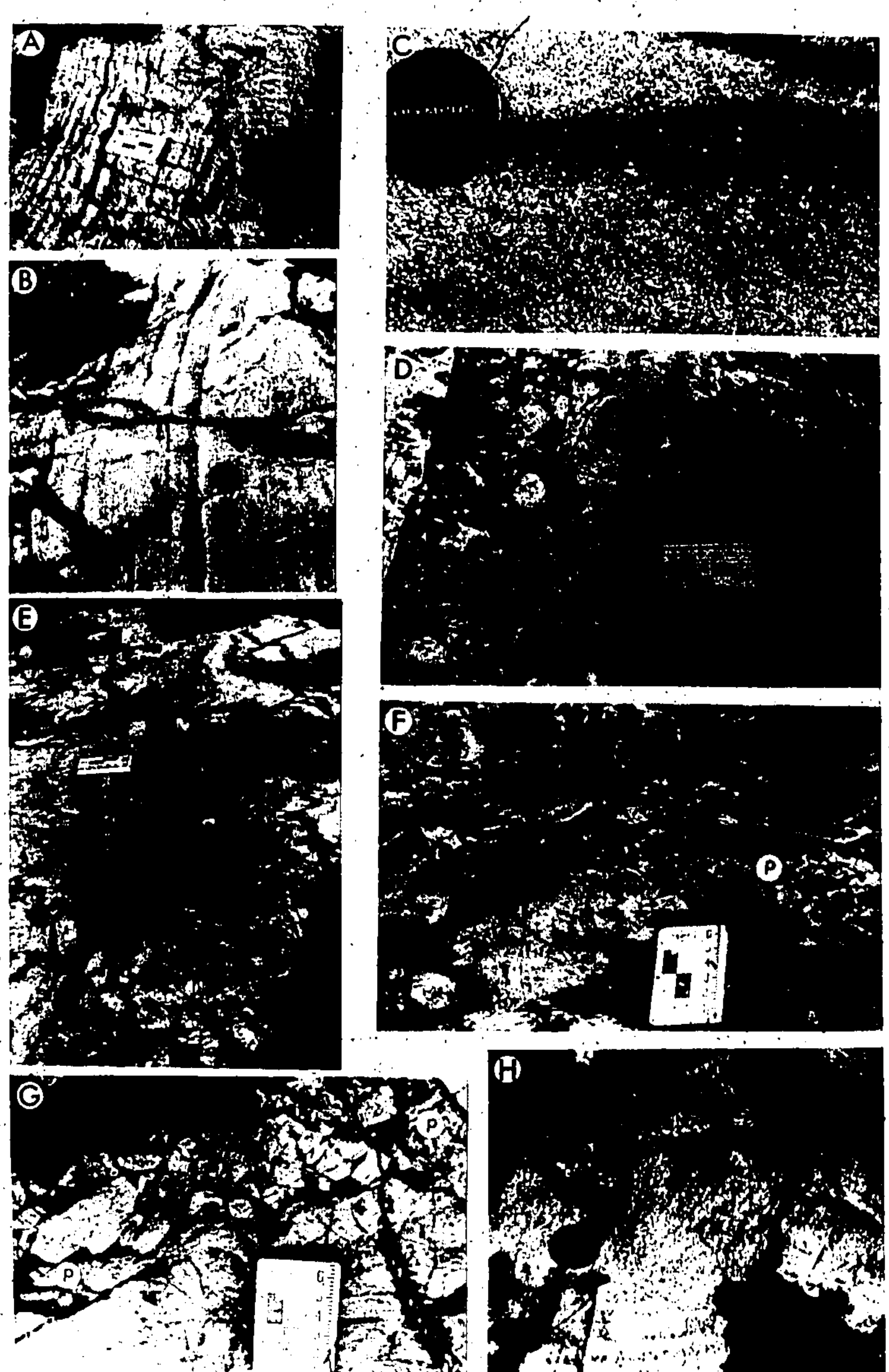
A
B
C
D
E
F
P
G
P
P
H

Some of the dykes contain pockets of pillow breccia (Figure 2-16e). The layered portions of the dykes are defined by centimeter thick graded units that are parallel to the dykes' contacts and, in places, are folded (Figure 2-16a). The graded units are the result of changes in plagioclase-mafic mineral ratios (Figure 2-16c) and vesicularity (Figure 2-16d).

2.1.1.9 interpretation

The depositional environment of the mafic rocks of unit 5 was primarily subaqueous. The pillow lavas, pillow breccias and hyaloclastites evidently resulted from extrusion under water. The volcaniclastic rocks, which are monolithic and the same rock type and grade into the pillow lavas and breccias, could represent 1) pillow breccia and hyaloclastite deposits and 2) pillows lavas, breccias and hyaloclastites reworked by density flows, slumping, and/or current/wave action within relatively shallow water. The flow lobes of volcaniclastic rocks indicate that some of the volcaniclastics are debris flow deposits.

Numerous local shoaling upward cycles are present within unit 5, as seen by increases upward in pillow and vesicle size and vesicle abundance and local grading upwards from pillowed lava to pillow breccia to volcaniclastic material (c.f. Cousineau & Dimroth, 1982 and Dimroth et al, 1978). A major shoaling upward sequence appears to be represented by the overall change from mainly pillowed flows /breccia at the bottom of the thickest part of the unit to a thick section of dominantly volcaniclastic rocks and minor pillowed flows in the middle part. Major deepening is suggested by the change upward from the thick section of volcaniclastic-dominated rocks to pillowed and massive rocks, seen to be lava flow-dominated, of the upper portion and the thin extremities of unit 5.

The layered dykes within the pillowed flows and breccia could be shallow dykes that were feeders to some of the pillowed lavas and breccias. DeWit and Stern (1978) describe graded units within dykes as being a number of chilled margins due to pulses of magma through the dykes. The folding of the graded units may be due to flowage of magma through the dykes deforming already formed graded units.

The globules that grade laterally into pillows (Figure 2-15b), and also seen within some of the volcaniclastic beds, could have an origin not fundamentally different from that of pillows (c.f. Carlisle, 1963).

The feeding fissures for the mafic deposits of unit 5 were probably separate from that of the felsic volcanic rocks, being on the eastern flank of the felsic volcanic pile, where the mafic volcanics are thickest.

2.1.2 sedimentary rocks

A sedimentary rock sequence (unit 6) surrounds the volcanic pile. The sequence is generally younger than the volcanic rocks, though a local exposure of sedimentary rocks within the southwest corner of the volcanic pile in unit 1 (Map sheet B) and three localities within unit 2 and 3 indicate sedimentation contemporaneous with volcanism. Northwest of the volcanic pile the sedimentary rocks appear to be older than the volcanic rocks (units 2 & 5). Though top directions were not seen in the sediments the mafic volcanics immediately south consistently face south, away from the sediments. The sediments have conformable, though locally faulted, and gossanous contacts with the volcanic rocks. At a few places along the southwestern part of the sedimentary and felsic volcanic contact the sediments contain rounded clasts of the felsic volcanic rocks. Also to the west of the volcanic pile, greywackes contain abundant, angular felsic volcanic clasts.

The sedimentary rocks are dominantly interbedded greywackes and mudstones (Figure 2-17a) metamorphosed to greenschist and lower amphibolite grade (Chapter 4). Greywackes weather light grey, tan or brownish grey and are coarse to fine grained and locally gritty. The mudstones are dark grey to black. The greywackes predominate within the sequence, repeatedly grading up into the mudstones. These graded couplets range from 1 cm to several meters in

FIGURE 2-17: TURBIDITE SEDIMENTARY ROCKS OF UNIT 6.

A) proximal and distal facies of turbidite sedimentary rocks. The proximal facies, left, is mainly greywacke (beds up to 35 cm thick) and the distal facies, right, mainly mudstone with thin (up to 5 cm) sandstone beds. B) complete Bouma sequence in turbidite sedimentary rocks. A (at stratigraphic base of sedimentation unit) is graded greywacke, B parallel laminated sandstone, C climbing ripples in sandstone, D laminated siltstone and E mudstone. C) trough cross bedded sandstone. Field of view is 15 cm. D) ripple drift cross bedding. Field of view is 10 cm. E) sandstone dyklet and load structures protruding into mudstone, stratigraphically below greywacke bed. F) synsedimentary, near isoclinal folds in sandstone. The isoclines are refolded by open tectonic structures. G) mud ripup clasts in sandstone. The E-W lineation is glacial. H) interbedded mudstones and sandstones. Note ripples (R), loads and flames (L) and rare flaser bedding (F). Stratigraphic top is upward. I) dewatering structure defined by an upside down teardrop in laminated sandstone. Field of view is 8 cm. Stratigraphic top is upward. J) & (K) microphotographs of greywacke showing abundant quartz grains (Q), felsic volcanic clasts (V) and a few metamorphosed granitic fragments (M). (J is with cross polarised light). Field of view is 3.5 mm.

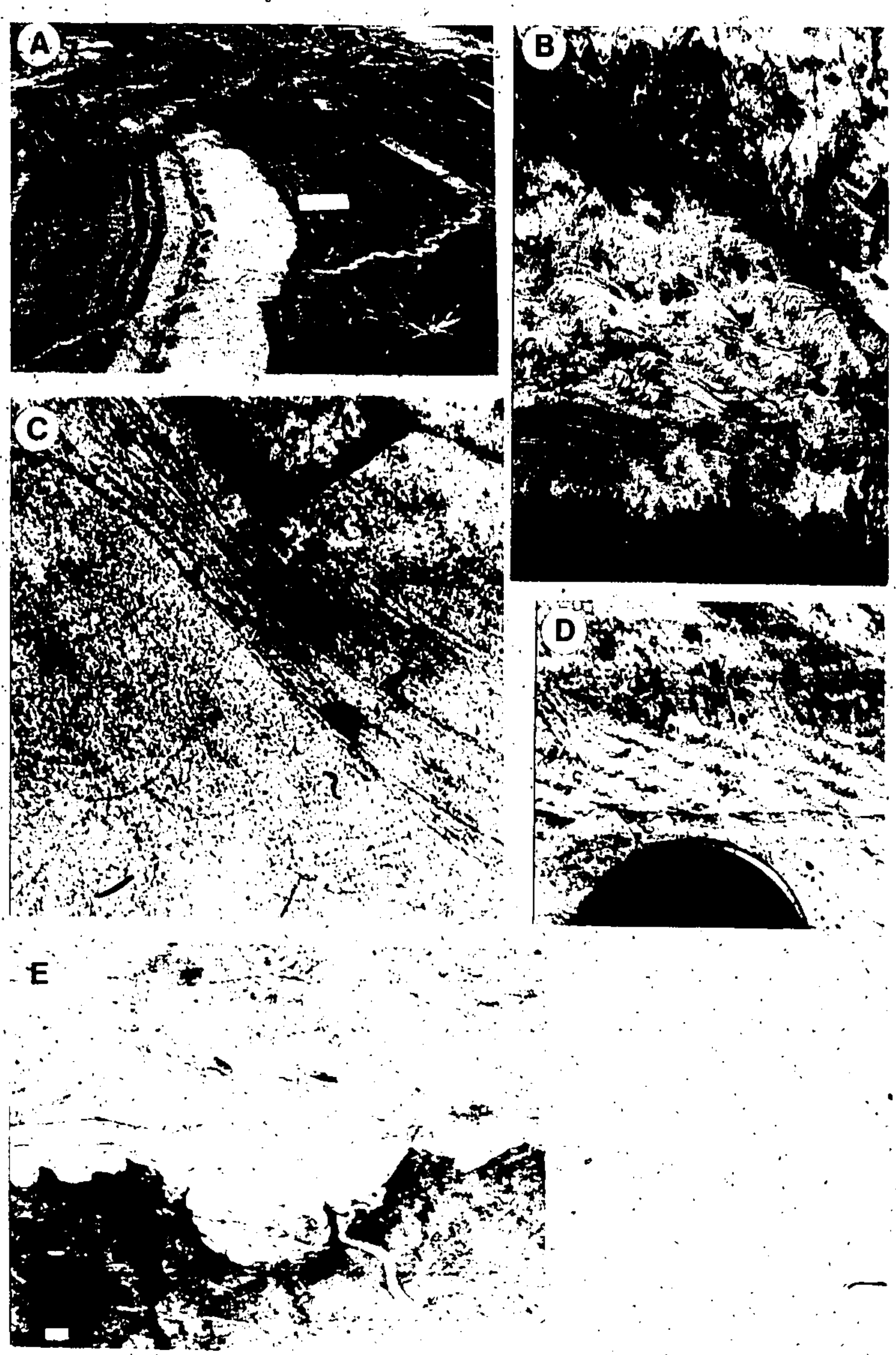
A
B
C
D
E

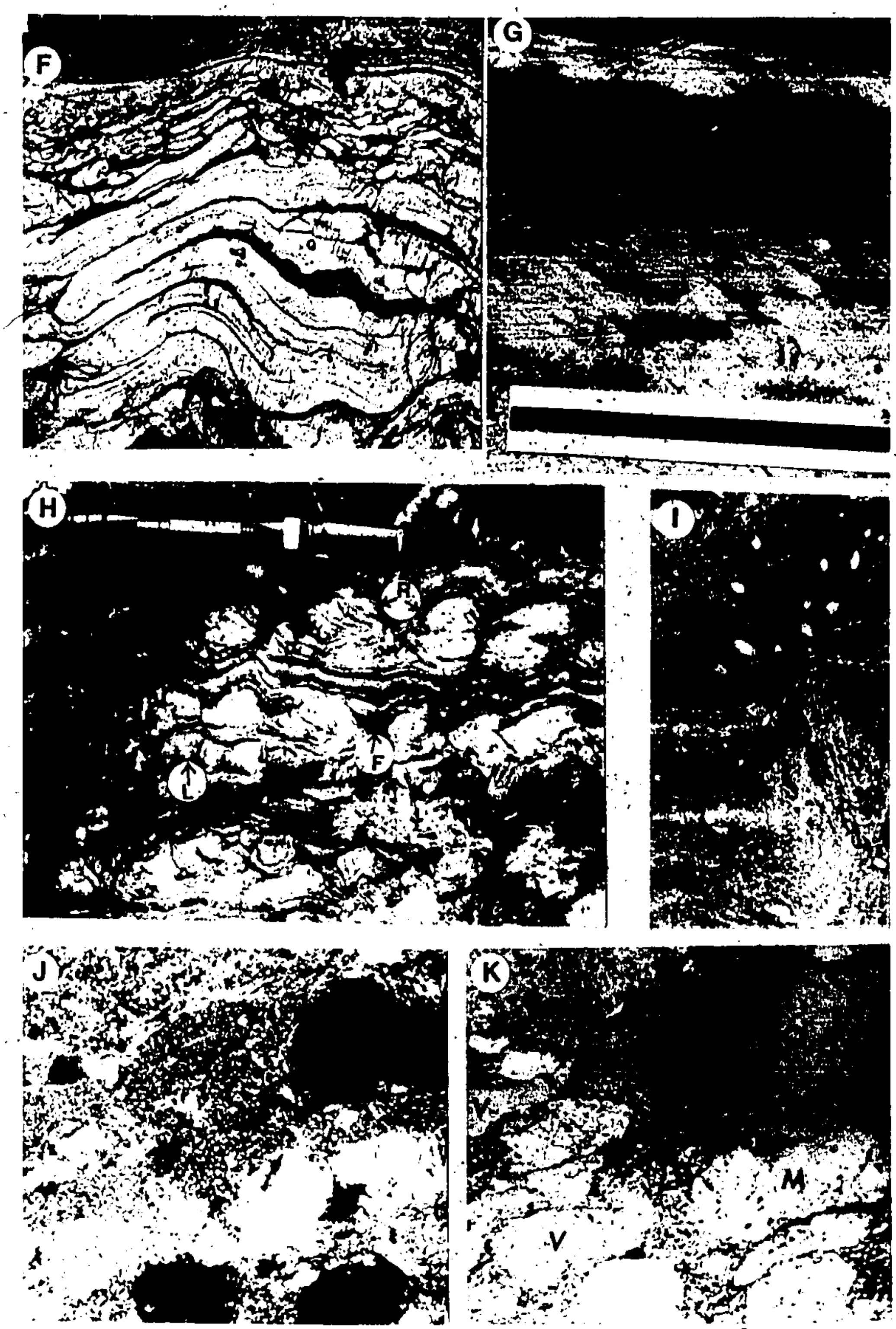
F
G
H
F
F
L
I
J
K
M
V

thickness and contain sedimentary features of the Bouma sequence (Bouma, 1962) (Figure 2-17b). Usually incomplete Bouma sequences are seen such as ABE, ACE or ABCE beds, with A as graded greywacke infilling scours at the base; B as parallel-laminated sandstone; C as cross-bedded (Figure 2-17c) to ripple-drift laminated (Figure 2-17d) sandstone; and E as mudstone. Rarely is the Bouma sequence complete with the D division, laminated siltstones, as seen in Figure 2-17b.

Sedimentary structures due to syn-sedimentary deformation are commonly present, particularly in the lower grade rocks. These include load and flame structures (Figure 2-17e,h), ball and pillow structures, convolute bedding, syn-sedimentary folds (Figure 2-17f), and dewatering structures such as sandstone dykelets (Figure 2-17e), conical forms in sandstone ('pseudo-ripples') at the contact with overlying mudstone and rarely upside-down teardrop shapes in laminated sandstone (Figure 2-17i). Other primary features are intraformational conglomerates (Figure 2-17g) and carbonate (now calcsilicate) concretions and beds.

The greywackes and mudstones are psammites and biotite schists in the higher grade metamorphic rocks. Though some of the primary features have been obliterated by metamorphism, many are preserved such as cross-bedding (Figure 4-5e), scours and grading. Grading is expressed by psammites grading into pelites and by cordierite porphyroblasts showing 'reverse grading' by size and abundance due to preferential growth in pelitic layers.

The greywackes, as seen in thin section, contain quartz and feldspar grains and felsic rock fragments (Figure 2-17h). The fragments include fine recrystallised felsic volcanic material and metamorphosed granitic fragments (mosaic of coarse, sutured crystals of quartz and feldspar). The felsic volcanic fragments are more deformed than other fragments and their outlines difficult to see, especially under polarised light.

2.1.2.1 interpretation

The sedimentary rocks of unit 6 contain all the features characteristic of turbidites discussed by Henderson (1975). They are not subdivided on the map (map sheets A,B,C) into turbidite subfacies because of changes over very short distances; for example a single outcrop may contain both distal and proximal turbidites (Figure 2-17a). One generalization, though, can be made: proximal sandstones predominate next to the volcanic pile. Thick A,B, and C divisions are topped by a thin mudstone E division and scours and gritty beds are common. As described above, the material for these sediments predominantly comes from the felsic volcanic and granitic rocks. In contrast, farther from the volcanic rocks, the sediments are a mixture of proximal and distal turbidites.

Sedimentation was going on during and after volcanism as seen by a few turbidite localities conformably within volcanic rock units 1, 2 and 3 and younger turbidites surrounding the volcanics and locally containing felsic volcanic material of possible pyroclastic origin.

### 2.1.3 paleogeographic interpretation

Five main stages can be recognised in the development of the Clan Lake volcanic pile and turbidite sedimentary rocks (Figure 2-18). During the first stage basaltic to andesitic lava (unit 1) was extruded in a subaqueous basin containing turbidites (Figure 2-18A ). This was followed by the build-up of an andesitic to dacitic volcanic cone by pyroclastic fall and flow and lava flow deposition (unit 2A), such that the cone eventually was subaerially exposed (Figure 2-18B). With subaerial exposure of part of the cone, volcaniclastic rocks of unit 3 (alluvial deposits) were deposited as a result of subsequent erosion and reworking of some of the unstable volcanic cone deposits. The third stage was the development of a dacitic dome complex on the volcanic cone, which included the deposition of crumble breccia and minor massive lava (unit 2b; Figure 2-18c). Subsequent mass wasting of this dome complex plus further reworking of unstable material from the volcanic cone resulted in continued deposition of volcaniclastic rocks of unit 3. Stage 4 (Figure 2-18D) was dacitic to rhyolitic pyroclastic flow and fall deposition. These pyroclastic deposits of unit 4 were preserved on the flank, presumably subaerially, of the volcanic cone. Prevailing winds may have also affected their distribution.

While the felsic volcanic pile developed (first subaqueously and later subaerially), mafic lava (unit 5) extruded from separate fissures on the submerged eastern flank of the volcanic cone. The mafic volcanic deposits built up into a shallow subaqueous environment where a thick section of mafic volcaniclastic rocks was deposited. Following deepening of the subaqueous environment, further extrusion of mafic lava produced pillowed and massive flows with minor volcaniclastic material within a turbidite depositional environment (Figure 2-18E). During this last stage, there was no felsic volcanism; the felsic pile was eroded down and became submerged and covered by turbidite sediments of unit 6.

## 2.2 INTRUSIVE ROCKS

The sedimentary and volcanic rocks were intruded by gabbroic bodies (unit 7), then by granitic bodies and dykes (unit 8) and lastly by diabase dykes (unit 9).

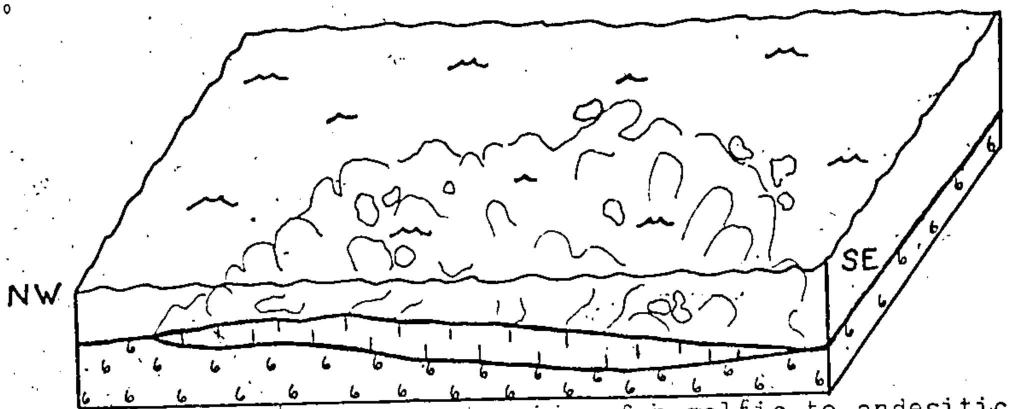


A stage: subaqueous extrusion of basaltic to andesitic lava (unit 1) in a turbidite sedimentary environment.

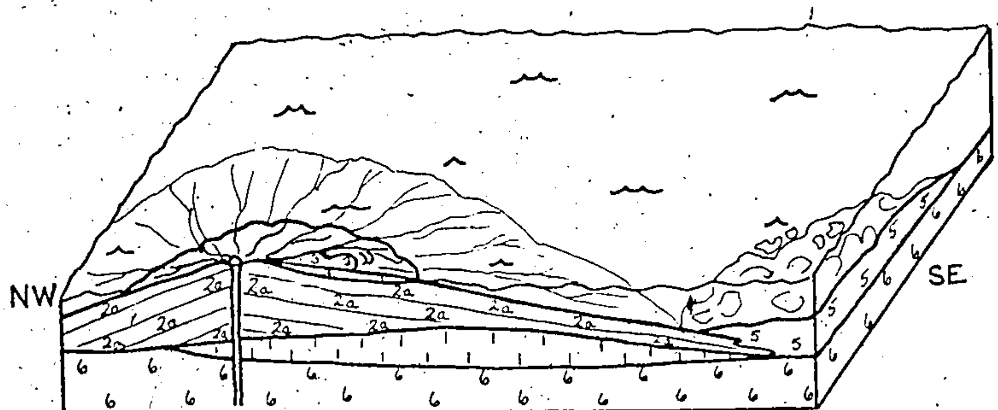


B stage: buildup of andesitic to dacitic volcanic cone (unit 2a) and, where subaerially exposed, reworking and redeposition of the cone's deposits (unit 3). Minor subaqueous extrusion of mafic lava (unit 5) to the east.

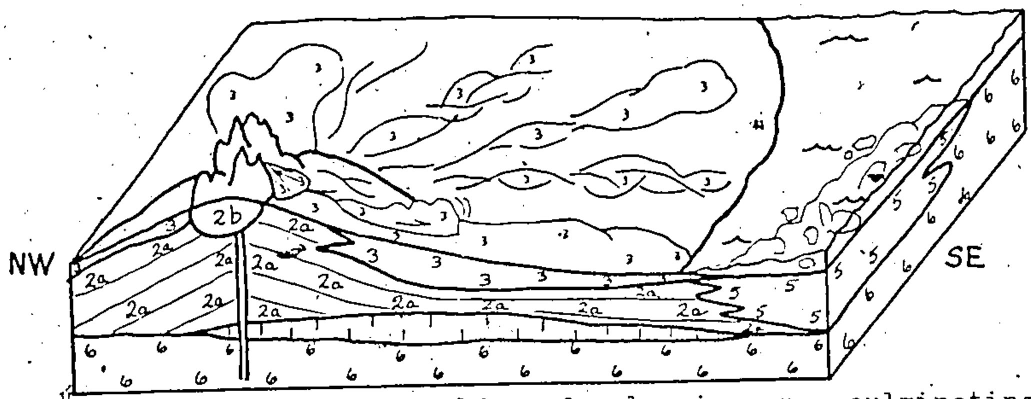


C stage: continued buildup of volcanic cone, culminating in development of a dome complex (unit 2b). Masswasting of dome complex and cone resulted in continued deposition of volcaniclastic rocks of unit 3. Shallow water extrusion of mafic lava to the east resulted in deposition of thick mafic volcaniclastic rocks (unit 5).

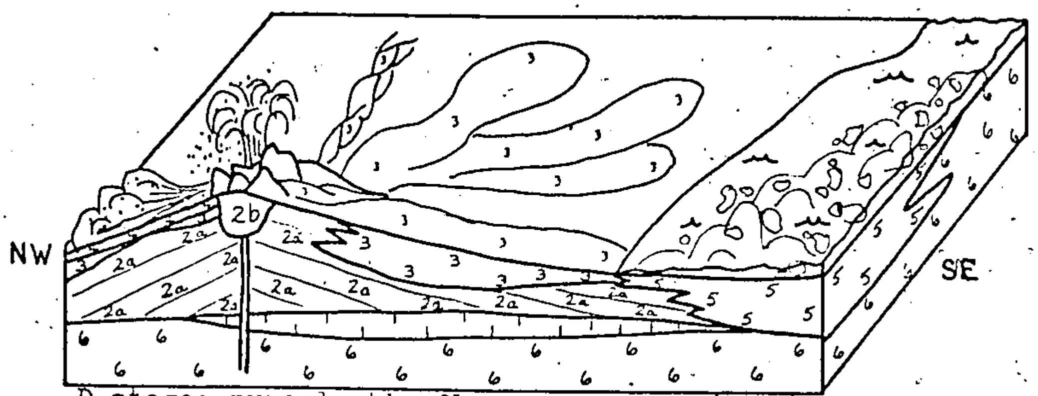


D stage: pyroclastic flow deposition (unit 4) followed by pyroclastic fall activity (unit 4). Subaqueous extrusion of mafic lava (unit 5) continued to the east.

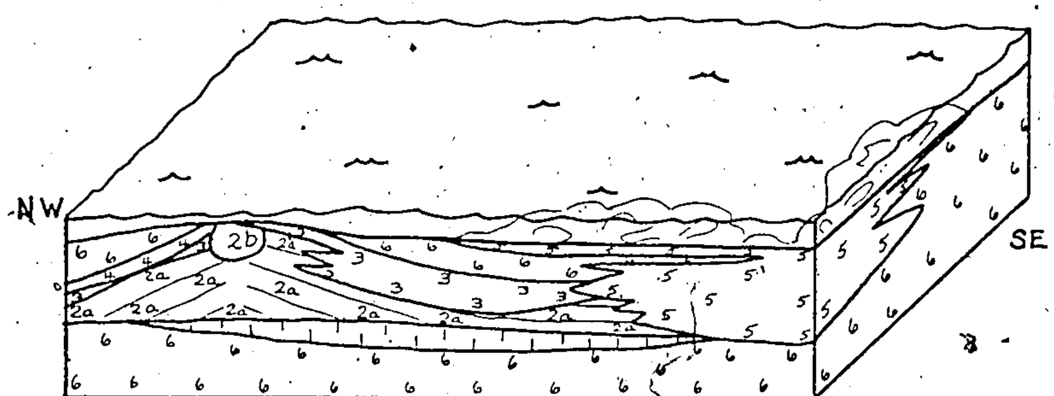


E stage: cessation of felsic volcanism. Felsic volcanic pile subsided and was covered by turbidite sediments (unit 6). Minor, deeper water, mafic extrusion (unit 5) continued to the east.

| | |
|---|---|
| 6 | turbidite sediments. |
| 5 | basaltic to andesitic massive and pillowed flows, pillow breccia and volcaniclastic rocks. |
| 4 | dacitic to rhyolitic tuffs. |
| 3 | andesitic to dacitic volcaniclastic rocks. (conglomerates, diamictites, arenites, lutites). |
| 2 | 2b: dacitic breccia and minor lava.<br>2a: dacitic and minor andesitic lavas and tuffs. |
| 1 | basaltic to andesitic pillowed and massive flows and pillow breccia. |

FIGURE 2-18:

Paleogeographic model for the Clan Lake volcanic-sedimentary succession.

### 2.2.1 gabbroic bodies

Gabbroic intrusive bodies are present in several localities within both the turbidite sedimentary and volcanic rocks (units 1 to 6). They form <1 to 75 m wide dykes; some are irregular-shaped plutons up to 500 m across. The gabbro, which has been metamorphosed, consists mainly of amphibole, biotite and plagioclase, and minor opaques and quartz. The bodies are crosscut by an undeformed S3 biotite foliation (see 3.2.4) and a few dykes are folded by F3 folds (see 3.2.4), indicating they were emplaced before D3 deformation.

The dykes trend northerly, generally not extending for more than a few kilometers (Map sheets A,B & C). In the thicker dykes, amphibole and plagioclase crystals increase in size from their margins to their centers. They also display rhythmic layering due to changes in plagioclase-mafic mineral ratio (Figure 2-19a). A few dykes have quartz amygdules and one, possibly a sill, has lenticular cavities at one of its margins with sedimentary rocks of unit 6 (Figure 2-19b). This is the upper margin, in accordance with top directions in the surrounding sediments.

### 2.2.2 granitic bodies and dykes (unit 8)

A granitic body is present in the western part of the map area, which borders on a region of granitic batholiths;

FIGURE 2-19: GABBROIC DYKES OF UNIT 7.

A) gabbroic dyke displaying rhythmic layering due to change in plagioclase-to-mafic mineral ratio. Grading is seen by an increase in plagioclase content and decrease in mafic mineral content (from dark to light) towards dyke margin. B) gabbroic dyke containing lenticular cavities at its margin with sedimentary rocks of unit 6. Stratigraphic top is upward. Pen is 15 cm long.

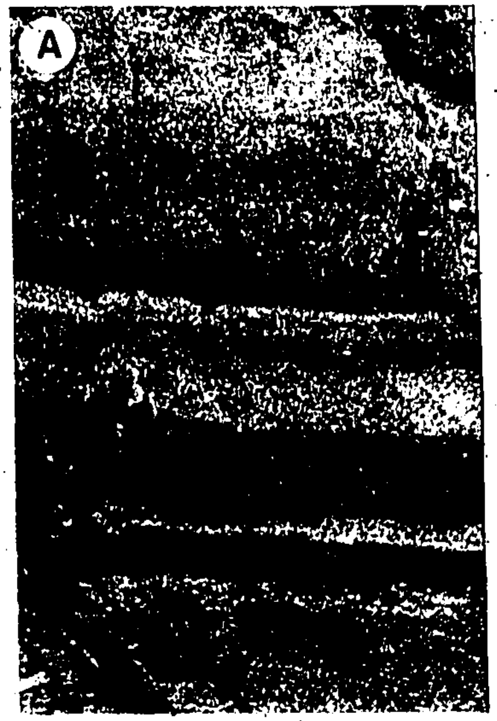
A


B

a few small granitic dykes are located just south of the eastern part of the volcanic pile. The granite is pink to white and commonly has sedimentary and volcanic xenoliths near its margin. The pluton has an intrusive contact with the sedimentary and volcanic rocks as shown by offshoots, dykes and veins that crosscut the supracrustal rocks. The contact is parallel to an S3 foliation present in the sedimentary rocks as well as in the granite.

Five samples of the granite contain mainly K-feldspar (~ 65% and mainly as microcline), some plagioclase (15%) and quartz (15%), and minor muscovite (3%) and biotite (2%).

The granite was emplaced during D3, indicated by its relationship to an S3-L3 fabric (described in chapter 3, section 4).

2.2.3 <u>diabase dykes</u> (<u>unit 9</u>)

Diabase dykes are abundant in the area. They weather rusty-brown but are generally resistant compared to the surrounding rock types, though in a few localities the dykes are recessive. They trend north- to northeastward; are generally discontinuous; and range from less than a meter to 50 meters in width. They are the youngest intrusive rocks of the area, being undeformed and unmetamorphosed and of Proterozoic age (McGlynn & Henderson, 1972). The dykes are, in a few localities, displaced by Proterozoic faults (Figure 2-1).

# Chapter III
# STRUCTURE

## 3.1 INTRODUCTION

Several deformational events, resulting in a succession of structures, affected the sedimentary and volcanic rocks of the Clan Lake area (Figure 3-1).

The earliest structures recognised are a macroscopic antiformal F0 structure and macroscopic F1 folds that are assigned to D0 and D1 deformations respectively and appear to have preceeded metamorphism. The next three deformations, D2 to D4, accompanied regional metamorphism. D2 deformation produced an S2-L2 fabric generally without accompanying folds; D3 deformation an S3-L3 fabric and F3 mesoscopic folds; and D4 deformation, during the peak of metamorphism, an S4 cleavage and F4 mesoscopic folds. Lastly, the rocks were faulted and fractured.

Each set of structures is described; pertinent features are discussed; and the deformational history of the map area summarised in the following sections. The terminology used for cleavages is after Powell, 1979 and Gray, 1977b (Figure 3-2) and fold types after Ramsay, 1967 (Figure 3-3).

| Deformational event | Structural succession | Morphology and distribution of structures | Orientation of structures |
|---|---|---|---|
| Proterozoic D5 | major faults | Prominant lineaments and highly fractured rocks. | N-NE strike for left laterals, E-ENE strike for right laterals. |
| | minor faults | Apparent left- and right-lateral faults. | N-NE-ENE strike for left laterals, E-SE strike for right laterals. |
| Archean D4 | F4 | Mesoscopic folds mainly in sedimentary rocks. Open to closed. Class IA to IC-type. | NE trends, steep plunges. |
| | L4 | Intersection lineation | |
| | S4 | Disjunctive to crenulation cleavage in low grade sedimentary rocks to mineral foliation and minor crenulation cleavage in higher grade rocks | N-NE strike, subvertical. |
| D3 | F3 | Mesoscopic folds in sedimentary and volcanic rocks. Open to isoclinal. Class IA to IC-type. | N trends, steep plunges. |
| | S3 | Disjunctive and continuous cleavage in low grade sedimentary and volcanic rocks to continuous mineral foliation in higher grade rocks. To a minor extent, defined by flattened primary features. | Generally N strike, varying from NW to NNE. steep dips to E, flattening near western granite. |
| | L3 | Defined by mineral alignment, quartz fibres and, to a minor extent, stretched primary features within S3 foliation plane. | Steep NE plunges. |
| D2 | S2 | Widely-spaced, disjunctive cleavage and flattened primary features mainly in volcanic rocks. Inclusion trails in biotite porphyroblasts in sedimentary rocks. | Generally NW-W strike, steep dips to N-NE, but NE strike in eastern mafic volcanic rocks. |
| | L2 | Stretched primary features. | Steep E-NE plunges. |
| D1 | F1B | Macroscopic folds in sedimentary and volcanic rocks. Isoclinal. | NE-NNE trends. |
| | F1A | Macroscopic folds in sedimentary and volcanic rocks. Isoclinal. | W-NW trends. |
| D0 | F0 | Defined by change in facing direction of F1 macroscopic folds | |

FIGURE 3-1:

Summary of structural succession in supracrustal rocks, C[illegible]an Lake area.

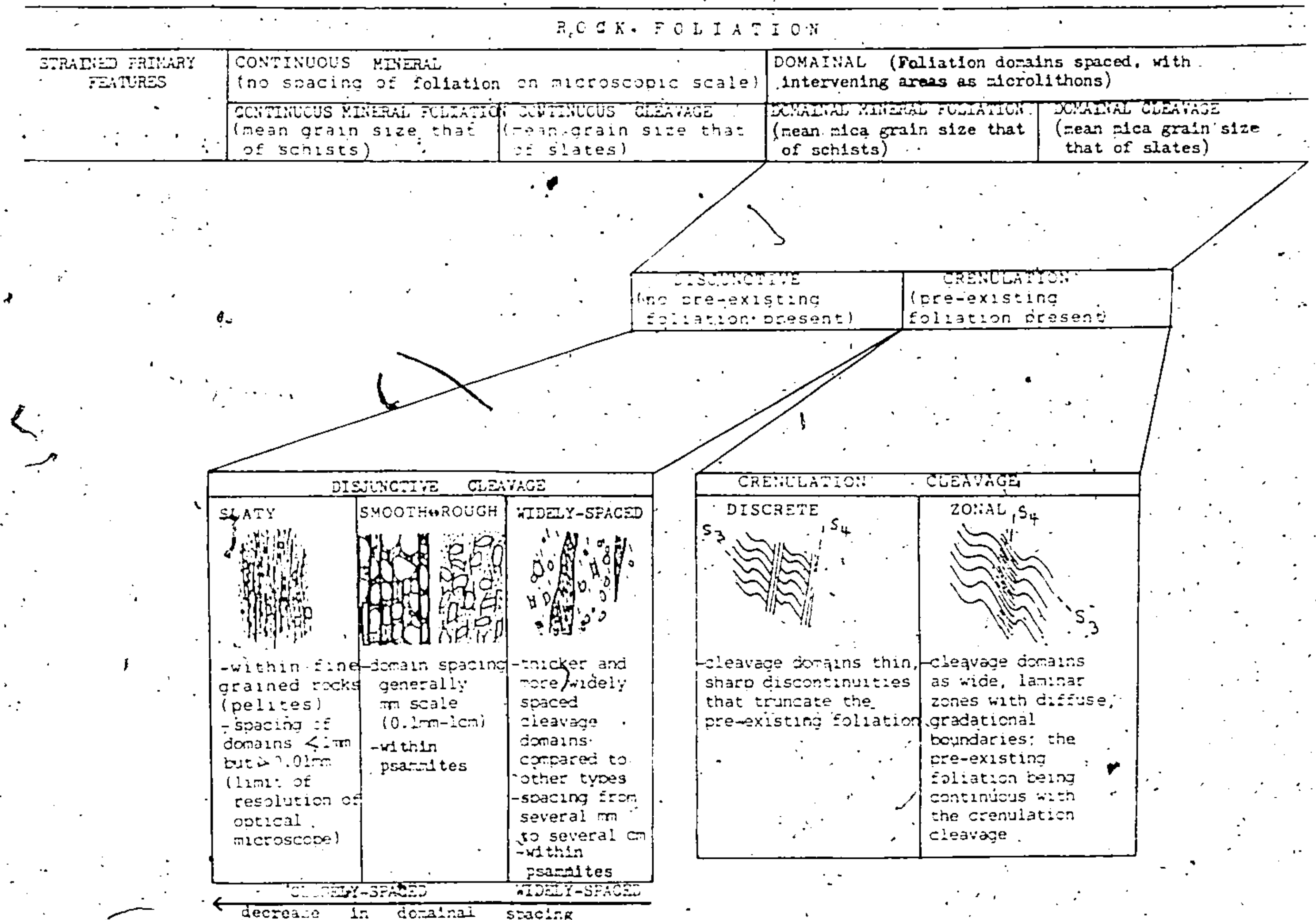


FIGURE 3-2:

Microscopic, morphological classification of rock foliation in Clan Lake area modified after schemes of Powell (1979) and Gray, 1977b).

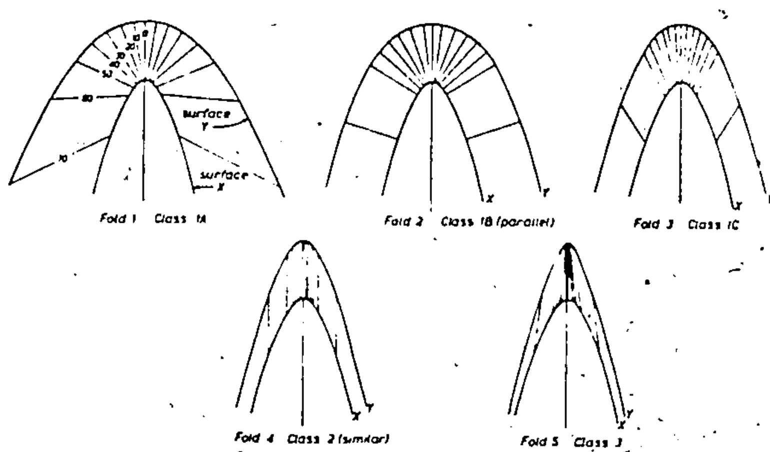


*Fundamental types of fold classes. Dip isogons have been drawn at 10° intervals from the lower to the upper surfaces X and Y.*

FIGURE 3-3:

Types of fold classes after Ramsay (1967).

Note that a mesoscopic, slaty cleavage in the Clan Lake area microscopically is a combination of a closely-spaced, domainal cleavage (referred to as a slaty cleavage in Figure 3-2) and a continuous cleavage.

## 3.2 STRUCTURES

### 3.2.1 D0 structure: F0 macroscopic fold

An F0 anticlinal or domal structure is outlined by changes in facing directions of F1 folds . As shown in Figure 3-4, F1 folds in sedimentary rocks face outward from the volcanic pile, northeastward, southwestward and westward. Some of these folds follow into outward facing structures within the volcanic rocks; the main body of which can be interpreted as forming a broad D0 domal structure before F1 folding.

### 3.2.2 D1 structures: F1 macroscopic folds

F1 macroscopic anticlines and synclines, delineated by major changes in bedding-top directions, form sets of folds with axial traces extending up to 6 km in two main directions (Figure 3-4). One set (F1A) trends northwest to westward within the central part of the volcanic pile and within sedimentary rocks farther west; the other set (F1B) trends northeastward within the southern and eastern parts of the pile and in sedimentary rocks immediately north and southeast of the pile.

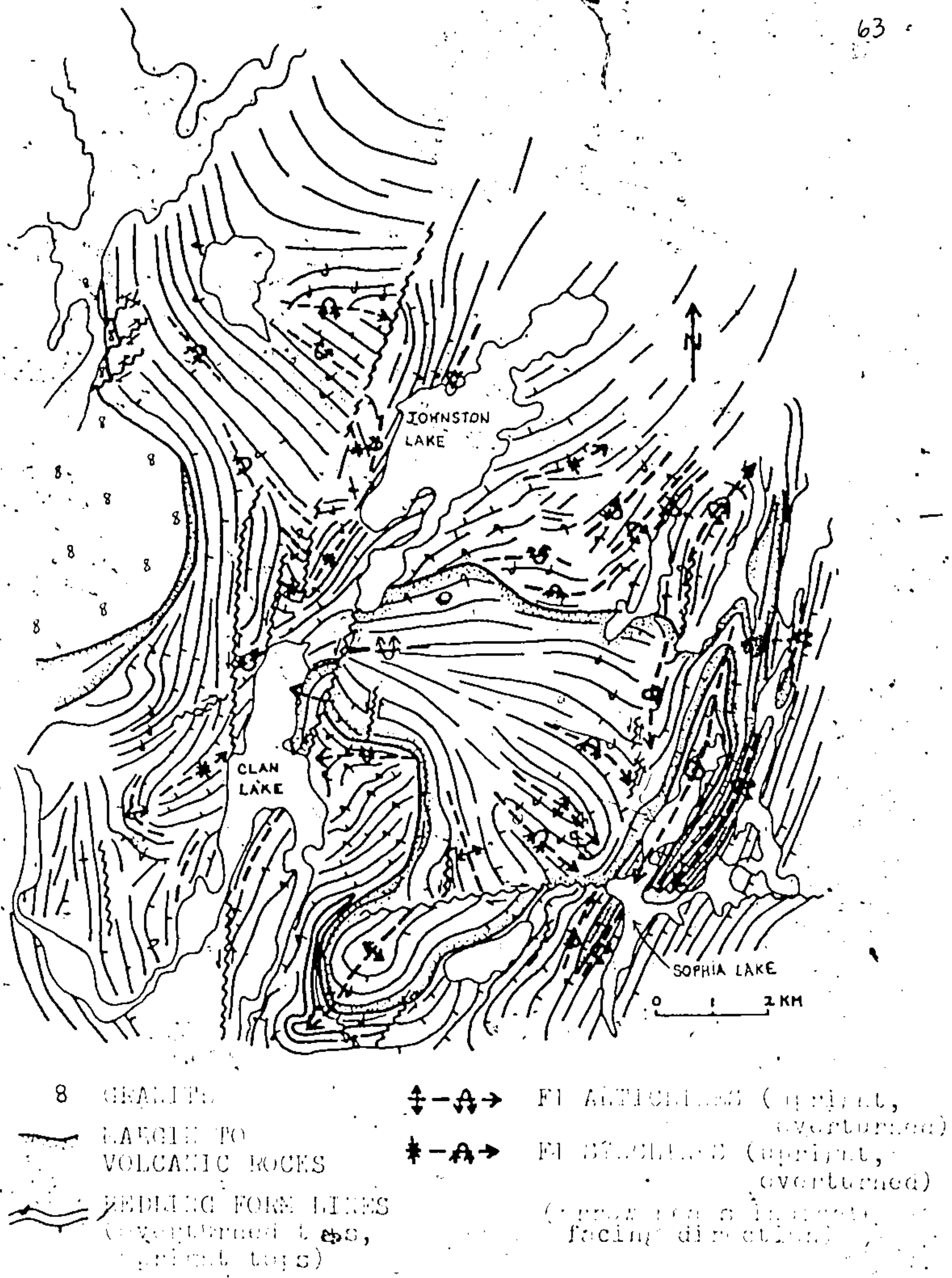


FIGURE 3-4:

Form line map, Clan Lake area. Macroscopic F1 folds are outlined. Form lines of bedding surfaces crosscut lithologic boundaries partly because of facies changes.

F1 folds are generally isoclinal, steeply inclined and dominantly overturned southwest or northwestward, towards the granitic rocks marginal to the supracrustal rocks. A few, for example west of Clan Lake, are upright or overturned away from the granitic rocks. The F1 folds are crosscut obliquely by S2 and S3 foliations, indicating they are older than D2 and D3 deformational events. Not as yet recognised is an S1 foliation associated with the F1 folds.

### 3.2.3 D2 structures: S2-L2 fabric

The earliest fabric recognised is a foliation, designated as S2, which is preserved mainly within the volcanic rocks. S2 is steeply dipping, mainly variably eastward (Figure 3-5) with an east plunging L2 lineation (Figure 3-6) but no associated mesoscopic folds. The foliation, though variable, generally strikes northwest to west except in the eastern mafic volcanic rocks where it strikes north to northeast. The S2-L2 fabric is younger than F1 folds because it strikes obliquely across these folds, for example at the axial trace of a northeast trending F1 fold in the southwest corner of the volcanic pile (Map sheet B).

S2 includes widely-spaced, disjunctive cleavage and rarely a continuous cleavage within felsic volcanic rocks and turbidite sandstones (Figure 3-7a,b). It also includes a foliation and/or L2 lineation of deformed and rotated

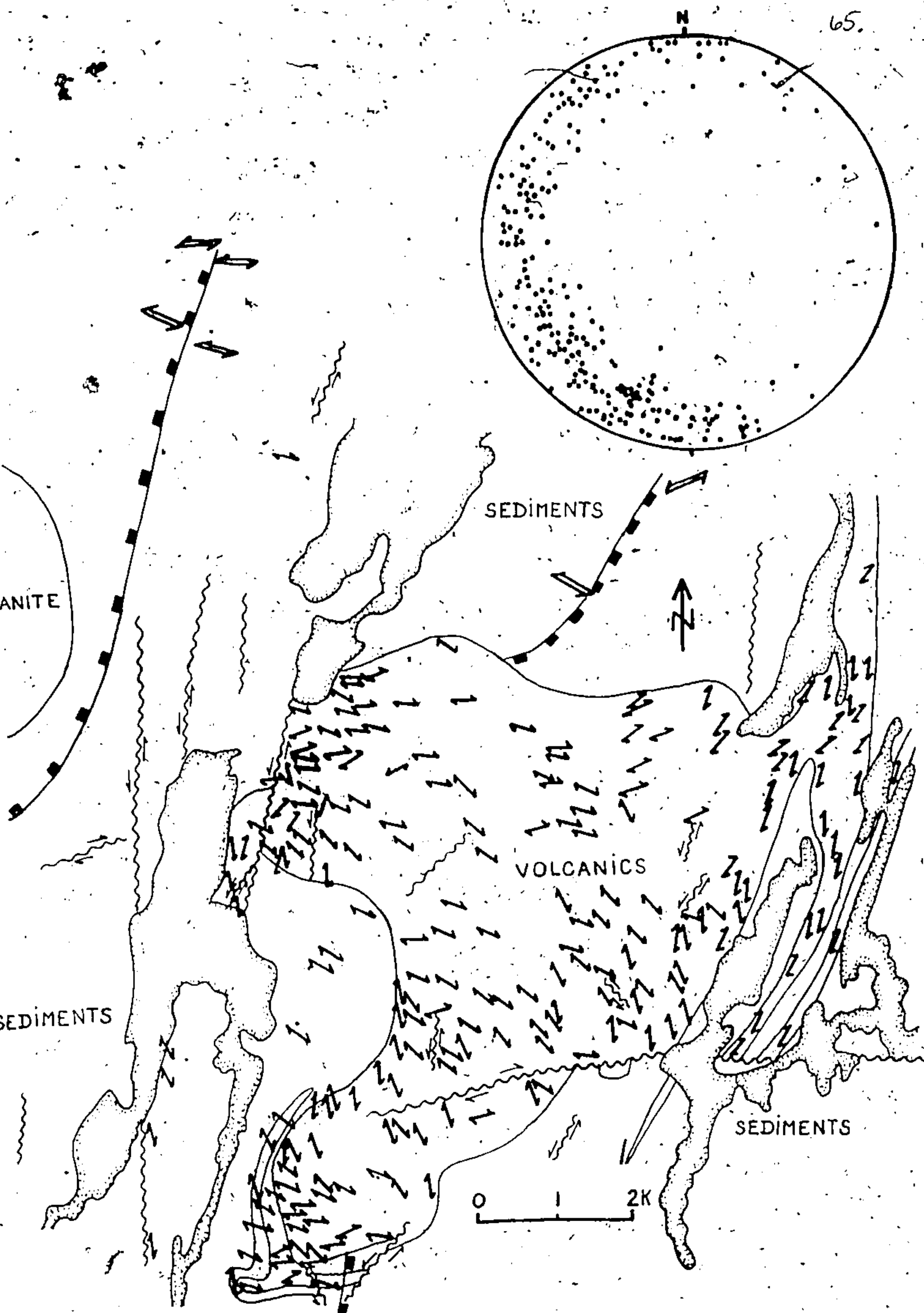


FIGURE 3-5:

S2 foliation. Map shows generalised S2 foliation trends; stereonet is a lower hemisphere projection of poles to S2 foliation. Note S2 biotite inclusion trail trends (⟵⟶) near cordierite isograds (-■-■-).

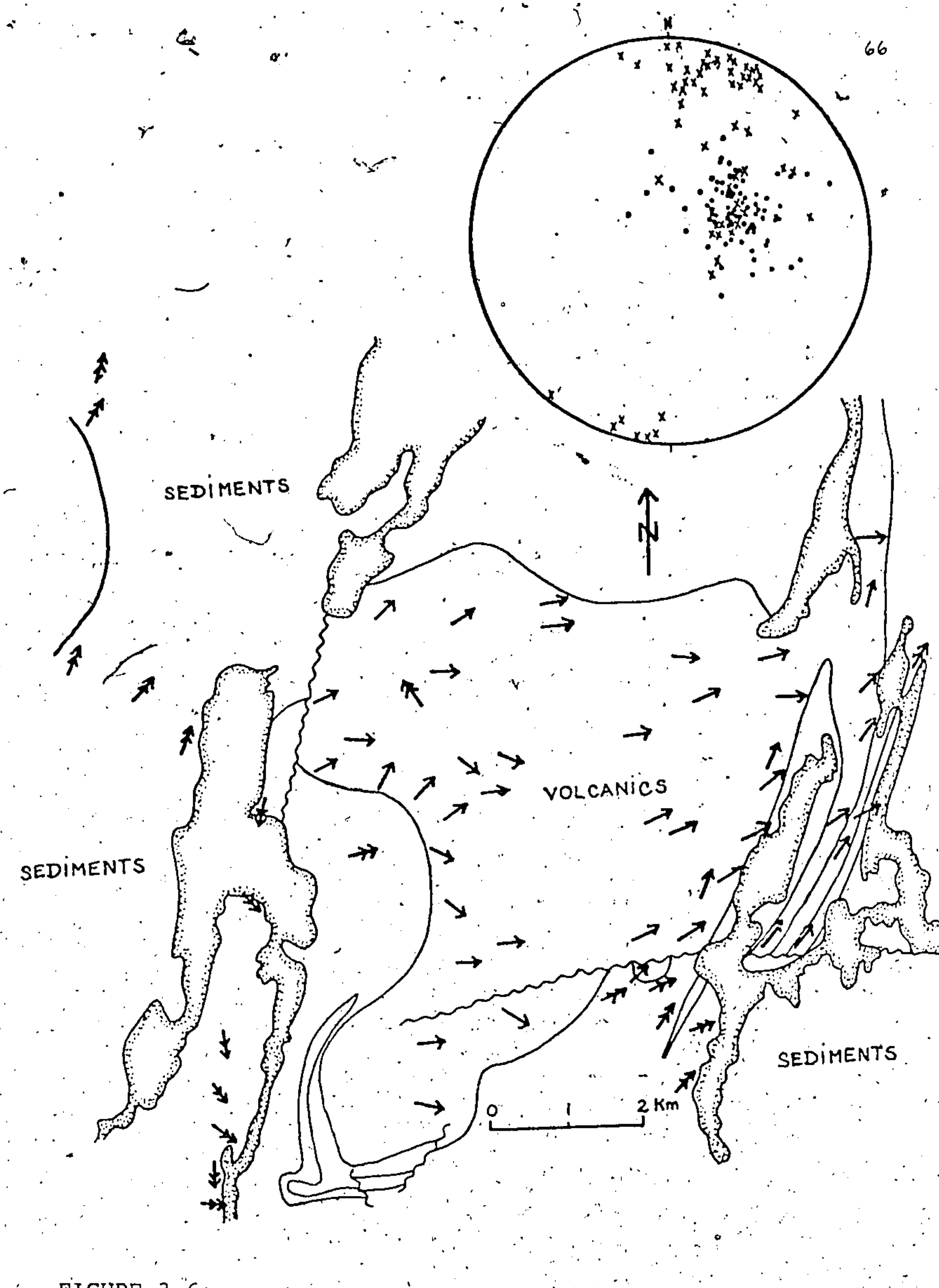


FIGURE 3-6:

L2 and L3 lineations. Map shows generalised L2 (⟶) and L3 (↠) lineation trends. Stereonet is a lower hemisphere projection of L2 (•) and L3 (×) orientations.

FIGURE 3-7: S2 FOLIATION.

A) S2 widely-spaced disjunctive cleavage (defined by white mica concentration) crosscut by an S3 rough cleavage (irregular, anastomising fractures), in felsic volcanic rock of unit 2. B) S2 widely-spaced disjunctive cleavage in sandstone (unit 6) defined by zones of concentrated and aligned white micas and opaques. S2 abruptly terminates at a contact with mudstone which contains an S3 slaty cleavage. C) highly strained mafic pillows (unit 5) defining S2 (parallel to pen). Tops are toward the bottom of the picture. D) photomicrograph of S2 widely-spaced disjunctive cleavage in sandstone (unit 6) defined by concentration of white micas. S2 is crosscut by an S3 foliation. Field of view is 2 mm. E) S2 continuous cleavage crenulated by S3 and S4 cleavages within a pelite (unit 6). Field of view is 2 mm. F) S2 quartz inclusion trails within biotite porphyroblasts (biotite A) in a pelite (unit 6). S2 is at an oblique angle to the exterior, S3 muscovite foliation. Field of view is 1 mm. G) S2 continuous to disjunctive cleavage defined by aligned muscovite and quartz, crenulated by a rare S3 crenulation cleavage in a felsic tuff (unit 4). Field of view is 2 mm.

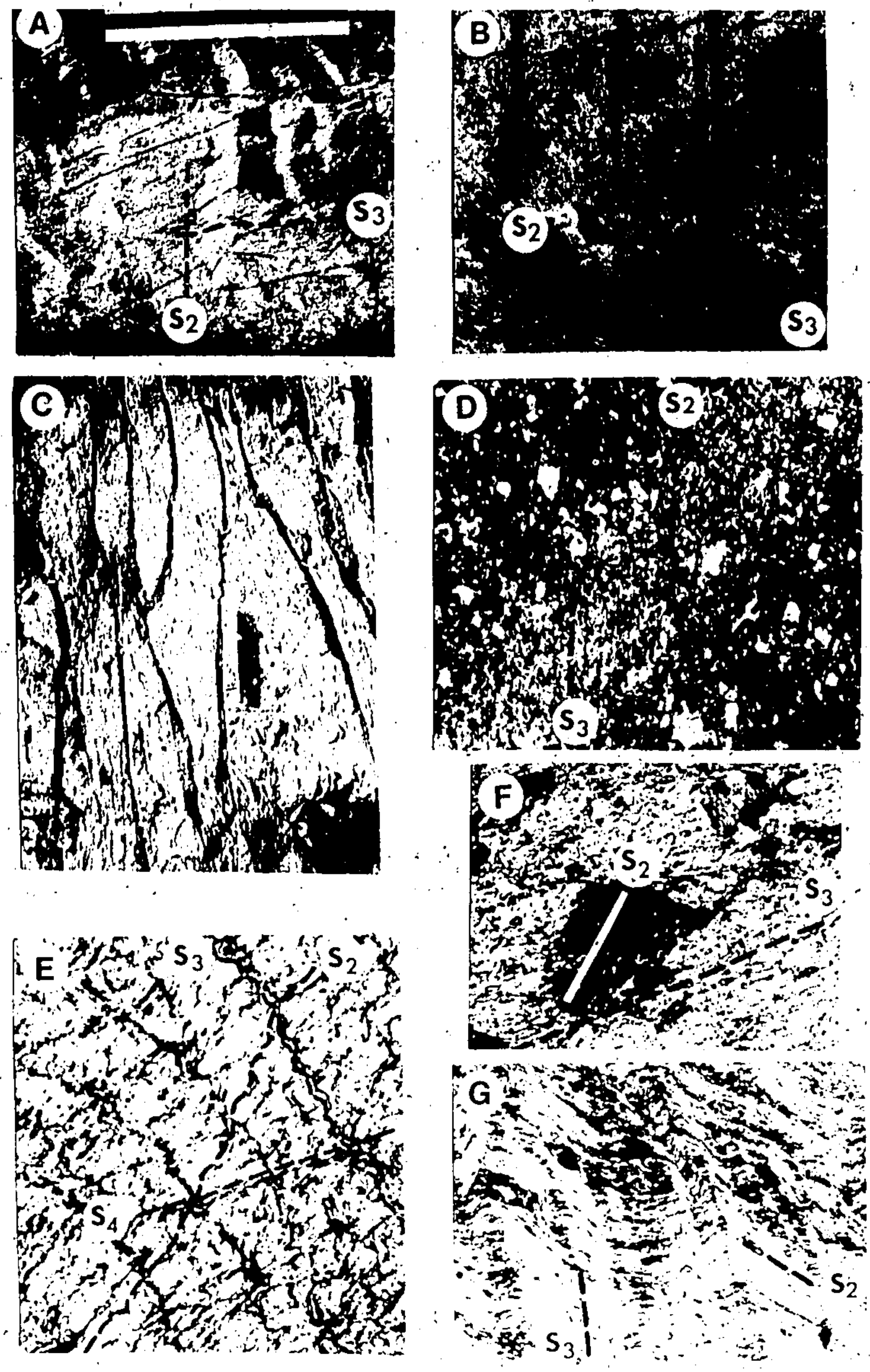
A
$S_3$
$S_2$
B
$S_2$
$S_3$
C
D
$S_2$
$S_3$
E
$S_3$
$S_2$
$S_4$
F
$S_2$
$S_3$
G
$S_2$
$S_3$

primary features such as clasts, amygdules, phenocrysts and pillows within volcanic rocks (Figure 3-7c), and mudchips, concretions and load structures within sedimentary rocks. The S2-L2 fabric of deformed primary structures varies considerably in character from where the structures are highly flattened, stretched and/or rotated to where they are weakly deformed. S2 is distinguished from a rare S3 foliation of strained primary structures by the presence of crosscutting S3 cleavage.

Widely-spaced disjunctive S2 cleavage in felsic volcanics and sandstones is defined by relatively straight (discounting later folding), discontinuous mica-rich zones 1 mm to 1 cm in width and 0.5 to 10 cm apart. Petrographically, the S2 widely-spaced disjunctive cleavage is defined by concentrations of white micas and less commonly, opaques (Figure 3-7d). The white micas are concentrated, though not necessarily aligned, within discontinuous zones that taper at the ends. The opaques form discontinuous, anastomising black seams within the mica-rich zones.

S2 continuous cleavage is rarely preserved in chlorite grade volcanic and sedimentary rocks as a chlorite and/or white mica foliation that, in places, is crenulated by later structures (Figure 3-7e,f). S2 is also rarely preserved as quartz inclusion trails within biotite porphyroblasts oblique or parallel to external S3 mica foliation within sediments near the cordierite isograd (Figure 3-7g).

### 3.2.4 D3 structures: F3 folds and associated S3-L3 fabric

#### 3.2.4.1 F3 folds

F3 mesoscopic folds, which are predominantly in sedimentary rocks and rarely in thin bedded volcaniclastic rocks, are open to isoclinal with steep to vertical plunges (Figure 3-9a). Some isoclinal F3 folds, with obscure hinges, are only recognised by a local change in bedding-top directions. The F3 folds are up to a few meters in amplitude with an associated S3 foliation that distinguishes them from macroscopic F1 folds. F3 folds vary from class IA- to class IC-type (Figure 3-3). Figure 3-9b shows a sandstone bed affected by F3 folds with variable profiles.

#### 3.2.4.2 S3-L3 fabric

An S3-L3 fabric is prevalent within both the sedimentary and volcanic rocks. It is usually distinguished from S2 by morphology and timing relationships such as S2, a widely-space disjunctive cleavage, crosscut by closely-spaced S3. Also S3 commonly is axial planar to mesoscopic folds whereas folds are not known to be associated with S2. S3 varies in trend, commonly lying subparallel to bedding in pelitic rocks and refracting into sandstones at an appreciable angle to bedding. Though variable, S3 predominantly strikes northward and is subvertical or dips steeply eastward (see net projection Figure 3-8. L3 plunges moderately to steeply, mainly

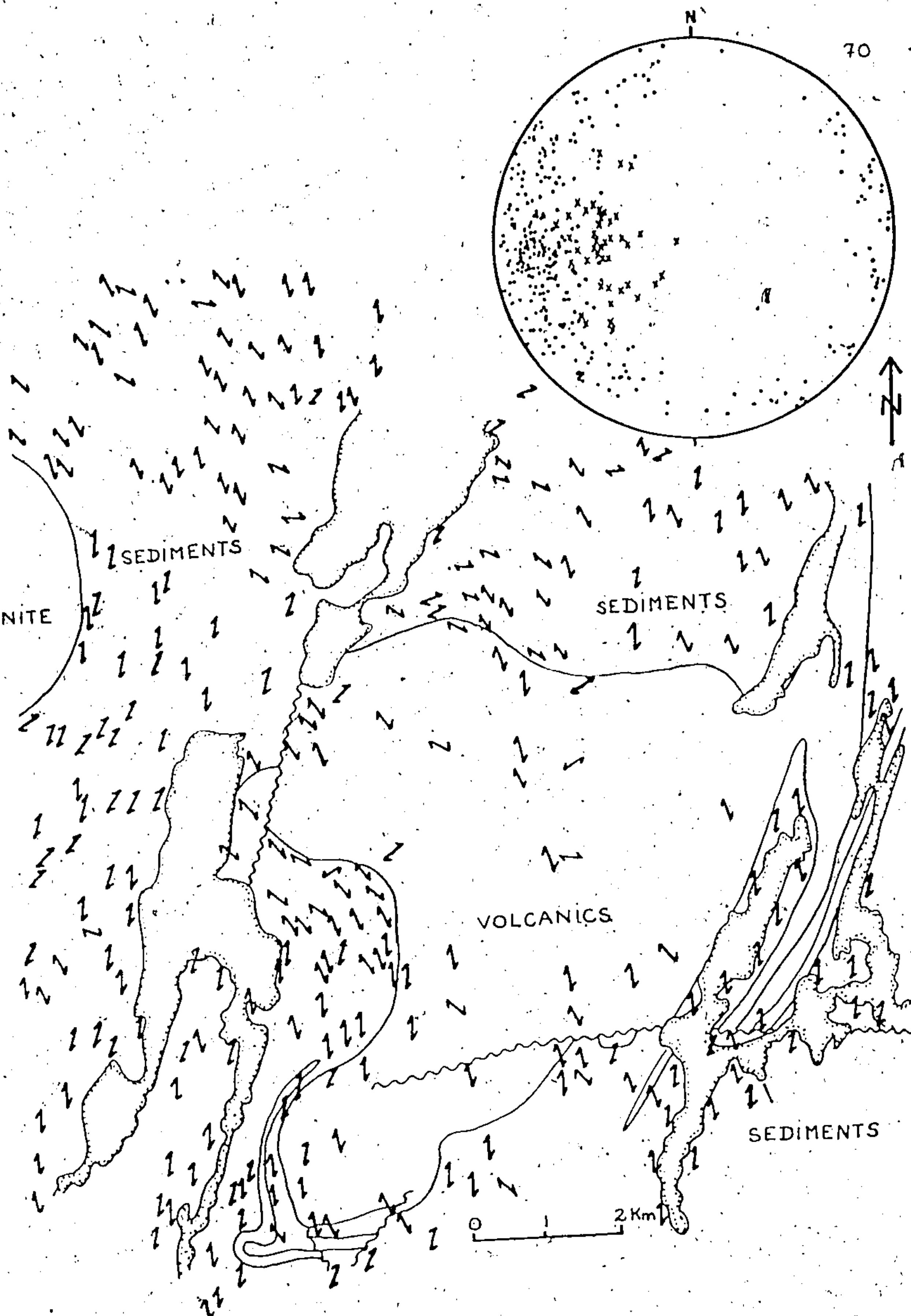


FIGURE 3-8:

S3 foliation. Map shows generalised S3 foliation trends; stereonet is a lower hemisphere projection of poles to S3 foliation orientations ( • ). The x's on the stereonet are poles to flattened S3 orientations near the western granite.

FIGURE 3-9: F3 MESOSCOPIC FOLDS AND S3 FOLIATION.

A) F3 folds in sedimentary rocks (unit 6). The fold is a closed, Class IB type fold with a steep plunge. B) F3 mesoscopic folds varying in profile shape along a sandstone bed (unit 6). C) S3 cleavage with strained ball and pillow structures in sandy layers and S4 crenulation cleavage in pelitic layers (unit 6). D) S3 slaty cleavage crenulated by S4 crenulation cleavage (parallel to pen) (unit 6). E) photomicrograph of S3 smooth disjunctive cleavage with long, straight folia in sandstone (unit 6). Folia are defined by concentrations of opaques and aligned white micas. Field of view is 4 mm. F) photomicrograph of S3 rough disjunctive cleavage with short, irregular folia of concentrated opaques and white micas in sandstone (unit 6). Field of view is 4 mm. G) photomicrograph of S3 rough cleavage in sandstones (unit 6). S3 folia of opaques and aligned white micas are concentrated at grain margins. Field of view is 2 mm. H) photomicrograph of S3 continuous cleavage in pelit (unit 6). White micas are aligned and quartz grains elongated along S3. Field of view is 1.5 mm. I)photomicrograph of S3 continuous cleavage in pelite (unit 6) defined by aligned white micas and quartz aggregates. S3 is weakly crenulated by an S4 cleavage (white streaks of white mica). Field of view is 2 mm. J) photomicrograph of S3 slaty cleavage disrupting a quartz vein (unit 6). Field of view is 1.5 cm. Offsets and terminations of vein at cleavage folia may represent pressure solution effects.

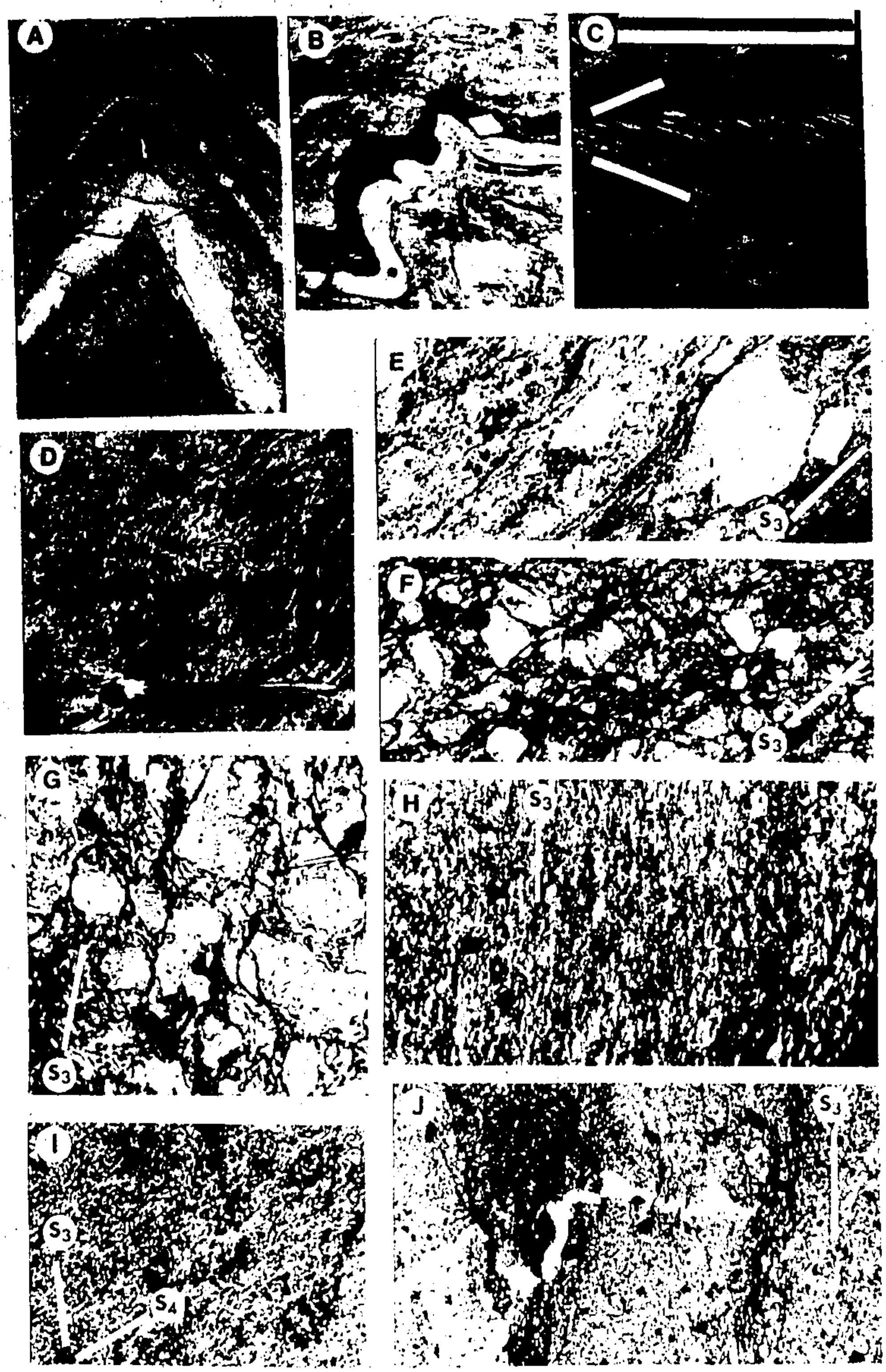
A
B
C
D
E
S3
F
S3
G
S3
H
S3
I
S3
S4
J
S3

northeastward (Figure 3-6). Major deviations of the fabric are shown on the map (Map sheets A, B, C). They include deviations around the western granite plutons (Figure 3-8) where S3 is shallow to moderately easterly dipping and L3 is shallow north-northeasterly plunging (Figure 3-6).

S3 foliation varies in character depending on rock type and metamorphic grade. Within chlorite to biotite grade sedimentary rocks of unit 6, S3 foliation is an irregular, disjunctive cleavage, in places accompanied by deformed and aligned primary features such as sandstone ball and pillow structures (Figure 3-9c). S3 may be crenulated by S4 (Figure 3-9d). Microscopically S3 disjunctive cleavage ranges from a rough to smooth type in sandstone (Figure 3-9e,f) to slaty in mudstone (Figure 3-9j) and is defined by concentrations and alignment of white mica, chlorite, opaques and/or minor biotite. It commonly disrupts quartz veins (Figure 3-9j) and, as a rough cleavage, is usually concentrated at sutured to planar margins of quartz grains, though in places it penetrates the grains. Quartz is present within the microlithons as strained, elongate grains parallel to S3 or unstrained equant grains. Other crystals are mica aligned parallel to S3 or random. In the pelitic rocks, S3 is also a continuous cleavage consisting of aligned white micas, chlorite, opaques, biotite, quartz and/or quartz aggregates (Figure 3-9h), commonly crenulated by S4 (Figure 3-9d,i), and rarely a crenulation cleavage where an S2 continuous cleavage is present (Figure 3-7f). This S3 crenulation cleavage is distinguished from S4 by the presence of a later S4 crenulation cleavage (Figure 3-7f).

In higher grade metasedimentary rocks of unit 6, biotite and cordierite grade rocks, S3 is a coarse continuous mineral foliation. Microscopically, it consists of aligned crystals of muscovite, biotite and minor opaques, and is locally crenulated by S4 (Figure 3-12a). Quartz grains are recrystallised and equant in shape, and do not contribute to the S3 fabric. S3 is also preserved in cordierite porphyroblasts as quartz inclusion trails (Figure 3-10a), some of which are crenulated (Figure 3-10b) and, outside the cordierite, are mainly obliterated by S4 biotite foliation. One sample showed the quartz inclusion trails continuous with an external S3 biotite foliation. In a few samples, chlorite porphyroblasts or clusters are aligned parallel to S3.

S3 varies in character in volcanic rocks. It is a mineral foliation; an irregular, closely-spaced disjunctive cleavage commonly crosscutting S2 cleavage in felsic volcanic rocks (Figure 3-7a); rarely a foliation of flattened primary features such as pillows and clasts; and rarely a crenulation cleavage affecting an S2 cleavage in felsic volcanic rock unit 4 (Figure 3-7e). Microscopically, S3 mineral foliation is continuous, mainly within the felsic volcanic

FIGURE 3-10: PHOTOMICROGRAPHS OF S3 AND S4 FOLIATIONS AND F3 AND F4 MICROSCOPIC FOLDS.

A) cordierite porphyroblast containing S3 inclusion trails and surrounded by an S4 continuous foliation in biotite schist (unit 6). Field of view is 3 mm. B) cordierite porphyroblast containing S3 quartz inclusion trails in biotite schist (unit 6). The S3 trails are crenulated inside the porphyroblast by an S4 cleavage whereas S3 is obliterated outside by S4. Field of view is 3 mm. C) S3 continouous cleavage in a volcaniclastic rock (unit 3). S3 is preserved as quartz inclusion trails in garnet porphyroblasts and passes without deviation into the matrix of quartz, chlorite and biotite. Field of view is 1 cm. D) S3 foliation defined by zonal arrangement of clusters of radiating hornblende in a mafic volcanic rock (unit 5). Field of view is 3 mm. E) rare S3 foliation defined by aligned biotite and amphibole within mafic lava (unit 5). Field of view is 1 cm. F) rare interference of F3 and F4 microscopic folds in quartz pelite (unit 6). Field of view is 3.5 mm.

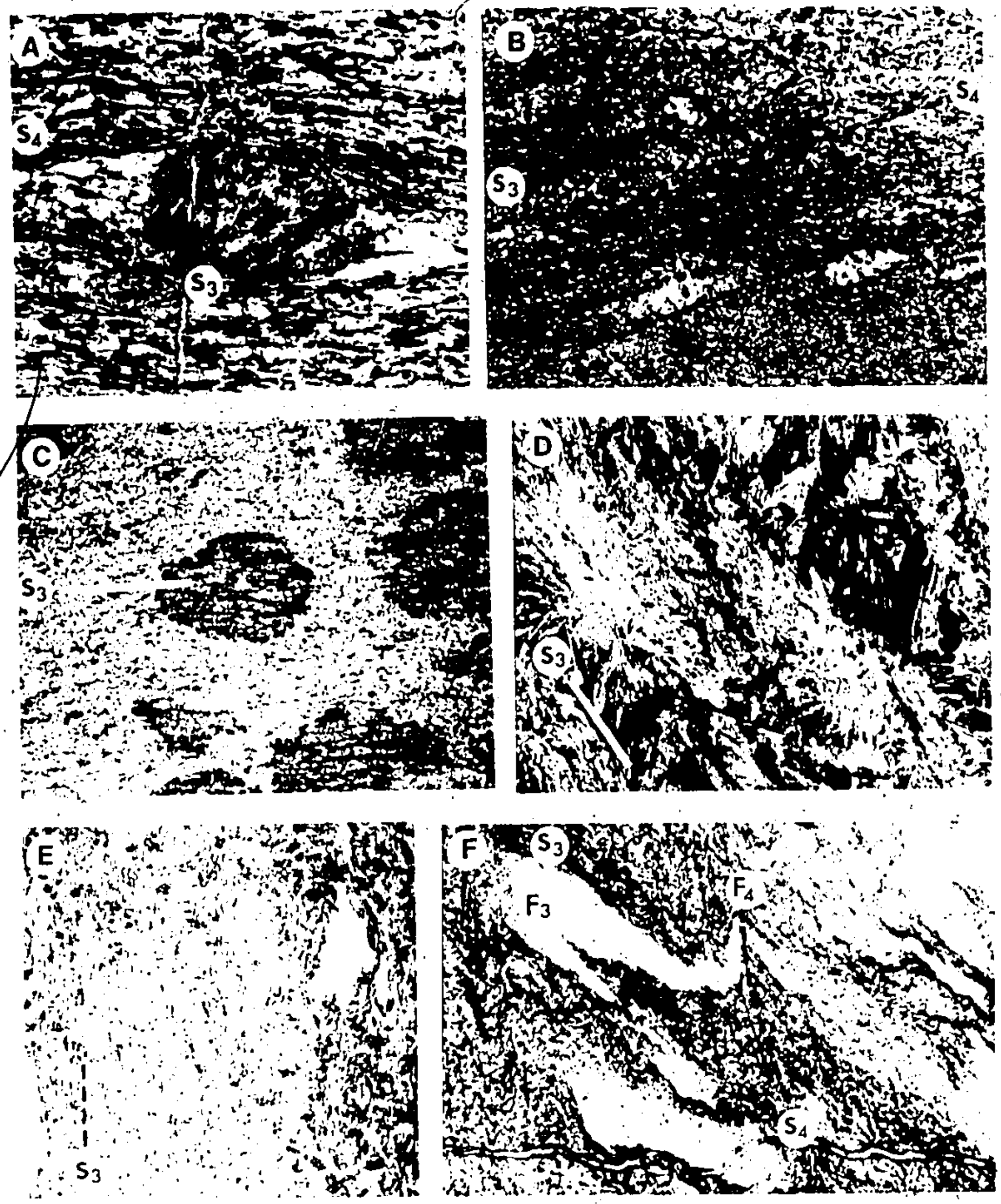
A
S4
S3
B
S4
S3
C
S3
D
S3
E
S3
F
S3
F3
F4
S4

rocks (units 2&3), defined by aligned muscovite, chlorite, opaques and/or biotite. Rarely S3 mineral foliation is as aligned amphibole in the mafic volcanic rocks (Figure 3-10e). It is also preserved in garnet porphyroblasts as quartz inclusion trails (Figure 3-10c) which are continuous with an external S3 biotite and chlorite foliation. A domainal S3 mineral foliation is also present as aligned biotite clusters, in which individual biotite crystals may be randomly oriented or aligned obliquely as S4. In higher grade and more mafic volcanic rocks (unit 5), this domainal mineral foliation is present as aligned amphibole clusters with individual amphiboles random or radiating (Figure 3-10d). S3 closely-spaced disjunctive cleavage within felsic volcanic rocks is defined by irregular black seams of opaques usually accompanied by a muscovite foliation.

S3 foliation defined by aligned primary structures such as ball and pillow and load and flame structures, and is similar in character and general trend to S2. Deformed structures are seen to represent an S3 foliation where parallel to an S3 disjunctive cleavage crossing an S2 cleavage.

An L3 lineation, which is within both the sedimentary and volcanic rocks and closely associated with S3 (together representing an S-L fabric), includes a mineral and mineral cluster lineation and quartz fibres along S3 foliation planes.

Within the granitic rocks in the western part of the map area, a coarse continuous cleavage of biotite and muscovite, accompanied by local rodding of quartz and feldspar, is considered to be an S3-L3 fabric because of similar orientations to S3-L3 in the surrounding sedimentary rocks.

### 3.2.5 D4 structures: F4 folds and an associated S4 cleavage

#### 3.2.5.1 F4 folds

F4 mesoscopic folds are similar in character to, and therefore indistinguishable from, F3 folds except where there is an associated S4 crenulation cleavage and a folded S3 foliation. F4 folds are open to isoclinal, class IA- to IC- type folds with steep to vertical plunges. They are up to a few meters in amplitude.

Interference of F3 and F4 folds is only observed microscopically by refolded quartz veins (Figure 3-10f).

#### 3.2.5.2 S4 cleavage

The youngest cleavage, S4, is prevalent within the sedimentary rocks and rare to absent in volcanic rocks. It generally is north- to northeast-trending, steep cleavage mainly dipping eastward (Fig. 3-11). Unlike S3, S2 is relatively unaffected in orientation near granitic rocks to the west.

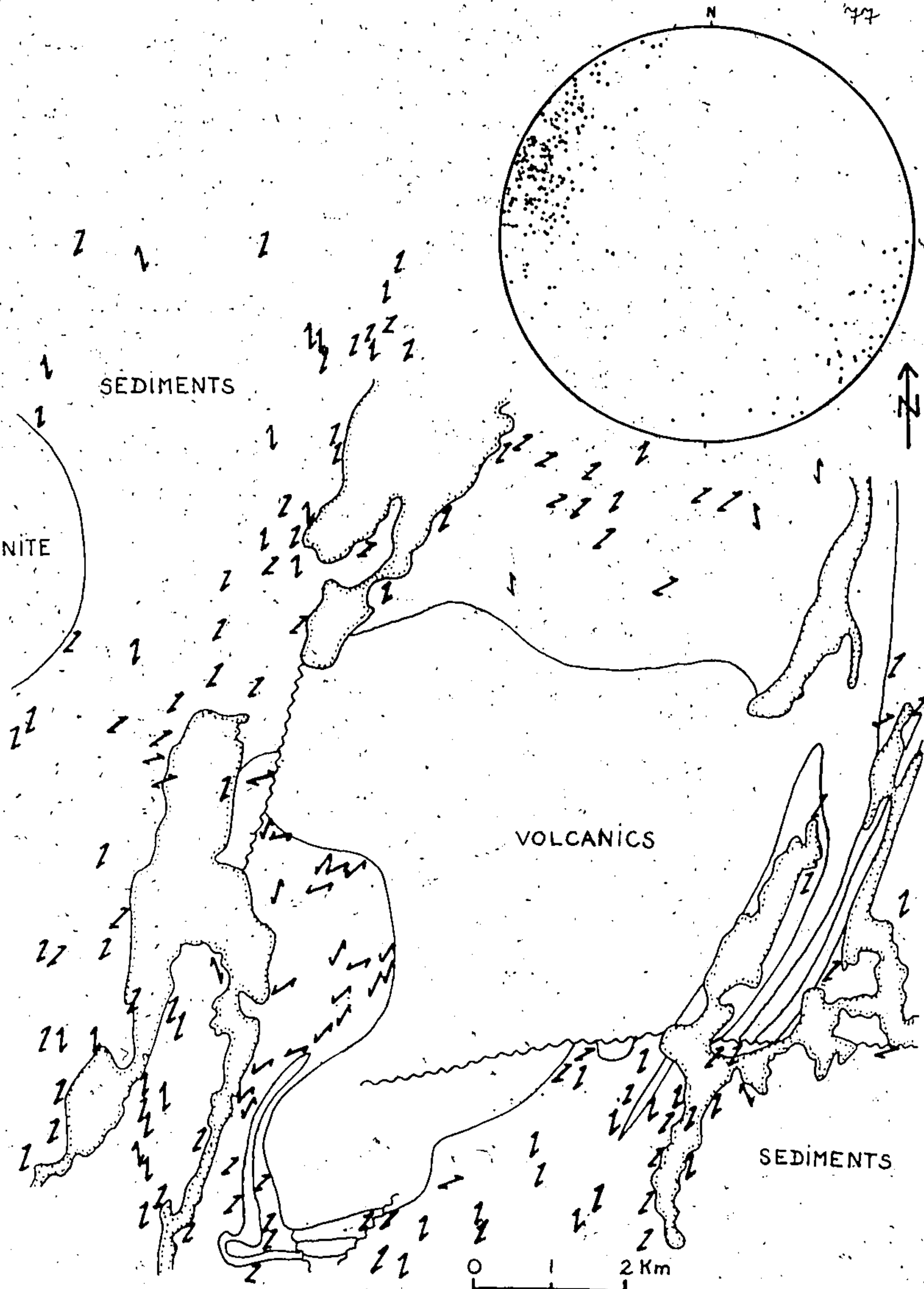


FIGURE 3-11:

S4 foliation. Map shows generalised S4 foliation trends; stereonet is lower hemisphere projection of poles to S4 foliation.

S4, like S3, varies in character, depending on rock type, metamorphic grade and other fabrics present. It is not as widespread as S3. In places only a lineation L4, formed by the axes of crenulations of S3, is obvious.

In chlorite grade sedimentary rocks, S4 is usually a slaty cleavage or a discrete crenulation cleavage in mudstones (Figures 3-9c&d) and a rough, disjunctive to incipient, discrete crenulation cleavage (Figures 3-12d) in sandstones. S4 discrete crenulation cleavage includes muscovite-rich zones with muscovite aligned parallel to S4, accompanied by black seams where opaques are concentrated (Figure 3-12b). The cleavage domains are less than 0.01 to 0.20 mm wide and spaced 0.05 to 0.10 mm apart. In one sample, a well-developed, discrete crenulation cleavage grades into a zonal crenulation cleavage (Figure 3-12c). S4 rough and incipient, discrete crenulation cleavages are concentrated at quartz grain boundaries as discontinuous dark seams of segregated white micas and opaques.

S4 foliation in biotite grade, pelitic rocks is a discrete to zonal crenulation cleavage, whereas in associated sandstones it is a continuous mineral foliation and, to a minor extent, a disjunctive cleavage. As a crenulation cleavage S4 has 0.1 to 0.2 mm spaced and 0.01 to 0.2 mm wide folia. The discrete crenulation cleavage is similar to that in chlorite grade rocks, with muscovite and opaque folia.

FIGURE 3-12: PHOTOMICROGRAPHS OF S3 AND S4 FOLIATIONS.

A) an S3 continuous foliation crenulated by an S4 zonal crenulation cleavage in pelite (unit 6). Field of view is 3 mm. B)S4 discrete crenulation cleavage in pelite (unit 6). Dark zones are quartz-rich (quartz is at extinction) and light zones are muscovite-rich. Field of view is 3.5 mm. C) S4 crenulation cleavage in pelite (unit 6) as both discrete (D) and zonal (Z) types in one sample. Field of view is 1.5 mm. D) interference of S3 and S4 cleavages in sandstone (unit 6). S3 is a rough cleavage with short discontinuous folia of opaques and white micas and S4 a discrete crenulation cleavage. Field of view is 3.5 mm. E) S4 zonal crenulation cleavage affecting S3 continuous cleavage in pelite (unit 6). The light zones (q) are quartz-rich and dark zones (m) muscovite-rich. Field of view is 3.5 mm. F) S3 slaty and S4 crenulation cleavages disrupting a quartz vein in pelite (unit 6). Field of view is 3.5 mm. G) S4 domainal biotite foliation crosscutting an S3 continuous biotite foliation in biotite schist (unit 6). Field of view is 1.5 cm. H) S3 and S4 biotite foliations in biotite schist (unit 6). S4 has thicker and stubbier biotites (biotite C) than S3 (biotite B). Field of view is 1.5 mm. I) S3 and S4 continuous mineral foliations in schist (unit 6). S3 is defined by aligned chlorite and muscovite whereas S4 is aligned biotite. Field of view is 3 mm. J) S3 and S4 continuous mineral foliations in biotite schist (unit 6). S3 is preserved as aligned biotite at the hinges of the folds and S4 as aligned biotite axial planar to the folds. Field of view is 3.5 mm.

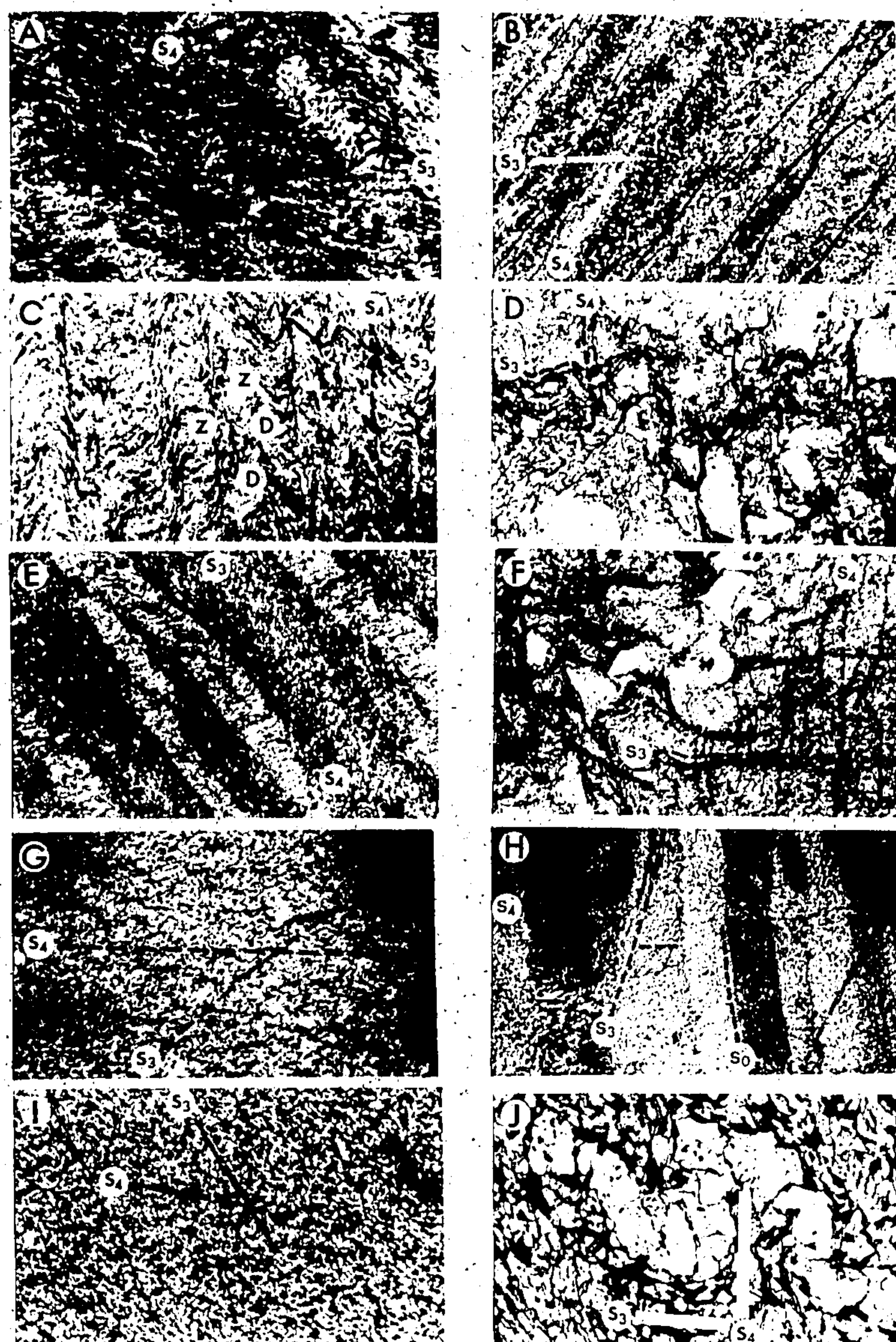
A
$S_4$
$S_3$
B
$S_3$
$S_4$
C
$S_4$
$S_3$
Z
Z
D
D
D
$S_4$
$S_3$
E
$S_3$
$S_4$
F
$S_4$
$S_3$
G
$S_4$
$S_3$
H
$S_4$
$S_3$
$S_0$
I
$S_3$
$S_4$
J
$S_3$
$S_4$

The zonal crenulation cleavage is defined by muscovite-rich zones, with the muscovite reoriented from S3, and quartz-rich zones (microlithons) with a minor S3 muscovite foliation (Figure 3-12a,e). As a continuous mineral foliation, S4 is defined by aligned biotite and muscovite.

Quartz veins in both chlorite and biotite grade rocks are disrupted or displaced where S4 is concentrated (Figure 3-12f). Quartz is occasionally concentrated and aligned parallel to S4 in pressure shadows.

S4 within cordierite grade rocks is a mineral foliation, less commonly a zonal crenulation cleavage and rarely a disjunctive cleavage. A continuous mineral foliation is defined by either aligned biotite, muscovite and/or chlorite. A domainal mineral foliation is present as aligned stringers of biotite/muscovite and quartz blebs, with individual biotite crystals within stringers aligned as S4 and ones outside as S3. These stringers are reminiscent of a zonal crenulation cleavage where individual biotite crystals lie along partly transposed S3 and along S4 (Figure 3-12g). S4 zonal crenulation cleavage has 0.01 to 4.0 mm wide folia 0.05 to 1.0 mm apart. It is in places preserved in cordierite porphyroblasts as quartz-rich zones axial planar to crenulations in S3 quartz trails and continuous with an external S4 zonal crenulation cleavage. The internal S3 trails may be obliterated by an S4 continuous cleavage (Figure 3-10b). S4 disjunctive cleavage consists of irregular black seams that are 0.01 to 0.03 mm wide and 0.1 to 0.25 mm apart and concentrated around cordierite porphyroblasts.

S4 may be distinguished from S3 where : 1) S4 crenulates S3. 2) S4 is a straighter or less irregular cleavage than S3. 3) S4 is characterized by thicker and stubbier biotites compared to S3 (Figure 3-12h) (see metamorphic chapter for biotite types). 4) In places S3 is defined by muscovite and chlorite whereas S4 is an oblique biotite foliation (Figure 3-12i). 5) S4 is an axial planar foliation to F4 folds which preserve a folded S3 at their hinges (Figure 3-12j).

S4 is uncommon in volcanic rocks. Where present, S4 within mafic volcanic rocks includes a rare amphibole foliation , lying oblique to S3 biotite foliation. Whereas within some dacite rocks, S4 is a domainal mineral foliation. The reason for the rarity of S4 foliation in the volcanic rocks could be related to S4 being not as strong a foliation as S3 and therefore favouring the more mica-rich rocks of the sediments over the volcanic rocks.

### 3.2.6 Faults

There are two sets of major faults in the map area, a north to northeast (minor northwest) trending, steeply-dipping set of left-lateral faults and, to a lesser extent, a northeast to east trending, steeply dipping set of right-lateral faults (Figure 3-5). The fault zones are characterised by prominent lineaments and highly fractured rock, an angular rubble that obscures primary features. These faults are thought to be of Proterozoic age because a left-lateral fault in the northwest part and one in the southern part of the volcanic pile displace a diabase dyke.

Many steeply-dipping minor faults are present with left- and right-lateral offsets . Most of the left-lateral faults strike from north to east-northeast and the right laterals east to southeast.

In summary, left-lateral faults strike from northwest to north to northeast and right-lateral faults from northeast to east to southeast. Because of these variable trends and the presence of faults of similar strike but opposite offset, a simple compressive fault regime cannot be established.

## 3.3 SUMMARY OF DEFORMATIONAL HISTORY

Several deformational events affected the rocks of the map area. D0 deformation produced a macroscopic anticlinal or domal structure centred on the volcanic pile. D1 deformation produced macroscopic F1 folds varying in trend from northwest to east-west to northeast in the sedimentary and volcanic rocks, D2 deformation resulted in an S2-L2 fabric mainly preserved in the volcanic rocks where it dominantly strikes northwestward but varies in the eastern part to northeastward. S2 is a well spaced, disjunctive cleavage as well as a foliation of aligned primary structures. D3 deformation is characterised by mesoscopic F3 folds and an associated subvertical to easterly dipping S3-L3 fabric that dominantly strikes northward in both sedimentary and volcanic rocks. S3 varies from a slaty cleavage in mudstones to a rough, disjunctive cleavage in sandstones at low grade and a continuous mineral foliation at higher grade; in volcanic rocks it includes the alignment of primary structures, a continuous mineral foliation and a disjunctive cleavage. L2 and L3 are stretch and mineral lineations in both the sedimentary and volcanic rocks.

D4 deformation produced F4 mesoscopic folds with an associated northeast striking S4 cleavage that is almost exclusively developed in the sedimentary rocks. S4 is commonly a crenulation cleavage affecting S3, generally changing from a discrete- to zonal-type with increase in metamorphic grade. It is also a continuous mineral foliation, and in a few places a slaty or a disjunctive cleavage, each of similar morphology to S3. L2 and L3 are stretch and mineral lineations in both the sedimentary and volcanic rocks.

Later brittle deformation produced northeast trending, left-lateral and east trending right-lateral faults.

## 3.4 DISCUSSION

From the field and petrographic observations, it is useful to consider a) the factors controlling type of fabric and its prevalence, b) the possible processes involved during the development of the fabrics, c) possible explanations for deviations in orientation of the fabrics d) relationships between fabrics and emplacement of granitic plutons e) tectonic setting for Clan Lake supracrustal rocks during the regional deformational events.

### 3.4.1 factors controlling fabric type and prevalence

The type of fabric and its prevalence are mainly controlled by rock composition, metamorphic grade and presence or absence of other fabrics.

Changes in fabric type according to rock composition have been described for S2 and S3 in lower grade rocks. Thus S2 is a disjunctive cleavage in the more competent rock types such as sandstones and felsic volcanic rocks, but not in the relatively incompetent pelites and mafic volcanic rocks. Also S3 varies from a rough cleavage in sandstones to a slaty or continuous cleavage in mudstones. The fabric type also changes with metamorphic grade as illustrated by S3 which changes from a disjunctive cleavage to a continuous mineral foliation with increase in grade, and S4, which is dominantly a discrete crenulation cleavage at lower grades, and a zonal crenulation cleavage or continuous mineral foliation at higher grades. These changes in fabric type reflect the processes involved in fabric formation (see below). Lastly, fabric type is affected by pre-existing fabrics as shown by S4, being a rough, slaty or continuous cleavage by itself but a crenulation cleavage where S3 is present.

As for fabric prevalence, the dominance of a particular fabric generation depends both on rock type and the presence or absence of other fabrics. Consider first rock type. Earlier fabrics are best preserved in the more competent rocks and later ones in the less competent. For example, on the mesoscopic or outcrop scale, S3 is mainly apparent in the sandstones whereas S4 is observed only in the pelites. Also S2 is seen mainly in the relatively competent volcanic rocks in contrast to S4 in the sedimentary rocks. This latter contrast could, however, be due to the fact that foliations such as S2 and, to a minor extent, S3 defined by aligned primary features are more likely to be seen in volcanic rocks with abundant deformable bodies than in the sedimentary rocks where these are less common.

Whether or not a cleavage is apparent depends to some extent on the presence of other cleavages. For example, S2 is mainly seen in the volcanic rocks which were not affected by an S4 foliation whereas it is only locally preserved in the sedimentary rocks displaying both S3 and S4 foliations. S3 is less obvious where affected by, and therefore to some extent obliterated by , S4.

3.4.2 processes involved in fabric development

Most of the foliations were probably formed by the interaction of several processes, but in some a single process seems to have predominated.

The prevalence of disjunctive and crenulation cleavages in the lower grade metamorphic rocks indicates that pressure solution was an important process. The disjunctive cleavages, which include S2 and S3, are defined by residual accumulations of relatively insoluble materials such as white micas, chlorite, opaques and carbonaceous material (Figures 3-9e,f,g,i). The cleavages are accented by the presence of new minerals such as muscovite, chlorite and biotite. The main process thus appears to have been dissolution and diffusion (Gray, 1979), accompanied or followed by crystal growth (Beach, 1979; Gray, 1978). Concentration of insoluble residues at truncated margins of quartz grains is good evidence for dissolution (Figure 3-9g). Quartz-rich and mica-rich zones following crenulations (Figures 3-12e) indicate that mineral differentiation (dissolution and diffusion at low grade) accompanied differential deformation (Gray, 1977b).

Offset quartz veins are also evidence of solution transfer. The veins are offset by S3 +/or S4 disjunctive cleavages (Figures 3-9j,3-12f), indicating pressure solution and/or shearing (Hobbs and Means, 1976 p.237). Because the veins are irregularly folded, a consistent sense of offset cannot be obtained and therefore which process was involved is unknown.

The alignment of quartz, biotite and chlorite crystals in pressure shadows adjacent to grains and large crystals indicates growth during the formation of S3 and S4 (c.f. Woodland, 1982).

In higher grade rocks, the dominant process involved in foliation formation appears to have been crystallization. Continuous mineral foliations predominate and are defined by coarser crystals than ones at lower grades. Disjunctive cleavages are less common. Large, undeformed biotite and muscovite crystals defining continuous mineral foliations and new mineral species such as cordierite and to a minor extent amphibole that to some extent grew during D3 and D4 (see Chapter 4 & Figure 4-2) indicate that crystallisation took place during deformation at these higher grades. Additionally, old quartz grains are absent, unstrained and recrystallised quartz is present, and S4 crenulation cleavages are dominantly a zonal-type versus a discrete-type which may also indicate that dissolution was less prevalent at higher grades. Zonal crenulation cleavages commonly develop into discrete crenulation cleavages with increased solution shortening (Gray, 1977a) but, because of higher temperatures and less water at higher grades, solution shortening may not have been as extensive so that zonal-type crenulation cleavages did not develop into discrete-types.

To summarise, with increase in metamorphic grade, the dominant fabrics generally change from disjunctive cleavages to continuous mineral foliations and from discrete crenulation cleavages to zonal crenulation cleavages. Therefore the dominant processes appear to have changed from pressure solution with minor crystallisation to crystallisation/recrystallisation with minor pressure solution. Rotation and plastic deformation took place at all grades of metamorphism as seen by strained and rotated primary features.

At a given metamorphic grade, the dominant processes involved in fabric formation also appear to have changed with rock type. Rough and widely-spaced, disjunctive cleavages, including both S2 and S3, are most common in the more competent rock types such as sandstones and felsic volcanic rocks, probably because of the predominance in these rocks of pressure solution. The disjunctive cleavages are not formed readily in pelites and mafic volcanic rocks, which have a relatively low proportion of soluble components such as quartz, compared to quartzo-feldspathic rocks (sandstones and felsic volcanic rocks), which have a high proportion of solubles. The mafic and pelitic rocks usually display a continuous mineral foliation due to either rotation and/or crystallisation of minerals.

### 3.4.3 deviations in fabric orientations

The following are possible explanations for deviations from the main fabric orientations, as mentioned above under fabric descriptions.

#### 3.4.3.1 deviation in S2 foliation

The S2 foliation, mainly defined by strained primary structures within the volcanic pile, changes in strike from northwesterly in most of the pile to north-northeasterly in the eastern part, particularly in the isoclinally folded mafic volcanic rocks within the sedimentary rocks (Figure 3-5). The deviation northeastward could be due to rotation of northwest striking S2 towards northeast striking S4 foliation in mafic volcanic rocks that are relatively, easily deformed. This may be due to the mafic volcanics containing a higher content of biotite than the felsic volcanics, making them less competent. Additionally, the mafic volcanics are, in part, present as thin units that were highly deformed in conformity with the enclosing incompetent sedimentary rocks.

3.4.3.2 deviation in S3 -L3 fabric

The S3 cleavage strikes predominantly north-northwestward but has scattered northeasterly trends. These local northeasterly trends could be due to folding of S3 by D4 with measurements taken on the rare, short limbs of these folds instead of the long limbs. Also S3 tends to be parallel to bedding in pelitic layers and these northeasterly trends were measured where bedding strikes northeasterly. Another possibility is that some of these foliations trending northeasterly are S4, rather than S3.

S3 cleavage in the sedimentary rocks generally dips steeply except where inclined at shallow angles away from the western granitic plutons. L3 generally plunges steeply except near the plutons where it plunges shallowly. S4 remains steep throughout the area. The shallow inclinations of S3 and shallow plunges of L3 are related to granite emplacement (see next section 3.4.4).

3.4.4 <u>evidence for syn-D3 granitic intrusion</u>

The granite was emplaced during D3, after the S3 fabric-producing phase had begun but before it had ended, as seen by: 1) the presence of shallow inclinations of S3 and shallow plunges of L3 near the granitic body in contrast with steep S3-L3 orientations elsewhere. This suggests that the granite rose during D3 and modified the regional strain (c.f. Fyson, 1980; Fyson & Frith, 1979). 2) margins of the granitic body conform to S3 foliation in the sedimentary rocks and do not truncate it. The granite also contains a foliation that is continuous with and parallel to an S3-type foliation in sedimentary xenoliths, This indicates that the pluton was emplaced before the S3-forming phase of deformation was completed. 3) granitic dykes and veins from the main granitic body lie along S3 foliation planes and contain an S3 foliation. Evidently they intruded after S3 had started but before it finished developing. 4) the S3 foliation within the granitic body is defined by muscovite and biotite alignment and, to a minor extent, tectonic elongation of quartz and feldspar crystals. This indicates that the granite was crystallising during D3.

### 3.4.5 deformational history for Clan Lake supracrustal rocks

Figure 3-1 summarises the deformational events and the structures they caused in the Clan Lake supracrustal rocks. D1, D2, D3 and D4 deformations produced structures similar in type to those at Ross-Gordon Lakes (Fyson, 1975), Cleft Lake (Fyson, 1980) and Yellowknife (Fyson, 1982). The foliations have regional trends (Fyson, 1984) which require regional stresses in the crust to account for them. The inferred direction of regional compression changed with time as seen by change in orientation of the successive structures. The regional compressive direction is only established for D4, namely WNW-ESE across S4, because S4 is unaffected by later deformation. Fyson (1975) proposed that proto-plate movements best account for these regional stresses in the crust.

# Chapter IV

# METAMORPHISM

## 4.1 INTRODUCTION

The rocks in the map area underwent greenschist to lower amphibolite facies metamorphism. The turbidite sedimentary rocks are subdivided into progressive metamorphic zones by north-northeasterly trending biotite and cordierite isograds (Figure 4-1). A central chlorite zone progrades to the east and west into biotite bearing and cordierite bearing zones. Despite the relatively high grade, primary features such as cross-bedding, scours and grading are fairly well preserved (Figure 4-5e). The volcanic rocks do not have any significant metamorphic zonation and therefore their grade of metamorphism is referred to by using the equivalent grade of adjacent sedimentary rocks.

Treated in the following sections are 1) field and petrographic descriptions of metamorphic minerals 2) metamorphic mineral assemblages (summarised in Figure 4-7) and possible metamorphic reactions and 3) a discussion of metamorphism with respect to time (deformation) and space (summarised in Figures 4-3&4-4), and a general model for the metamorphic history of the map area. Supplementary petrographic data is in Appendix I. Textural criteria used in establishing

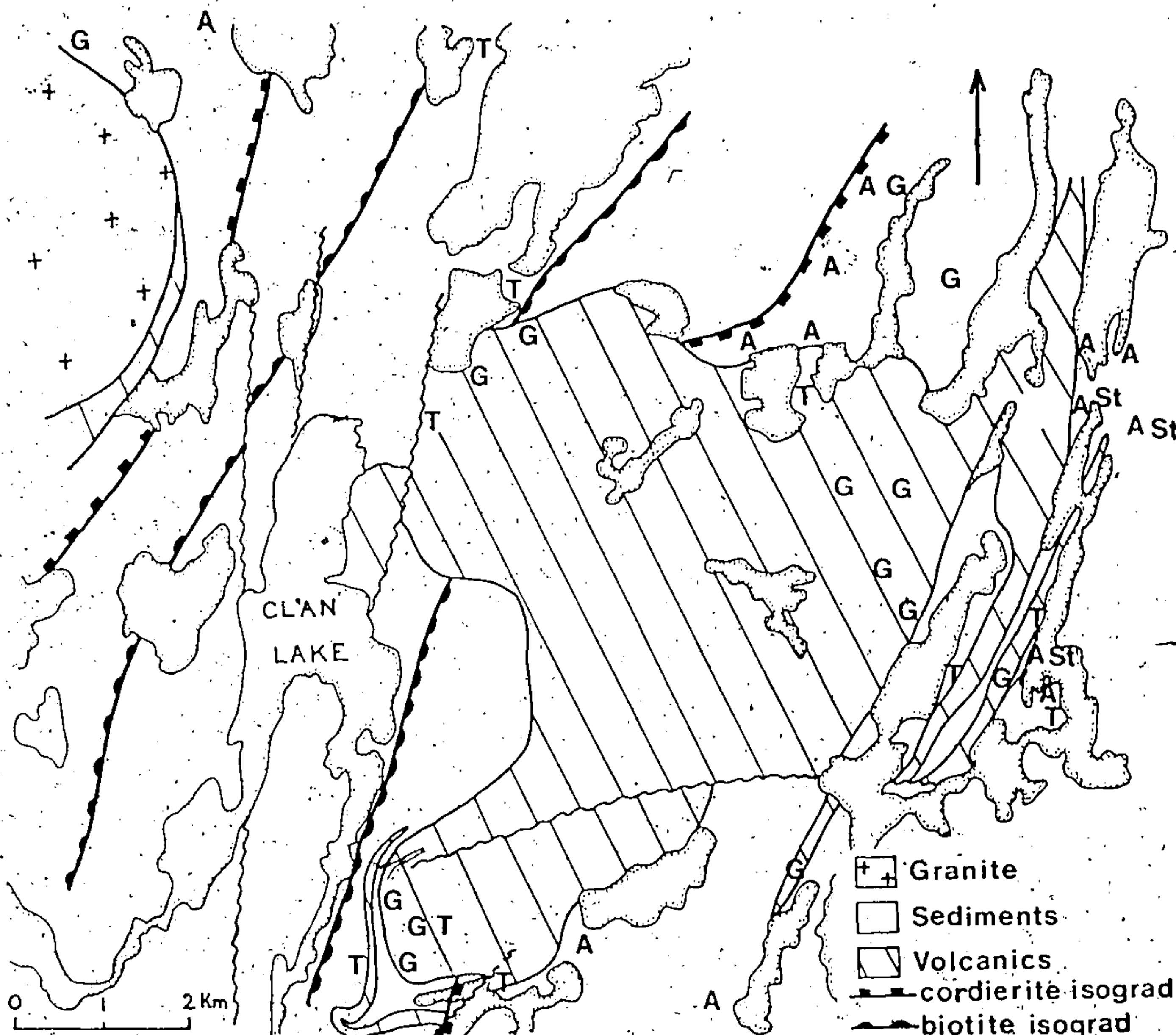


FIGURE 4-1:

Sketch map of metamorphic zonation, Clan Lake area. A low grade zone centred on Clan Lake is bounded east and west by biotite and cordierite isograds. Garnet (G), andalusite (A), tourmaline (T) and possibly staurolite (St) are present.

| MINERAL | TEXTURE | FIGURE | TIMING OF GROWTH |
|---|---|---|---|
| CHLORITE | a) aligned plates parallel to S3 and locally to S2.<br>b) rarely as S2 inclusions within biotite porphyroblasts.<br>c) random crystals overprinting S3.<br>d) interleaved with and replacing biotite. | a) 3-7e,g | prograde growth from D2 to post D3. retrograde growth post D4. |
| MUSCOVITE | a) aligned plates parallel to S3 and locally to S2.<br>b) concentrated as an S2 widely-spaced disjunctive cleavage.<br>c) random crystals over S3. | a) 3-7e,f,g, 3-9h<br>b) 3-7d | from D2 to D4. |
| BIOTITE | a) random porphyroblasts containing S2 inclusion trails (biotite A), in places wrapped around by S3.<br>b) aligned plates parallel to S3 (biotite B).<br>c) aligned stubby plates parallel to S4 and random plates overprinting S3 (biotite C). | a) 3-7f; 4-5b<br>b) 3-12g,h,j; 4-5a<br>c) 3-12g,h,j; 4-5a | from post D2 to D4. |
| GARNET | porphyroblasts containing S2 inclusion trails that are:<br>a) continuous with an undeformed, external S3 foliation.<br>b) continuous with a crenulated, external S3 foliation.<br>c) discontinuous with an external S4 foliation. | a) 3-10c; 4-5c | between D3 and D4. |
| CORDIERITE | a) porphyroblasts containing S4 inclusion trails continuous with undeformed external S4 foliation. The S4 foliation, in places, deviates around the porphyroblasts. | a) 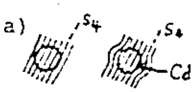 | from post D3 to post D4, the main growth during D4. |
| | b) porphyroblasts containing S3 inclusion trails crenulated by F4 microfolds with axial planes parallel to external S4 foliation. | b) 3-10b 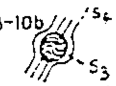 | |
| | c) porphyroblasts containing S3 inclusion trails continuous with an undeformed external S3 foliation. | c)  | |
| | d) porphyroblasts containing S3 inclusions discontinuous with an external S4 foliation wrapped around the porphyroblasts. | d) 3-10a 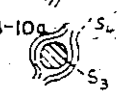 | |
| ANDALUSITE | a) porphyroblasts containing S3 inclusion trails in cores and S4 inclusion trails in rims. | a)  | post D3 to late D4. |
| | b) porphyroblasts with an external S4 foliation wrapped around them. | b)  | |
| | c) porphyroblasts with an external S3 crenulated by S4 in pressure shadows and an external S4 foliation deflected around. | c)  | |

FIGURE 4-2:

Textural criteria used for establishing timing of mineral growth.

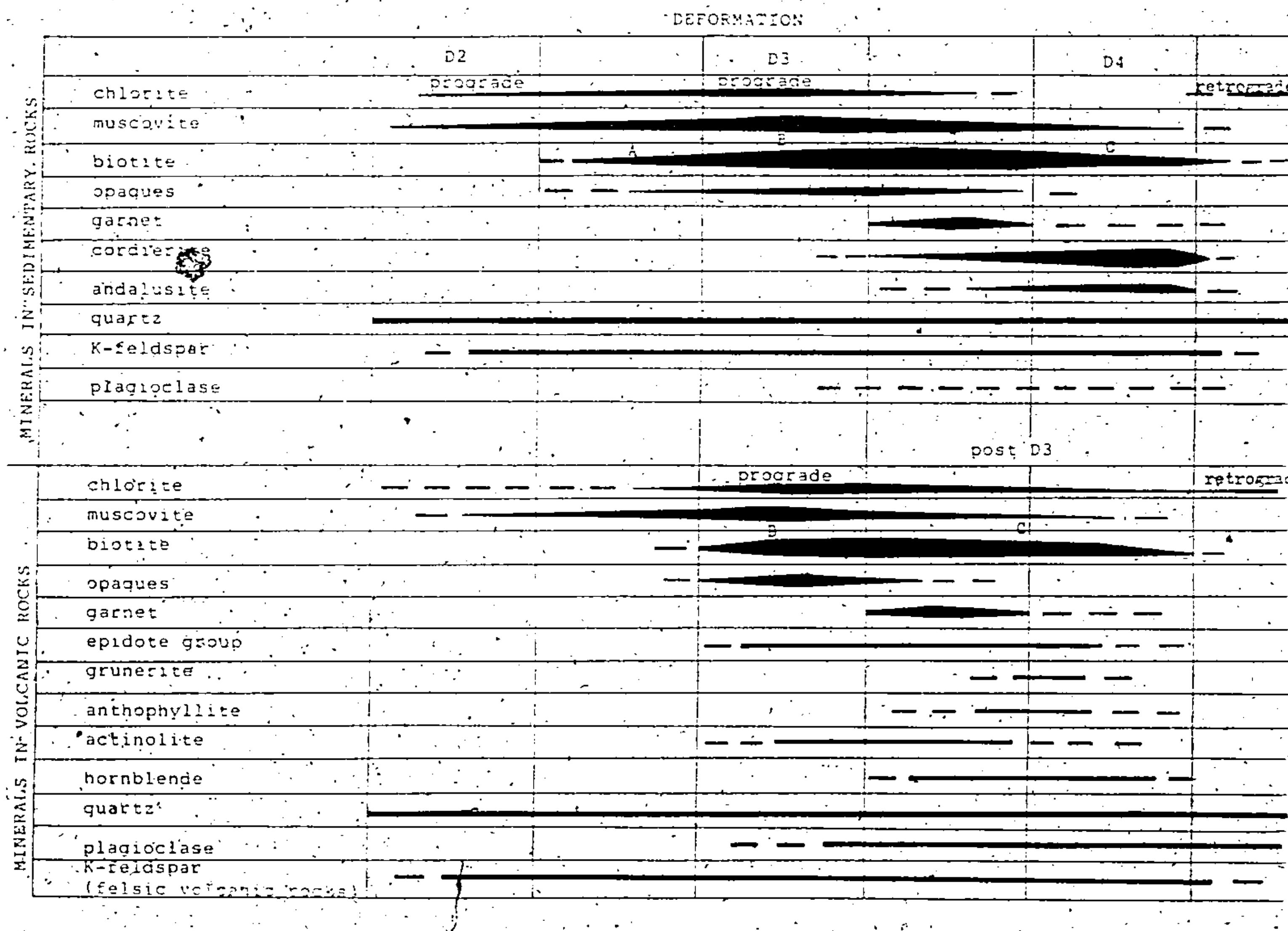


FIGURE 4-3:

Mineral growth with respect to deformation (time).

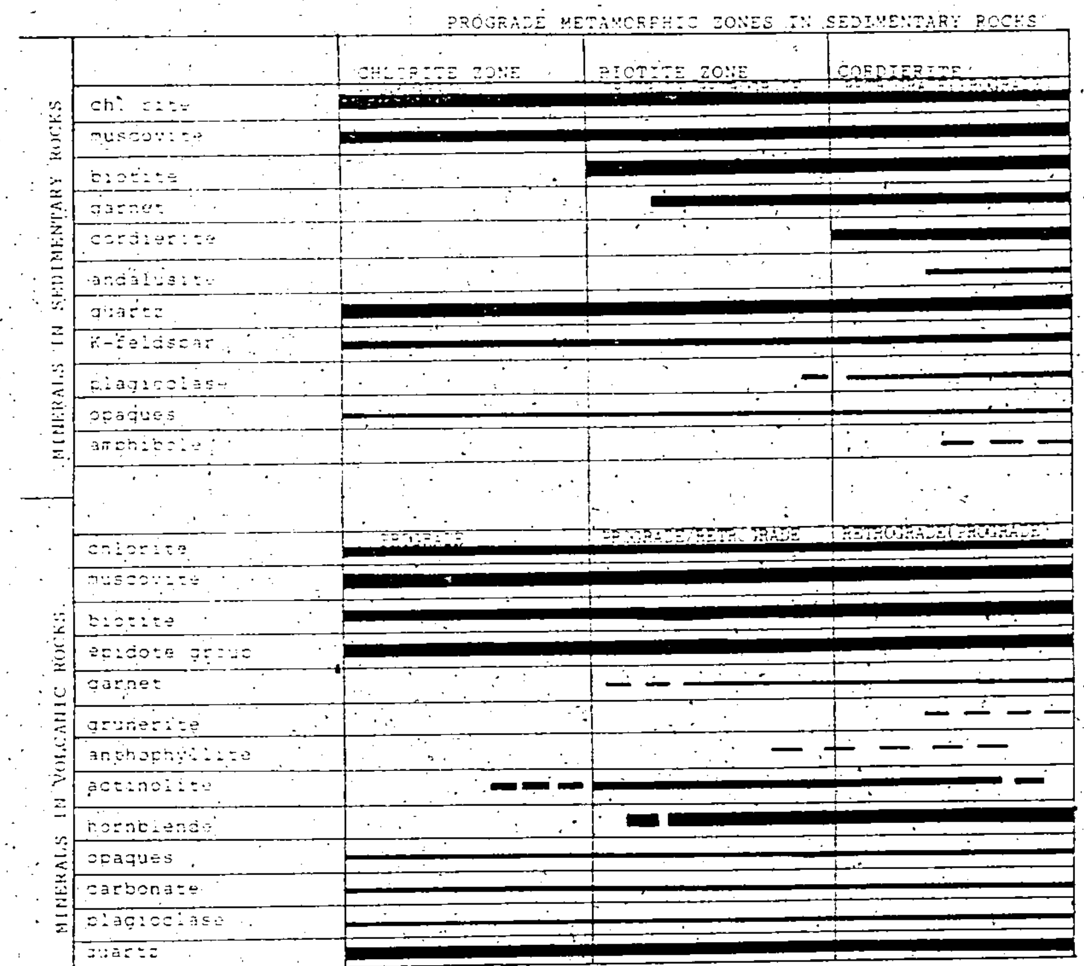


FIGURE 4-4:

Mineral growth with respect to metamorphic grade (space).

timing of mineral growth is summarised in Figure 4-2. Mineral growth includes crystallisation, recrystallisation and to a minor extent, metasomatism.

## 4.2 METAMORPHIC MINERALS

The following mineral descriptions are based on field observations and petrographic work on 173 rock samples tabilised in Appendix I.

### 4.2.1 Chlorite

Chlorite generally is not observed in hand specimen. It is present as microscopically aligned plates, imparting a cleavage to the rocks.

Petrographic work reveals chlorite is common as aligned plates in the lower grade rocks and as large random crystals and an alteration product in the higher grade rocks. In sedimentary and volcanic rocks of the chlorite zone, chlorite forms .02 to .07 mm-sized plates aligned along an S3 foliation and locally an S2 foliation. In the biotite zone, chlorite is 1) an alteration product of biotite, 2) similar to the chlorite zone as .01 to .05 mm sized plates along S3 foliation, or 3) rarely, randomly oriented plates over S3. In the cordierite zone, chlorite is mainly an alteration product of biotite, interleaved or totally replacing it and rarely with quartz as S2 inclusion trails within biotite porphyroblasts.

In summary, prograde chlorite is more common in the lower grade rocks than in the higher grade rocks (Figure 4-4) and crystallised mainly during D3 and to some extent during D2 and post D3 (Figure 4-2&4-3). Retrograde chlorite is more common in the higher grade rocks and crystallised post D4.

4.2.2 Muscovite

Muscovite, like chlorite, is usually too fine to see mesoscopically but imparts a cleavage to the rocks.

Petrographically, muscovite is present as oriented plates, in places aligned with chlorite or biotite. In sedimentary rocks of the chlorite zone, muscovite includes .01 to .03 mm sized plates aligned parallel to an S3 foliation. Locally, muscovite is aligned along an S4 foliation or concentrated, but not necessarily aligned, as an S2 disjunctive cleavage. In sedimentary and volcanic rocks of the biotite zone, muscovite crystals ranging from .01 to .05 mm in size, as in the chlorite zone lie aligned parallel to S3 and locally to S4. Muscovite is also locally concentrated as an S2 segregation cleavage within felsic volcanic rocks. Within sediments of the cordierite zone, muscovite forms .04 to .10 mm sized plates aligned parallel to S3 and less commonly to S4; it is also present as large random crystals overprinting S3. In cordierite grade volcanic rocks, muscovite crystals mainly randomly cross S3.

In summary, muscovite is present in rocks of each metamorphic grade as plates dominantly aligned along S3 (Figure 4-4), generally increasing in size with increase in grade. It crystallised mainly during D3 and to some extent during D2, post D3 and during D4 (Figure 4-2&4-3).

### 4.2.3 Biotite

Biotite is visible in the field as aligned plates, defining a schistosity, and less commonly as lineated aggregates.

Microscopically biotite is of three types within the sedimentary rocks (two types discussed by Ramsay and Kamineni, 1977). The most common type is subhedral, thin elongate plates aligned parallel to an S3 foliation and referred to here as biotite B (Figure 4-5a). Another type, biotite C (Figure 4-5a), is euhedral, thick stubby plates randomly oriented over an S3 foliation (usually within the lower grade end of the biotite zone) or aligned as an S4 foliation (usually within the higher grade end of the biotite zone). The least common type, biotite A (Figure 4-5b), is subequant ragged crystals randomly oriented over an S2 foliation and wrapped around by an S3 foliation. Biotite types B and C generally increase in size upgrade from 0.03 - 0.15 mm in the biotite zone to 0.08 - 0.30 mm in the cordierite zone. Biotite A is only present in sedimentary rocks immediately above and below the cordierite isograd.

FIGURE 4-5:

A) photomicrograph of biotite B and C in biotite schist (unit 6). Thinner plates aligned as S3 (N-S in photo) are biotite B whereas biotite C includes the thicker crystals aligned as S4 (E-W) containing S3 quartz inclusion trails. Field of view is 3 mm. B) photomicrograph of ragged, biotite A porphyroblasts in schist (unit 6). S3 is defined by small, aligned plates of muscovite and biotite B. Field of view is 3 mm. C) photomicrograph of garnetiferous volcarenite (unit 3). Garnet porphyroblast contains S3 quartz inclusion trails and matrix contains an S3 foliation defined by aligned aggregates of quartz crystals and aligned concentrations of radiating amphibole crystals. Field of view is 3 mm. D) garnet porphyroblast (left half of photomicrograph) containing black, fibrous skeletons reminiscent of amphibole (actinolite?) in volcaniclastic rock (unit 3). Field of view is 3 mm. E) cordierite porphyroblasts in sandstone (unit 6). Cross bedding is preserved despite cordierite grade. F) garnet porphyroblasts in volcanic lutite (unit 3). G) andalusite porphyroblasts in pelitic beds (unit 6). The crystals are of the chiastolite variety. H) staurolite? porphyroblasts in biotite schist (unit 6).

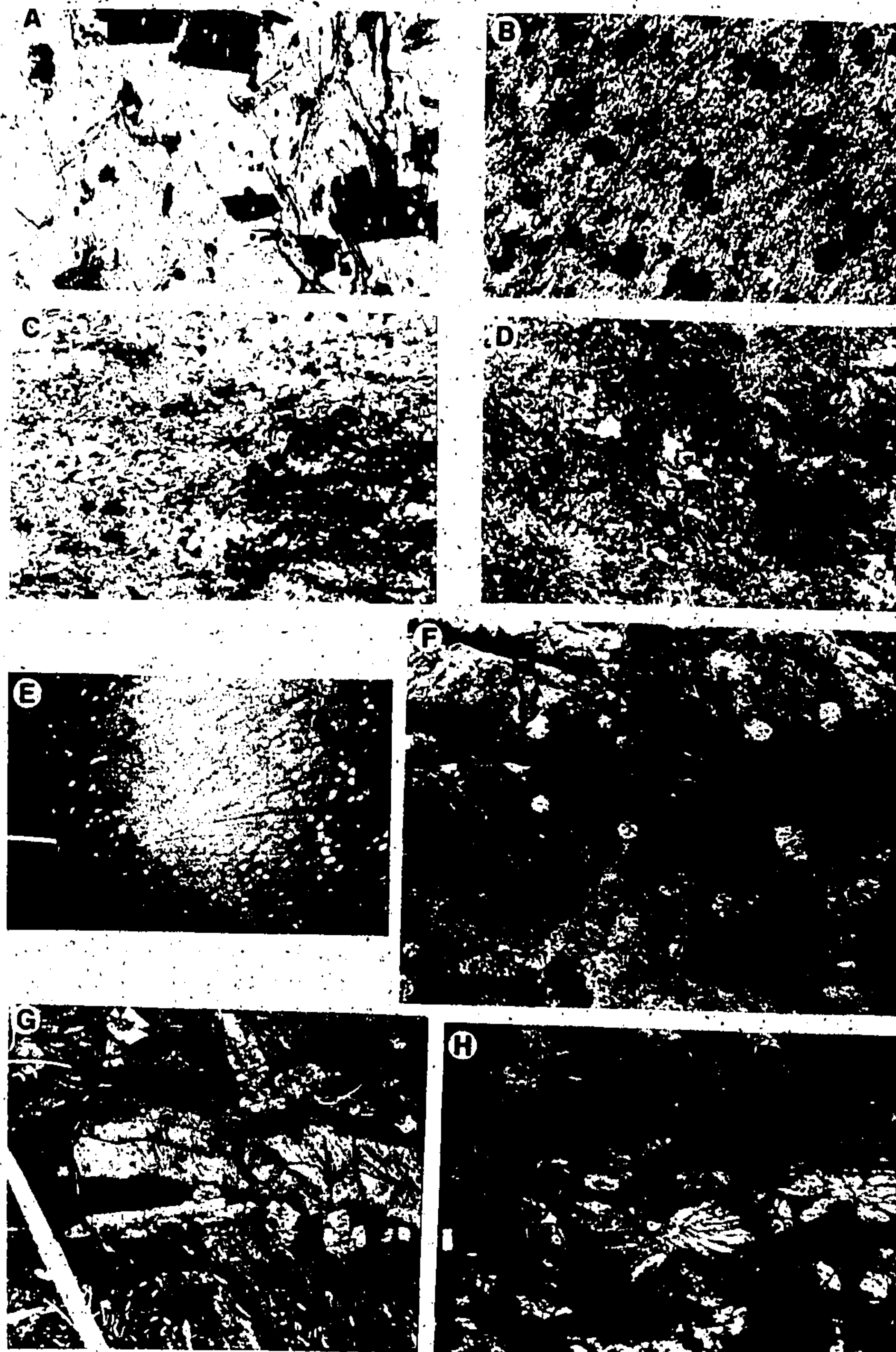
A
B
C
D
E
F
G
H

It is absent in lower grade rocks probably because of the temperatures required for its growth between D2 and D3 were not attained. Biotite A is not seen above the cordierite isograd because it was used up or obliterated by later mineral growth such as cordierite and biotite B+/or C.

The first appearance of biotite A probably marks the position of the biotite isograd between D2 and D3 (Figure 4-6a). As metamorphism progressed with time, the biotite isograd shifted towards the thermal low centered on Clan Lake (Figure 4-1) and subsequent biotites B and C crystallised (Figure 4-6b&c), The present position of the biotite isograd marks the first appearance of biotite C during D4.

Within the mafic volcanic rocks, biotite is present mainly as aligned plates representing an S3 foliation (biotite B) and/or random plates overprinting S3 (biotite C) and rarely as S4. Biotite is not present in felsic volcanic rock unit (4) because of this unit's felsic lithology and its position within the chlorite zone. In the other volcanic lithologies biotite generally increases in size upgrade, ranging in size from .02 to .10 mm for biotite B and .05 to .15 mm for biotite C.

All three types of biotite are to some extent interleaved with or replaced by chlorite, especially the ones in the higher grade rocks.

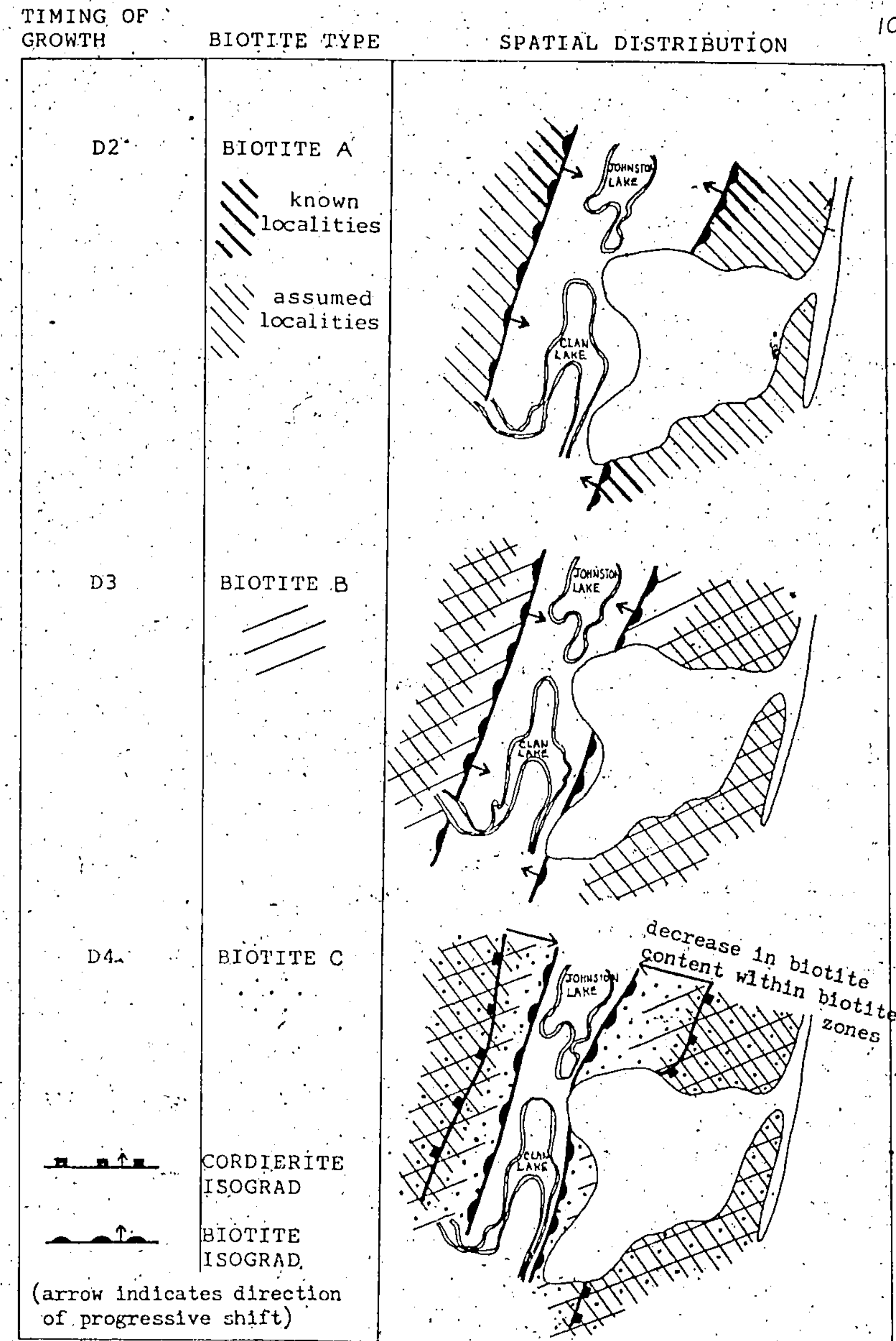


FIGURE 4-6:

Biotite growth through space with time.

In summary, biotite is an index mineral in the sedimentary rocks . It generally increases in size upgrade from the biotite isograd to within the cordierite zone. Crystallisation was mainly from D3 to D4 (biotites B and C) and to a some extent between D2 and D3 (biotite A) (Figure 4-2&4-3).

### 4.2.4 Garnet

Pink to purplish red garnet porphyroblasts are present mainly within mafic volcanic and volcaniclastic rocks (units 3&5; Figure 4-5f) at metamorphic grades equivalent to the biotite and cordierite zones in the sediments. They are locally developed in felsic volcanic (unit 2) and sedimentary rocks. The crystals range in size from less than 1 mm to 2 cm.

Within the volcanic rocks subhedral porphyroblasts of garnet generally contain aligned inclusions of quartz and opaques. The inclusion trails display three main relationships to the external matrix. They are parallel and continuous with an undeformed external S3 foliation (Figure 4-5c), indicating garnet crystallisation was post D3, or continuous with an external S3 foliation crenulated by F4 (indicating garnet crystallisation was between D3 and D4); or discontinuous with an external S4 foliation which deviates around the garnet porphyroblasts, also indicating crystallisation between D3 and D4. In some mafic volcanic rocks, garnet contains fibrous crystal skeletons of actinolite(?) (Figure 4-5d), particularly within rims of porphyroblasts. Garnet is commonly intergrown with hornblende and biotite B.

### 4.2.5 Cordierite

The first appearance of cordierite marks two north-northeasterly trending isograds through the sedimentary rocks (Figure 4-1). Cordierite increases from less than 1 mm to 1-3 cm in size within a few meters above the cordierite isograd. Farther upgrade size variation is dependent on lithology. The cordierite evidently grew in pelites in preference to psammites. Thus primary graded bedding in psammite-pelite turbidites is reflected by an apparent inverse grading of cordierite. With the increase in mudstone stratigraphically up a Bouma sequence, the porphyroblasts increase in size and number, though the uppermost, extremely fine part is commonly void of them.

Cordierite is present as anhedral porphyroblasts (Figure 4-5e) partially to completely altered to pinnite and/or sericite. The porphyroblasts are poikiloblastic and contain abundant inclusions of quartz, opaques, muscovite, biotite and chlorite which are commonly aligned along an S3 or S4 foliation. The varying relationships between the internal foliation and the foliation in the external matrix are summarised in Figure 4-2. Most commonly an S4 internal foliation is continuous with an S4 exterior foliation, the latter being wrapped around the poikiloblasts indicating they grew towards the end of D4 deformation. In a few examples, S4 is a crenulation of S3 quartz inclusion trails within the poikiloblasts that changes to a continuous S4 cleavage externally, suggesting growth at an early stage during the formation of S4. Rarely, the internal foliation is an undeformed S3 whereas the external is either an S3 continuous with the internal indicating growth post S3 or an S4 wrapped around the porphyroblasts, suggesting growth between D3 and D4. One sample has cordierite with an internal foliation of S4 biotite C but an external foliation of both S3 biotite B and S4 biotite C. Further, the external S3 biotite is partially replaced by cordierite where it abuts the porphyroblast, indicating cordierite crystallised at the expense of biotite B.

The cordierite porphyroblasts are commonly elongated parallel to the external foliation. From the porphyroblast/foliation relationships above, this is probably due to the cordierite having crystallised after deformation preferentially along anisotropy provided by the foliation, or less commonly during the foliation-producing deformation preferentially in the direction of least stress, in the foliation plane.

In summary, cordierite is an index mineral that defines a metamorphic zone within the sedimentary rocks. It crystallised mainly during D4 and after D4 and, to a minor extent, between D3 and D4.

4.2.6 Andalusite

Andalusite is only present at a few localities within sedimentary rocks of the cordierite zone (Figure 4-1) and therefore is not useful as an index mineral. Andalusite occurs within carbonaceous, pelitic rocks or within sediments containing abundant quartzofeldspathic veins. It is of the chiastolite variety; is white to pink in colour ; and ranges from 1 mm to 4 cm in length(Figure 4-5g).

The andalusite is present as subhedral to euhedral porphyroblasts partially altered to sericite . The porphyroblasts locally contain inclusions of biotite and opaques. The inclusions are commonly aligned along an S3 foliation and locally aligned in rim zones as an S4 foliation continuous with S4 in the external matrix (Figure 4-2). The external foliation is usually an S4 foliation that is wrapped around the porphyroblasts. Rarely S3 is crenulated by an S4 foliation in pressure shadows of the porphyroblasts and obliterated elsewhere by S4 which deviates around the porphyroblasts. From these textural relations it is apparent that the porphyroblasts crystallised after D3 deformation. Initial growth could have been before D4, but, as shown by inclusion of S4 in rim zones, some growth was after initial

D4 deformation. The deviations of external S4 around the porphyroblasts suggests that the latter were present before the end of D4.

### 4.2.7 Staurolite

Three possible sites near the eastern margin of the volcanics are recognised where staurolite porphyroblasts may have been present within sedimentary rocks of the cordierite zone (Figure 4-1). Pseudomorphs of the porphyroblasts (Figure 4-5h) are elongate, up to 5 cm in length, and display radiating black lines in the long dimensional face. The crystals are pseudo-hexagonal in cross-section. Thin section study reveals that the porphyroblasts are composed entirely of aggregates of biotite, muscovite and chlorite. The morphology suggests that the crystals may originally have been staurolite, but this is not certain.

### 4.2.8 Quartz and feldspar

Quartz and K feldspar are ubiquitous throughout the sedimentary and felsic volcanic rocks. Detrital grains and, to a minor extent, fine recrystallised material are present in the lower grade rocks; recrystallised material and minor detritus in higher grade rocks; and coarse, completely recrystallised material in the highest grade rocks.

Evidence that the recrystallised, quartzofeldspathic material was produced continuously during the period of metamorphism includes 1) the presence of quartz and K-feldspar throughout the metamorphic zones with an increase in amount and crystal size upgrade ; 2) the presence of S2 quartz inclusion trails within biotite A as well as S3 quartz inclusion trails in garnet and cordierite; and 3) elongate crystals of quartz and k feldspar in the matrix parallel to both S3 and S4.

Quartz and K feldspar are therefore assumed to have crystallised during most of the period of metamorphism.

### 4.2.9 Plagioclase

Plagioclase is seen microscopically in the mafic volcanic rocks (unit 5) and to a minor extent in the felsic volcanic and volcaniclastic rocks (unit 2&3). The plagioclase is present as fine crystals and forms < 5% of quartzofeldspathic material; it appears to be albite, but includes oligoclase at higher grades.

In the sedimentary rocks (unit 6) plagioclase (oligoclase and to a minor extent andesine) was only identified in cordierite grade rocks near granitic plutons or gabbroic dykes. Possibly albite is present in biotite and cordierite grade rocks but was not identified.

### 4.2.10 Carbonate and sericite

Carbonate and sericite are present as alteration products. They are common throughout the volcanic rocks and are responsible for the bleaching of some of the mafic volcanic rocks such that in colour they resemble felsic volcanic rocks.

### 4.2.11 Opaque minerals

Opaque minerals of metamorphic origin are present throughout the sedimentary and volcanic rocks. Though they were not studied in detail with a reflecting microscope, most were identified as magnetite, ilmenite and rutile. The crystals are usually aligned parallel to an S3 foliation but in places are randomly oriented with an S3 wrapped around them, creating pressure shadows. Random crystals also overprint an S3 foliation. The opaque minerals are therefore seen to have crystallised mainly during D3 and to a minor extent before and after D3.

### 4.2.12 Epidote group

Epidote is common as subequant crystals throughout the volcanic rocks of varying metamorphic grade. It usually is associated with D3 and post D3 minerals such as biotite, amphibole and chlorite, and therefore is thought to have crystallised during and post D3.

### 4.2.13 Tourmaline

Tourmaline needles are present at several localities within both sedimentary and volcanic rocks of variable metamorphic grade. Figure 4-1 shows the localities as being near the contact between the volcanic and sedimentary rocks, evidently where boron was readily available. In the volcanic rocks, tourmaline commonly contains S3 opaque inclusion trails indicating crystallised after D3. In the sedimentary rocks, tourmaline crystals are randomly oriented with respect to S3 and therefore grew after D3.

### 4.2.14 Amphibole group

Four types of amphiboles are present within the volcanic rocks, predominantly within the mafic and volcaniclastic ones. These are 1) hornblende (the most abundant and widespread) 2) actinolite ( commonly associated with hornblende) 3)anthophyllite ( present in a few scattered localities) and 4) grunerite (at two localities). These minerals are present in rocks of each metamorphic grade, though actinolite tends to become less prevalent and and hornblende more prevalent going upgrade (from studying 23 volcanic rock samples of units 2&5). Hornblende is of the blue-green variety and changes from pale, pleochroic colours to darker ones up grade. Hornblende is also commonly intergrown with garnet and/or biotite C and generally forms random crystals overprinting an S3 foliation. Actinolite crystals are aligned parallel to S3 or they randomly overprint an S3 foliation.

Cummingtonite and hornblende were observed at one locality in the sedimentary rocks, next to a metagabbroic dyke.

## 4.3 MINERAL ASSEMBLAGES AND REACTIONS

The preceeding petrographic descriptions of metamorphic minerals, fabrics and textural relationships suggest changes in mineral assemblages with respect to lithology, space and time (Figure 4-7).

The following are lists of prograde mineral assemblages within the sedimentary rocks. All are assumed to include quartz and K-feldspar. Variations in mineral assemblage due to lithologic changes in rocks of the same grade are minor and not discussed.

Within the chlorite zone the main mineral assemblages are:

1. MUSCOVITE+CHLORITE+OPAQUES(syn D3+minor syn D2/D4)
2. CHLORITE+OPAQUES (syn D2)

Within the biotite zone they are:

1. BIOTITE+MUSCOVITE+CHLORITE+OPAQUES (syn D3)
2. BIOTITE+OPAQUES (syn D3, post D3 + pre D4, syn D4)
3. MUSCOVITE+CHLORITE+OPAQUES (syn D3)

and a minor assemblage is:

DEFORMATION (TIME)

| PROGRADE METAMORPHIC ZONES (SPACE) | | D2 | | D3 | | D4 | |
|---|---|---|---|---|---|---|---|
| CHLORITE ZONE | sediments | chl<br>chl-musc | chl-musc | chl-musc±opaq<br>musc±opaq | | | |
| | felsic volcanics | musc-chl | musc-chl-epid<br>biot±musc-epid | | musc-chl | | |
| | mafic volcanics | | | chl-epid±opaq<br>biot-opaq | biot-musc±epid±amph | | |
| BIOTITE ZONE | sediments | chl | biot | biot-musc±opaq<br>biot-musc-chl±opaq<br>biot±opaq<br>musc-chl±opaq | garn-musc±opaq<br>biot-garn±opaq<br>garn±opaq | biot±opaq<br>biot-chl±opaq | |
| | felsic volcanics | chl-musc | | biot-musc±epid<br>biot-musc-chl<br>biot-chl±actin<br>biot±epid | hnblnde-biot±epid<br>biot-chl | | |
| | mafic volcanics | | | biot-epid±musc<br>biot-chl±epid | anth-plag<br>hnblnde-actin-plag-biot±musc±epid<br>hnblnde-garn-plag±biot±chl±epid | | |
| CORDIERITE ZONE | sediments | chl | biot | biot-musc±opaq<br>biot±opaq<br>biot-chl<br>cord-musc-biot | biot±opaq<br>garn±opaq<br>cord-biot-musc | cord-biot<br>cord-biot-musc<br>cord-biot-chl<br>and-biot±opaq<br>garn-biot | cord |
| | felsic volcanics | musc | | musc±opaq<br>musc-biot±epid±opaq | musc-biot±chl±epid±amph±garn | | |
| | mafic volcanics | | | biot±epid±opaq<br>biot-chl-±epid±opaq | anth-plag<br>actin/hnblnde-plag-garn±biot±epid<br>hnblnde/actin-plag-biot±epid | | |

chl-chlorite
musc-muscovite
biot-biotite
opaq-opaques
epid-epidote
cord-cordierite
garn-garnet
plag-plagioclase
amph-amphibole
actin-actinolite
hnblnde-hornblende
anth-anthophyllite

FIGURE 4-7:

Metamorphic mineral assemblages with respect to deformation (time) and grade of rocks (space). The underlined assemblages are the most common ones. Quartz and K-feldspar are assumed to be part of all the assemblages.

FIGURE 4-7:

Metamorphic mineral assemblages with respect to deformation (time) and grade of rocks (space). The underlined assemblages are the most common ones. Quartz and K-feldspar are assumed to be part of all the assemblages.

4. GARNET+BIOTITE+MUSCOVITE+OPAQUES (post D2)

Within the cordierite zone they are:

1. BIOTITE+CORDIERITE+CHLORITE+MUSCOVITE (syn D3)
2. BIOTITE+ANDALUSITE (syn D3)
3. CORDIERITE+BIOTITE (syn D3+D4, post D3+D4 and minor pre D3)
4. BIOTITE+MUSCOVITE+CHLORITE (syn D3)

and to a minor extent:

5. GARNET+BIOTITE+MUSCOVITE+CORDIERITE (post D3, syn D4).

Using the textural relationships of minerals and the timing and spatial relationships of mineral assemblages, the following mineral reactions possibly took place:

1. PHENGITE(MUSCOVITE)+CHLORITE MUSCOVITE+BIOTITE+QUARTZ+$H_2O$ (Kamineni + Carrara, 1973)
2. CHLORITE+MUSCOVITE+ILMENITE BIOTITE + MUSCOVITE + (QUARTZ, RUTILE, K-FELDSPAR) + $H_2O$ (Ramsay + Kamineni, 1977)

The above two reactions could account for the first appearance of biotite. The very first appearance of biotite would have been biotite A (post D2). This would have been followed by the first appearance of biotite B during D3 and then by the first appearance of biotite C (after D3 and during D4). The spatial relationships of these first appearances indicate that the biotite isograds progressively shifted toward the thermal low centered at Clan Lake (Figure 4-1) with time as shown in Figure 4-6. That is, biotite-forming reactions were continuously going on from post D2 to D4 over a range of temperatures. This could account for the decrease in biotite content going downgrade through the biotite zone (Figure 4-6). Another biotite-forming reaction could have been:

3. CHLORITE+MUSCOVITE +QUARTZ BIOTITE + GARNET+$H_2O$ (Kretz, 1973) but only to a minor extent after D3 when garnet grew locally in the biotite zone. Minor garnet in the cordierite zone is not associated with cordierite and probably formed from the reaction:

4. CORDIERITE+BIOTITE GARNET+MUSCOVITE (Kretz, 1973)

Other reactions that took place within the cordierite zone are ones that produced cordierite, mainly during D4 and to a minor extent during and after D3.

5. CHLORITE +MUSCOVITE+QUARTZ BIOTITE+CORDIERITE+$H_2O$ (Thompson, 1978)

6. CHLORITE+MUSCOVITE+BIOTITE A+/or B+(ALBITE+ILMENITE) CORDIERITE+BIOTITE+$H_2O$ (Ramsay and Kamineni, 1977)

Because of biotite A disappearing abruptly upgrade away from the cordierite isograd and some of the textural relationships showing cordierite replacing biotite B , biotite A+/or B are assumed to be used in forming cordierite and biotite C.

A possible reaction for the production of andalusite is:

7. CHLORITE+MUSCOVITE+QUARTZ ANDALUSITE+BIOTITE C+CORDIERITE+H2O (Hess, 1969)

Because andalusite usually occurs without cordierite, the following three reactions are more likely:

8. CORDIERITE+MUSCOVITE+QUARTZ ANDALUSITE+BIOTITE C (Thompson, 1978)
9. CHLORITE+MUSCOVITE+QUARTZ ANDALUSITE+BIOTITE C+H2O (Miyashiro, 1973).
10. MUSCOVITE + QUARTZ ANDALUSITE + K-FELDSPAR (Turner, 1981)

All four reactions for andalusite occurred during D4.

The last reaction is the only reaction that can be used to obtain an approximate pressure and temperature attained during regional metamorphism. Temperature was between 550 and 650 C and pressure was between 0.1 and 2.0 kb. assuming P=PH2O (Turner, 1981: p. 154).

Within the volcanic rocks, the mineral assemblages change going upgrade but, because of no significant metamorphic zonation or index minerals, the grade that these particular mineral assemblages are in is referred to by using the equivalent grade of the sediments (Figure 4-1 ).

The mineral assemblages change with volcanic lithology but, because of radical facies changes over short distances it is difficult to monitor mineralogical changes throughout one lithology across grade. However, several generalities can be made.

The significant changes with time and up grade are:

1. the disappearance of prograde chlorite and prevalence of retrograde chlorite
2. the change from assemblages containing actinolite to ones containing actinolite- hornblende to those that are hornblende dominant
3. the appearance of biotite during D3 and post D3 which is below the biotite isograd of the sediments ie. biotite crystallised at a lower temperature in volcanics than in sediments (c.f. Miyashiro, 1973)
4. the appearance of garnet, which more or less coincides with the biotite isograd within the sediments and
5. the change up grade from Na plagioclase to more calcic plagioclase.

Therefore possible reactions that took place are:

1. pyroxene/olivine/plagioclase chlorite/epidote/biotite/calcite/albite

2. chlorite+calcite+quartz  actinolite+$CO_2$+$H_2O$ (syn-D3, post-D3); (Miyashiro,1973).
3. chlorite+actinolite  hornblende/anthophyllite (post-D3) (Miyashiro, 1973)
4. actinolite  actinolite+blue-green hornblende (post-D3); (Schimann,1978; Miyashiro,1973)
5. epidote+chlorite  plagioclase+hornblende (post-D3); (Froese,1980).
6. biotite- and garnet-forming reactions similar to ones in the sedimentary rocks such as muscovite+chlorite+quartz  biotite+garnet+$H_2O$ and chlorite+quartz  garnet (both post-D3 and to a minor extent syn-D3; after Kretz,1973)
7. Na plagioclase (albite)  more calcic plagioclase (oligoclase) (post-D3; after Winkler,1974 and Schimann,1978).

## 4.4 MAP PATTERNS OF ISOGRADS

The first appearances of the minerals biotite and cordierite within the sedimentary rocks mark two biotite and two cordierite isograds (Figure 4-1). These isograds trend north-northeasterly and outline a thermal 'trough' centered at Clan Lake. The axis of the 'trough' is notably parallel to S4 foliation. The isograd pattern could be explained by:

1. different heat sources at depth or more than one thermal dome such that one to the west and one to the east created a thermal low centered at Clan Lake.

2. folding of isograds such that the low grade rocks of the thermal low represent exposed, high crustal levels preserved in a synformal structure and the progressively higher grade rocks to the west and the east represent progressively lower crustal levels.

Evidence for an original thermal low comes from the distribution of granitic plutons; one group of plutons lies along the western margin of the Clan Lake area and another group of scattered plutons to the east (see preliminary map of Fortier, 1946). On the other hand, there is little evidence for folding of the isograds. The present exposed position of the isograds was determined during D4 (peak of metamorphism), as seen by textural criteria for timing of growth of cordierite and andalusite. Therefore, if the isograds were folded into a synformal structure subsequent to D4, the S4 foliation should also show the effects of this folding. However, S4 shows no obvious change in orientation across the map area (Figure 3-11).

## 4.5 SUMMARY AND DISCUSSION

Metamorphism of greenschist to lower amphibolite grade progressed with time and space as shown by the distribution of metamorphic minerals and the timing of the growth of these minerals with respect to deformation (Figure 4-3&4-4).

Metamorphism began during D2, progressed until it peaked during and just after D4, and waned post D4. Three prograde zones are defined in the sedimentary rocks by the first appearance of the index minerals biotite and cordierite. Distribution of other metamorphic minerals such as garnet and andalusite cannot be so readily described because of their sporadic occurrence. Within the volcanic rocks, prograde zones are not easily defined, but prograde metamorphism is manifested by change in type of amphibole, increase in An content of plagioclase and disappearance of prograde chlorite.

Variations in metamorphic grade through space reflect:

1. spatial variations in temperature and pressure (at a single time) (c.f.. Thompson,1978)
2. changes in pressure and temperature regime through time (ie. thermal peak was during D4)
3. the amount of subsequent uplift and erosion (c.f. Thompson, 1978).

The changes in temperature with space and time can be explained by combining regional metamorphic models for the Slave Province proposed by Ramsay and Kamineni, 1977 and Thompson, 1978. Metamorphism was a single continuous cycle which can be subdivided into phases with respect to deformation. The first phase, during D2, was the beginning of thermal doming (Thompson, 1978) which imprinted an aureole of low grade zones on the rocks. Continued thermal doming resulted in two succeeding phases, during D3 and D4 plus partial melting and concurrent granitic emplacement. The last or waning phase, post D4, was the decay of the thermal dome. Thermal doming, and therefore regional metamorphism, was caused by high geothermal gradients in thick sialic crust (Thompson, 1978). The crust was thickened by regional horizontal compression (Thompson, 1978).

## Chapter V

# SUMMARY AND PALEOGEOTECTONIC ANALYSIS

The volcanic and sedimentary succession at Clan Lake represents a small segment of a depositional basin in the southwest Slave Province that developed during the Archean.

A paleogeotectonic model for the Clan Lake area, within an Archean plate tectonic regime, is as follows:

1. rifting of preexisting sialic crust due to regional extension to form a depositional basin. The volcanic and sedimentary rocks at Clan Lake are assumed to have been deposited on sialic crust by analogy with similar supracrustal rocks elsewhere in the Slave Province which a) lie unconformably above older granitic rocks (Henderson, Loveridge and Sullivan, 1982; Krogh and Gibbins, 1978; Henderson and Easton, 1977; Baragar and McGlynn, 1976) and b) are largely derived from a granitic source and emergent felsic volcanic islands (Henderson, 1981; Baragar and McGlynn, 1976; McGlynn and Henderson, 1970).
2. extrusion of the 1300 meter thick Clan Lake volcanic pile was concommittent with turbidite sedimentation within part of this basin. The volcanic pile developed into a felsic volcanic island but was later in-

undated by turbidite sediments. Material for the turbidite sediments came mainly from the emerged felsic volcanics and sialic basement highs.

3. gabbroic intrusion of the volcanic and sedimentary rocks

4. regional deformation (D1-D4), regional metamorphism (D2-post D4) and granitic intrusion (syn-D3) of the volcanic and sedimentary rocks due to regional horizontal compression, crustal thickening and thermal doming. The complex structures and metamorphic aureoles of Archean rocks commonly have been attributed to granitic emplacement (Drury, 1977; Gorman et al, 1978; Stephansson, 1977; and Young, 1978). However, regional structural and metamorphic trends in the Slave Province cannot be directly related to the granitic plutons and emplacement of the plutons is mainly after extensive deformation (such as shown by D2 and earlier structures) and metamorphism had begun. Most of the structures require regional stresses in and beyond the Clan Lake area (c.f. Fyson, 1975,1978) and metamorphic aureoles require a regional heat source such as a thermal dome (Thompson, 1978; Ramsay and Kamineni, 1977), with the plutons representing merely subsidiary effects. Plate interaction is thought best to account for the regional stresses (Fyson, 1975), possibly plate convergence.

The resultant crustal thickening led to thermal doming.

5. intrusion of diabase dykes, as the result of regional extension, and later faulting during the Proterozoic (McGlynn and Henderson, 1972).
6. uplift and erosion of the metavolcanic, metasedimentary and granitic rocks to their present-day configuration.

# Chapter VI

## SUGGESTIONS FOR FURTHER WORK

Future geochemical work would complement the present study. The following warrant particular attention: determination of the tectonic affinity of the volcanic rocks through major element and rare earth element analyses, establishment of the nature of alteration zones within the volcanic pile and evaluation of progressive metamorphism across the volcanic rocks. Together with the mapping undertaken in the present study, these may help to define zones of potential mineralisation and thus explain the presence, locally within the volcanic rocks, of gold.

## REFERENCES


Baragar, W.R.A. and McGlynn, J.C.,1976: Early Archean basement in the Canadian Shield: A review of the evidence. Geol. Surv. Can., Pap. 76-14: 21p.

Beach, A., 1979: Pressure solution as a metamorphic process in deformed terrigenous sedimentary rocks. Lithos. 12: 51-58.

Bouma, A.H., 1962: Sedimentology of some flysch deposits; a graphic approach to facies interpretation. Amsterdam, Elsevier: 168p.

Carlisle, D., 1963: Pillow breccias and their aquagene tuffs, Quadra Island, B.C. Jour. Geol. vol. 71: 48-71.

Cas, R., 1978: Silicic lavas in Paleozoic flyschlike deposits in New South Wales, Australia: behaviour of deep subaqueous silicic flows. Geol. Soc. Amer., Bull., vol. 89: 1708-1714.

Cousineau, P. and Dimroth, E., 1982: Interpretations of the relations between massive, pillowed and brecciated facies in the Archean submarine andesite volcano-Amulet Andesite, Rouyn-Noranda, Canada. Jour. Volc. & Geotherm. Res. 13: 83-102.

Crowe, B.M. and Fisher, R.V., 1973: Sedimentary structures in base-surge deposits with special reference to cross-bedding Ubehebe Craters, Death Valley, California. Geol. Soc. Amer. Bull., vol. 84: 663-682.

deWit, M.J. and Stern, C., 1978: Pillow talk. Jour. Volc. Geotherm. Res. 4: 55-80.

Dimroth, E., Cousineau, P., Leduc, M. and Sanschagrin, Y., 1978: Structure and organization of Archean subaqueous basalt flows, Rouyn-Noranda area, Quebec, Canada. Can. Jour. Earth Sci., vol.15: 902-918.

Drury, S.A., 1977: Structures induced by granite diapirs in the Archean greenstone belt at Yellowknife, Canada: implications for Archean geotectonics. Jour. Geol., vol. 85: 345-358.

Fisher, R.V., 1960: Criteria for recognition of laharic breccias, Southern Cascade Mountains, Washington. Geol. Soc. Amer. Bull., vol. 71: 127-132.

-----, 1966: Rocks composed of volcanic fragments and their classification. Earth Sci. Rev. 1: 287-298.

-----, 1982a: Debris flows and lahars. In L.D. Ayres (Ed) Pyroclastic Volcanism and deposits of Cenozoic intermediate to felsic volcanic islands with implications for PreCambrian greenstone-belt volcanoes. Geol. Assoc. Can., Short course notes, vol. 2: 136-220.

-----, 1982b: Pyroclastic flows and pyroclastic surges in L.D. Ayres (Ed) Pyroclastic Volcanism and deposits of Cenozoic intermediate to felsic volcanic islands with implications for PreCambrian greenstone-belt volcanoes. Geol. Assoc. Can., Short course notes, vol. 2: 71-131.

----- and Schmincke, H.-U., 1984: Pyroclastic rocks. Springer-Verlag, Germany: 472p.

Flint, R.F., Sanders, J.E. and Rodgers, J., 1960: Diamictite, a substitute term for symmictite. Geol. Soc. Amer. Bull., vol. 71: 1809.

Fortier, Y.O., 1946: Notes on the Yellowknife-Beaulieu region, N.W.T., Preliminary map, Geol. Surv. Can. Pap. 46-23.

Frisch, T.,1973: Clues to the recognition of ignimbrites in deformed and metamorphosed terrains. In Volcanism and volcanic rocks. Geol. Surv. Can. Open File 164, : 39-45.

Frith, R.A., Fyson, W.K. and Hill, J.D., 1977: The geology of the Hackett -Back River greenstone belt-second preliminary report. In Rpt. of Activities, Part A, Geol. Surv. Can. Pap., 77-1A: 415-423.

Froese, E., 1980: A reaction grid for medium grade mafic rocks. Geol. Surv. Can. Pap., 80-1A: 53-55.

Fyson, W.K., 1975: Fabrics and deformation of Archean metasedimentary rocks, Ross Lake-Gordon Lake area, Slave Province, N.W.T. Can. Jour. Earth Sci. 12: 765-776.

-----, 1978: Structures induced by granite diapirs in the Archean greenstone belt at Yellowknife, Canada: implications for Archean geotectonics: a discussion. Jour. Geol. vol. 86: 767-769.

-----, 1980: Fold fabrics and emplacement of an Archean granitoid pluton, Cleft Lake, N.W.T. Can. Jour. Earth Sci., vol.17: 325-332.

-----, 1982: Complex evolution of folds and cleavages in Archean rocks, Yellowknife, N.W.T. Can. Jour. Earth Sci., vol.19: 878-893.

-----, 1984: Fold and cleavage patterns in Archean metasediments of the Yellowknife supracrustal domain, Slave Province, Canada. PreCambrian Tectonics 19: 281-293.

----- and Frith, R.A., 1979: Regional deformations and emplacement of granitiod plutons in the Hackett River greenstone belt, Slave Province, Northwest Territories. Can. Jour. Earth Sci. 16: 1187-1195.

Gorman, B.E., Pearce, T.H. and Birkett, T.C., 1978: On the structure of Archean greenstone belts. PreCambrian Res. 6: 23-41.

Gray, D.R., 1977a: Some parameters which effect the morphology of crenulation cleavages. J. Geol., vol. 85: 763-780.

-----, 1977b: Morphologic classification of crenulation cleavage. J. Geol., vol. 85: 229-235.

-----, 1978: Cleavages in deformed psammitic rocks from southeastern Australia: Their nature and origin. Geol. Soc. Amer. Bull., vol.89: 577-590.

-----, 1979: Microstructure of crenulation cleavages: an indicator of cleavage origin. Amer. Jour. Earth Sci. 279: 97-128.

Henderson, J.B., 1970: Stratigraphy of the Archean Yellowknife Supergroup, Yellowknife Bay-Prosperous Lake area. Geol. Surv. Can. Pap. 70-26.

Henderson, J.B., 1975: Sedimentology of the Archean Yellowknife Supergroup at Yellowknife, District of Mackenzie. Geol. Surv. Can. Bull. 246: 62p.

Henderson, J.B., 1976: Geology maps, 1:125,000 85J,I (Hearne Lake and Yellowknife map sheets). Geol. Surv. Can. Open File 353.

-----, 1981: Archean basement evolution in the Slave Province, Canada. In A. Kroner (Ed) PreCambrian plate tectonics, Elsevier, Amsterdam: 213-236.

----- and Easton, R.M., 1977: Archean supracrustal-basement rock relationships in the Keskarrah Bay map-area, Slave Structural Province, District of Mackenzie. In Rpt. of Activities, Part A, Geol. Surv. Can., Pap. 77-1A: 217-221.

-----, Loveridge, W.D. and Sullivan, R.W., 1982: A U-Pb study of zircon from granitic basement beneath the Yellowknife Supergroup, Point Lake, District of Mackenzie. In Rpt. of Activities, Part C, Geol. Surv. Can., Pap. 82-1c: 173-178.

Hess, P.C., 1969: The metamorphic paragenesis of cordierite in pelitic rocks. Contr. Mineral. and Petrol. 24: 191-207.

Hobbs, B.E., Means, W.D. and Williams, P.F., 1976: An outline of structural geology. J. Wiley & Sons, New York: 571p.

Hurdle, E.J., 1983: Geology of the Clan Lake area, District of Mackenzie, N.W.T. Preliminary maps, E.G.S. 1983-5 sheets A, B, C.

Jolliffe, A.W., 1939: Preliminary maps, Quyta Lake and parts of Fishing Lake and Prosperous Lake areas, N.W.T. Geol. Surv. Can. Pap. 39-6.

-----, 1940: Quyta Lake and parts of Fishing Lake and Prosperous Lake areas, N.W.T. Geol. Surv. Can. Pap. 40-14.

Jones, J.G., 1969: Pillow lavas as depth indicators. Amer. Jour. Sci., vol. 267: 181-195.

Kamineni, D.C. and Carrara, A., 1973: Comparison of the composition of porphyroblastic and fabric-forming biotite in two metamorphic rocks. Can. Jour. Earth Sci. 10: 948-953.

Kretz, R., 1973: Kinetics of the crystallization of garnet at two localities near Yellowknife. Can. Min. 12: 1-20.

Krogh, T.E. and Gibbins, W., 1978: U-Pb isotopic ages of basement and supracrustal rocks in the Point Lake area of the Slave Structural Province, Canada; in Geol. Assoc. Can.-Mineral. Assoc. Can. Abst. with Progs. 3: 438.

Lajoie, J., 1979: Facies Models 15: Volcaniclastic rocks. Geoscience Can., vol. 6: 129-139.

Lambert, M., 1975: Anatomy of a greenstone belt, Slave Province, N.W.T.. In Baragar, W.R.A., Coleman, L.C. and Hall, J.M. (Eds.) Volcanic Regimes in Canada, Spec. Geol. Ass. Can. 16: 331-340.

-----, 1982: Felsic flows and flank deposits of the Back River volcanic complex, District of Mackenzie. Geol. Surv. Can. Pap. 82-1A: 159-164.

MacDonald, G.A., 1972: Volcanoes. Prentice-Hall Inc., Englewood Cliffs, N.J.: 510p.

McGlynn, J.C. and Henderson, J.B., 1970: Archean volcanism and sedimentation in the Slave Structural Province. In A.J. Baer (Ed) Basins and Geosynclines in the Canadian Shield, Geol. Surv. Can. Pap. 70-40: 31-40.

----- and -----, 1972: The Slave Province. In R.A. Price and R.J.W. Douglas (Eds), Geol. Ass. Can., Spec. Pap. 11: 506-526.

Miyashiro, A., 1973: Paired and unpaired metamorphic belts. Tectonophysics 17: 241-254.

Mullineaux, D.R. and Crandell, D.R., 1962: Recent lahars from Mt. St. Helens, Washington. Geol. Soc. Amer. Bull., vol.73: 855-870.

Parsons, W.H., 1969: Criteria for the recognition of volcanic breccias: a Review. Geol. Soc. Amer. Mem. 115: 263-304.

Powell, C.McA., 1979: A morphological classification of rock cleavage. Tectonophysics 58: 21-34.

Ramsay, C.R. and Kamineni, D.C., 1977: Petrology and evolution of an Archean metamorphic aureole in the Slave Craton, Canada. Jour. of Petrol., vol. 18 : 460-486.

Ramsay, J.G., 1967: Folding and fracturing of rocks. McGraw-Hill, New York: 568p.

Reading, H.G., 1978: Sedimentary environments and facies. Elsevier, New York: 557p.

Rose, W.I. Jr., 1972: Santiaguito volcanic dome, Guatemuala. Geol. Soc. Amer. Bull., vol. 83: 1413-1434.

Ross, C.S. and Smith, R.L., 1961: Ash-flow tuffs: their origin, geologic relations and identification. U.S. Geol. Surv. Prof. Pap. 366: 1-81.

Schimann, K., 1978: On regional metamorphism in the Wakeham Bay area, New Quebec. In J.A. Fraser and W.W. Heywood (Eds) Metamorphism in the Canadian Shield, Geol. Surv. Can., Pap. 78-10: 245-248.

Schmincke, H-U., 1974: Pyroclastic rocks. In Fuchtbauer, H. (Ed) Sediments and sedimentary rocks 1, Sedimentary petrology part II: 160-169.

Self, S., 1982: Lava flows and domes; Nature of subaerial pyroclastic deposits based on a facies concept. In L.D. Ayres (Ed); Pyroclastic volcanism and deposits of Cenozoic intermediate to felsic volcanic islands with implications for Precambrian greenstone-belt volcanoes. Geol. Assoc. Can., Short course notes, vol. 2, Winnipeg: 71-131.

Sigvaldson, G.E., 1968: Structure and products of subaquatic volcanoes in Iceland. Contr. Mineral. and Petrol. 18: 1-16.

Sparks, R.S.J., 1976: Grain size variations in ignimbrites and implications for the transport of pyroclastic flows. Sedimentology 23: 147-188.

Stephansson, O., 1977: Granite diapirism in Archean rocks. J. Geol. Soc. Lond., vol. 133: 357-361.

Thompson, P.H., 1978: Archean regional metamorphism in the Slave structural Province- a new perspective on some old rocks. In J.A.Fraser and W.W. Heywood (Eds.) Metamorphism in the Canadian Shield, Geol. Surv. Can. Pap. 78-10: 85-102.

Turner, F.J., 1981: Metamorphic petrology, McGraw-Hill, New York.

Walker, G.P.L. and Croasdale, R., 1970: Characteristics of some basaltic pyroclastics. Bull. Volc. 35: 303-317.

Winkler, H.G.F., 1974: Petrogenesis of Metamorphic Rocks. Third edition. Springer-Verlag, New York: 320p.

Woodland, B.G., 1982: Gradational development of domainal slaty cleavage, its origin and relation to chlorite porphyroblasts in the Martinsburg Formation, E. Pennsylvania. Tectonophysics, vol. 82: 89-124.

Wright, J.V., Smith, A.L. and Self, S., 1980: A working terminology of pyroclastic deposits. Jour. Volc. and Geotherm. Res. 8: 315-336.

Young, G., 1978: Some aspects of the evolution of Archean crust, Geoscience canada no. 5: 140-149.

# Appendix A

# APPENDICES

APPENDIX 1:

Mineralogy of rock samples. The types of minerals present are indicated ( -abundant; -few) and, where known, the time of growth with respect to deformation is shown.

APPENDIX 2:

XRF analyses of samples from rock units 1, 2a, 2b and 5.

| | SAMPLE NO | CHLORITE | MUSCOVITE | BIOTITE | EPIDOTE GP | GARNET | AMPHIBOLE | TOURMALINE | OPAQUES | CARBONATE | QUARTZ | PLAGIOCLASE |
|---|---|---|---|---|---|---|---|---|---|---|---|---|
| UNIT 4 | 32-1 | ✓ $S_2$ | ✓ $S_2,S_3$ | | | | | | ✓ $S_3$? | | ✓ .02 mm | |
| | 10-1a | | ✓ $S_2$ | | | | | | | ✓ | ✓ .01 mm | |
| | 10-1b | ✓ R | ✓ $S_2$ | (✓) .01-.02 mm | | | | | ✓ $S_3$? | ✓ | ✓ .01-.02 mm | |
| | 10-4 | | ✓ post $S_2$ $S_1$ | | ✓ | | | | ✓ | ✓ | ✓ .02 mm | |
| | 32-7 | ✓ | ✓ $S_2$ | | ✓ | | | | | | ✓ .02 mm | |
| | 27-3 | ✓ R | ✓ $S_2$? | | | | | (✓) | | | ✓ .03 mm | |
| | 15-6a | ✓ R | | | ✓ | | | | | | ✓ .02 mm | |
| | 25-10 | ✓ R | ✓ $S_2$ | | | | | | | | ✓ .03 mm | |
| | 15-24 | | ✓ | | | | | | ✓ | | ✓ .02 mm | |
| | 30-2b | ✓ R, $S_3$ | ✓ $S_2$ | | | | | | | ✓ | ✓ .03 mm | |
| | 78-34 | | ✓ $S_3$ | ✓ .03-.05 mm | | | | ✓ | | | ✓ .04 mm | |
| UNIT 3 | 32-23 | ✓ $S_3$ | | | ✓ | | | | | ✓ | ✓ .01-.02 mm | |
| | 25-12 | ✓ | | | | ✓ | ✓ | | ✓ | ✓ | ✓ | |
| | 25-15b | ✓ R | | ✓ $S_3$ .02-.03 mm | | | | | ✓ | ✓ | ✓ .01 mm | |
| | 74-18 | ✓ R | ✓ post $S_3$ | ✓ .02-.03 mm | ✓ | | ✓ ANTHOPHYLLITE | | ✓ | ✓ | ✓ .03 mm | |
| | 25-26 | ✓ | | ✓ $S_3$, post $S_3$ .05 mm | ✓ | ✓ | ✓ | | | | ✓ .03 mm | |
| | 12-9a | ✓ | | ✓ $S_3$ .02-.05 mm | | | ✓ | | ✓ $S_3$ | ✓ | ✓ .04 mm | |
| | 12-14a | ✓ $S_3$ | | | | ✓ post $D_3$, pre D | | | ✓ | | ✓ | |
| | 12-14 | ✓ $S_3$ | | ✓ $S_4$ .05-.1 mm | | ✓ post $D_3$ | ✓ | | | | ✓ .03-.04 mm | |
| | 31-3 | | | ✓ .03 mm $S_3$, .15 mm post $S_3$ | | ✓ | ✓ | | | (✓) | ✓ .04 mm | |
| | 26-5 | ✓ post $S_3$ | | ✓ .02-.03 mm $S_3$, .1 mm post $S_3$ | (✓) | ✓ | ✓ ANTHOPHYLLITE | | ✓ | ✓ | ✓ .03 mm | |

APPENDIX 1: Mineralogy of rock samples. The types of minerals present are indicated ( -abundant; -few) and, where known, the time of growth with respect to deformation (S2, S3, post S3, S4) is shown. Also biotite types (A, B, C) are indicated.

| | SAMPLE NO. | CHLORITE | MUSCOVITE | BIOTITE | EPIDOTE GP. | GARNET | AMPHIBOLE | TOURMALINE | OPAQUES | CARBONATE | QUARTZ | PLAGIOCLASE |
|---|---|---|---|---|---|---|---|---|---|---|---|---|
| UNIT 3 | 23-20 | | ✓ | .04mm $S_3$, .1-.15mm post $S_3$ | ✓ | | | | ✓ $S_3$ | ✓ | ✓ .04 mm | |
| | 26-22 | ✓ | | ✓ $S_3$, post $S_3$ | ✓ | (✓) | | | | | ✓ $S_3$ trails in garnet | |
| | 31-46 | ✓ | ✓ | | ✓ | ✓ post $S_3$ | ✓ actinolite, hornblende | | | ✓ | ✓ .05-.07 mm | ✓ |
| | 23-27b | | | | | ✓ | ✓ | | ✓ | ✓ | ✓ .06 mm | |
| | 35-27 | ✓ R | | ✓ $S_3$ .07-.1mm, $S_4$ | | ✓ post $S_3$ | ✓ anthophyllite actinolite ?$S_3$ | | | | ✓ .04 mm | |
| | 36-21 | | ✓ | | | ✓ post $S_3$ | ✓ hornblende | | ✓ | | ✓ .08-.1 mm | |
| | 36-56 | | | | | | ✓ hornblende | | ✓ | | ✓ .07 mm | |
| | 43-40 | | | ✓ $S_3$ .05-.1 mm, $S_4$ .1 mm | ✓ | ✓ post $S_3$ | ✓ | | | | ✓ .01 mm | ✓ |
| UNIT 2 | 74-7 | ✓ $S_3$ | ✓ $S_3$ | | | | | | ✓ $S_3$ | ✓ | | |
| | 73-9 | ✓ R | ✓ $S_3$ | (✓) post $S_3$ | ✓ | | | | | ✓ | ✓ .03 mm | |
| | 64-8 | ✓ | (✓) $S_3$ | ✓ $S_3$ .05mm | ✓ | | | | ✓ | ✓ | ✓ | |
| | 64-7 | | (✓) $S_3$ | $S_3$ .05-.07mm post $S_3$ .1mm | ✓ | | | | ✓ | ✓ | ✓ .03 mm | |
| | 20-43a | | | $S_3$ .05-.07 post $S_3$ .07mm | | | ✓ $S_3$? + random hornblende | | | | | |
| | 34-44 | ✓ R | | $S_3$ .05 mm post $S_3$ .1-.2 mm | | | ✓ | | ✓ | ✓ | ✓ .02 mm | |
| | 64-5 | ✓ $S_3$ | | ✓ $S_3$ .05-.1mm | | | hornblende actinolite - $S_3$ | | | | ✓ .02-.03 mm | |
| | 30-7 | | ✓ $S_3$ | ✓ $S_3$ .05mm | ✓ | | | | | ✓ | ✓ .04-.05 mm | |
| | 59-9 | | (✓) | | | | hornblende actinolite | | ✓ | ✓ | ✓ .02-.03 mm | ✓ |
| | 71-6 | ✓ | .1-.2 mm ✓ | $S_3$ .05 mm post $S_3$ .1mm | (✓) | | | | | | ✓ .03 mm | |
| | 31-18 | | $S_3$ .05-.1 post $S_3$ .2 mm | $S_3$ .02-.1 mm post $S_3$ .1 mm | (✓) | | | | | ✓ | ✓ .03 mm | |
| | 67-14 | | | $S_3$ .06 mm post $S_3$ .1mm | ✓ | | ✓ hornblende | | | | ✓ | |
| | 42-31 | (✓) $S_3$ + post $S_3$ | ✓ | $S_3$ .02-.03mm post $S_3$ .1mm | ✓ | (✓) | ✓ | (✓) | ✓ | ✓ | ✓ .03 mm | |

APPENDIX I: cont'd.

| Unit | SAMPLE NO. | CHLORITE | MUSCOVITE | BIOTITE | EPIDOTE GP. | GARNET | AMPHIBOLE | SPHENE/ TOURMALINE | OPAQUES | CARBONATE | QUARTZ | PLAGIOCLASE |
|---|---|---|---|---|---|---|---|---|---|---|---|---|
| UNIT 2 | 23-25 | ✓ $S_3$, R | | ✓ $S_3$ .1 mm | | | ✓ | | | | ✓ .05 mm | ✓ plagioclase |
| UNIT 2 | 23-27 | ✓ | | $S_3$ .07-.1 mm post $S_3$ .1 mm | (✓) | ✓ | (✓) hornblende | | | ✓ | ✓ .07 mm | |
| UNIT 2 | 78-34 | | ✓ $S_3$ | ✓ ≥.1 mm | (✓) | | (✓) | tourmaline | | | ✓ .04 mm | |
| UNIT 2 | 51-3 | ✓ | ✓ | $S_3$ .08 mm post $S_3$ .1 mm | | | | | | ✓ | ✓ .05 mm | |
| UNIT 2 | 37-9 | ✓ | ✓ $S_3$, post $S_3$ | $S_3$ .05 mm; post $S_3$ .1 mm | (✓) | ✓ | | | | | ✓ .05 mm | |
| UNIT 2 | 49-22 | ✓ | ✓ $S_3$ | ✓ $S_3$ .05-.1 mm | | | | tourmaline | ✓ | ✓ | ✓ .02-.07 mm | |
| UNIT 2 | 49-10 | ✓ | ✓ $S_2$? | ✓ $S_3$ .06 mm | | | | | | | ✓ .06 mm | |
| UNIT 2 | 48-4a | ✓ $S_3$ | ✓ | ✓ $S_3$ ≥.1 mm | | | | | | ✓ | ✓ .06 mm | |
| UNIT 2 | 39-13 | ✓ R | ✓ | ✓ $S_3$ ≥.1 mm | | | | | | ✓ | ✓ .06 mm | |
| UNIT 1 | 12-19 | ✓ | ✓ $S_3$, post $S_3$ | $S_3$ .02-.04 post $S_3$ .1-.2 mm | | (✓) | | tourmaline | ✓ | ✓ | ✓ .05-.1 mm | |
| UNIT 1 | 30-8 | ✓ $S_3$ .03 mm | ✓ post $S_3$ | | | | | | | | ✓ | |
| UNIT 1 | 55-13 | ✓ post $S_3$ | | $S_3$ .05-.1 mm post $S_3$ .1-.15 | | | ✓ | | ✓ | | ✓ .05 mm | |
| UNIT 5 | 35-37 | | | ✓ post $S_3$ .1 mm | | | hornblende, minor actinolite | sphene | ✓ $S_3$ | (✓) | ✓ .04 mm | .1 mm |
| UNIT 5 | 47-21 | ✓ $S_3$ | | ✓ post $S_3$ | (✓) | | hornblende actinolite? | | ✓ $S_3$ | | ✓ | ✓ |
| UNIT 5 | 78-25 | | | $S_3$ .02-.04 mm post $S_3$ .1 mm | | | hornblende, actinolite? | | ✓ $S_3$ | ✓ | ✓ | albite |
| UNIT 5 | 78-20 | | | $S_3$ .05-.1 mm post $S_3$ .15 mm | ✓ | | hornblende | (sphene) | ✓ $S_3$ | ✓ | ✓ .02-.05 mm | |
| UNIT 5 | 42-21 | ✓ R | ✓ | ✓ post $S_3$ .1-.2 mm | ✓ | ✓ | hornblende, grunerite? | | ✓ | ✓ | ✓ .03-.05 mm | ✓ albite .1 mm |
| UNIT 5 | 53-8 | (✓) R | | $S_3$ .03-.05 mm post $S_3$ .1-.15 | | | hornblende | | ✓ | ✓ | ✓ .02-.06 mm | |
| UNIT 5 | 42-16 | (✓) | | $S_3$ .05-.1 post $S_3$ .2-.5 mm | | ✓ post $S_3$ | hornblende actinolite? | | ✓ $S_3$ | ✓ | ✓ .07 mm | ✓ albite |
| UNIT 5 | 35-41 | | | | ✓ | ✓ post $S_3$ | hornblende | | ✓ $S_3$ | ✓ | ✓ inclusion trails in [illegible] | |
| UNIT 5 | 35-6 | | (✓) post $S_3$ | $S_3$ .02-.05 mm post $S_3$ .1-.3 mm | | | ✓ hornblende | | ✓ $S_3$ | ✓ | ✓ .02-.06 mm | ✓ albite .1 mm |

APPENDIX I: cont'd.

| | SAMPLE NO. | CHLORITE | MUSCOVITE | BIOTITE | EPIDOTE GP. | GARNET | AMPHIBOLE | SPHENE/ TOURMALINE | OPAQUES | CARBONATE | QUARTZ | PLAGIOCLASE |
|---|---|---|---|---|---|---|---|---|---|---|---|---|
| UNIT 5 | 35-5 | ✓ A | | | | | actinolite? | | ✓ $S_3$ ? | ✓ | ✓ .06 mm | ✓ oligoclase |
| | 37-2 | ✓ A | | | | ✓ | actinolite? | | ✓ $S_3$ ? | | | |
| | 40-48 | | | ✓ .05-.1 mm | ✓ | ✓ | hornblende | sphene | ✓ $S_3$ | ✓ | ✓ | (✓) |
| | 39-39 | ✓ $S_3$ | | | ✓ | | hornblende grunerite | | ✓ $S_3$ | | ✓ .10 mm | (✓) |
| | 39-16 | ✓ $S_3$ | | | ✓ | ✓ post $S_3$ | hornblende anthophyllite actinolite $S_3$ | ✓ post $S_3$ | ✓ $S_3$ | | | |
| | 37-22 | | | ✓ post $S_3$ .1mm | | | | | ✓ $S_3$ | | ✓ .05 mm | ✓ oligoclase |
| | 25-12 | ✓ | | | | | hornblende (actinolite) | | ✓ | | ✓ .05 mm | |
| | 37-3 | ✓ | | $S_3$ .1-.2 mm post $S_3$ | (✓) | | actinolite anthophyllite | | | | ✓ .02-.05 mm | ✓ .07 mm |
| | 78-32 | | $S_3$, post $S_3$ | $S_3$ .03 mm post $S_3$ .06-.1mm | ✓ | | actinolite | | | ✓ | ✓ .05 mm | |
| UNIT 6 (SUB BIOTITE ZONE) | 77-25 | ✓ $S_3$ | ✓ $S_3$ | | | | | tourmaline | ✓ | | ✓ | |
| | 24-32a | | ✓ $S_3$ .03 mm | | | | | | ✓ | ✓ | ✓ .02-.03 mm | |
| | 24-32b | ✓ | ✓ $S_3$ | | | | | | ✓ | ✓ | ✓ | |
| | 62-2 | ✓ | ✓ $S_3$ | | | | | | ✓ | | ✓ | |
| | 25-24 | | $S_3$ .01 mm $S_4$ | | | | | (tourmaline) | ✓ | | ✓ .02 mm | |
| | 60-14 | ✓ | ✓ $S_3$ | | | | | | | | ✓ | |
| | 29-1 | ✓ | ✓ $S_2/S_3$ | | | | | | ✓ | | ✓ | |
| | 60-15 | ✓ $S_3$ .007 | ✓ $S_3$ .01 mm | | | | | | ✓ | | ✓ .01 mm | |
| | 60-15b | | ✓ $S_2$? | | | | | | | | ✓ | |
| | 76-21 | ✓ | ✓ $S_3$ | | | | | | ✓ | | ✓ | |
| | 18-39b | ✓ $S_2$ ? | ✓ $S_2$ ? | | | | | | ✓ | | ✓ | |
| | 77-27 | ✓ | ✓ $S_3$ | | | | | | | ✓ | ✓ | |

APPENDIX I: cont'd.

| Zone | SAMPLE NO. | CHLORITE | MUSCOVITE | BIOTITE | CORDIERITE | GARNET | ANDALUSITE | TOURMALINE | OPAQUES | CARBONATE | K-FELDSPAR/QUARTZ | PLAGIOCLASE |
|---|---|---|---|---|---|---|---|---|---|---|---|---|
| UNIT 6 (SUB BIOTITE ZONE) | 19-37 | | ✓ | | | | | | | | ✓ | |
| | 19-33 | | ✓ $S_2$? | | | | | | | ✓ | ✓ .02 mm | |
| | 69-5 | | ✓ $S_2$ | | | | | | ✓ | | ✓ | |
| | 64-1 | ✓ $S_3$ | ✓ $S_2$ | | | | | | ✓ | | ✓ | |
| | 18-35 | | ✓ $S_2$ | | | | | | | | ✓ .02 mm | |
| | 15-4 | | ($S_2$) $S_3$ .03 mm | | | | | | ✓ | | ✓ | |
| | 18-37 | | ✓ | | | | | | | | ✓ | |
| | 60-1 | ✓ | ✓ $S_2$ | | | | | | | ✓ | ✓ | |
| | 8-6 | (✓) $S_3$ | ✓ $S_3$ .01-.02 mm | | | | | | | | ✓ .01 mm | |
| | 22-2 | | $S_3$ ($S_2$) .01 mm | | | | | | | | ✓ $S_3$ .01-.02 mm | |
| HIGHER GRADE ← UNIT 6 (WESTERN BIOTITE ZONE) → LOWER GRADE | 60-12 | ✓ $S_3$ | | B 0.05 mm | | | | | ✓ | | ✓ | |
| | 70-20 | ✓ $S_3$, R | ✓ $S_3$ | B 0.1 mm $S_3$ | | | | | ✓ | | ✓ | |
| | 77-17 | ✓ $S_3$ | ✓ $S_3$ | A .1-.2 mm $S_3$; B .03 mm $S_3$ | | | | | ✓ | | ✓ | |
| | 76-11 | | ✓ $S_3$ | B .1 mm $S_3$; C .15 mm $S_3$ | | | | | ✓ | | ✓ | |
| | 76-13 | ✓ R | ✓ $S_3$ | A .2-.5 mm $S_3$; B .2 mm $S_3$ | | | | | ✓ | | ✓ | |
| | 77-18 | ✓ $S_3$ | ✓ $S_3$ | A .09-.12 mm $S_3$ | | | | | ✓ | | ✓ | |
| | 62-8 | | ✓ $S_3$ | B .04 mm $S_3$; C .09 mm $S_4$ | | | | | ✓ | | ✓ | |
| | 77-21 | | ✓ $S_3$ | B .05 mm $S_3$ | | | | | ✓ | | ✓ | |
| | 60-3 | ✓ | ✓ $S_3$ | B .04 mm $S_3$; C .07 mm $S_4$ | | | | | ✓ | | ✓ | |
| | 70-26 | | ✓ | C .1 mm $S_4$ | | | | | ✓ | | ✓ | |
| | 69-14 | | ✓ $S_3$ | B .03 mm $S_3$ | | | | | ✓ | | ✓ | |

APPENDIX I: cont'd.

LOWER GRADE ← UNIT 6 (EASTERN BIOTITE ZONE) → HIGHER GRADE

| SAMPLE NO. | CHLORITE | MUSCOVITE | BIOTITE | CORDIERITE | GARNET | ANDALUSITE | TOURMALINE | OPAQUES | CARBONATE | K-FELDSPAR/ QUARTZ | STAUROLITE |
|---|---|---|---|---|---|---|---|---|---|---|---|
| 63-14 | ✓ $S_3$ .05 mm | (✓) | B .03-.1 mm $S_3$ | | | | | ✓ | | ✓ .03 mm | |
| 72-11 | | ✓ $S_3$ .03-.04 mm | A .2-.5 mm post $S_3$; B .06 mm $S_3$; C .1-.2 mm $S_4$ | | | | | ✓ | | ✓ .03 mm | |
| 75-16 | | ✓ $S_3$ | A .25 mm; B .04, $S_3$ post $S_3$; C .07 mm, $S_4$ | | | | | ✓ $S_3$ | | ✓ | |
| 75-9 | | ✓ $S_3$ | B .02 mm $S_3$; C .06 mm $S_4$ | | | | | ✓ | | ✓ | |
| 75-10 | ✓ $S_3$, R | ✓ $S_3$ | | | ✓ | | | ✓ | | ✓ .03 mm | |
| 61-3 | | ✓ $S_3$ | B .03 mm $S_3$ | | | | | ✓ $S_3$ | | ✓ | |
| 59-5 | | ✓ $S_3$ .03 mm | B .02 mm $S_3$ | | | | ✓ | ✓ | | ✓ .02 mm | |
| 59-3 | ✓ $S_3$? | ✓ $S_3$? | B .01-.03 mm | | | | | ✓ | | ✓ | |
| 65-3 | ✓ $S_2$, R | ✓ $S_3$ | B $S_3$; C post $S_3$ | | | | | ✓ | ✓ | ✓ .03 mm | |
| 18-32 | ✓ | | C .05 mm | | | | | ✓ | ✓ | ✓ | |
| 18-29 | ✓ $S_3$ | ✓ $S_3$ | C .05-.1 mm post $S_3$ | | ✓ | | | ✓ | | ✓ | |
| 18-12 | ✓ R | ✓ | B .03 mm | | | | | | ✓ | .03 mm ✓ | ✓ |
| 72-20 | ✓ | ✓ $S_3$ | C .04 mm post $S_3$ | | | | | ✓ | | ✓ | |
| 67-4 | | ✓ $S_3$ .01-.02 mm | B .05 mm $S_3$; C .03 mm $S_4$ | | | | | | | ✓ .01-.02 mm | |
| 72-7 | | ✓ | C .05-.1 mm | | | | | ✓ | | ✓ | |
| 75-20 | | ✓ $S_3$ | C .04 mm post $S_3$ | | | | | ✓ | | ✓ | |
| 64-2 | | ✓ $S_3$ | C .04-.08 mm post $S_3$ | | | | | ✓ | | ✓ | |
| 72-23 | | ✓ $S_3$ | C .02 mm post $S_3$ | | | | | ✓ | | ✓ | |
| 59-1 | | ✓ $S_3$ .03 mm | C .07 mm post $S_3$ | – | | | | ✓ | | ✓ .03 mm | |
| 50-9 | ✓ | (✓) | B 0.3 mm $S_3$; C 0.2 mm $S_4$ | ✓ | | | | ✓ | | ✓ | |
| 50-9a | | (✓) | B .25-.5 $S_3$; C .3 mm $S_4$ | ✓ | | | | | | ✓ | |

APPENDIX I: cont'd.

HIGHER GRADE ← UNIT 6 (EASTERN CORDIERITE ZONE) → LOWER GRADE

| SAMPLE NO. | CHLORITE | MUSCOVITE | BIOTITE | CORDIERITE | GARNET | ANDALUSITE | TOURMALINE | OPAQUES | PLAGIOCLASE | K-FELDSPAR/ QUARTZ | STAUROLITE |
|---|---|---|---|---|---|---|---|---|---|---|---|
| 41-31 | ✓ | ✓ .08 mm | C ✓ .1-.2 mm | ✓ | | ✓ | (✓) | | (✓) | ✓ .13 mm | |
| 41-32 | ✓ R | ✓ $S_4$ | C ✓ $S_4$ | ✓ | | | | | | ✓ | ✓? |
| 46-12 | | ✓ $S_3$ | B .2 mm | | | | | | | ✓ | |
| 46-13 | | ✓ $S_3$ | C .5 mm | ✓ | | | | | | ✓ | |
| 44-5 | ✓ R | | B .15 mm $S_3$<br>C .2 mm $S_4$ | | | ✓ $S_3$ | | ✓ | | ✓ | |
| 44-5b | ✓ R | ✓ $S_3$ | B .1 mm $S_3$<br>C .2 mm $S_4$ | ✓ | | | | | | ✓ | |
| 46-3 | ✓ R | ✓ $S_3$ | B .1 mm $S_3$ | ✓ | | | | | | ✓ | |
| 41-43c | | (✓) | B .06 mm $S_3$<br>C .1 mm $S_4$ | (✓) | | ✓ $S_3$ | ✓ | ✓ | | ✓ | |
| 46-10 | | | B .02-.04 $S_3$<br>C .05 mm $S_4$ | ✓ | | | ✓ | ✓ | | ✓ | |
| 39-30 | (✓) | | B .1 mm<br>C .1 mm | ✓ | | | | | | ✓ | |
| 39-29 | ✓ G | | C .07 mm | ✓ | | | | ✓ | | ✓ | |
| 39-27 | ✓ R | ✓ $S_4$ | C .04 mm $S_4$ | ✓ | | | | | | ✓ | |
| 41-3 | ✓ R | ✓ $S_3$ | C .08-.1 mm post $S_3$, $S_4$ | ✓ | | | | ✓ | | ✓ | |
| 46-14 | ✓ R | ✓ | B .25 mm $S_3$<br>C .15-.3 mm $S_4$ | ✓ | | | | ✓ | | ✓ | |
| 35-45a | | (✓) | B .05-.1 mm $S_3$ | ✓ | | | | | | ✓ | |
| 49-33 | | (✓) $S_3$ | B .08-.1 mm $S_3$ | | | | | | | ✓ | |
| 44-33b | | ✓ $S_3$ | C .25-.3 mm $S_4$ | | | | | | | ✓ | |
| 56-15 | | | B .1-.25 mm $S_3$? | | ✓ | | | ✓ | | ✓ | |
| 56-4 | ✓ R | ✓ R | B $S_3$<br>C $S_4$ | | | | | | | ✓ | ✓? |
| 56-3 | ✓ R | (✓) $S_3$ | B .1 mm $S_3$<br>C .05 mm $S_4$ | ✓ | | | | ✓ | | ✓ .03-.06 mm | |
| 56-8 | | ✓ $S_3$ | B $S_3$ | | | | | ✓ | | ✓ | |

APPENDIX I: cont'd.

| SAMPLE NO. | CHLORITE | MUSCOVITE | BIOTITE | CORDIERITE | GARNET | ANDALUSITE | AMPHIBOLE/ TOURMALINE | OPAQUES | PLAGIOCLASE | K-FELDSPAR/ QUARTZ | STAUROLITE |
|---|---|---|---|---|---|---|---|---|---|---|---|
| 40-28 | ✓ | ✓ $S_3$ * | B .1 mm | | | ✓ $S_3$ | | ✓ $S_3$ | | ✓ | ✓ ? |
| 63-9 | ✓ | | C .05-.1 mm | | | | | | | ✓ | |
| 63-11 | ✓ | | C .1-.2 mm | | | | | ✓ | | ✓ | |
| 33-24 | | ✓ $S_3$ | B $S_3$ C .05-.1 mm $S_3$ | ✓ | | | tourmaline ✓? | | | ✓ | |
| 75-15 | ✓ | (✓) $S_3$ | B .25 mm $S_3$ C .1 mm | ✓ | | | | ✓ | | ✓ | |
| 63-12a | ✓ | | B .07 mm $S_3$ | | | | | ✓ | | ✓ | |
| 7-2 | | (✓) | ✓ B $S_3$ | ✓ | | | | | | ✓ | |
| 3-4 | | | B ✓ $S_3$ | ✓ | | (✓) | | | (✓) | ✓ | |
| 3-5a | | | C .1-.2 mm $S_4$ | ✓ | | | | | ✓ oligoclase/albite | ✓ | |
| 3-5b | | | B .2 mm $S_3$ C .2 mm $S_4$ | | ✓ | | | | ✓ oligoclase/albite | ✓ | |
| 3-6 | | | B .15-.3 mm $S_3$ C .15-.3 mm $S_4$ | ✓? | | | | | | ✓ | |
| 3-14 | | ✓ $S_4$ | C .15-.1 mm $S_4$ | (✓) | | | | | ✓ oligoclase | ✓ | } |
| 2-34 | (✓) | | C $S_4$ | | ✓ | | | ✓ | | ✓ | } |
| 2-12 | | | (✓) | | | | cummingtonite/ hornblende | ✓ | ✓ andesine | ✓ | |
| 1-7 | | | C .15 mm $S_4$ | (✓) | ✓ | | | | (✓) | ✓ | |
| 7-5 | | | C .15 mm $S_4$? | (✓) | | | | ✓ | ✓ oligoclase | ✓ | |
| 77-2 | | ✓ $S_3$ | B .06 mm $S_3$ | | | ✓ | | ✓ | (✓) | ✓ | |
| 1-12a | | | ✓ .25 mm | ✓ | | | | ✓ | | ✓ | |
| 1-27 | | | C .2 mm $S_4$? | ✓ | | | | | | ✓ | |
| 1-23 | ✓ R | | | | | | — | ✓ | | ✓ | |
| 1-18 | | | .10 mm $S_4$? | | | | | ✓ | | ✓ | |

LOWER GRADE ←— UNIT 6 (WESTERN CORDIERITE ZONE) —→ HIGHER GRADE

APPENDIX I: cont'd.

| SAMPLE NO | CHLORITE | MUSCOVITE | BIOTITE | CORDIERITE | GARNET | AMPHIBOLE | TOURMALINE | OPAQUES | CARBONATE | K-FELDSPAR/ QUARTZ | STAUROLITE |
|---|---|---|---|---|---|---|---|---|---|---|---|
| 77-15 | ✓ | ✓ $S_3$ | A $S_2$ B $S_3$ | | | | | | | ✓ | |
| 4-16 | ✓ | ✓ | .25 mm | ✓ | | | | ✓ | | ✓ | |
| 70-8 | ✓ R | ✓ | C .15 mm $S_4$ | ✓ $S_4$ | / | | | ✓ | | ✓ | |
| 60-13 | ✓ R | | B .01-.02 mm C .06 mm | ✓ | | | | ✓ | | ✓ | |

APPENDIX II, cont'd.

Samples from unit 1:

| | | SAMP.NC. 84-6 | SAMP.NC. 84-7 | SAMP.NC. 84-5 |
|---|---|---|---|---|
| % | SIO2 | 66.45 | 62.13 | 74.50 |
| | AL2O3 | 12.33 | 16.00 | 10.91 |
| | FE2O3T | 4.73 | 9.08 | 4.16 |
| | MGO | 1.55 | 2.44 | 1.31 |
| | CAO | 5.55 | 4.55 | 3.01 |
| | NA2O | 3.34 | 0.38 | 2.07 |
| | K2O | 2.77 | 3.44 | 1.43 |
| | TIO2 | 0.58 | 0.63 | 0.70 |
| | P2O5 | 0.07 | 0.11 | 0.17 |
| | MNO | 0.09 | 0.12 | 0.11 |
| | S | 0.00 | 0.00 | 0.01 |
| PPM | BA | 379. | 185. | 193. |
| | CR | 4. | 58. | 8. |
| | ZR | 197. | 153. | 150. |
| | SR | 61. | 33. | 103. |
| | RB | 78. | 63. | 33. |
| | Y | 51. | 18. | 30. |
| | NB | 6. | 5. | 5. |
| | ZN | 129. | 73. | 77. |
| | NI | 0. | 46. | 0. |
| | TOTAL | 96.568 | 95.947 | 98.469 |
| RATIO | K/RB | 294.78 | 345.52 | 372.90 |
| | RB/SR | 0.98 | 1.90 | 0.32 |
| | BA/SR | 4.74 | 2.01 | 1.89 |

APPENDIX II: XRF analyses of samples from rock units 1, 2a, 2b, and 5.

Samples from unit 2a:

| | | SAMP.NO. 61-15 | SAMP.NO. 64-5 | SAMP.NO. 73-14 |
|---|---|---|---|---|
| % | SIO2 | 64.70 | 65.56 | 63.63 |
| | AL2O3 | 15.35 | 15.10 | 14.94 |
| | FE2O3T | 5.55 | 4.82 | 6.17 |
| | MGO | 1.68 | 2.18 | 1.96 |
| | CAO | 4.70 | 6.33 | 5.22 |
| | NA2O | 3.65 | 2.89 | 3.58 |
| | K2O | 1.75 | 0.70 | 0.39 |
| | TIO2 | 0.59 | 0.60 | 0.70 |
| | P2O5 | 0.12 | 0.09 | 0.13 |
| | MNO | 0.09 | 0.11 | 0.12 |
| | S | 0.00 | 0.00 | 0.03 |
| PPM | BA | 894. | 435. | 315. |
| | CR | 35. | 25. | 34. |
| | ZR | 236. | 159. | 205. |
| | SR | 318. | 391. | 247. |
| | RB | 50. | 18. | 7. |
| | Y | 22. | 20. | 28. |
| | NB | 8. | 7. | 10. |
| | ZN | 95. | 113. | 177. |
| | NI | 21. | 8. | 21. |
| | TOTAL | 98.391 | 98.517 | 96.999 |
| RATIO | K/RB | 297.97 | 341.04 | 539.45 |
| | RB/SR | 0.16 | 0.05 | 0.03 |
| | BA/SR | 2.82 | 1.14 | 1.28 |

APPENDIX II: cont'd.

Samples from unit 2a:

| | SAMP.NO. 5A-19 | SAMP.NO. 51-10 | SAMP.NO. 49-8A | SAMP.NO. 61-16DUP | SAMP.NO. 61-6 |
|---|---|---|---|---|---|
| % SIO2 | 61.93 | 65.70 | 68.60 | 64.19 | 65.98 |
| AL2O3 | 15.58 | 15.69 | 14.27 | 15.18 | 15.80 |
| FE2O3T | 6.27 | 4.15 | 5.44 | 5.49 | 4.66 |
| MGO | 1.95 | 1.73 | 1.03 | 1.66 | 2.02 |
| CAO | 5.22 | 4.56 | 1.18 | 4.67 | 4.20 |
| NA2O | 3.17 | 4.48 | 7.21 | 3.59 | 3.22 |
| K2O | 2.10 | 1.12 | 0.20 | 1.75 | 1.91 |
| TIO2 | 0.72 | 0.61 | 0.41 | 0.59 | 0.65 |
| P2O5 | 0.18 | 0.13 | 0.09 | 0.13 | 0.13 |
| MNO | 0.13 | 0.07 | 0.06 | 0.09 | 0.07 |
| S | 0.00 | 0.02 | 0.02 | 0.00 | 0.00 |
| PPM BA | 572. | 387. | 207. | 878. | 327. |
| CR | 21. | 21. | 3. | 35. | 35. |
| ZR | 196. | 210. | 311. | 203. | 211. |
| SR | 336. | 311. | 178. | 317. | 304. |
| RB | 55. | 33. | 1. | 41. | 44. |
| Y | 24. | 25. | 44. | 25. | 26. |
| NB | 7. | 8. | 8. | 6. | 7. |
| ZN | 96. | 102. | 117. | 112. | 126. |
| NI | 11. | 10. | 0. | 11. | 23. |
| TOTAL | 97.377 | 98.387 | 98.600 | 97.536 | 98.774 |
| RATIO K/RB | 316.53 | 282.07 | 999.99 | 353.93 | 368.89 |
| RB/SR | 0.16 | 0.11 | 0.00 | 0.13 | 0.14 |
| BA/SR | 1.70 | 1.25 | 1.16 | 2.77 | 1.08 |

APPENDIX II: cont'd.

Samples from unit 2b:

| | | SAMP.NO. 84-2 | SAMP.NO. 84-3 |
|---|---|---|---|
| % | SIO2 | 64.03 | 61.58 |
| | AL2O3 | 15.12 | 17.02 |
| | FE2O3T | 6.10 | 5.69 |
| | MGO | 2.08 | 2.25 |
| | CAO | 6.00 | 6.25 |
| | NA2O | 3.23 | 3.20 |
| | K2O | 0.74 | 1.06 |
| | TIO2 | 0.70 | 0.74 |
| | P2O5 | 0.10 | 0.12 |
| | MNO | 0.10 | 0.08 |
| | S | 0.01 | 0.02 |
| PPM | BA | 234. | 552. |
| | CR | 35. | 44. |
| | ZR | 205. | 247. |
| | SR | 244. | 344. |
| | RB | 14. | 43. |
| | Y | 24. | 27. |
| | NB | 7. | [illegible] |
| | ZN | 127. | 115. |
| | NI | 23. | 33. |
| | TOTAL | 98.332 | 98.165 |
| RATIO | K/RB | 471.13 | 204.41 |
| | RB/SR | 0.06 | 0.13 |
| | BA/SR | 0.96 | 1.46 |

APPENDIX II: cont'd.

Samples from unit 5:

| | | SAMP.NO. 47-5 | SAMP.NO. 55-8A | SAMP.NO. 54-11 |
|---|---|---|---|---|
| | SIO2 | 56.50 | 55.51 | 50.81 |
| | AL2O3 | 13.39 | 16.38 | 15.53 |
| | FE2O3T | 9.14 | 7.57 | 10.07 |
| | MGO | 3.97 | 4.78 | 6.19 |
| | CAO | 7.63 | 5.79 | 8.02 |
| | NA2O | 4.33 | 4.13 | 3.84 |
| | K2O | 0.09 | 0.58 | 0.69 |
| | TIO2 | 2.17 | 1.20 | 2.02 |
| | P2O5 | 0.07 | 0.65 | 1.19 |
| | MNO | 0.17 | 0.13 | 0.25 |
| | S | 0.00 | 0.01 | 0.01 |
| PPM | BA | 28. | 264. | 634. |
| | CR | 134. | 176. | 310. |
| | ZR | 133. | 230. | 258. |
| | SR | 245. | 433. | 710. |
| | RB | 0. | 14. | 7. |
| | Y | 30. | 36. | 43. |
| | NB | 6. | 3. | 9. |
| | ZN | 140. | 112. | 164. |
| | NI | 78. | 125. | 142. |
| | TOTAL | 97.609 | 97.600 | 98.899 |
| RATIO | K/RB | 999.99 | 431.50 | 952.64 |
| | RB/SR | 0.0 | 0.03 | 0.01 |
| | BA/SR | 0.11 | 0.61 | 0.85 |

APPENDIX II: cont'd.

# E.G.S. 1983-5 sheet "A"

MAP LEGEND

**9** PROTEROZOIC DIABASE DYKE (db)

ARCHEAN

**8** GRANITIC INTRUSION

**7** METAGABBRO DYKE/INTRUSIVE BODY

**6** TURBIDITE METASEDIMENT; GREYWACKE AND MUDSTONE

**5** BASALT/(ANDESITE)
- a. massive flow; $a_1$ layered dyke
- b. volcaniclastic rock
- c. pillowed flow
- d. pillowed breccia

**4** RHYOLITE/DACITE
- a. crystal tuff
- b. lithic-pumice tuff / deformed +/or welded tuff
- c. laminated tuff
- d. massive, phyric + aphyric dacite
- e. dacite breccia

**3** FELSIC TO INTERMEDIATE VOLCANICLASTIC ROCK
- a. tuffaceous sandstone, mudstone
- b. diamictite
- c. breccia
- d. conglomerate

**2** DACITE/(ANDESITE),
- a. massive, phyric; $a_1$ vesicular patches; $a_2$ clastic
- b. aphyric; $b_1$ clastic
- c. volcaniclastic rock
- d. pillowed flow; pillow breccia
- e. crumble breccia

**1** ANDESITE/BASALT
- a. massive flow
- b. pillowed flow
- c. pillow breccia

63° 00'

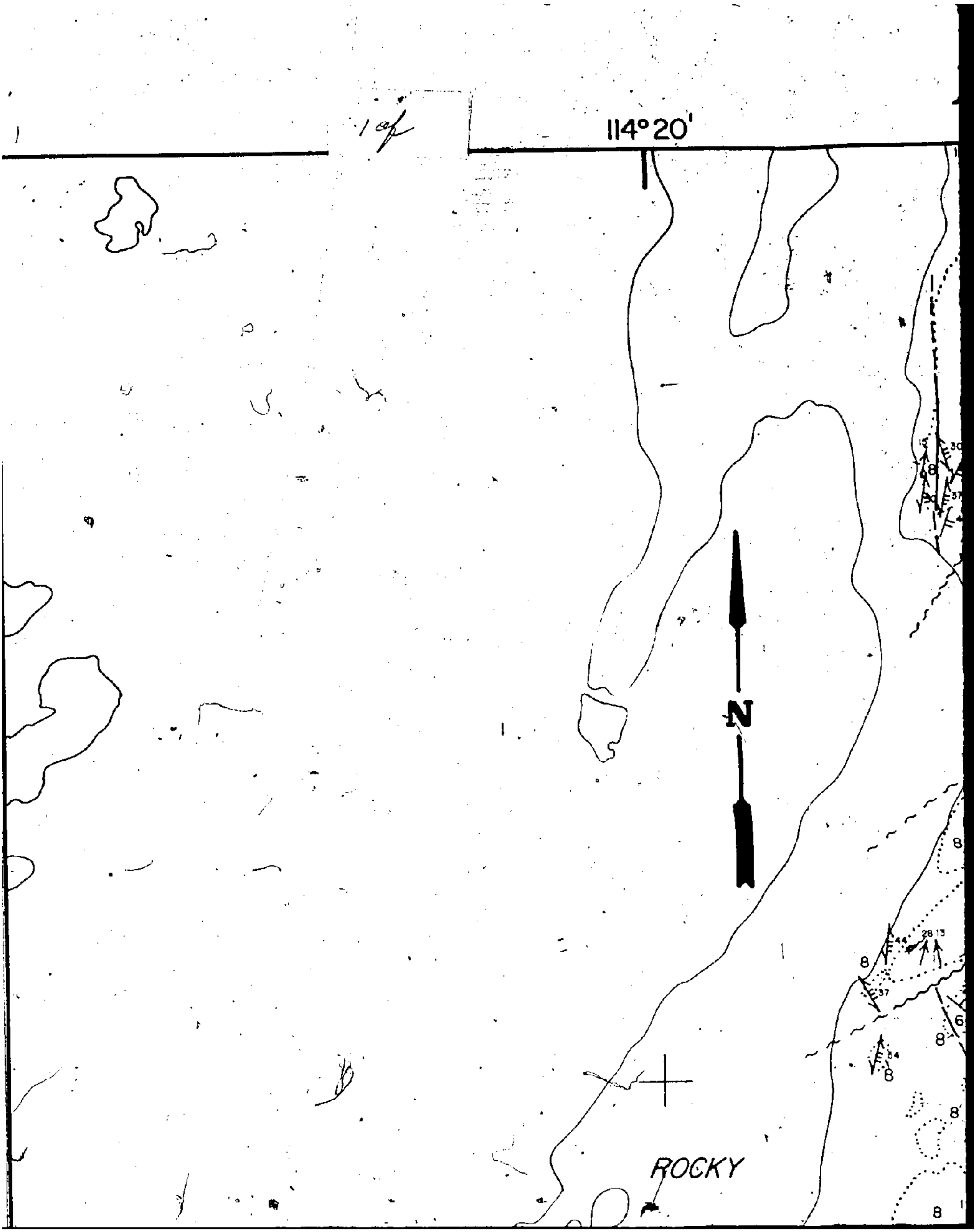
114° 20'
N
ROCKY

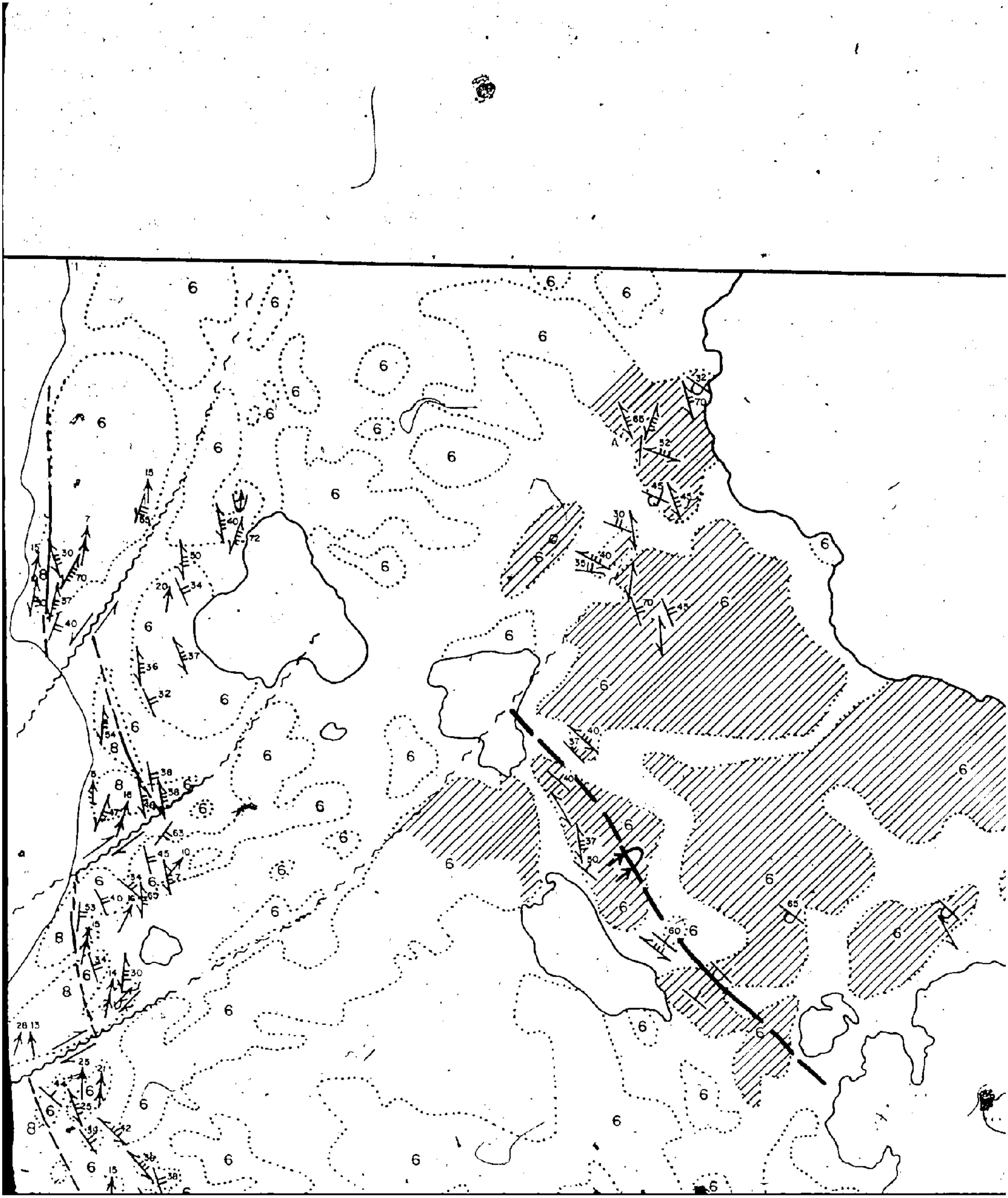

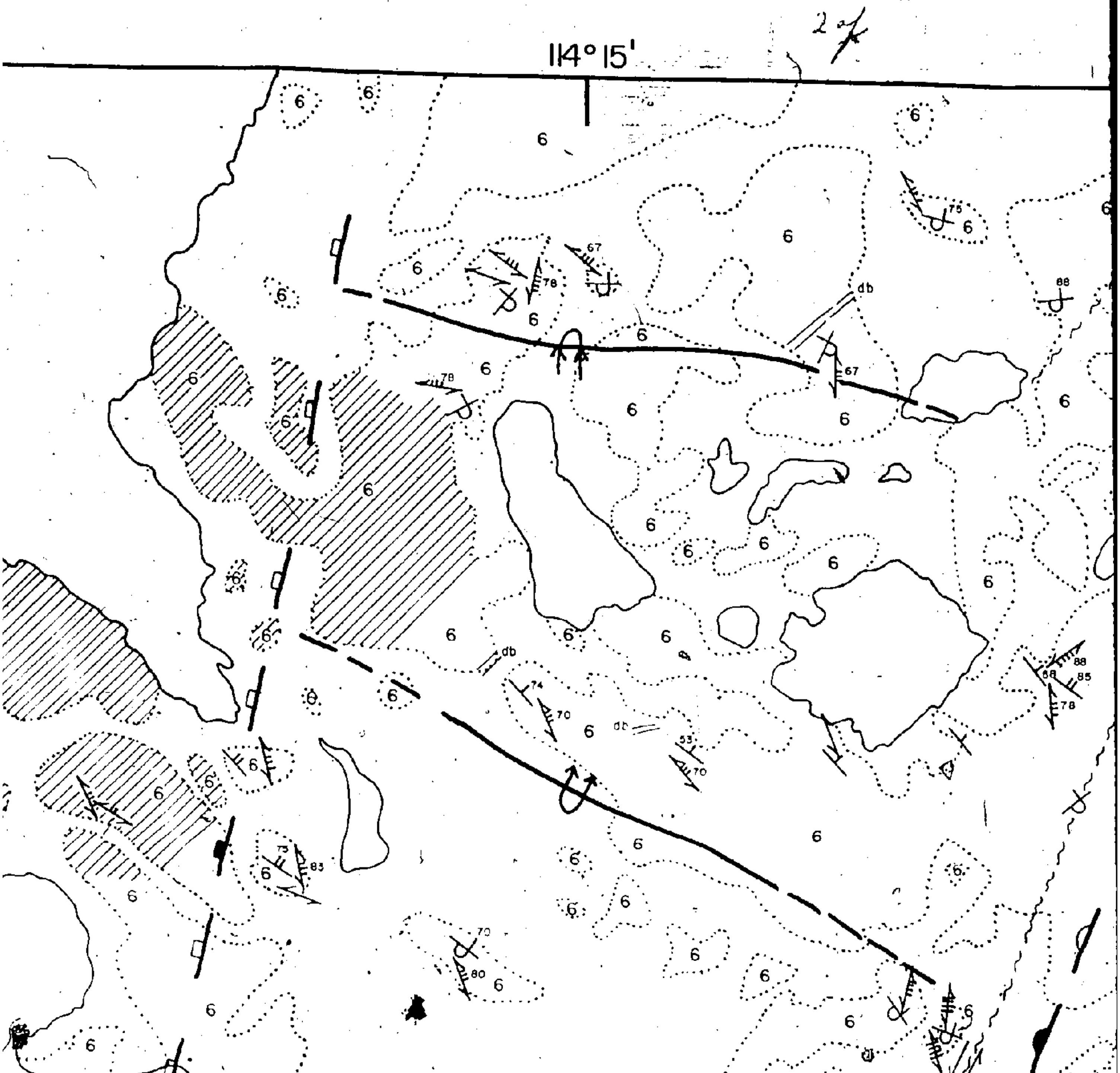
114° 15'
6
db
67
78
75
88
74
70
53
73
83
80
85

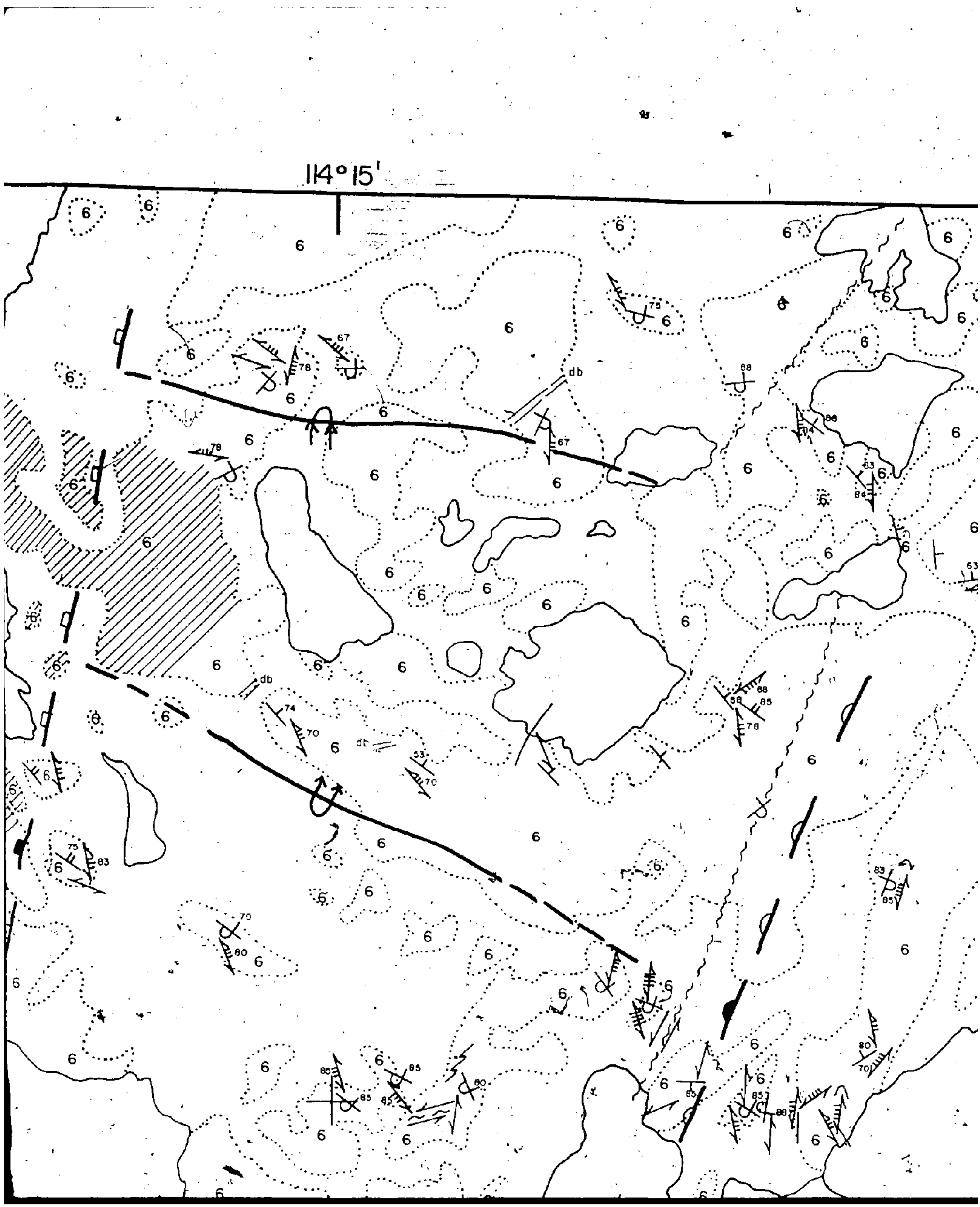
114°15'
db
db
db

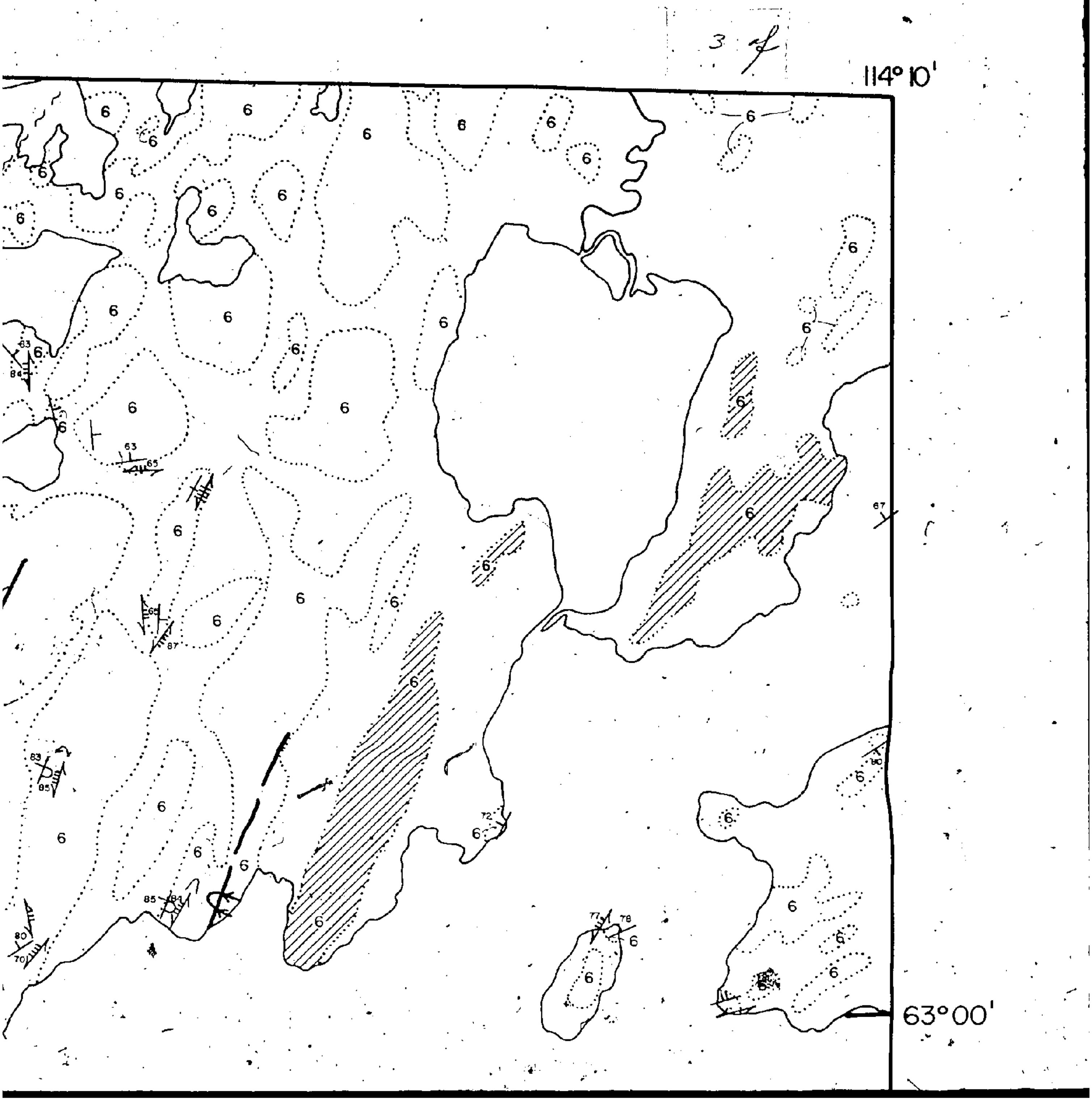
114° 10'
63°00'

48

d.. pillowed flow; pillow breccia
e. crumble breccia

| 1 | ANDESITE/BASALT

a. massive flow
b. pillowed flow
c. pillow breccia

## MAP SYMBOLS

GEOLOGICAL BOUNDARY

(defined, approximate, inferred)

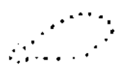

OUTCROP BOUNDARY

BEDDING, TOPS KNOWN

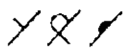

(inclined, overturned, pillowed)

BEDDING, TOPS UNKNOWN

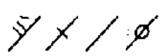

(inclined, vertical, dip unknown, pillowed)

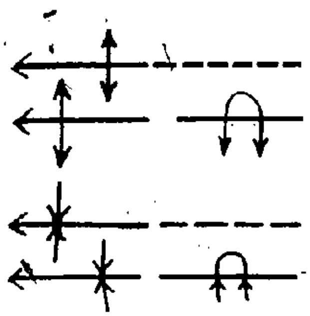

MAJOR FOLD: ANTICLINE, AXIAL TRACE

(defined, approximate) (arrowhead indicates facing direction)

(upright, overturned)

: SYNCLINE, AXIAL TRACE

(defined, approximate) (arrowhead indicates facing direction).

(upright, overturned)

MINOR FOLD

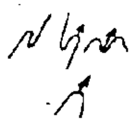

symmetry

symmetry unknown

FOLIATION:

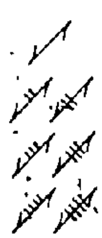

$S_1$ (inclined, vertical)

$S_2$ (inclined, vertical)

$S_3$ (inclined, vertical)

LINEATION

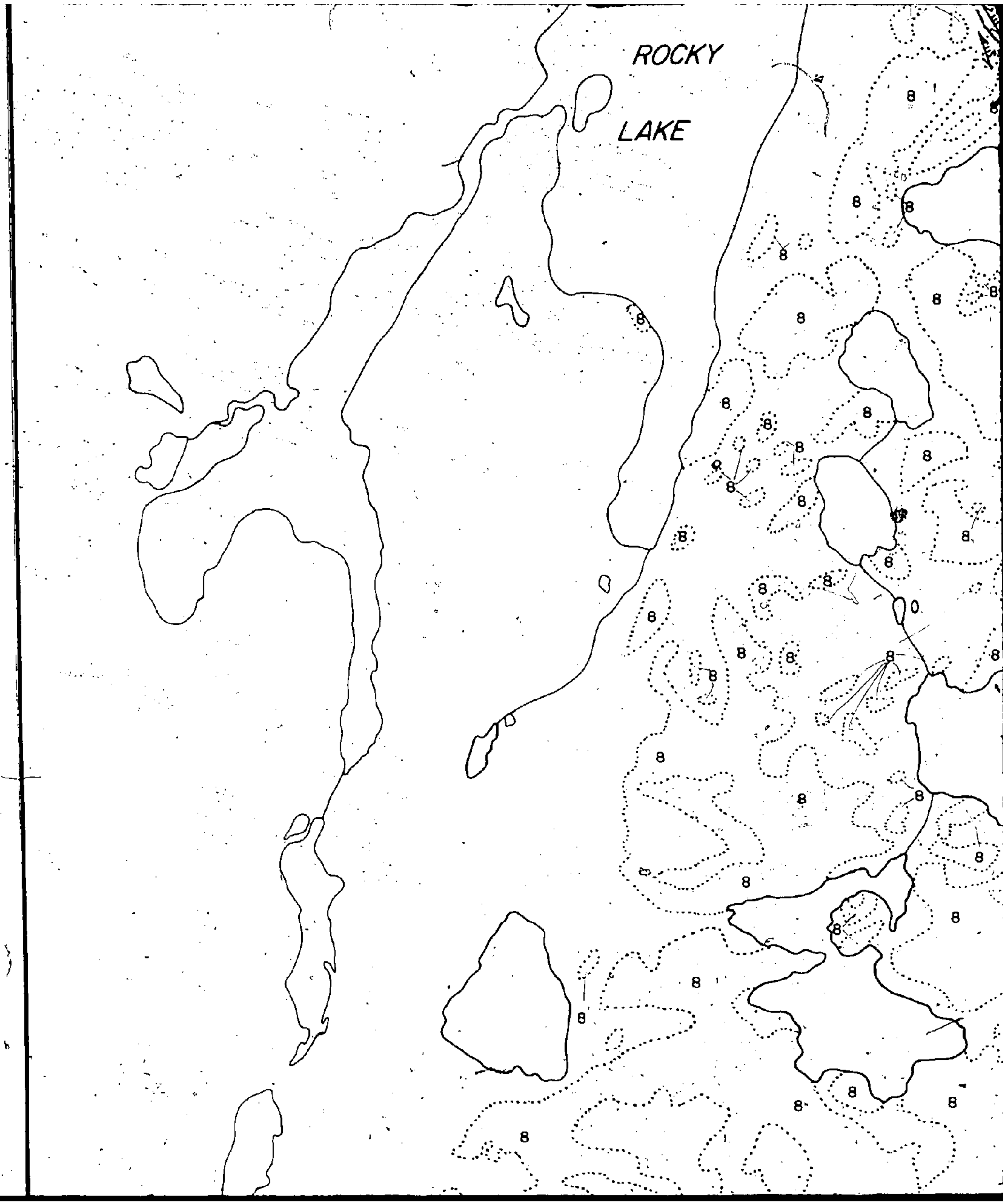
ROCKY
LAKE

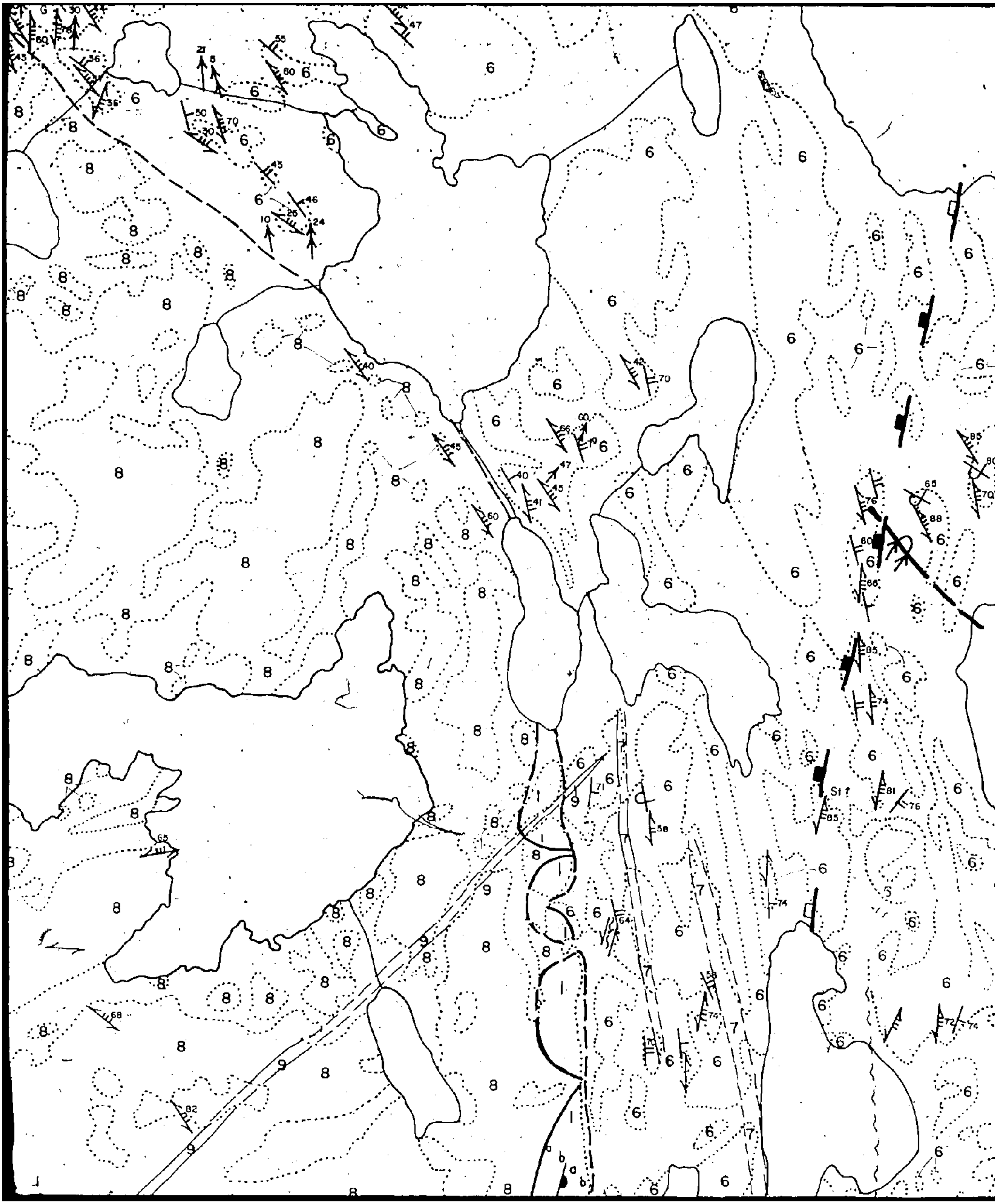

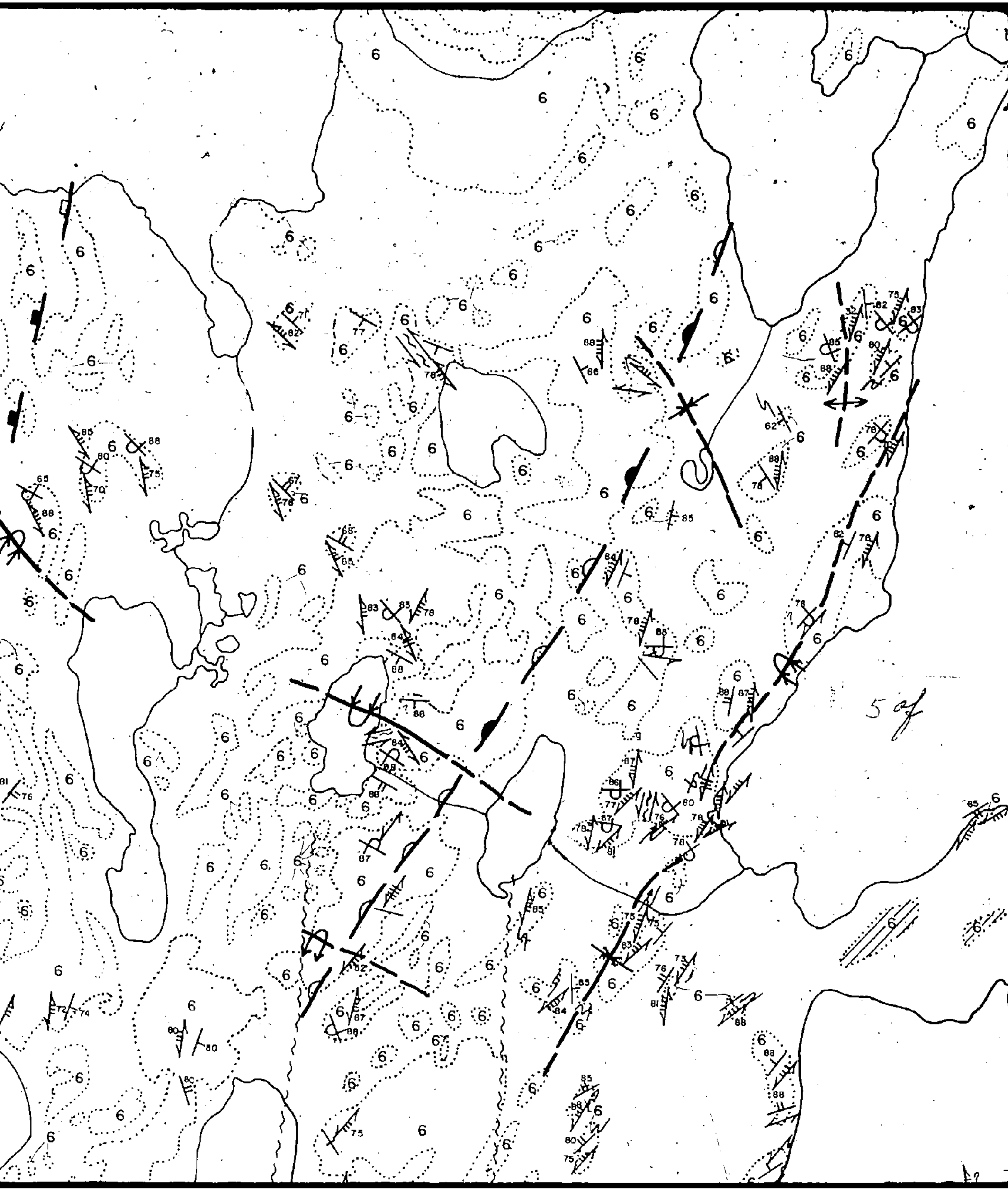
5 of

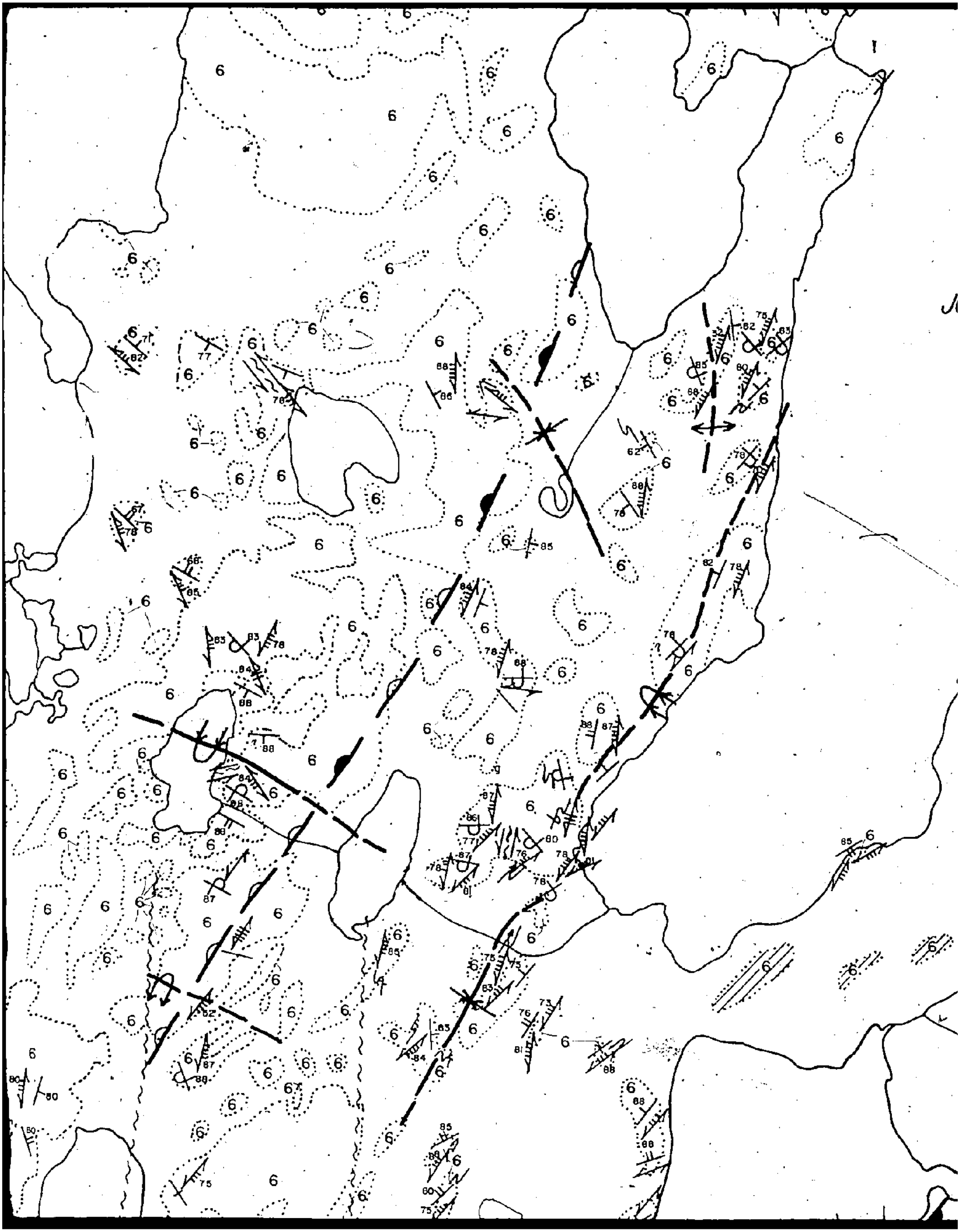

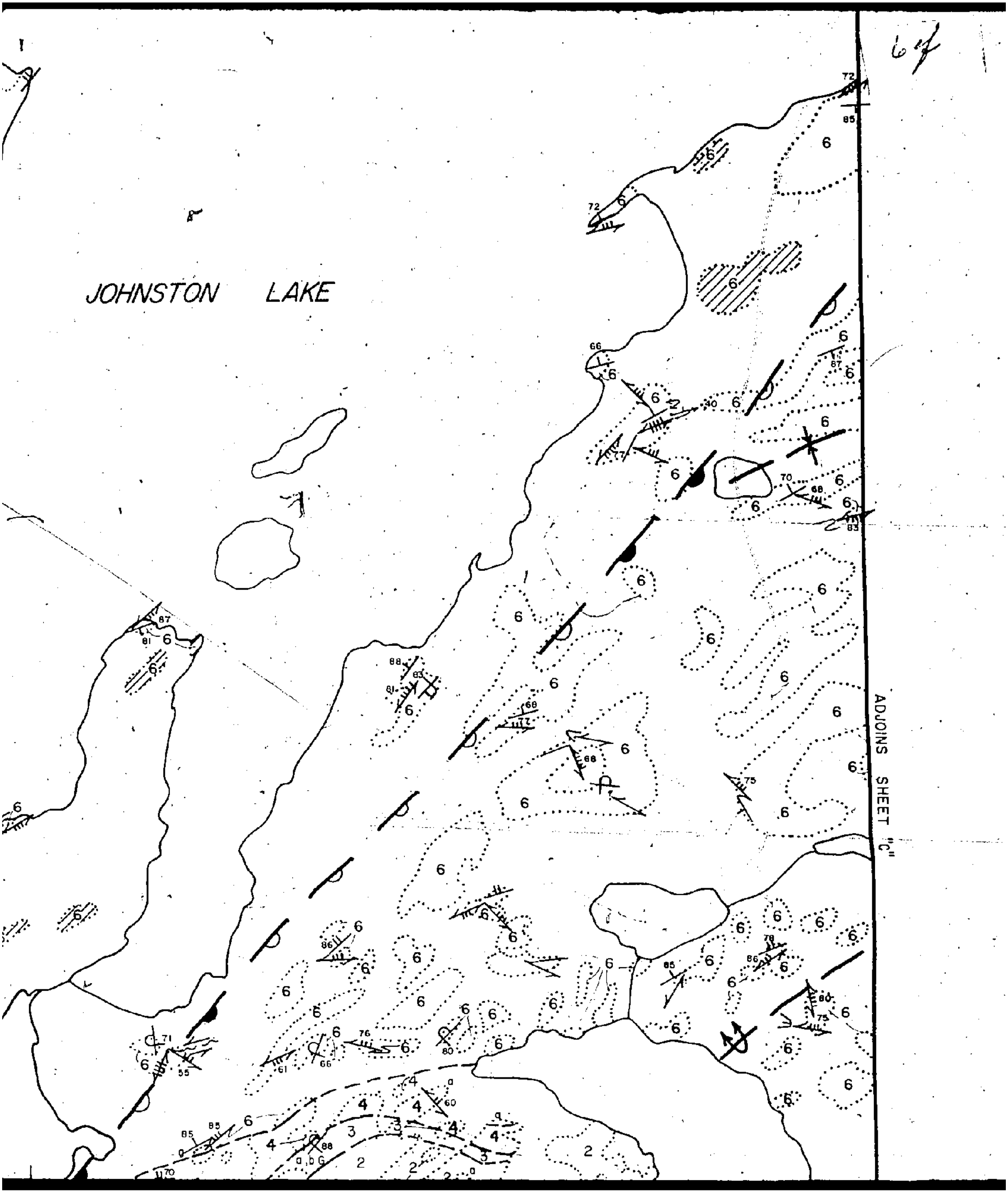
JOHNSTON LAKE
ADJOINS SHEET "C"

LINEATION

(mineral, elongation, cleavage/bedding)

(quartz fibres, slickensides)

MAJOR FAULT (with sense of offset)

(defined, approximate, inferred)

MINOR FAULT

MINERAL ISOGRAD: CORDIERITE

(defined, approximate)

: BIOTITE

(defined, approximate)

A MINERAL: ANDALUSITE

G GARNET

St STAUROLITE

g GOSSAN/IRON STAINING

TR TRENCH

UNBURNED AREA

☆ **NOTE**: see sheet "C" for marginal notes and description.

**SCALE : 1:10,000 (approx.)**

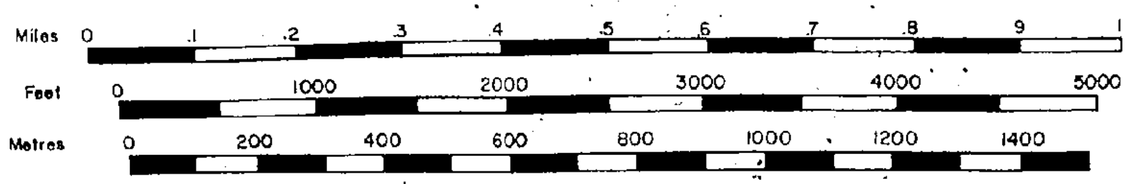

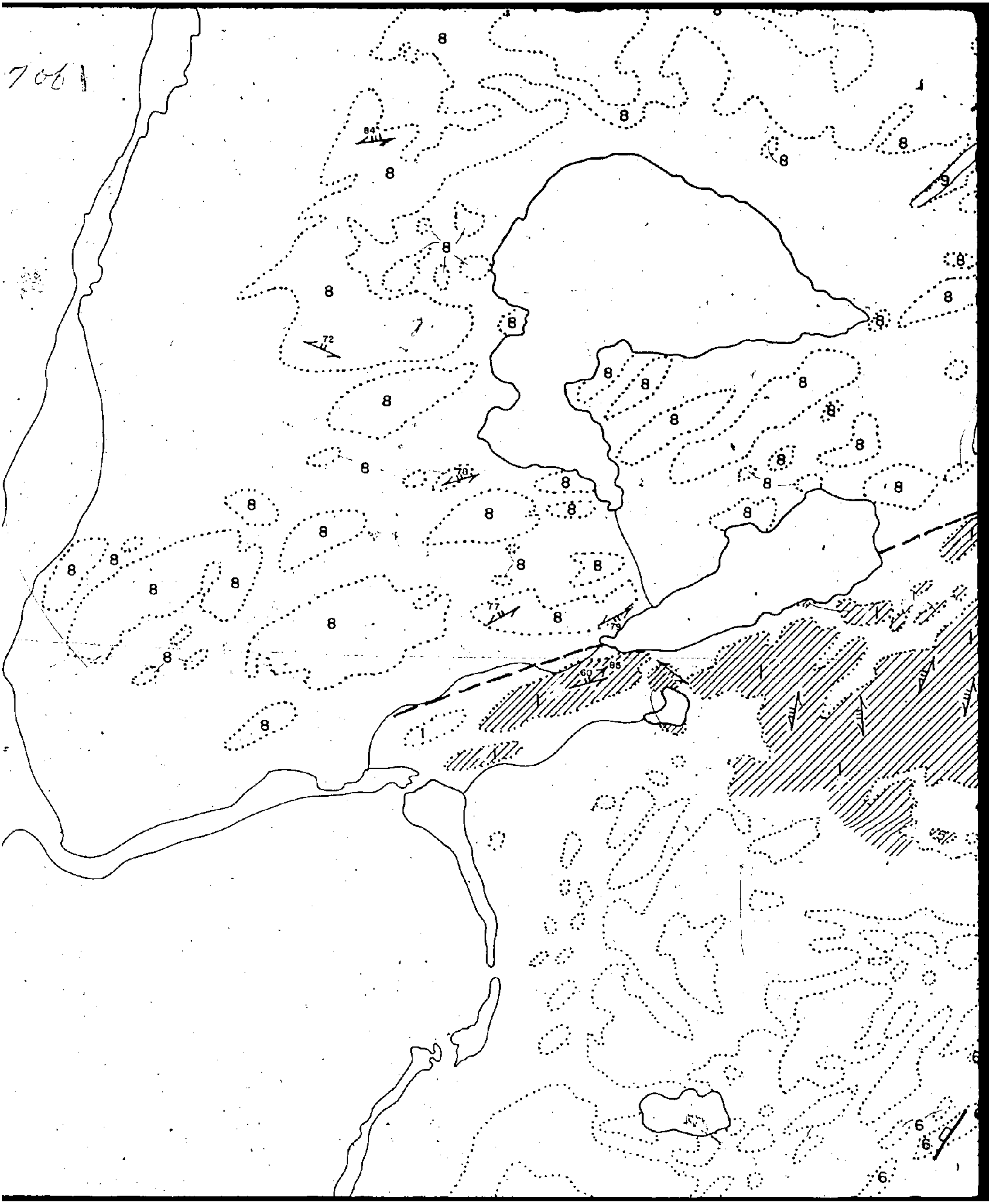

8
9
84
72
70
77
73
60
65
1
6

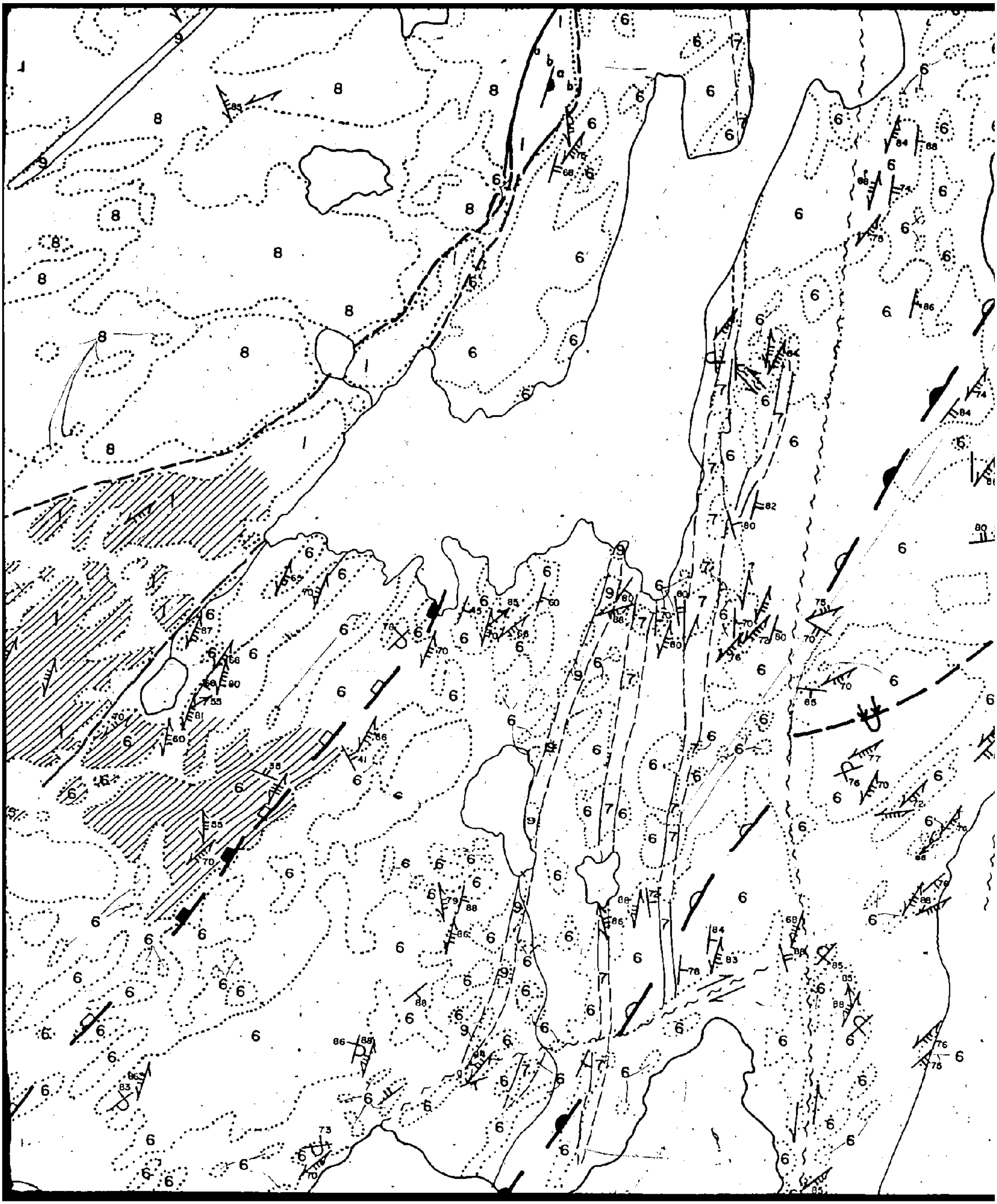

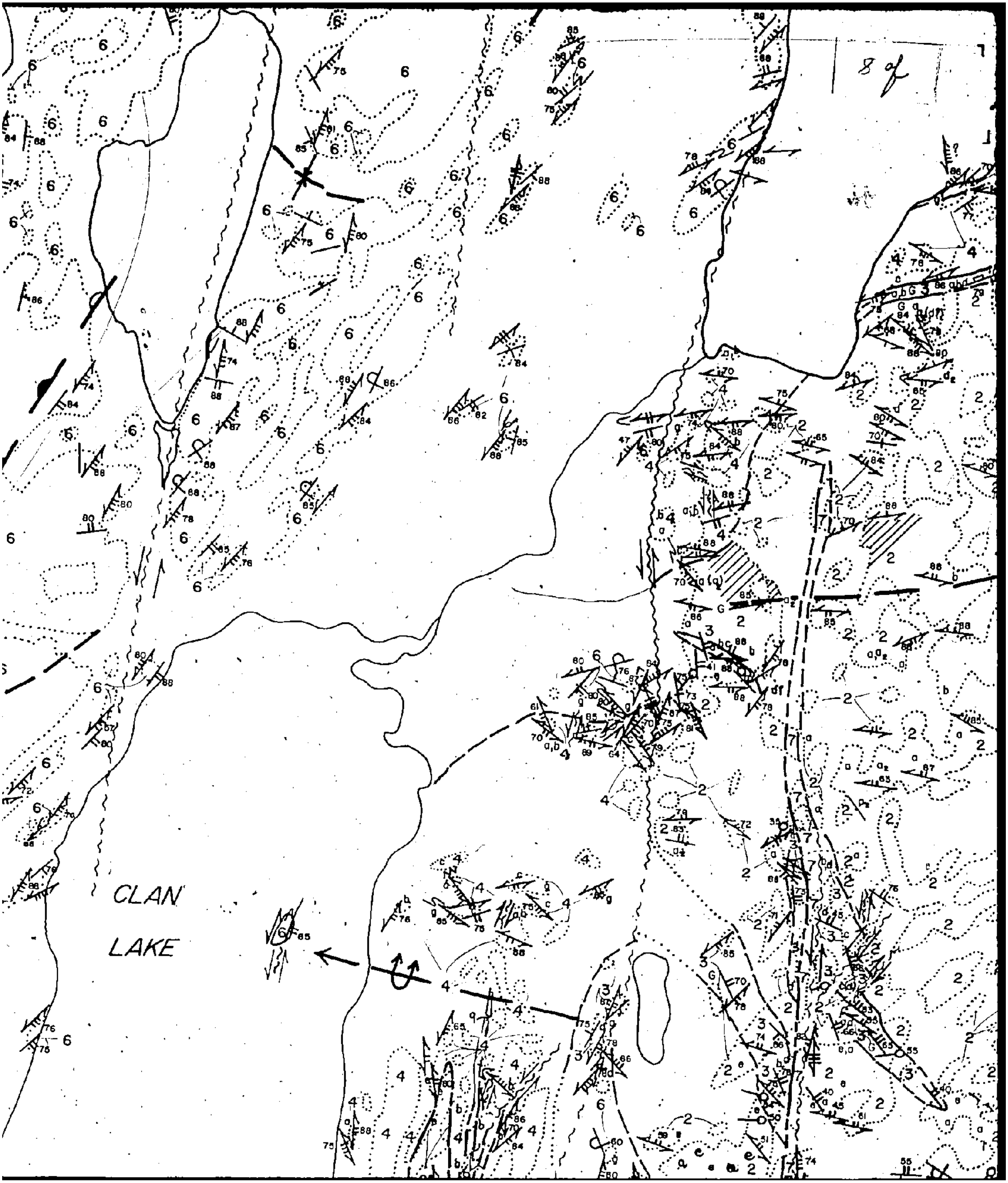
8 of
CLAN
LAKE

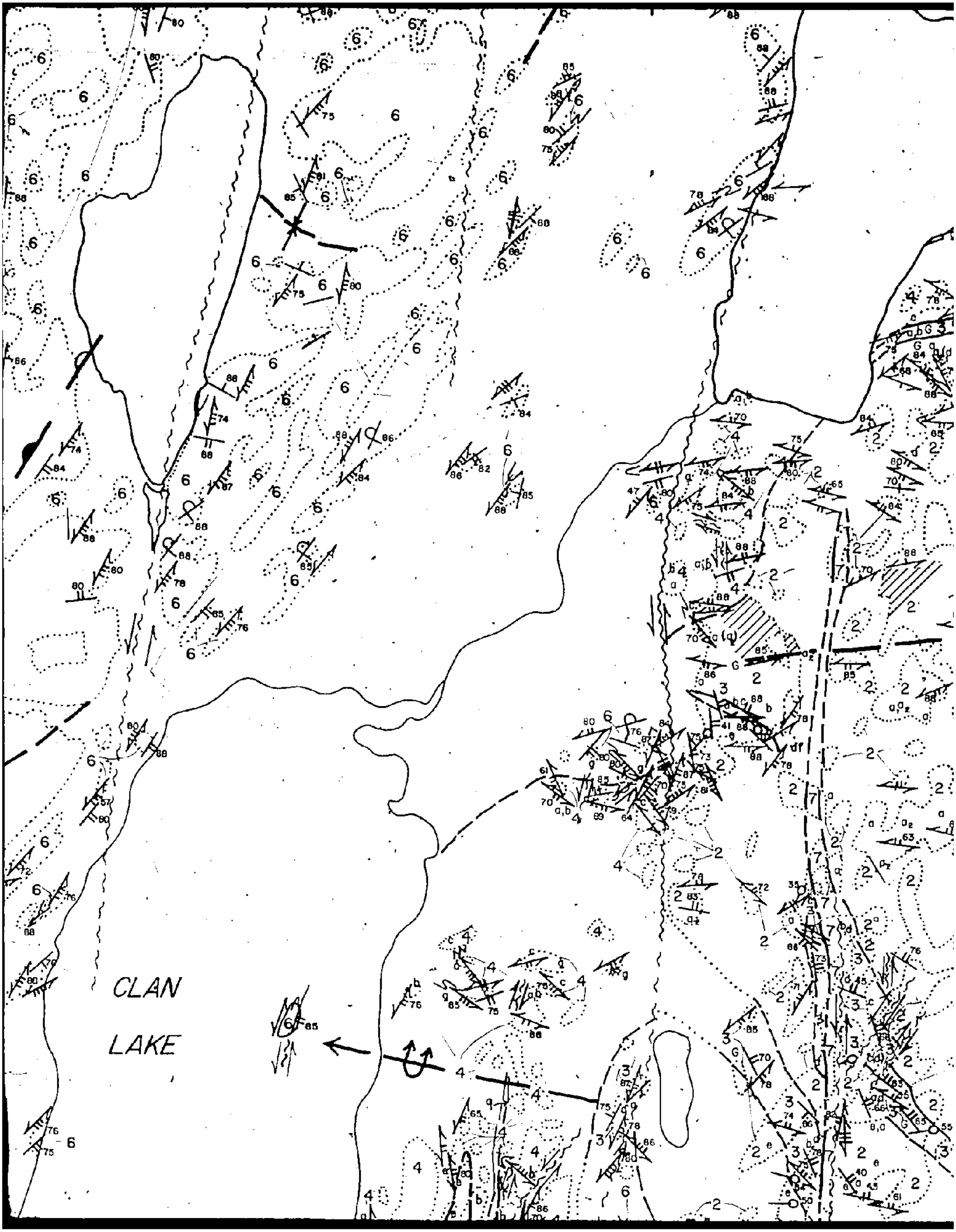
CLAN
LAKE

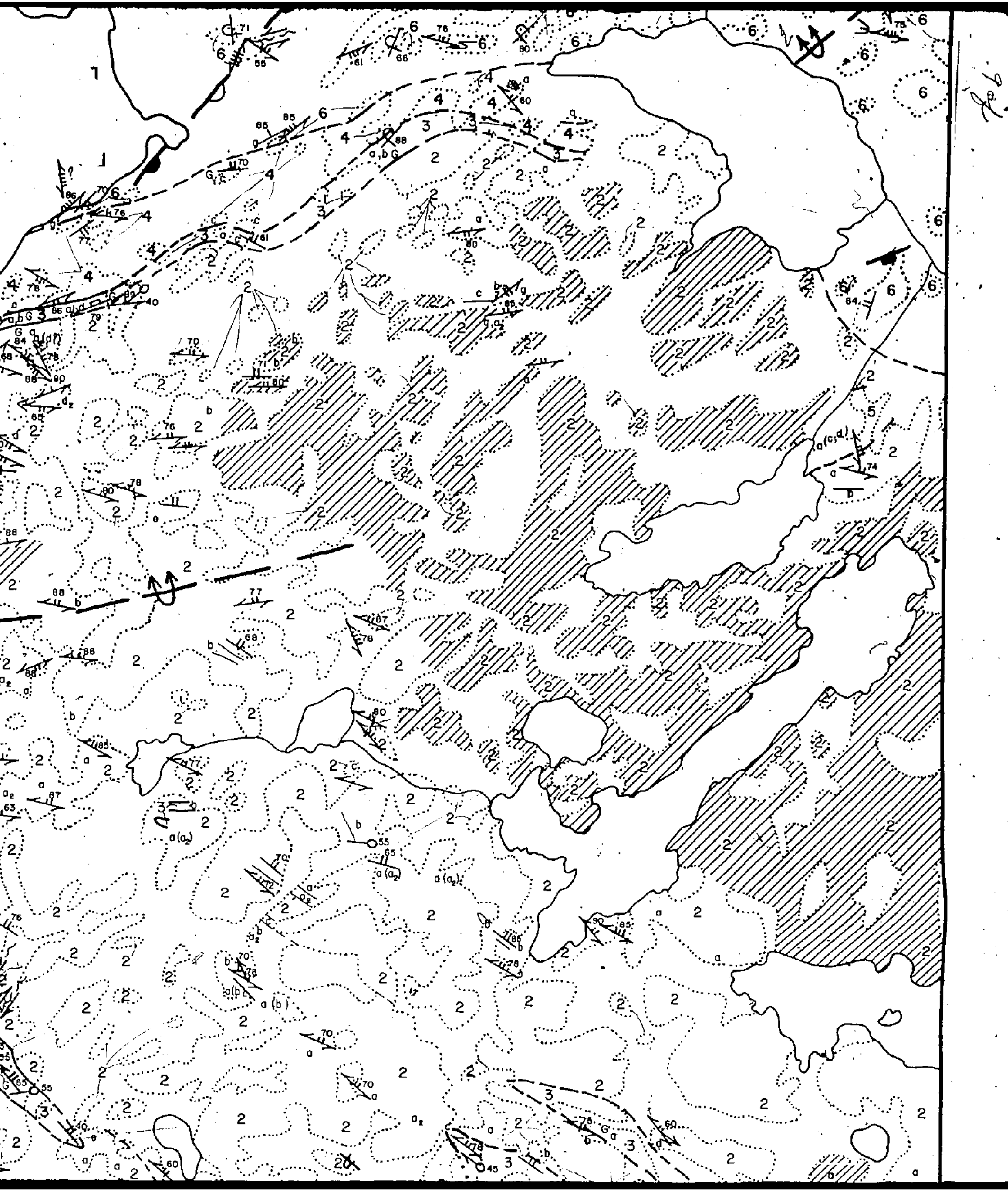

10 of

UNBURNED AREA

☆ **NOTE**: see sheet "C" for marginal notes and description.

SCALE : 1:10,000 (approx.)

Miles 0 .1 .2 .3 .4 .5 .6 .7 .8 .9 1

Feet 0 1000 2000 3000 4000 5000

Metres 0 200 400 600 800 1000 1200 1400

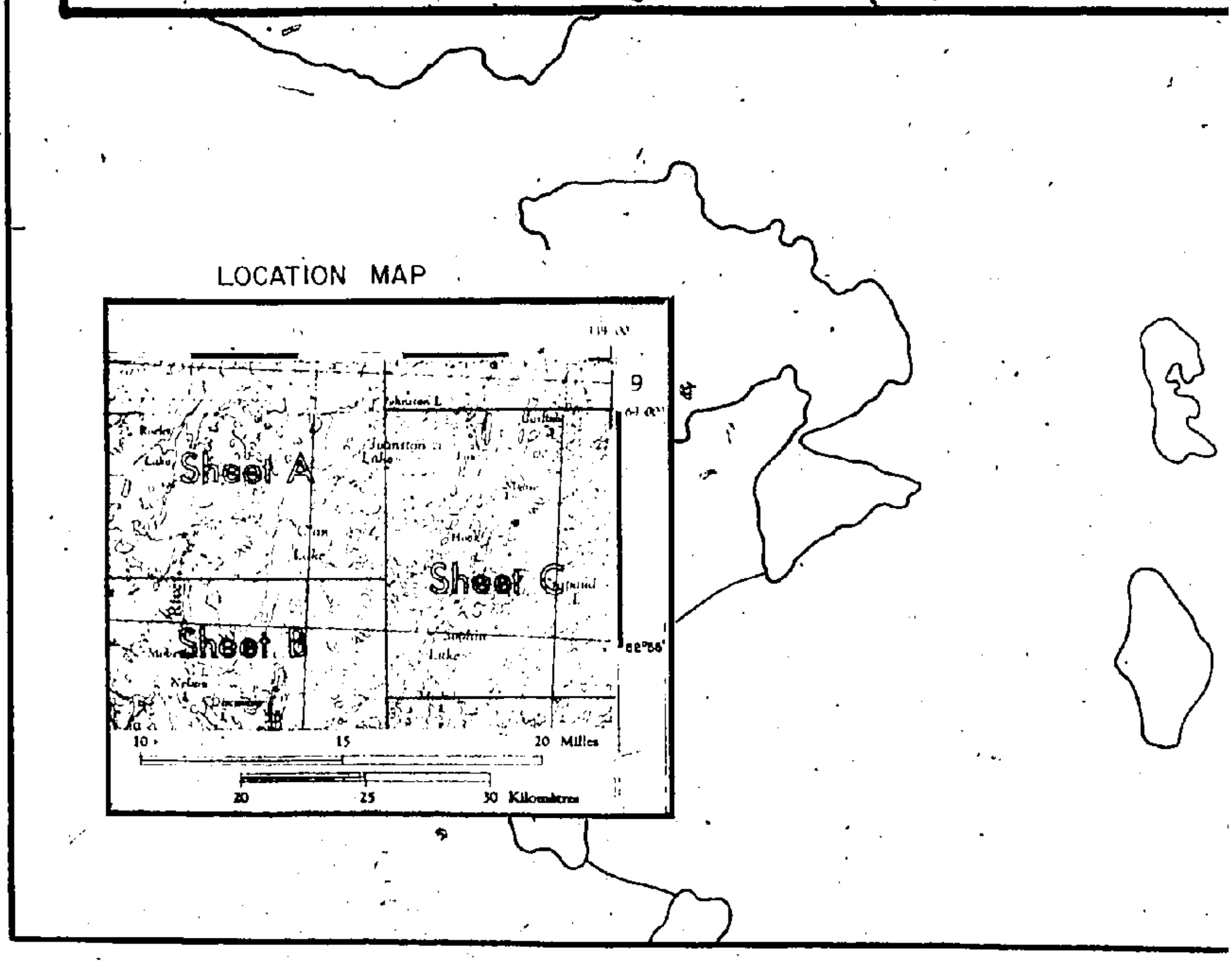

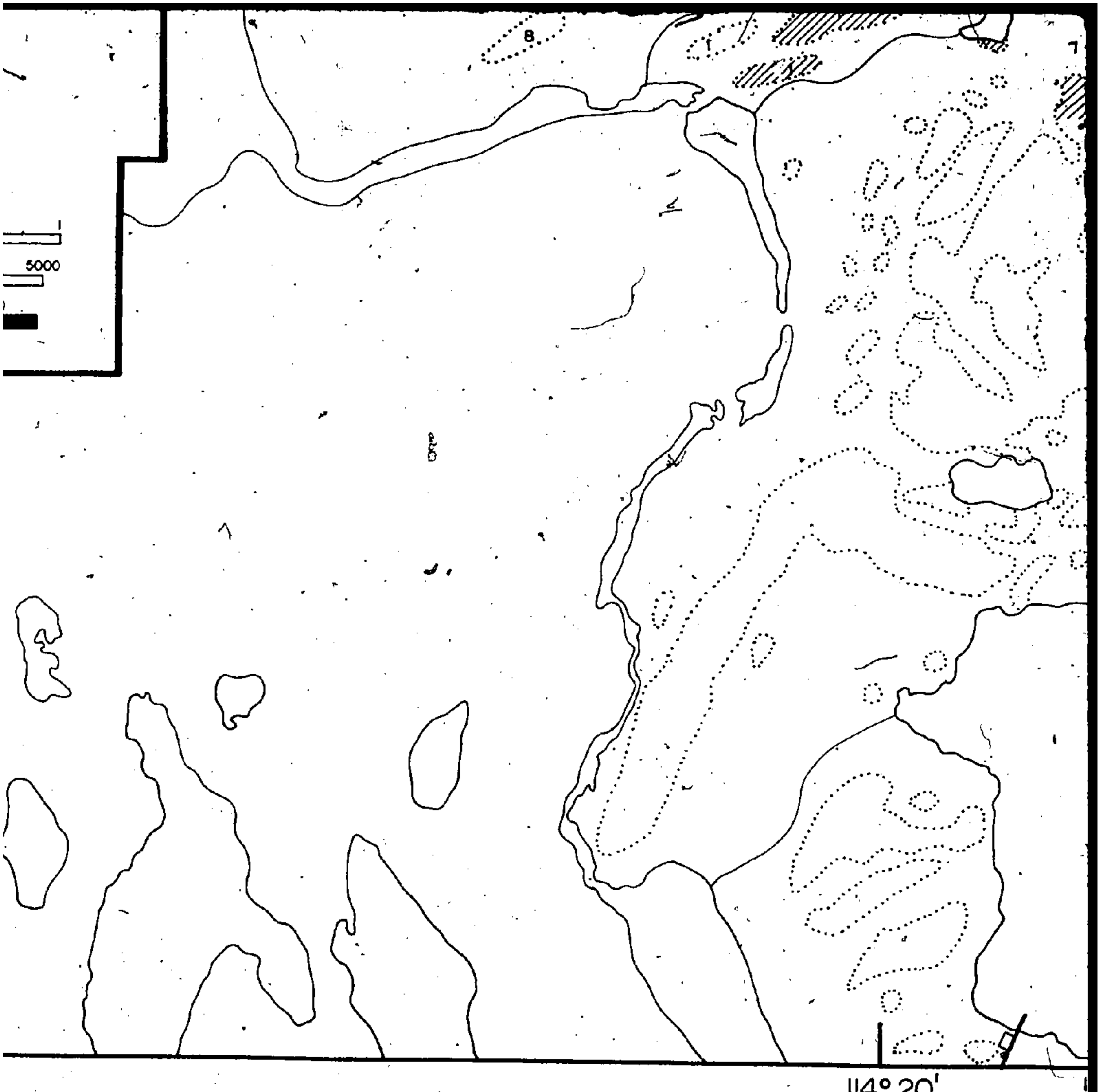

8
7
5000
114° 20'

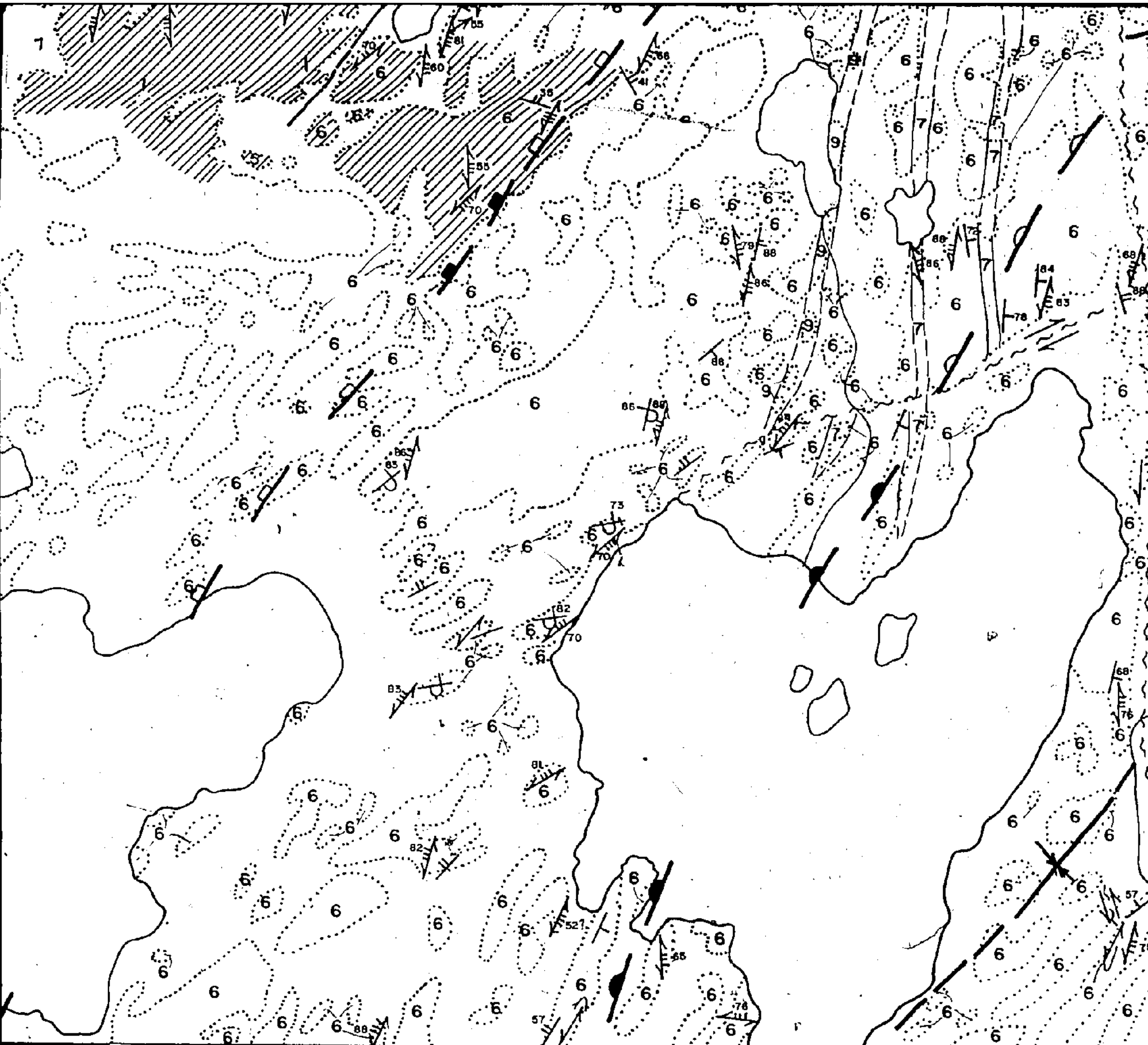

11 of

ADJOINS SHEET "B"

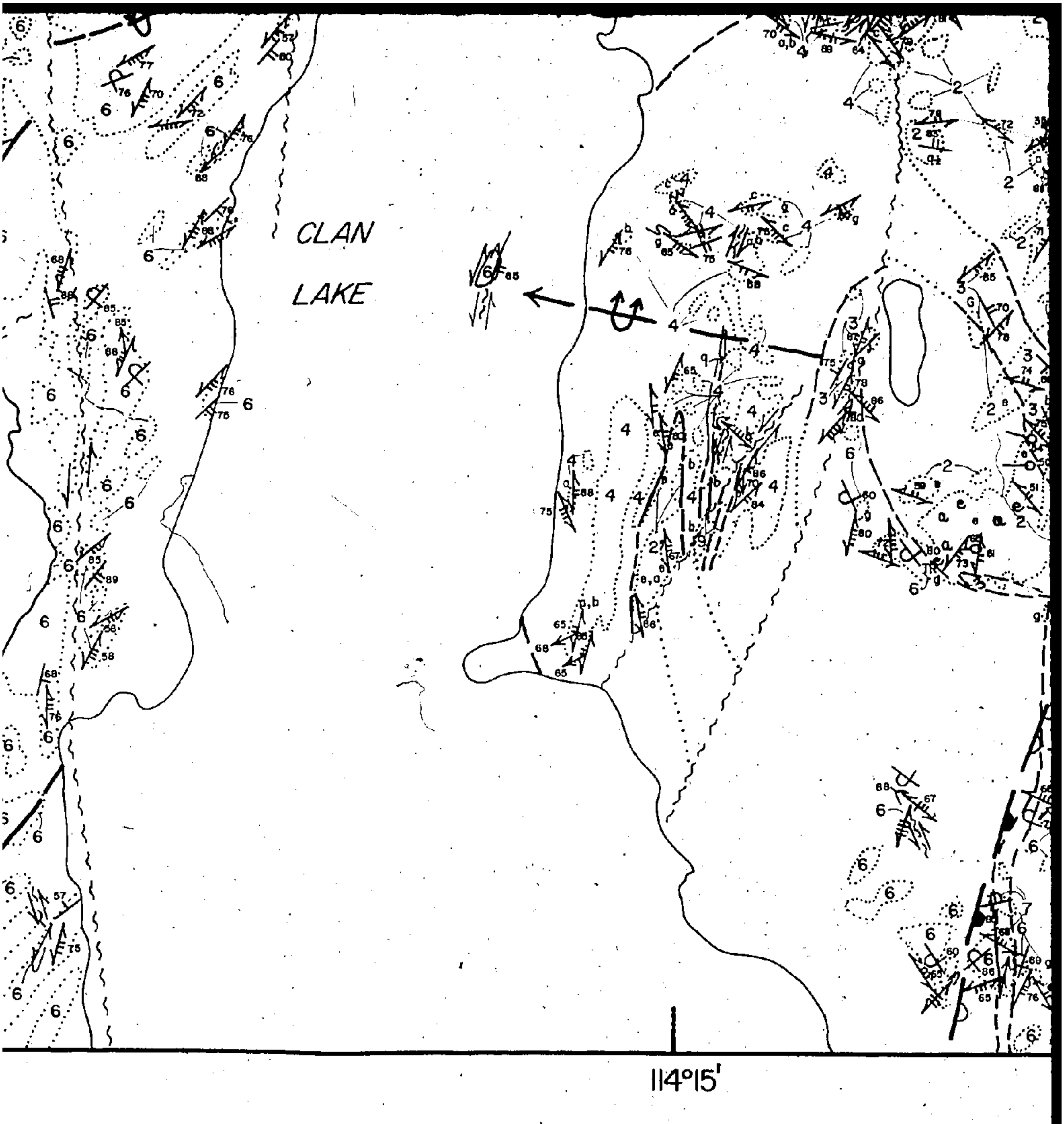
CLAN
LAKE
114°15'

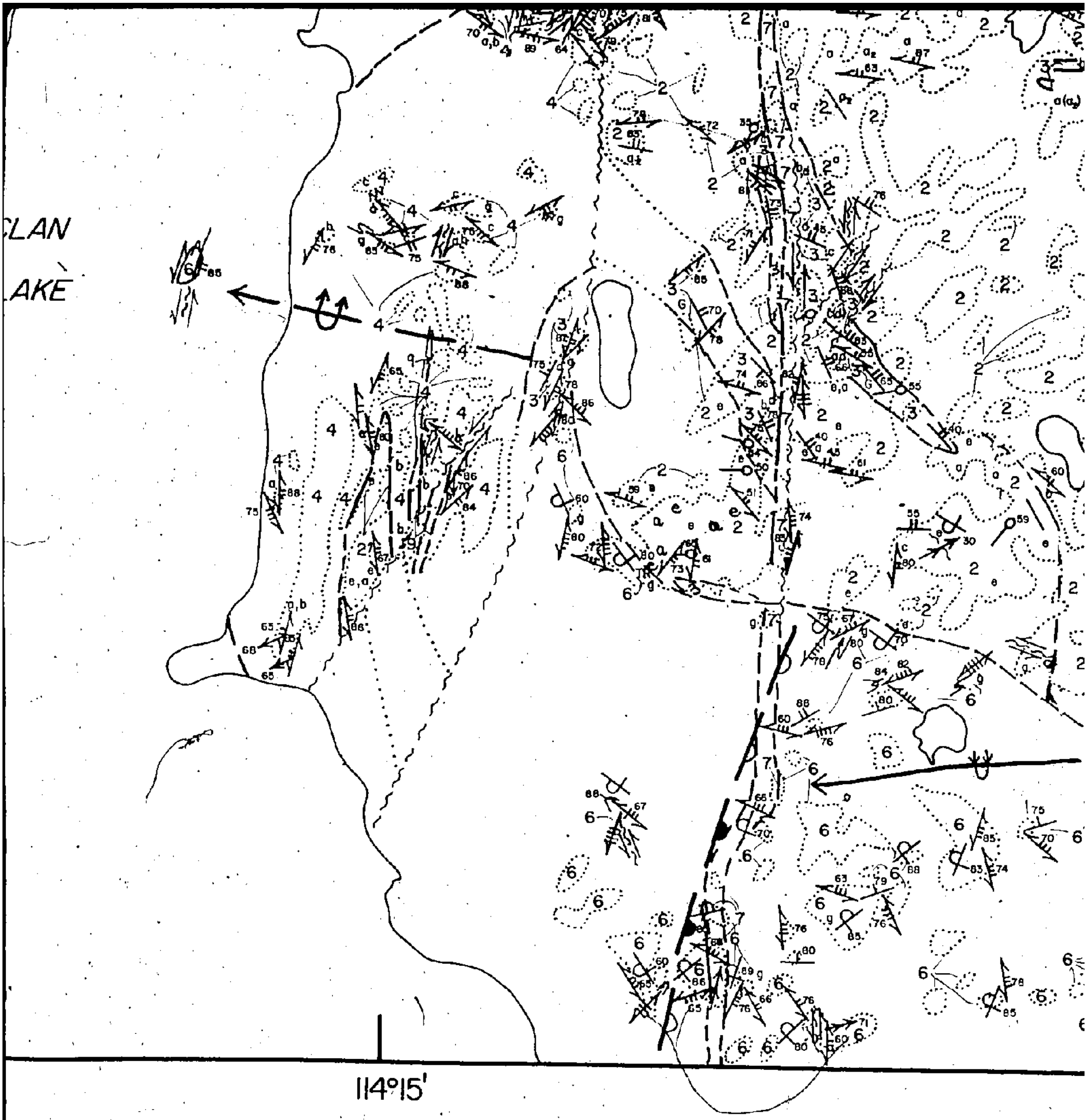

CLAN
LAKE
114°15'

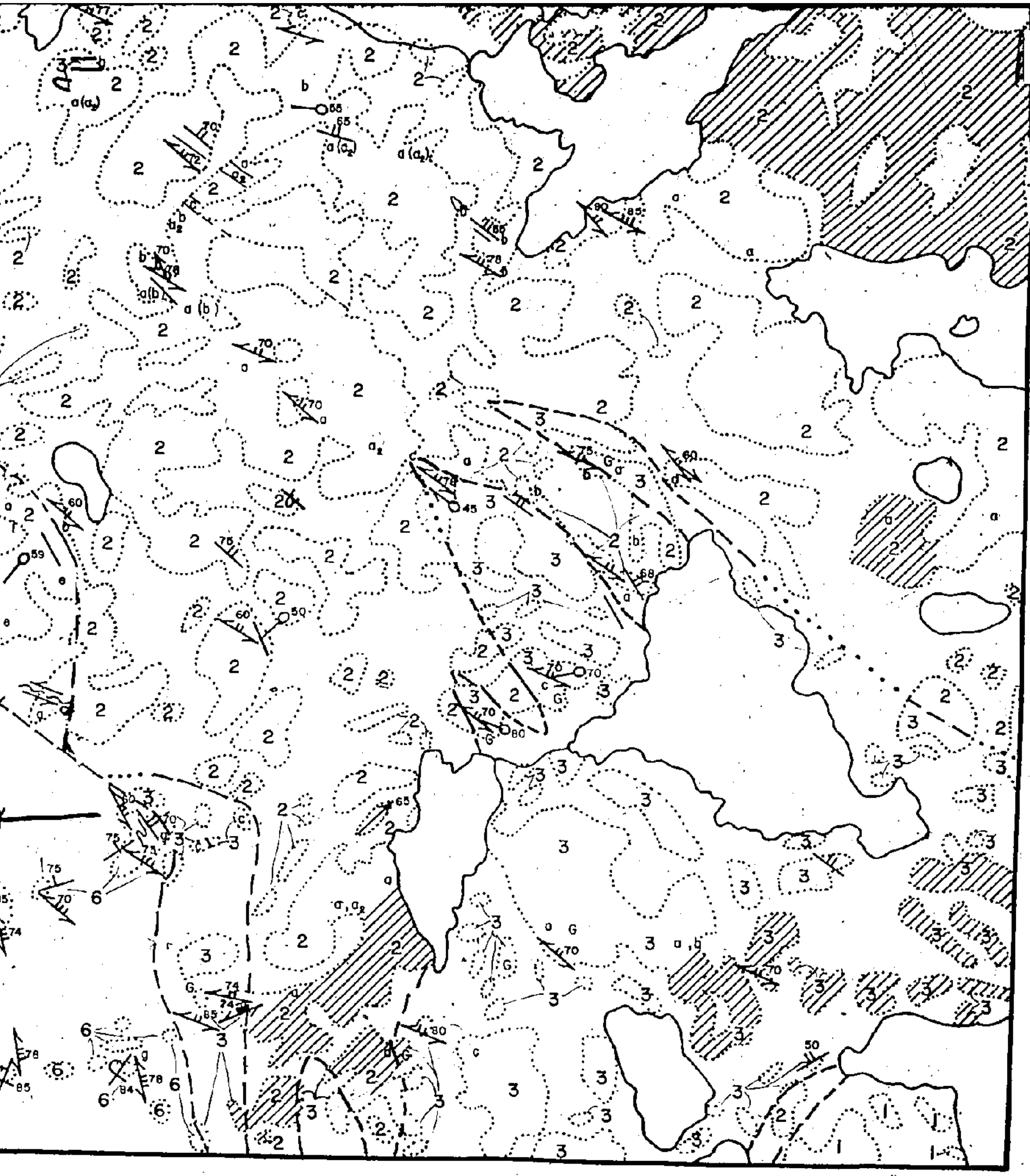

$ 5.00 ea / $ 15.00 set

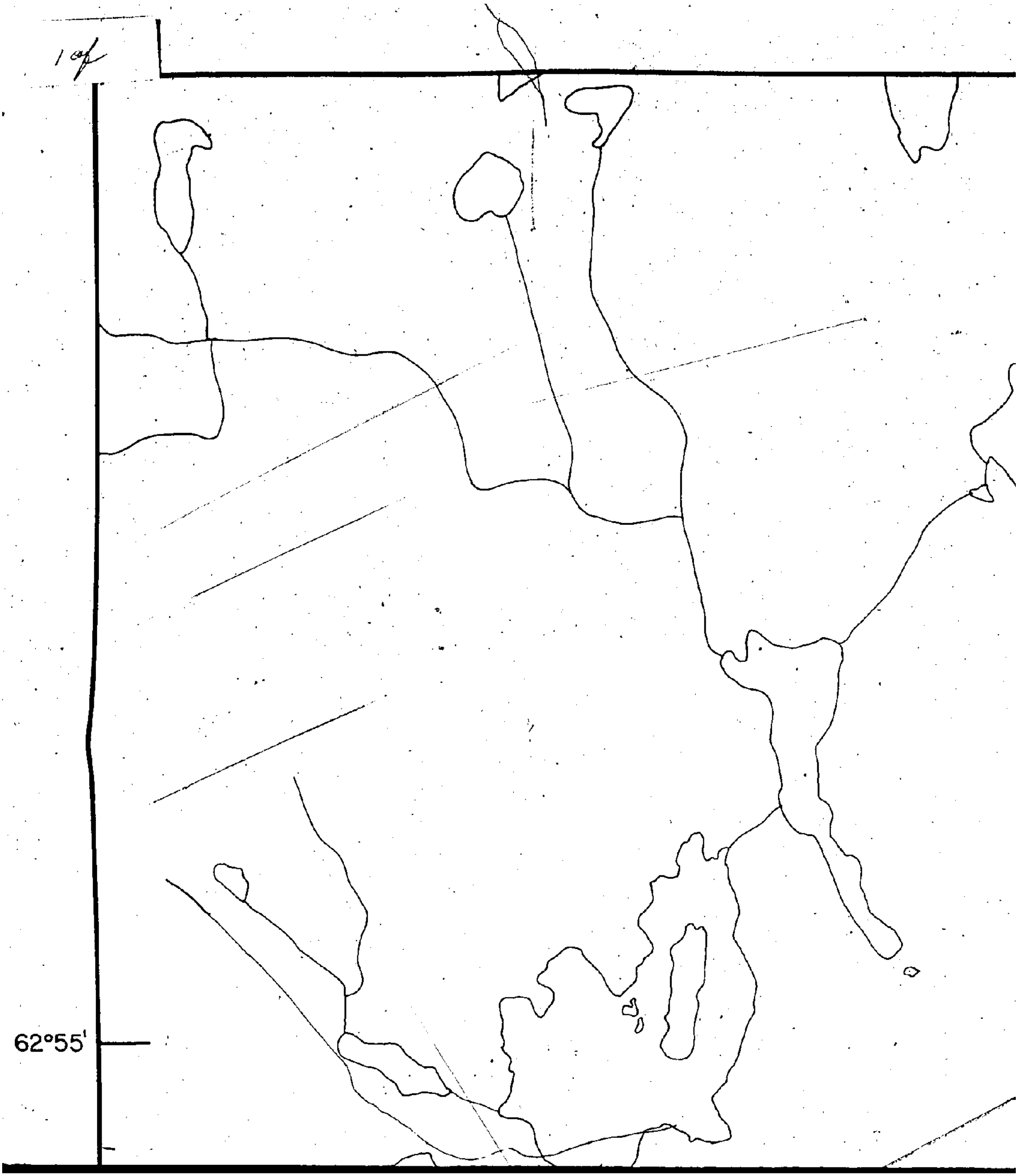
1 of
62°55'

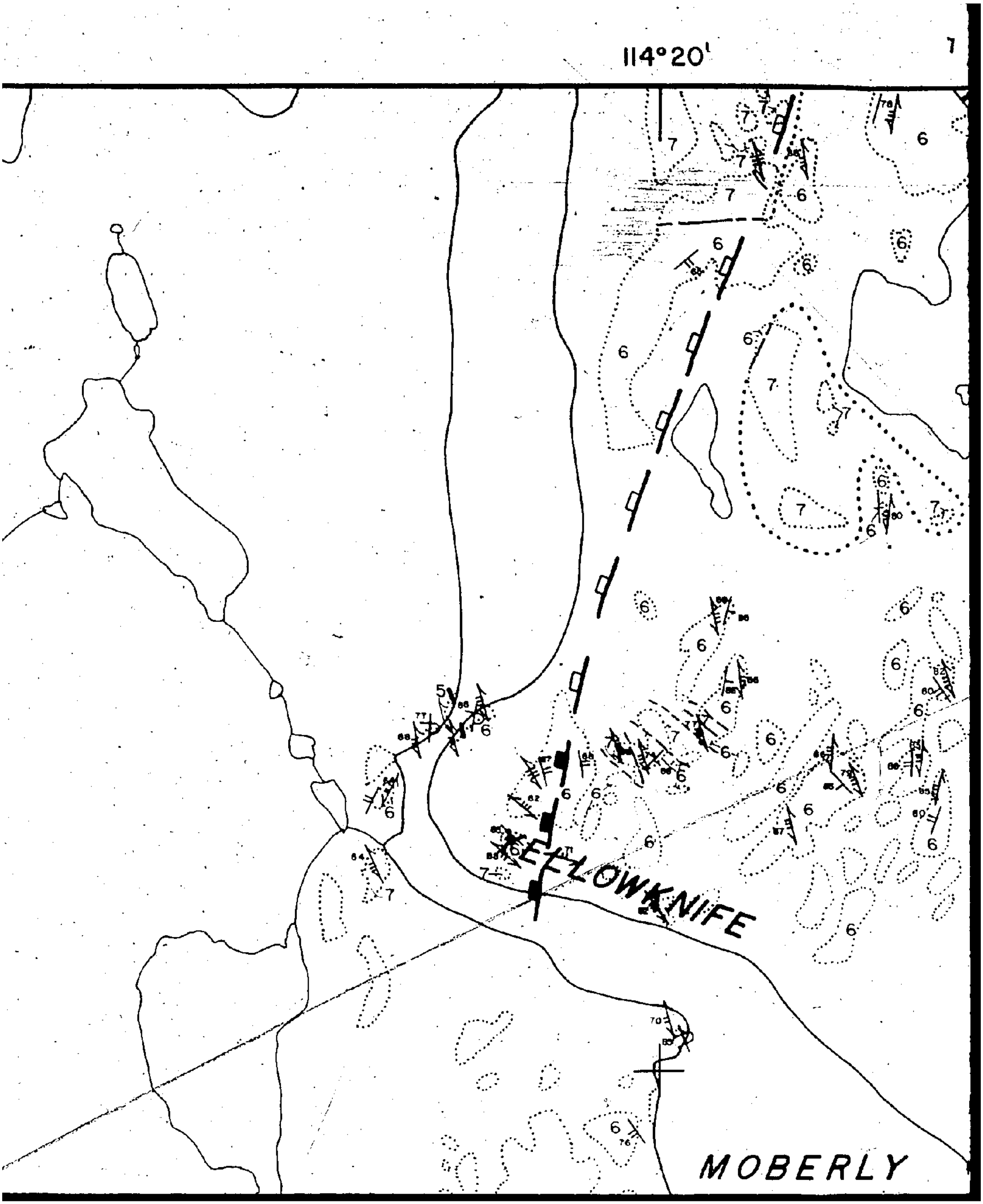

114°20'
MOBERLY

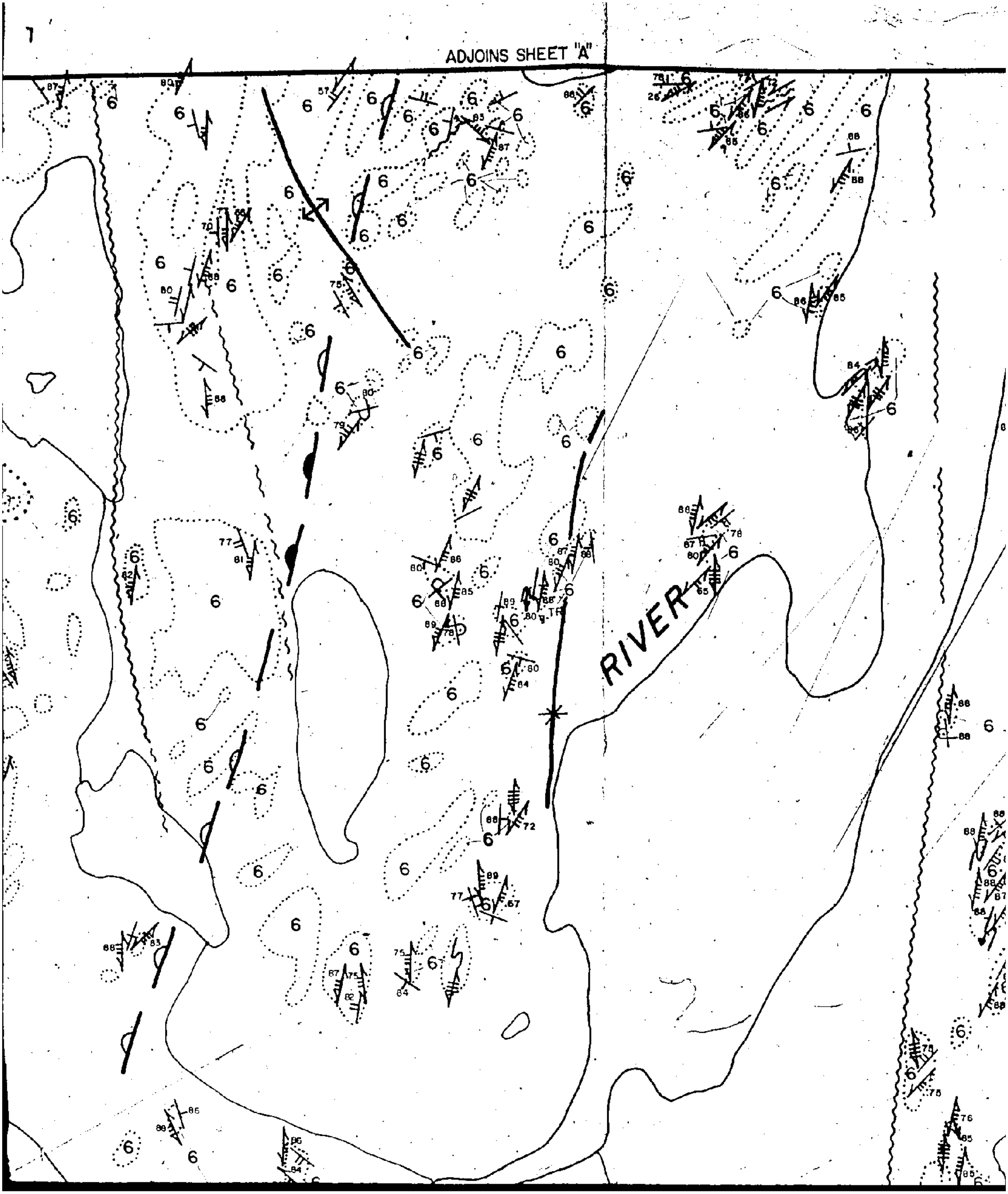
ADJOINS SHEET "A"
RIVER


114° 15'
2 of
CORE
SHED
TR
PIT


114° 15'
CORE
SHED
PIT
TR

E.G.S. 1983-5 Sheet "B"

408

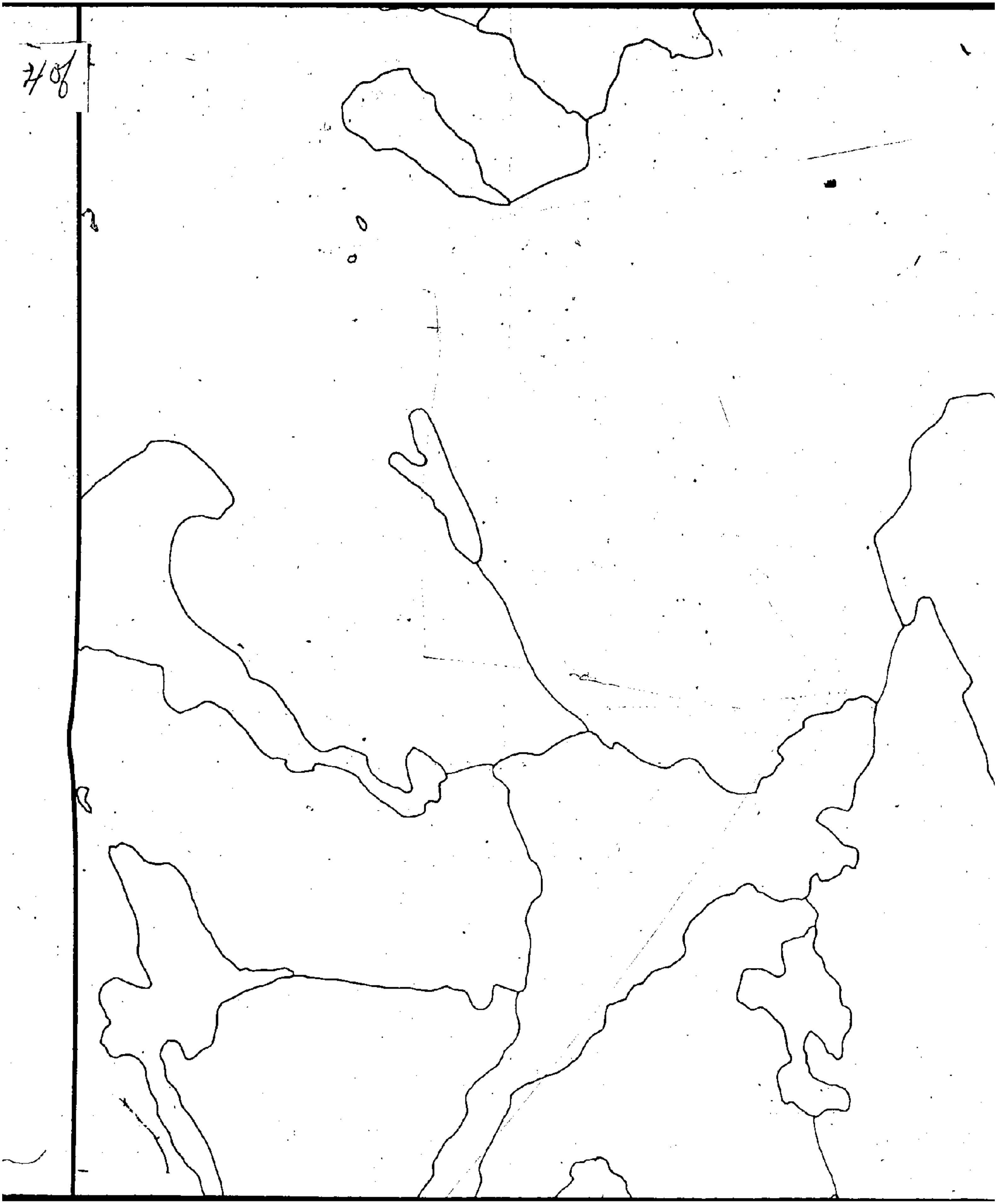

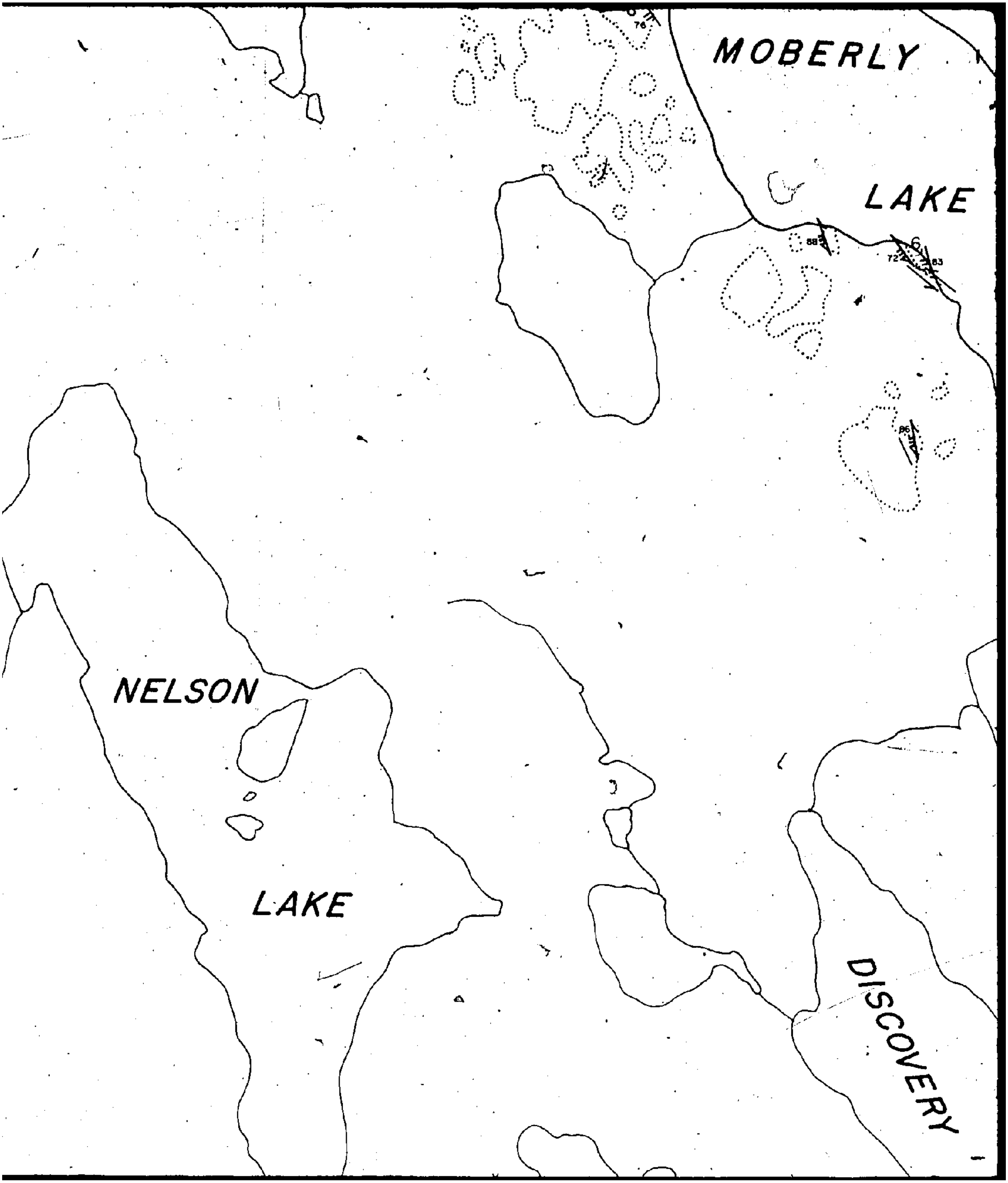
MOBERLY
LAKE
NELSON
LAKE
DISCOVERY


ELLOWKNIFE
6
7

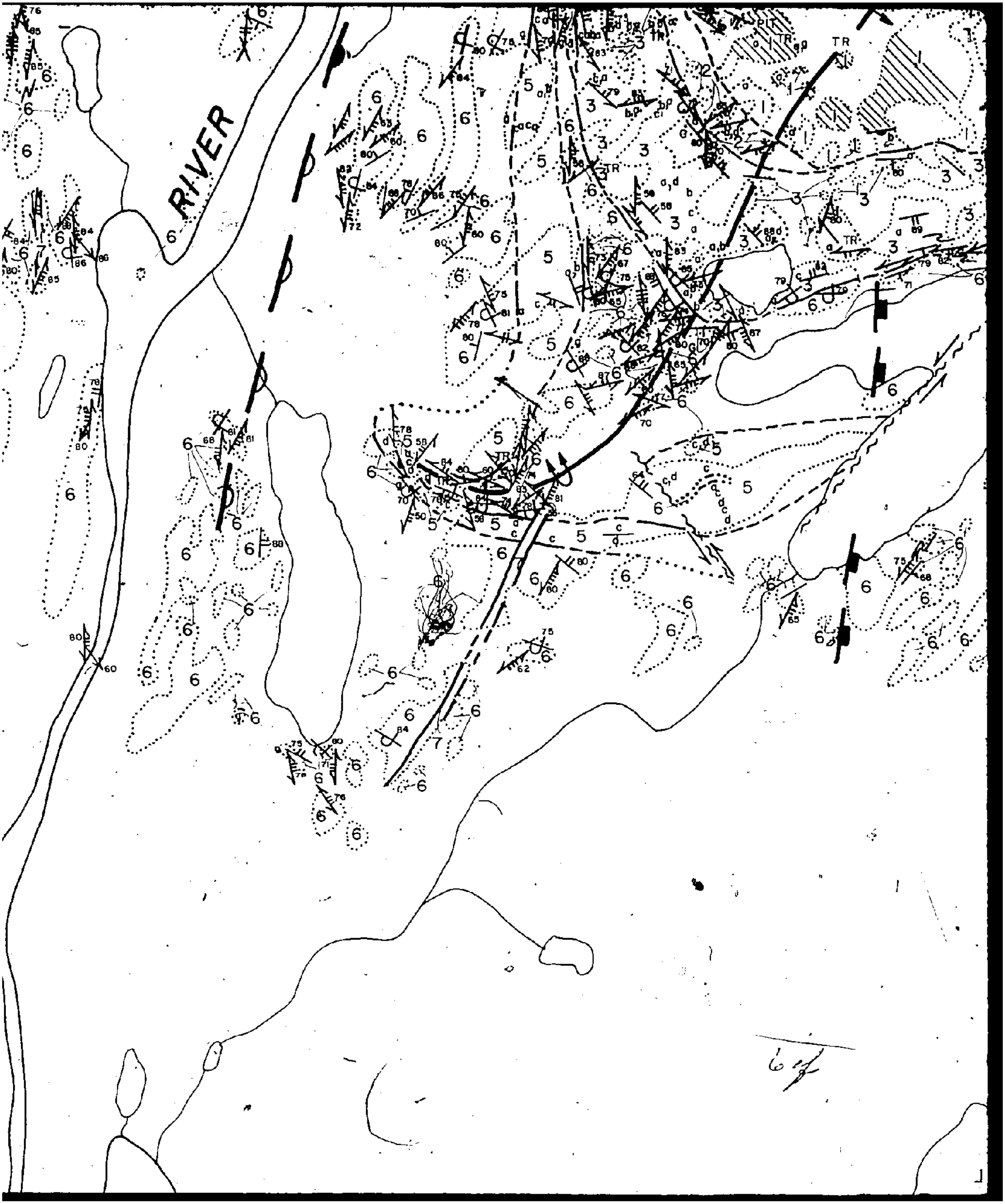
RIVER
TR


RIVER

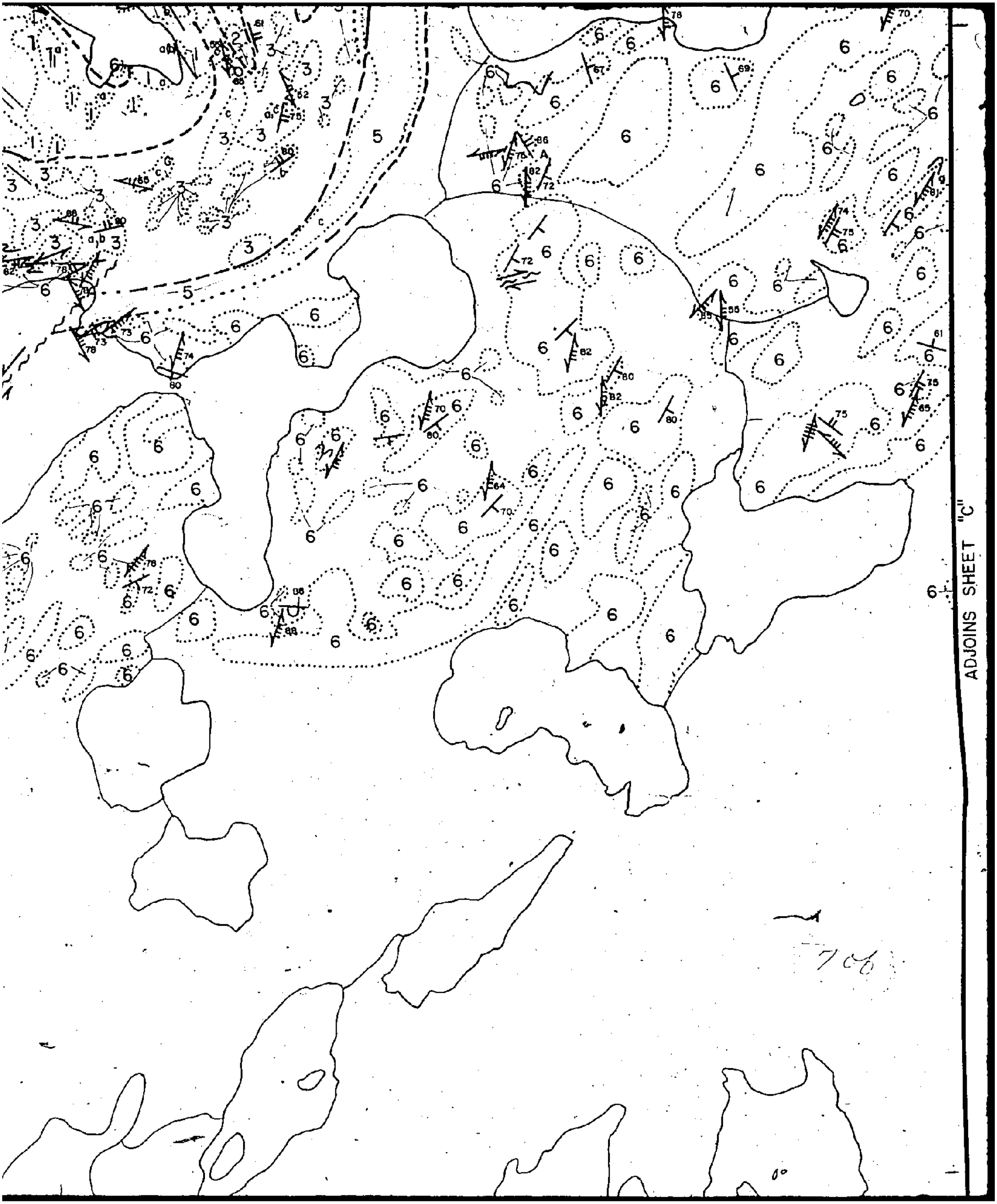
ADJOINS SHEET "C"

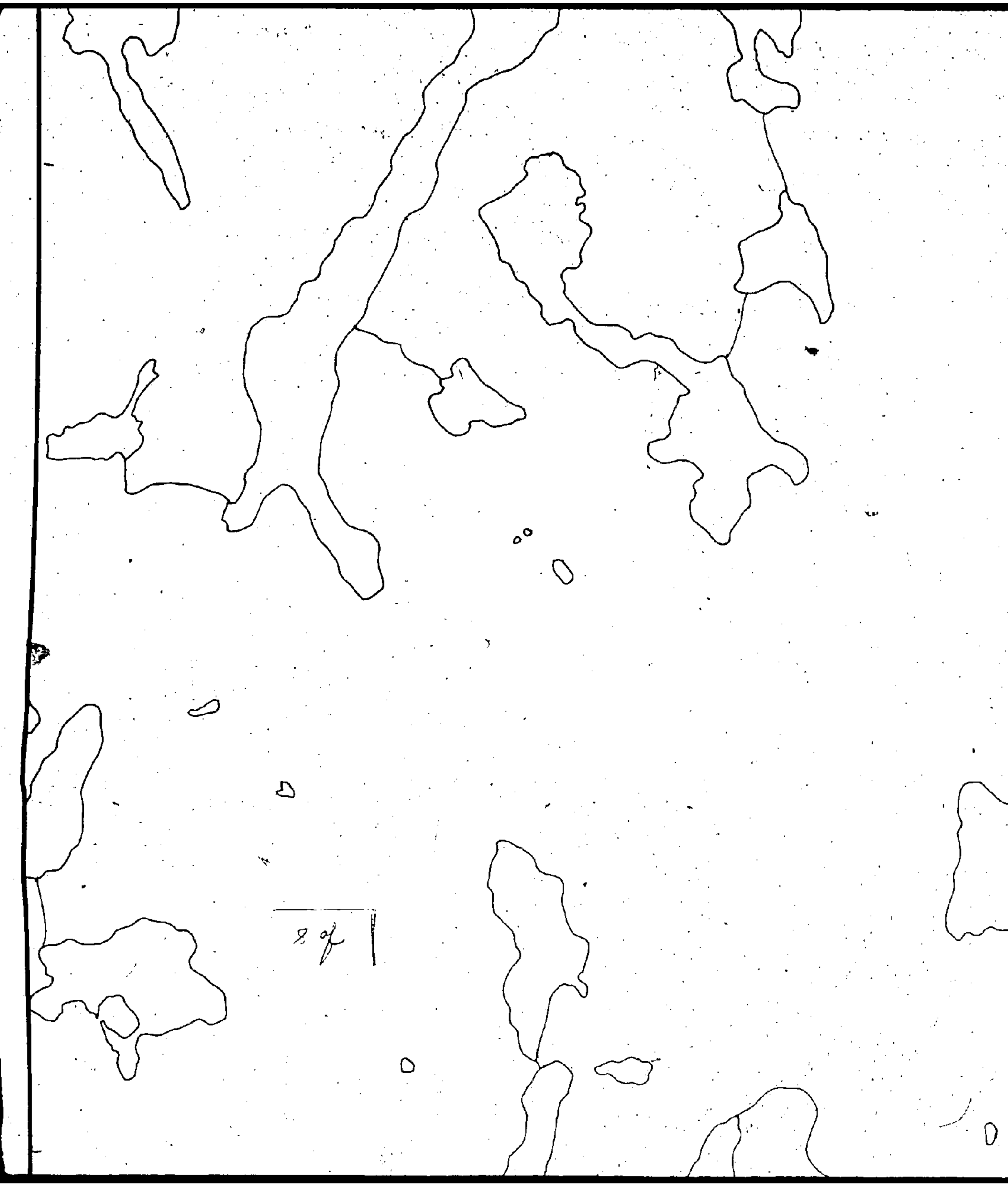

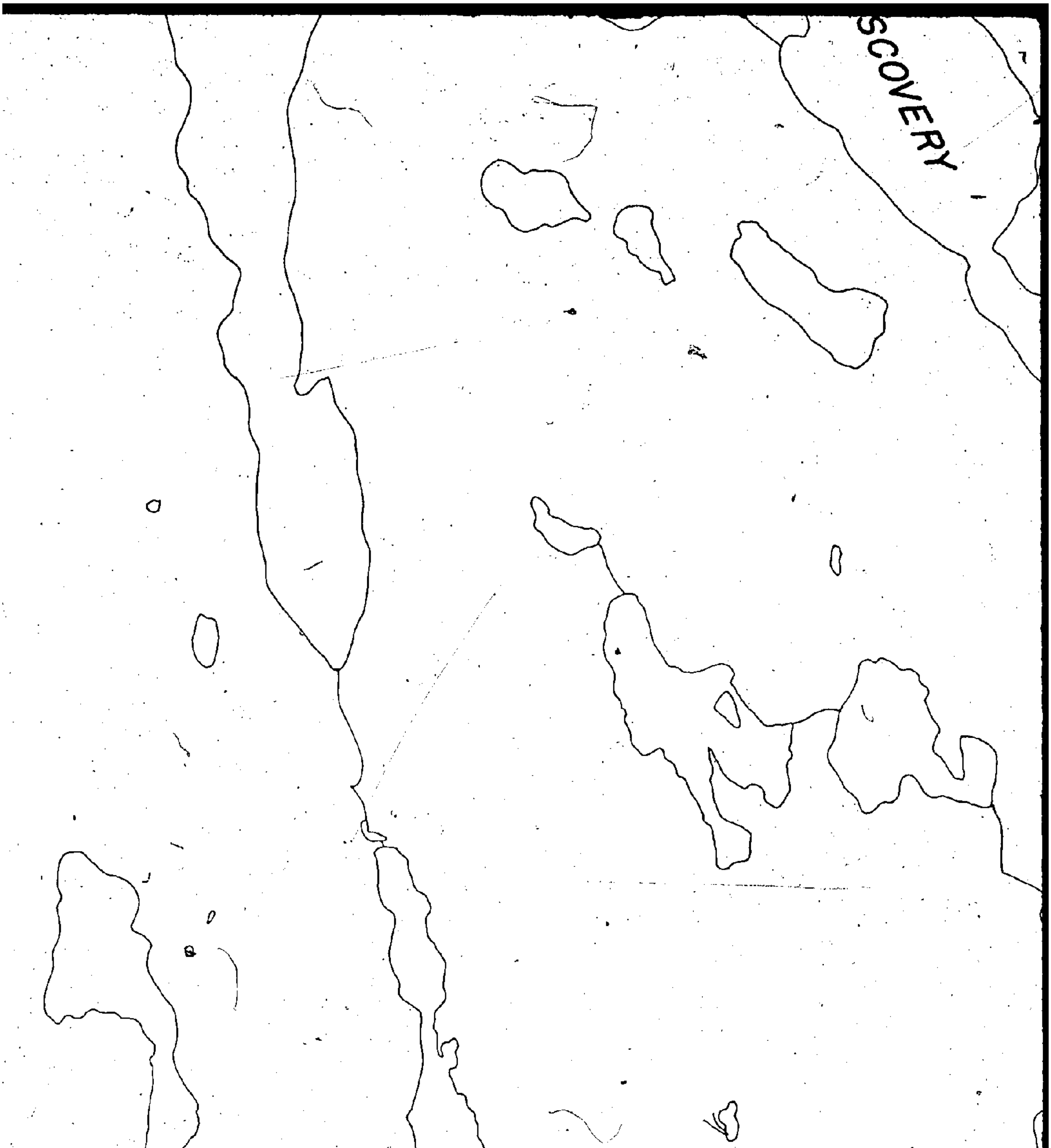
SCOVERY

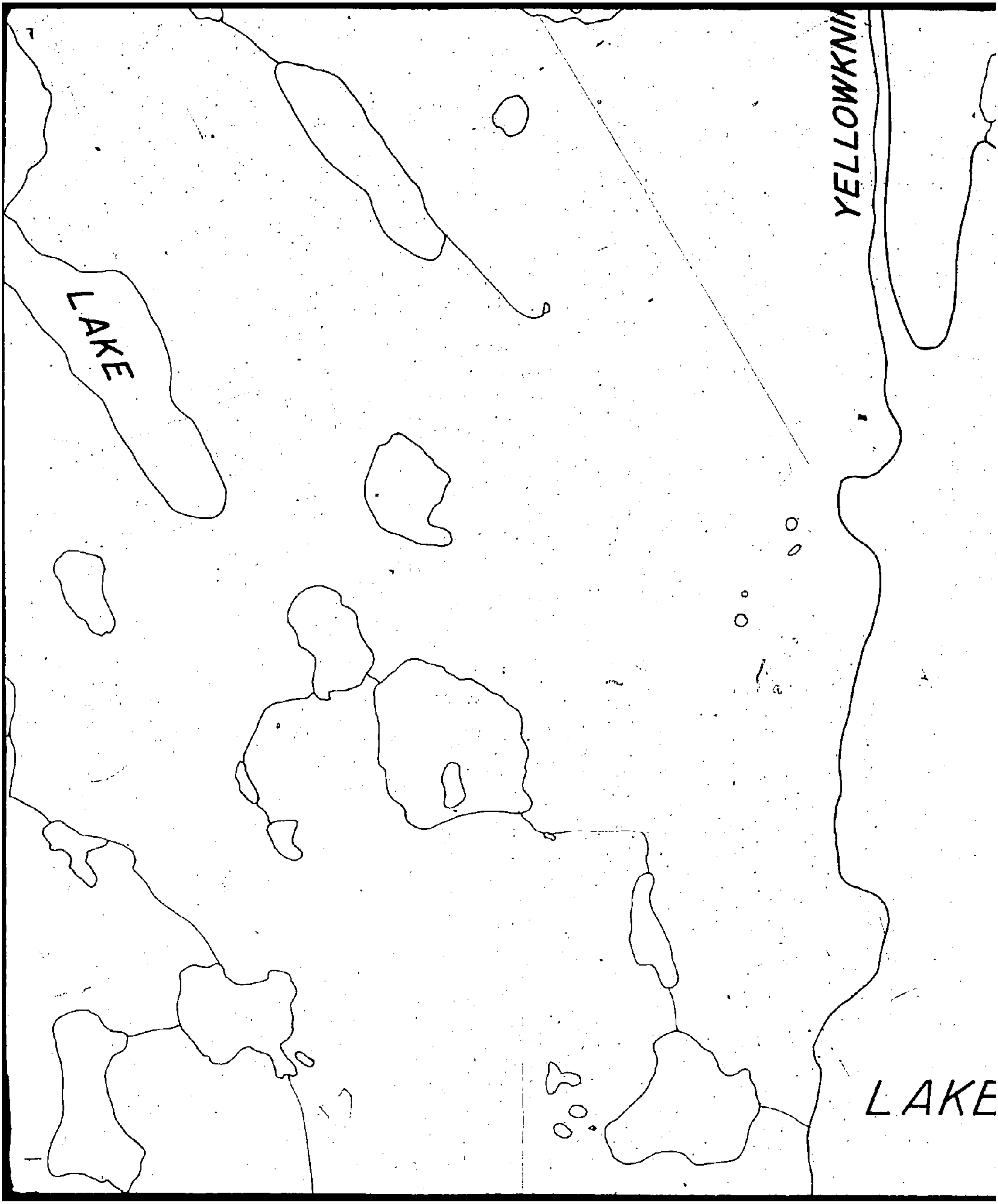
LAKE
YELLOWKNI
LAKE

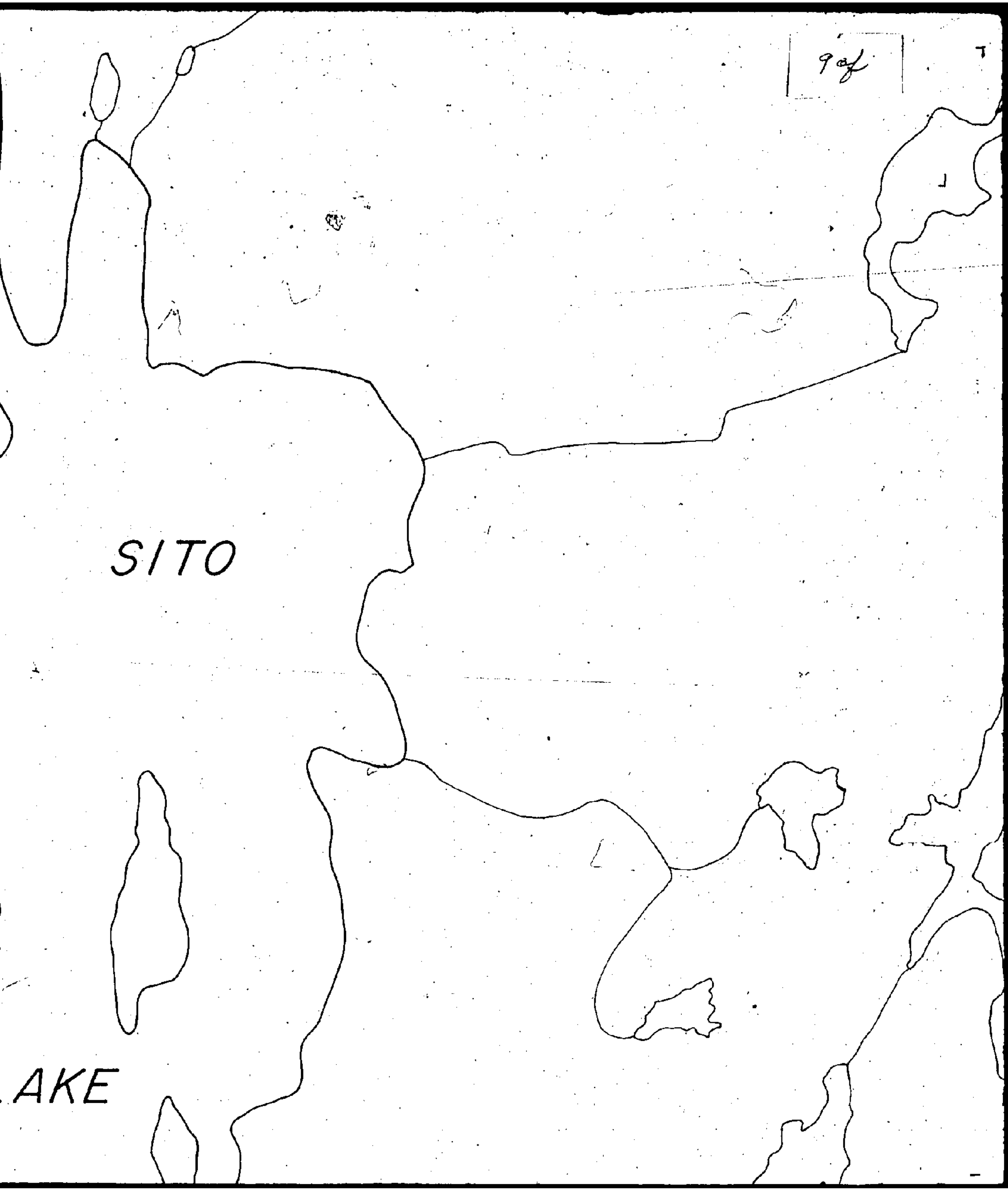

9 of
SITO
AKE

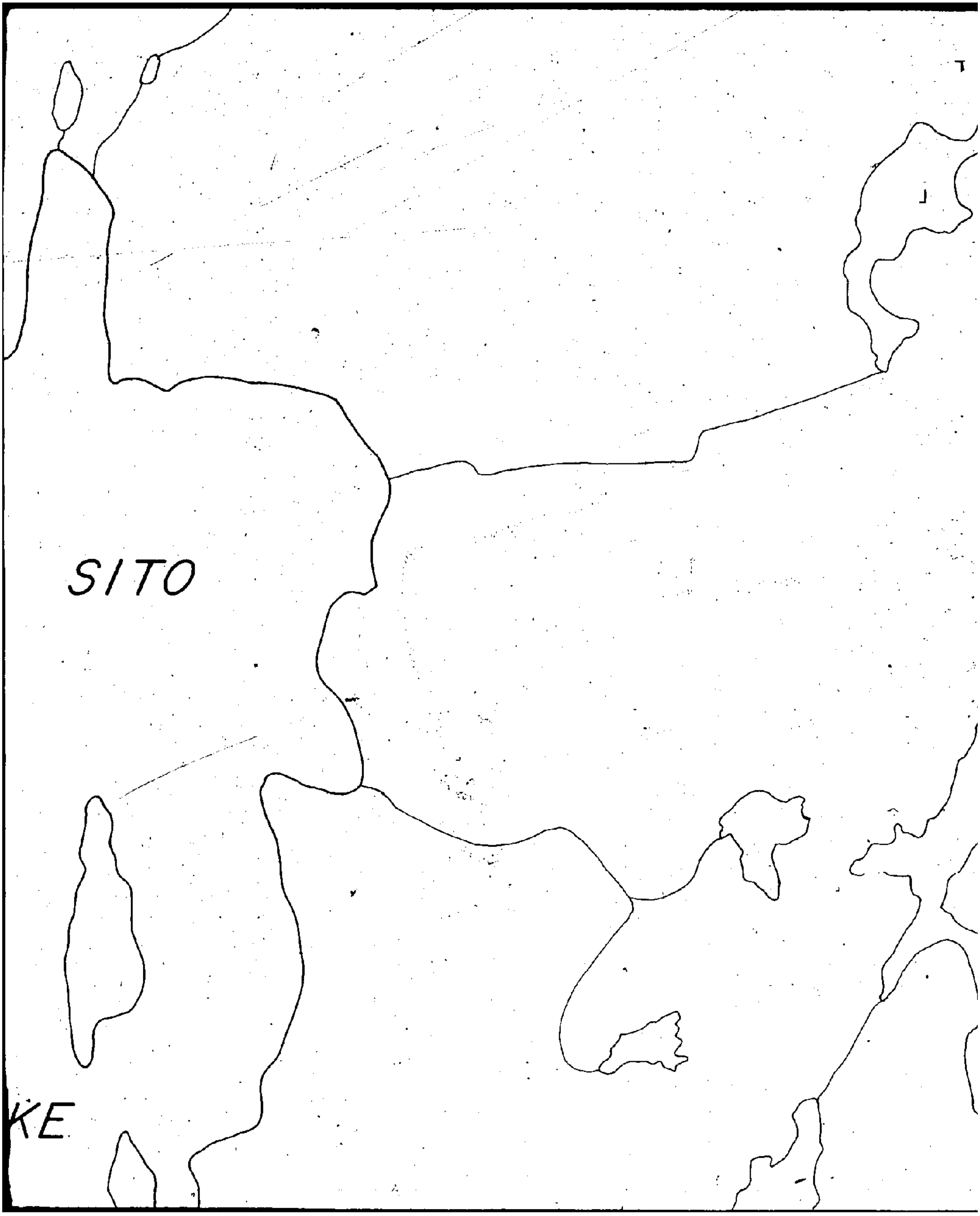
SITO
KE

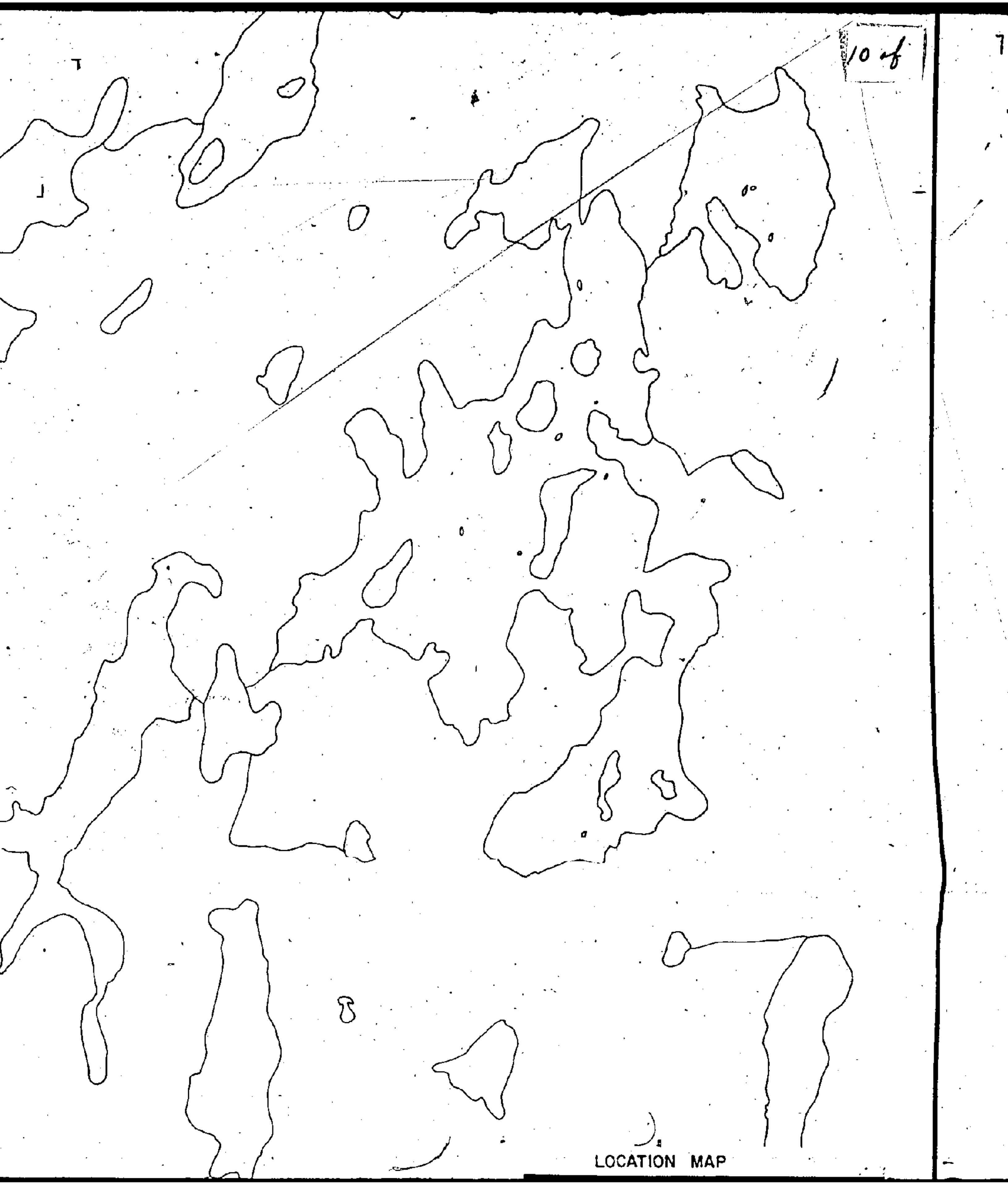
10 of
LOCATION MAP

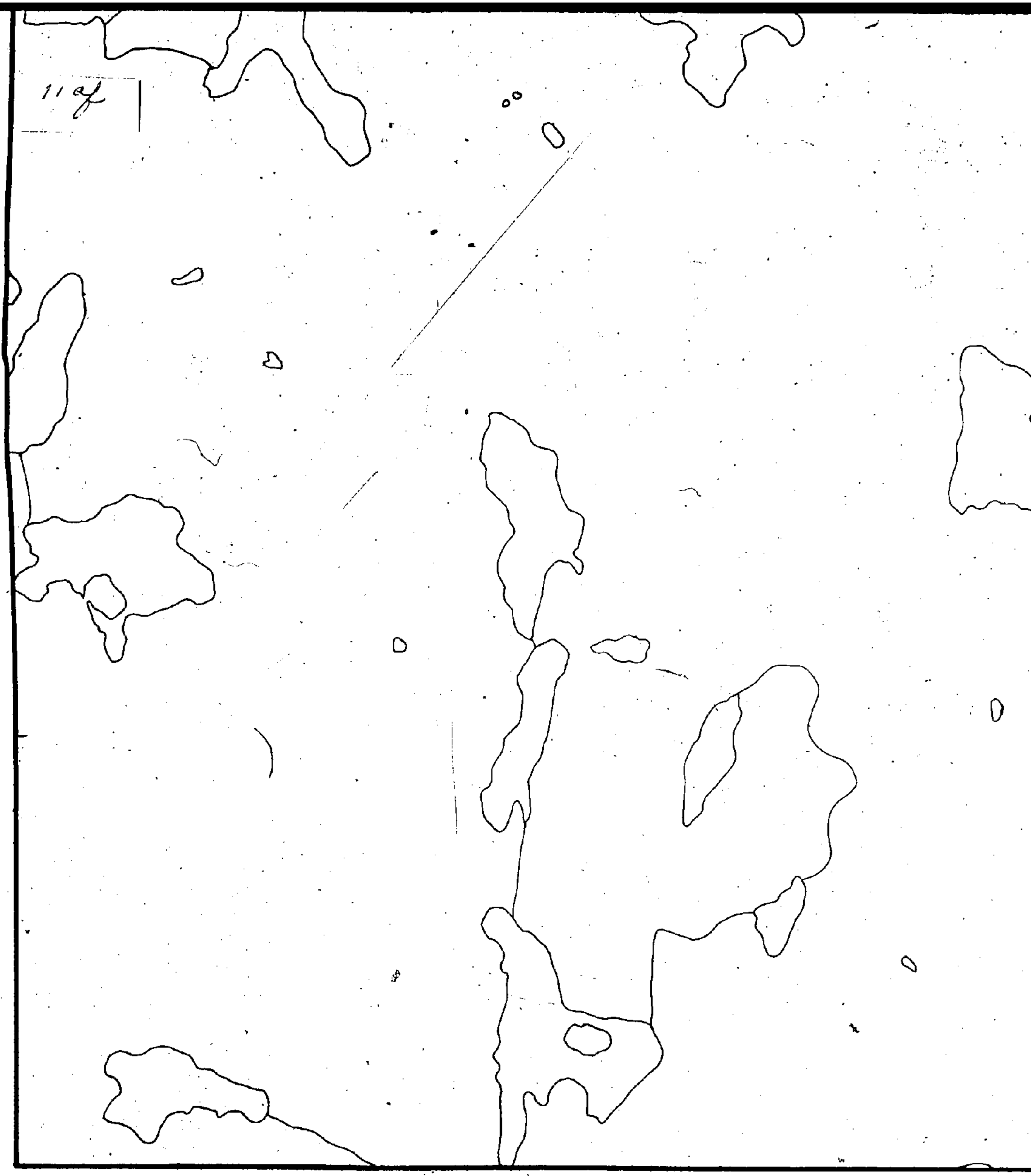
11 af

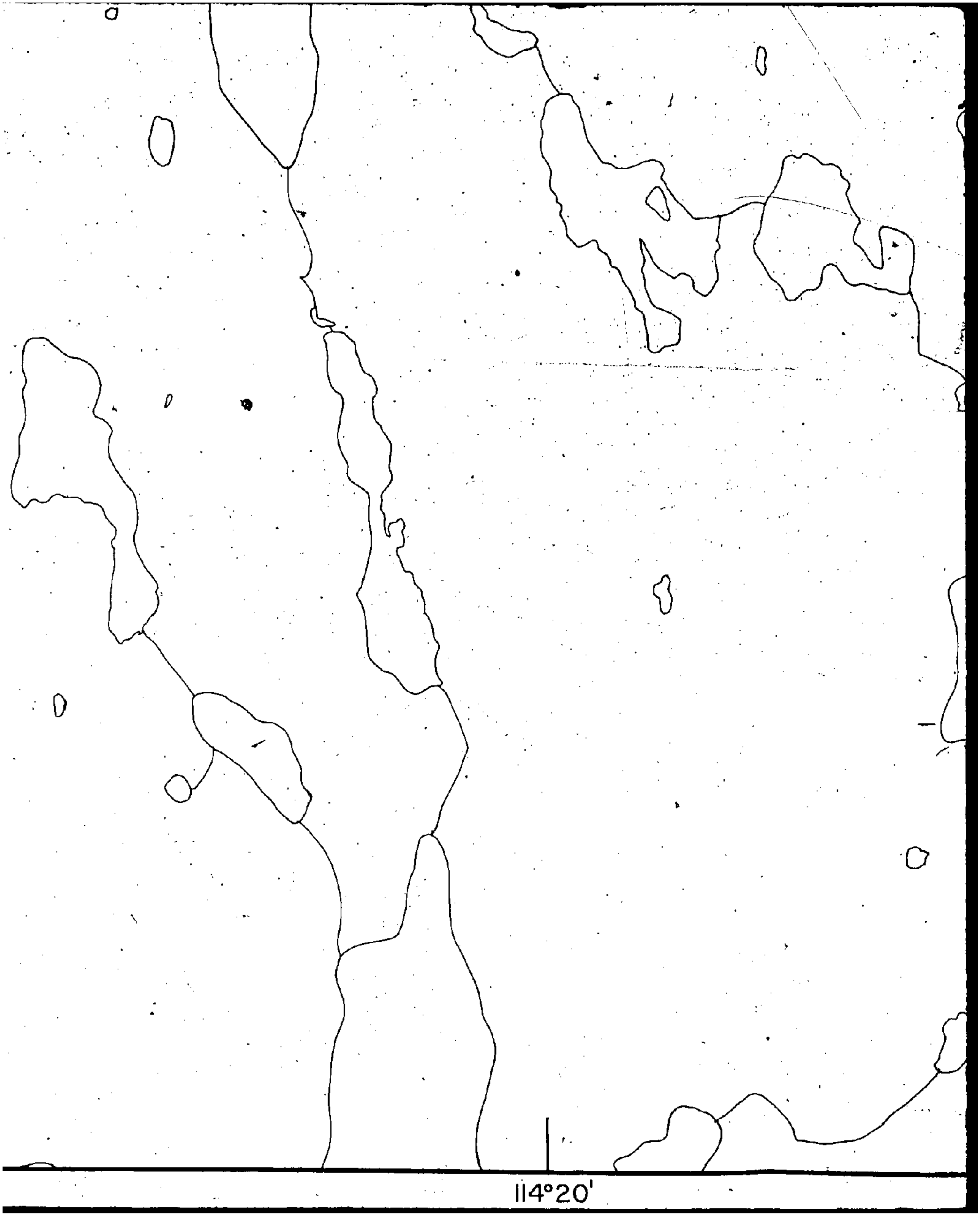
114°20'

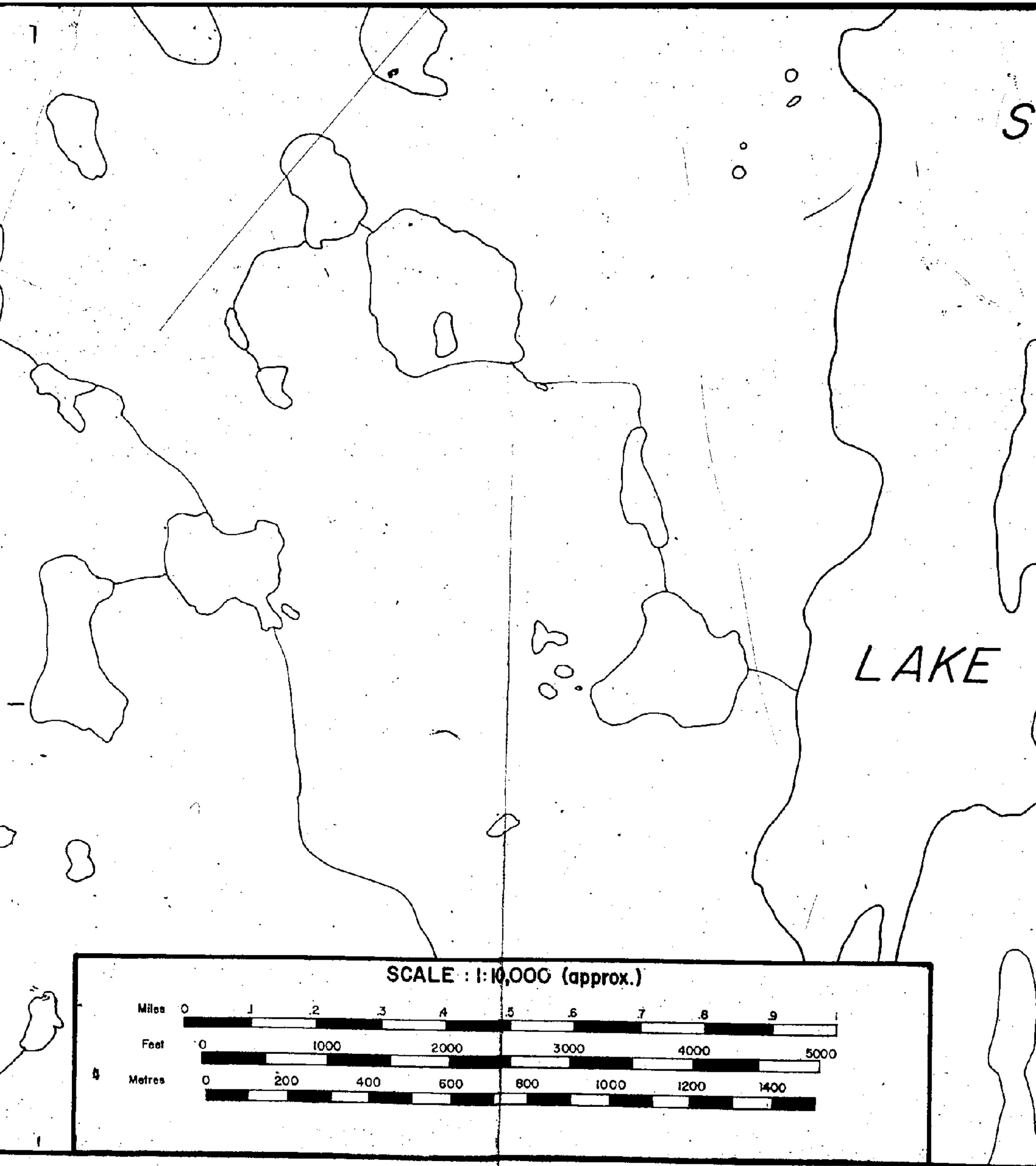
S
LAKE
SCALE : 1:10,000 (approx.)
Miles 0 .1 .2 .3 .4 .5 .6 .7 .8 .9 1
Feet 0 1000 2000 3000 4000 5000
Metres 0 200 400 600 800 1000 1200 1400

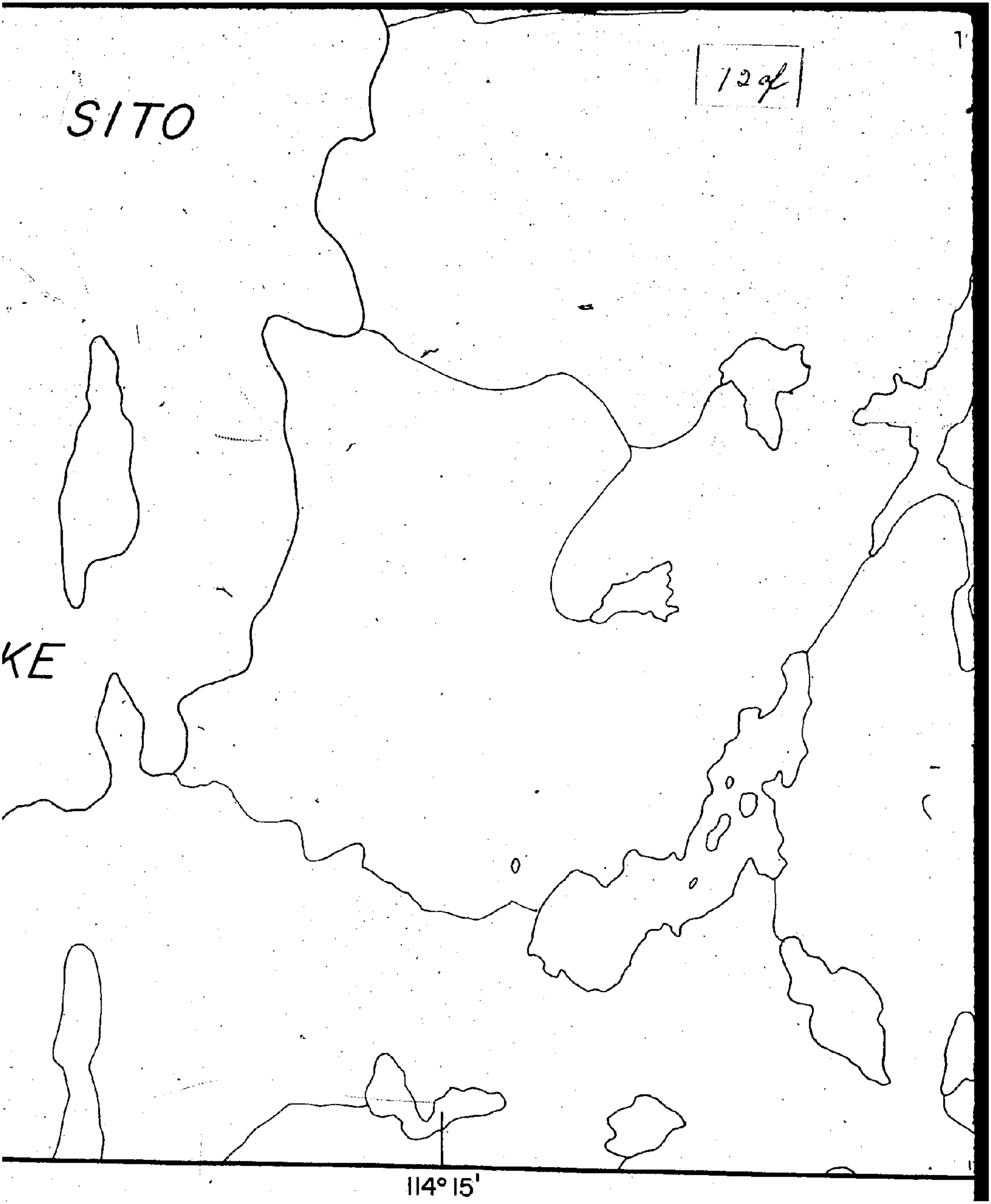
SITO
KE
12 gl
114° 15'

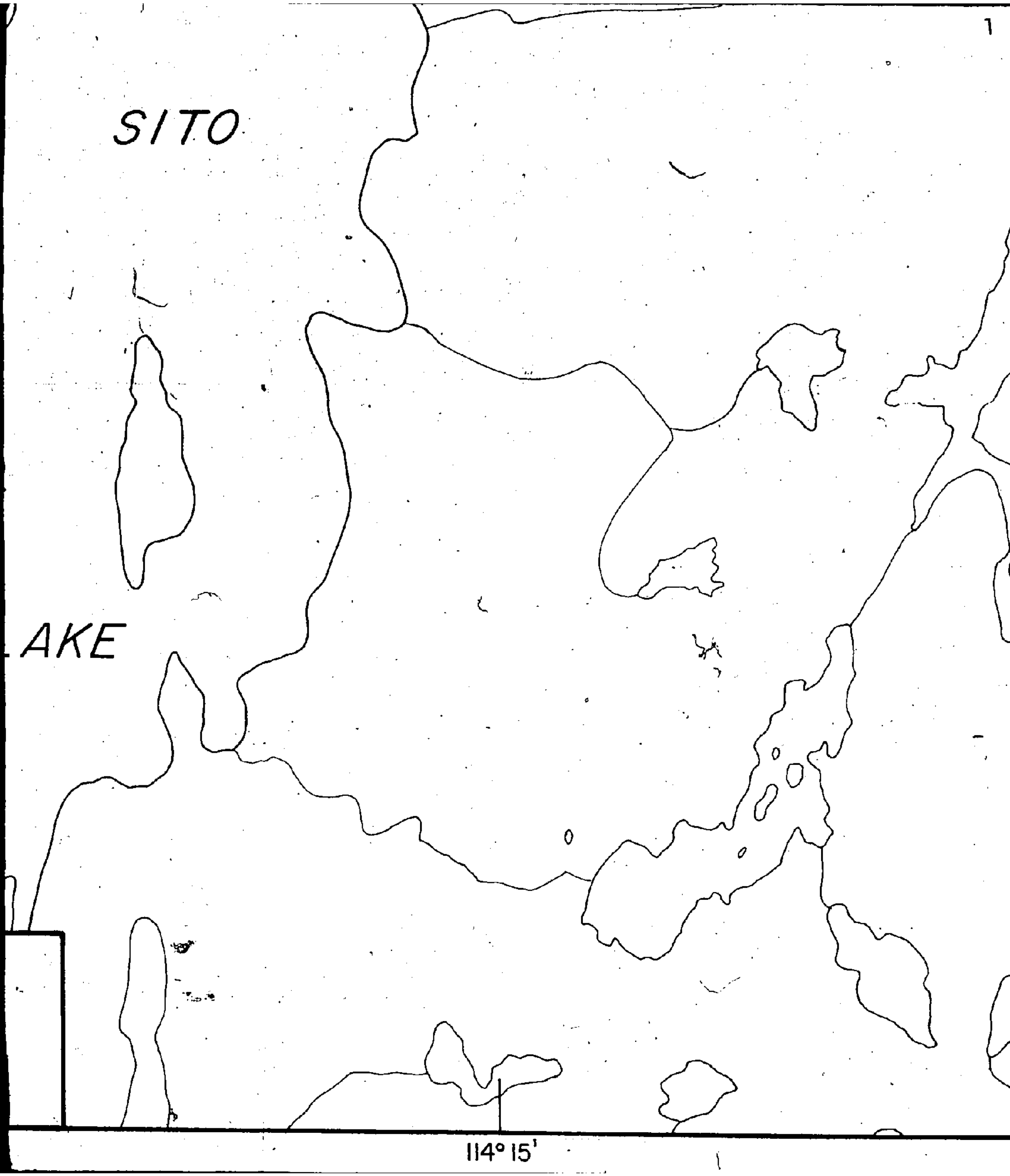
1
SITO
LAKE
114° 15'

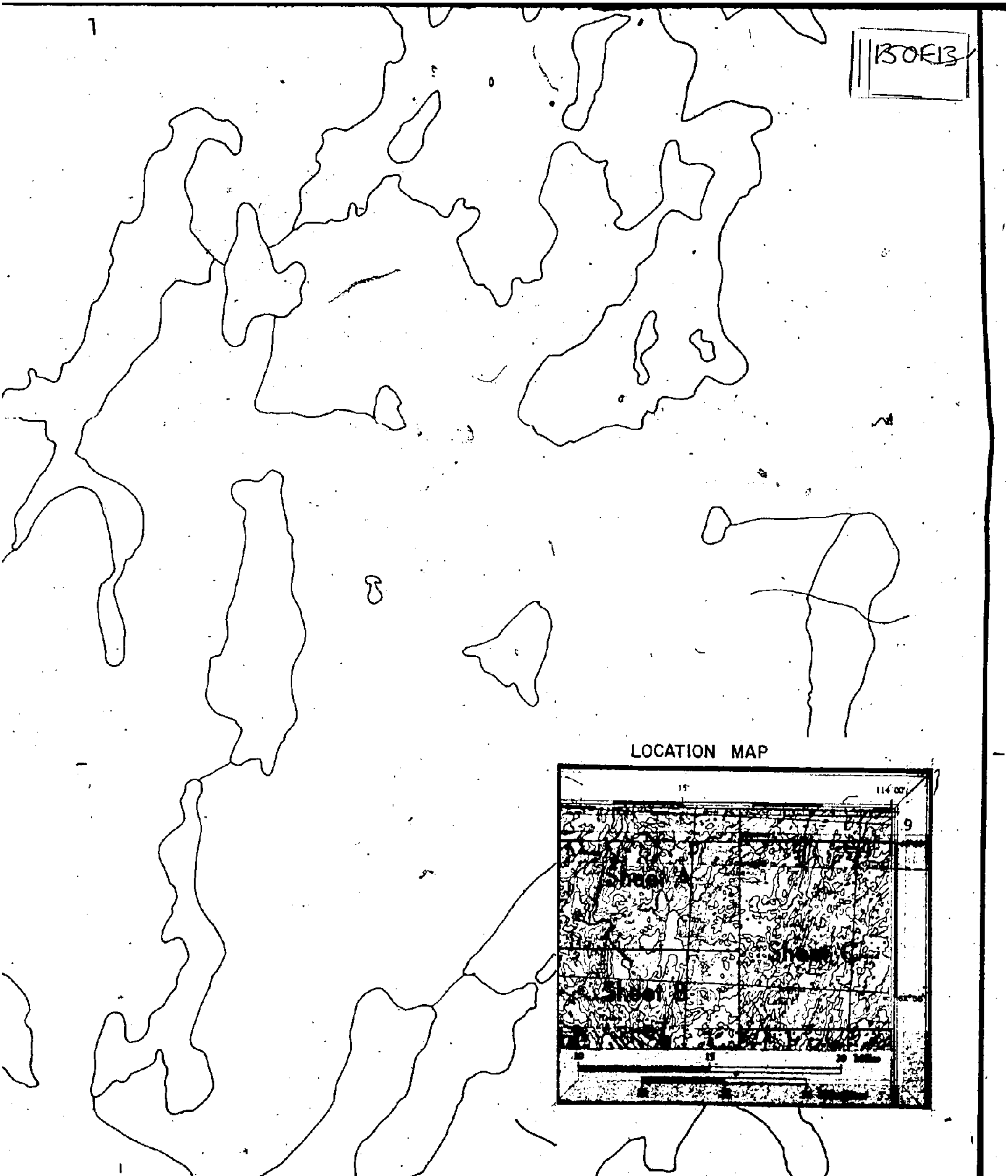


$5.00 ea/$15.00 set

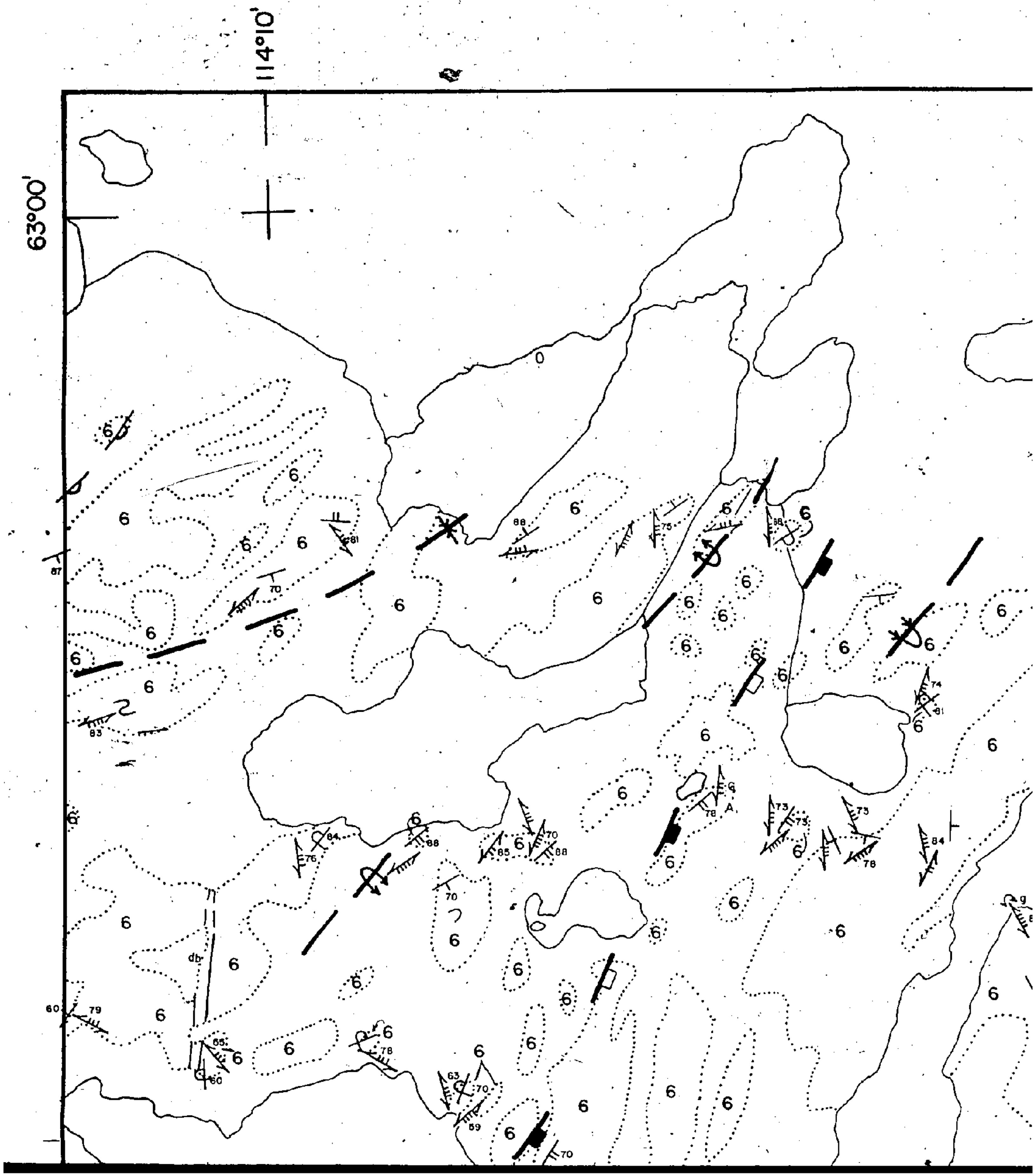

114°10'
63°00'

1 of

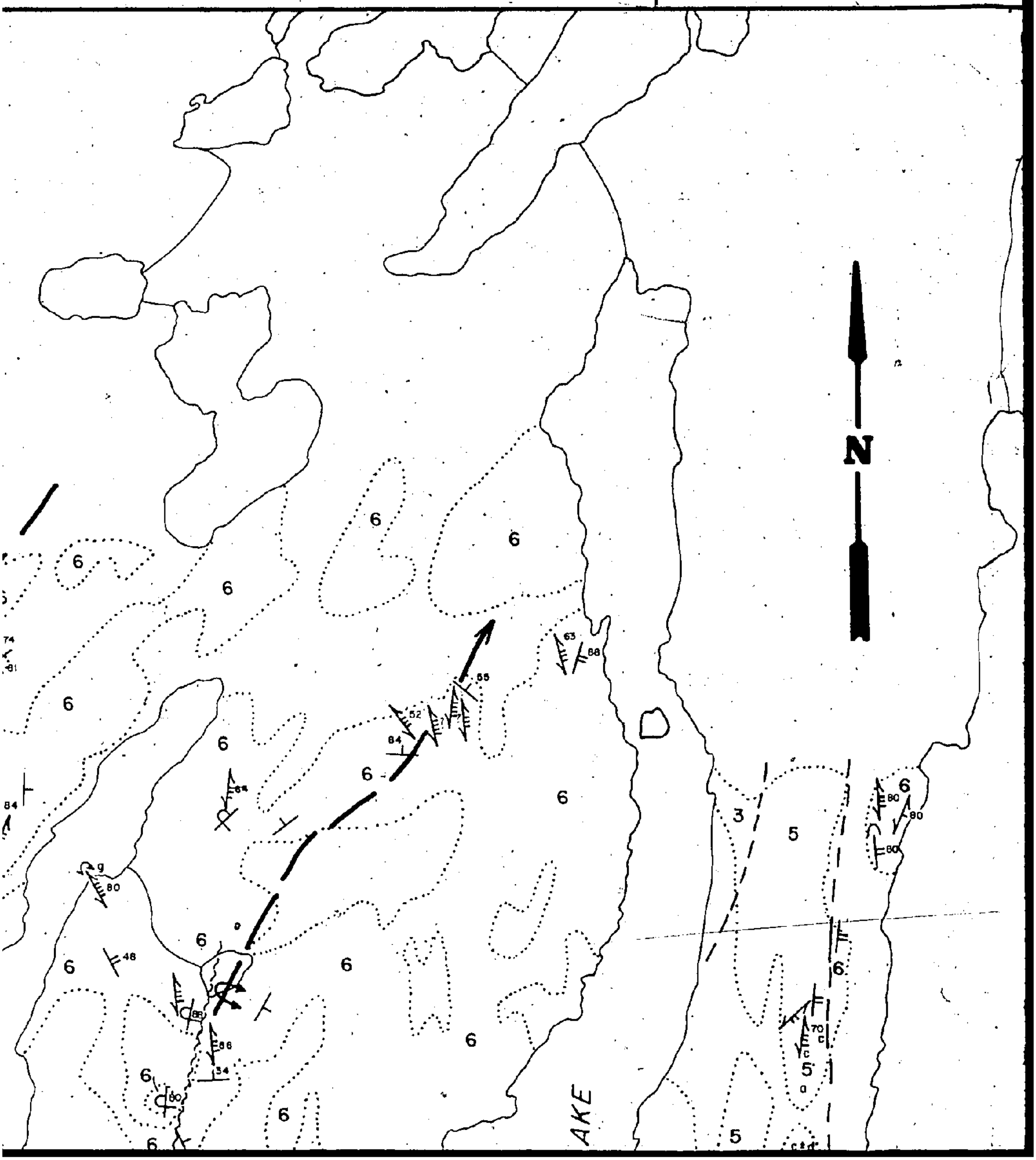

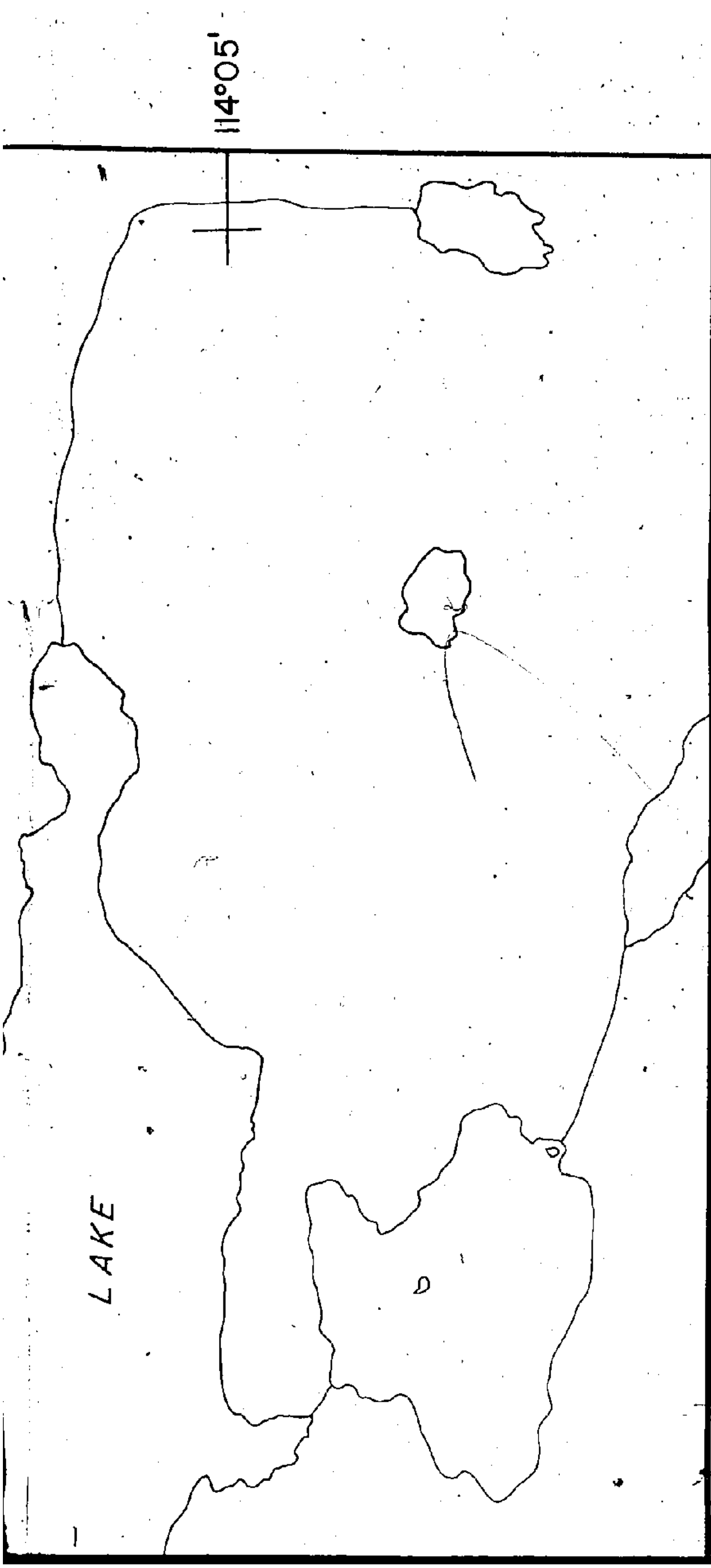


E

INTRODUCTION

The Clan Lake volcanic belt, about
and by Henderson (1976) at a scale of 1
The rock units, part of the Archea
scale of 1:10,000 for an M.Sc. Thesis.
truded by metagabbro dykes and granitic

DESCRIPTION OF ROCK TYPES

The volcanic pile has been subdivi
rhyolite (4), and basalt (5) (Figure 1)
individually include considerable litho
present-day configuration (minus foldin
The oldest unit, (1), is plagiocla
amygdules (up to 2 cm in size). Unit 2
aphyric or plagioclase phyric, in place
dacite lacks primary features and its m
fall and lava flow. The dacite breccia
breccia of a dome complex. The breccia
less than 1 cm to more than a meter in
clast size and the presence of a few ma
Unit 3, volcaniclastic rock, inclu
breccia, the predominant rock types, ar
breccia. Heterolithic conglomerate and
Unit 4, rhyolite and dacite restri
Massive and brecciated dacite form a mi
crysts in a brownish grey, tuffaceous m
zones).
Unit 5, the uppermost unit of the
well-bedded volcaniclastic rocks, with
reworked pillows, pillow breccia and la
and are commonly vesicular. Some clast
(layered flow fragments). The upper pa
character, some being massive, some var
trated at the pillow margins. One flow
Associated with all these volcanic unit
The turbiditic sediments (unit 6)
primary features within incomplete Boum

2 of

114°00'
63°00'

# E.G.S. 1983-5 sheet-"C"

GEOLOGY OF A VOLCANIC PILE AT CLAN LAKE, N.W.T.

E. Hurdle

lt, about 55 km north of Yellowknife, was previously mapped by Jolliffe (1939) at a scale of 1 in. = ½ mile
cale of 1:125,000.
he Archean Yellowknife Supergroup (Henderson, 1970) within the Slave Structural Province, were mapped at a
Thesis. The general geology is that of a volcanic pile surrounded by younger turbidite metasediments in-
granitic rocks. Proterozoic diabase dykes crosscut these rocks.

n subdivided into five lithologic units: andesite (unit 1), dacite (2), volcaniclastic rock (3), dacite/
Figure 1). The rock units are generally in stratigraphic order, though they interfinger with each other and
ble lithologic variation and facies changes. Figure 2 is a facies model for these volcanic units, with the
us folding and faulting) shown on the front side of the block diagram.
plagioclase phyric andesite and includes massive and pillowed flows containing numerous vesicles and quartz
. Unit 2 has been subdivided into a massive dacite and a dacite breccia. The massive dacite is either
in places with a few floating andesite clasts, more rarely with packed clasts. Elsewhere the massive
and its mode of deposition is difficult to determine; probably it includes a combination of ash flow, ash
e breccia is confined to a prominent hill in the NW part of the volcanic pile. It is interpreted as crumble
e breccia is poorly sorted, monomictic, clast-supported and has little matrix. Angular clasts, ranging from
meter in size, are commonly cemented by pink carbonate. The breccia has crude layering due to variations in
a few massive dacite layers. The rock is additionally brecciated in shear zones.
ck, includes interbedded diamictites, breccia, conglomerate, sandstone and pelite. The diamictite and
types, are debris flow deposits. Monomictic conglomerate near the dome complex is fluvially reworked crumble
erate and rippled and crossbedded sandstone form other fluvial deposits.
te restricted to the western flank of the volcanic pile, consists mainly of ash fall and ash flow deposits.
form a minor component. Ash fall tuff, predominantly at the top of the unit, has abundant plagioclase pheno-
faceous matrix. Ash flow tuff is a light grey tuffaceous rock with discrete, dark, lenticluar zones (welded

t of the volcanic pile, is andesite and basalt. The lower part of this unit is predominantly meter-scale,
ks, with minor interbeds of pillowed and layered flows, pillow breccia and hyaloclastite. The clasts are
ia and layered flows; most are well rounded, sometimes white due to alteration by carbonate and sericite,
ome clasts are concentrically zoned with vesicles (lava tube fragments?) and others are parallel zoned
upper part of unit 5 is composed predominantly of pillowed and massive flows. The pillows vary in size and
some variolitic, and others vesicular, with vesicles either uniformly distributed, radiating, or concen-
One flow unit grades from small, non-vesicular pillows to large, vesicular ones (shallowing upwards).
anic units, in varying amounts, are airfall deposits.
(unit 6) are mainly greywackes and mudstones, which, despite metamorphism and deformation, preserve numerous
lete Bouma cycles. Sedimentary structures that are good top indicators include grading, crossbedding

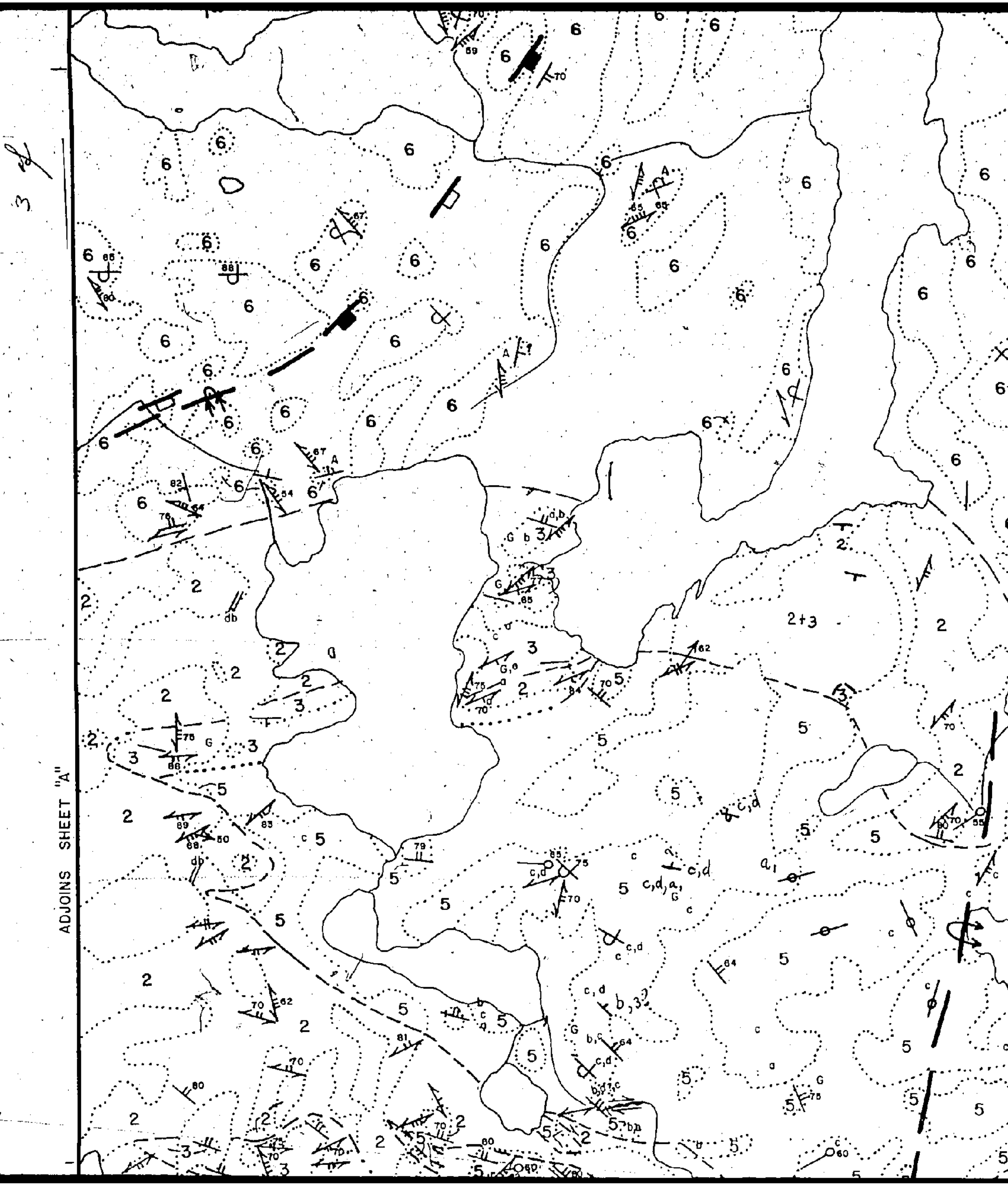
ADJOINS SHEET "A"

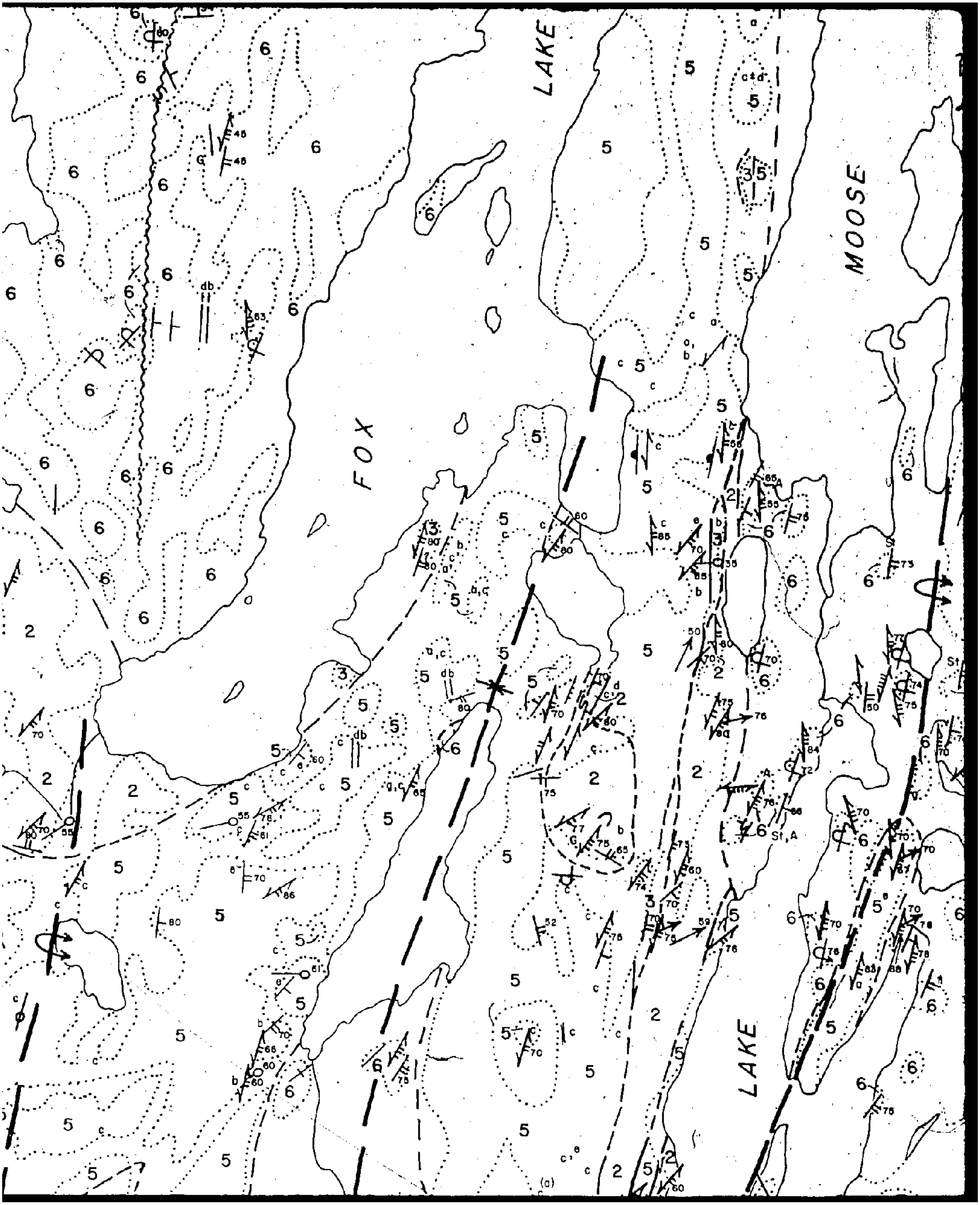

LAKE
FOX
MOOSE
LAKE
(a)

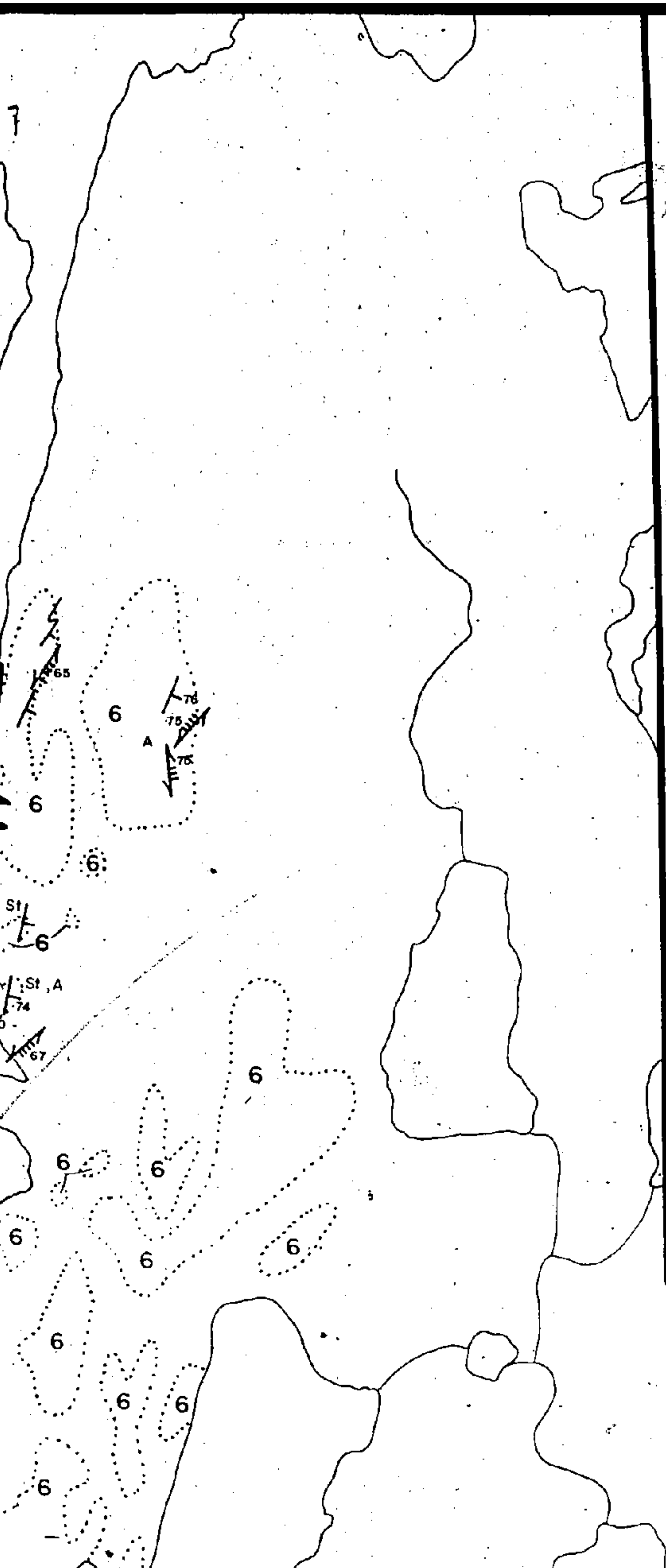


character, some being massive, some variolitic, and ot
trated at the pillow margins. One flow unit grades fr
Associated with all these volcanic units, in varying a
The turbiditic sediments (unit 6) are mainly grey
primary features within incomplete Bouma cycles. Sedi
scours, load and flame structures, ball and pillow str
clasts and rare flaser bedding are also present. The
sediments are exposed within the core of an anticline
3/4 and mafic volcanics of unit 5. The turbidites loc

Metagabbroic dykes and other bodies (unit 7) intr
show primary, rhythmic layering.

Granitic rocks (unit 8) intrude both the sediment
white and contain both biotite and muscovite.

Proterozoic diabase dykes crosscut all the above

DEFORMATION AND METAMORPHISM

The rocks have undergone a complex history of def
are present, a northeast- to north-trending set and a w
facing direction of both fold sets indicate earlier fo
deformation. The earliest foliation is characterised b
is widespread in the felsic volcanics, rare in the maf
by later cleavages in the mudstone, except as incl
locally northeast across all the rock types. In th
cleavage in the greywacke forms a closely-spaced anast
is expressed as a well-defined, slaty cleavage in the
the earlier $S_1$ segregation cleavage. In both the fel
aligned parallel to $S_2$ to form a foliated and/or linea
north-northeast and is axial planar to minor isoclinal
present, it is a fine, continuous cleavage in greywack
felsic volcanics (unit 4), as a crenulation cleavage w

Proterozoic faults crosscut the area, with a majo

The rocks were metamorphosed to greenschist and
the sediments, outlining a zone of low grade (inclu
narrow zone around the granitic intrusions in the west
dant within units 3 and 5 of the volcanics and are onl
Andalusite and staurolite are sporadically distributed

Chlorite, muscovite and biotite grew throughout
grew during the end of and after the last deformation

REFERENCES


Henderson, J.B., 1970:
Stratigraphy of the Archean Yellowknife Supergro
Paper 70-26.

Henderson, J.B., 1976:
Geology Yellowknife (85J), District of Mackenzie

Jolliffe, A.W., 1939:
Preliminary Maps, Quyta Lake and parts of Fishin


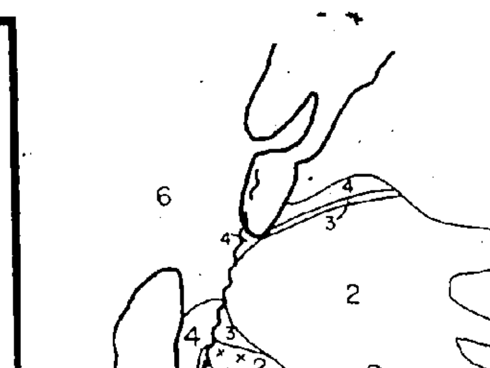

olitic, and others vesicular, with vesicles either uniformly ...
unit grades from small, non-vesicular pillows to large, vesicular ones (shallowing upwards).
, in varying amounts, are airfall deposits.
re mainly greywackes and mudstones, which, despite metamorphism and deformation, preserve numerous
cycles. Sedimentary structures that are good top indicators include grading, crossbedding,
and pillow structures, and convolute bedding. Sandstone dyklets, climbing ripples, mud rip-up
present. The turbidites are mainly younger than the volcanic rocks, though some similar older
an anticline at the SW end of the volcanic pile and also nearby between felsic volcanics of unit
turbidites locally contain felsic volcanic clasts near the contact with the volcanics.
s (unit 7) intrude both the sediments and the volcanics. The rocks are now amphibolites, but still

th the sediments and volcanics and contain xenoliths of these rocks. The granites are pink to
ovite.
all the above rock types.

history of deformation and metamorphism. Two sets of moderately-to steeply-plunging major folds
ing set and a west to northwest one. The time relationship of these sets is not clear. Changes in
cate earlier folding. Overprinting these folds are foliations developed during three periods of
characterised by an easterly-striking set of discontinuous, spaced segregation cleavage ($S_1$), which
rare in the mafic volcanics and locally developed in the greywacke. $S_1$ is completely obliterated
ept as inclusion trails in biotite porphyroblasts. The second foliation ($S_2$) strikes northwest to
ypes. $S_2$ in the sediments is an axial planar cleavage to minor isoclinal to closed folds. The
ly-spaced anastomosing or wavy pattern, and primary structures tend to be aligned subparallel. $S_2$
leavage in the mudstone. In the felsic volcanics $S_2$ is a fine, continuous cleavage crosscutting
n both the felsic and mafic volcanics primary features such as pillows, amygdules, and clasts are
ed and/or lineated fabric. The third foliation ($S_3$) is mainly confined to the turbidites, strikes
minor isoclinal to closed folds. $S_3$ is dominantly a crenulation cleavage, though, where $S_2$ is not
age in greywacke and a slaty cleavage in mudstone similar to $S_2$. $S_3$ is only locally seen in the
tion cleavage which is axial planar to chevron folds affecting $S_2$.
ea, with a major set trending north-northeast and a minor set trending easterly.
eenschist and lower amphibolite grade. Two major cordierite isograds trend north-northeast through
grade (including sub-biotite) rocks in the center and higher grade rocks to the east and west. A
ions in the west is cordierite-free, despite being above the cordierite isograd. Garnets are abun-
nics and are only locally apparent in the turbidites, both above and below the cordierite isograd.
ally distributed within the sediments above the cordierite isograd.
rew throughout the last three deformation periods and cordierite, garnet, andalusite and staurolite
ast deformation.


wknife Supergroup, Yellowknife Bay-Prosperous Lake area, District of Mackenzie; Geol. Surv. Can.,

ct of Mackenzie; Geol. Surv. Can., Open File 353.

parts of Fishing Lake and Prosperous Lake areas, Northwest Territories; Geol. Surv. Can., Paper 39-6.


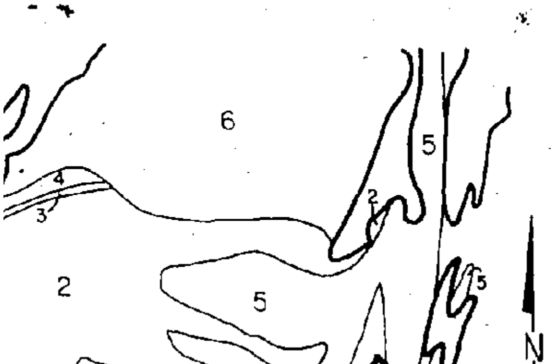


LEGEND
(for fig. 1 and 2)

| | |
|---|---|
| 6 | TURBIDITE SEDIMENTS |
| 5 | BASALT/ANDESITE |
| 4 | RHYOLITE / DACITE |

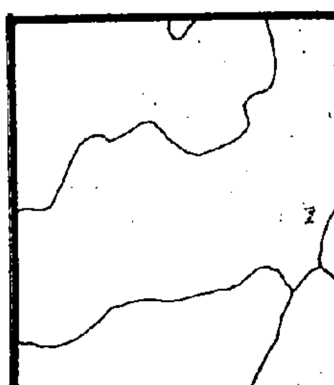

5 of

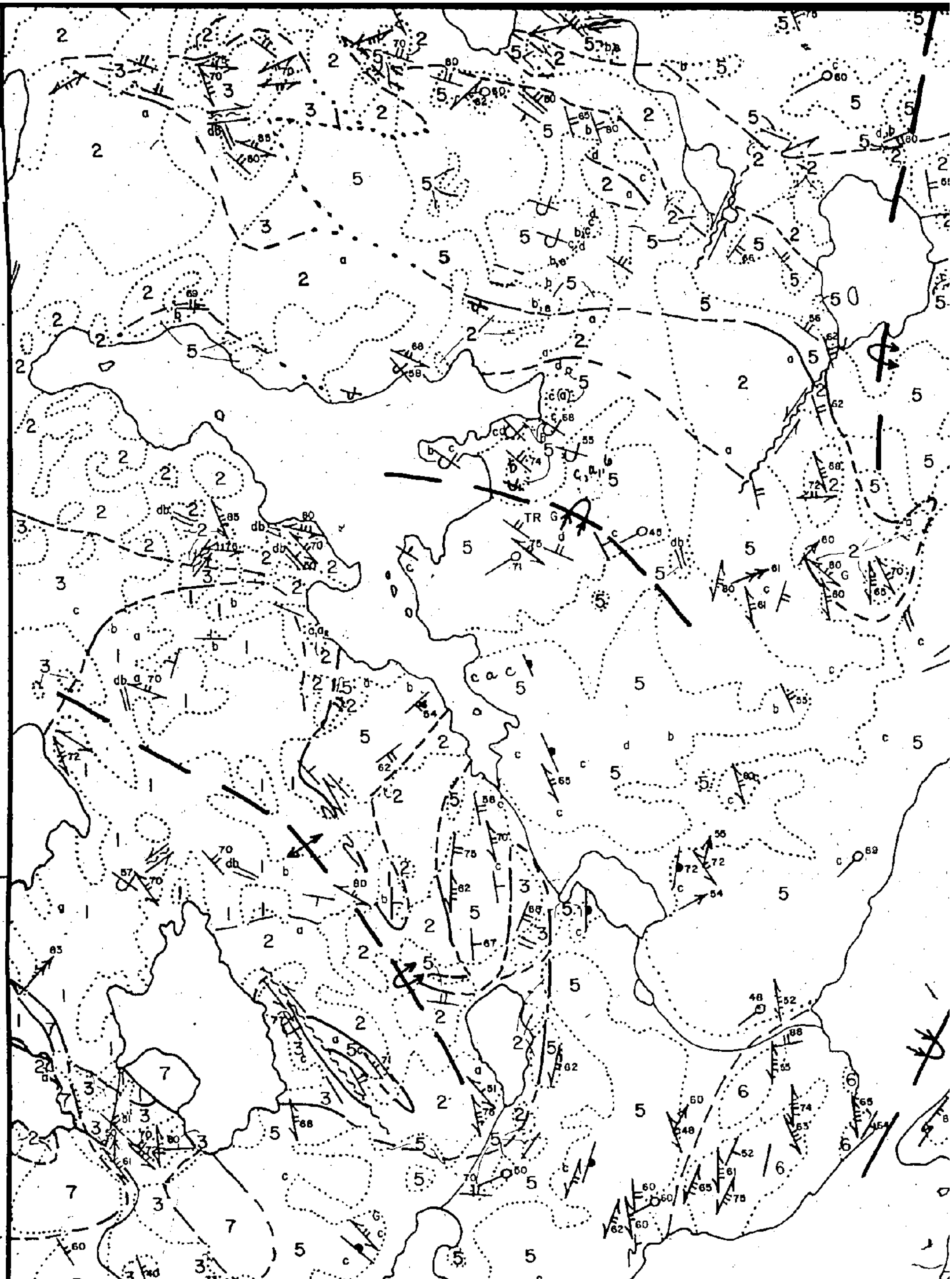

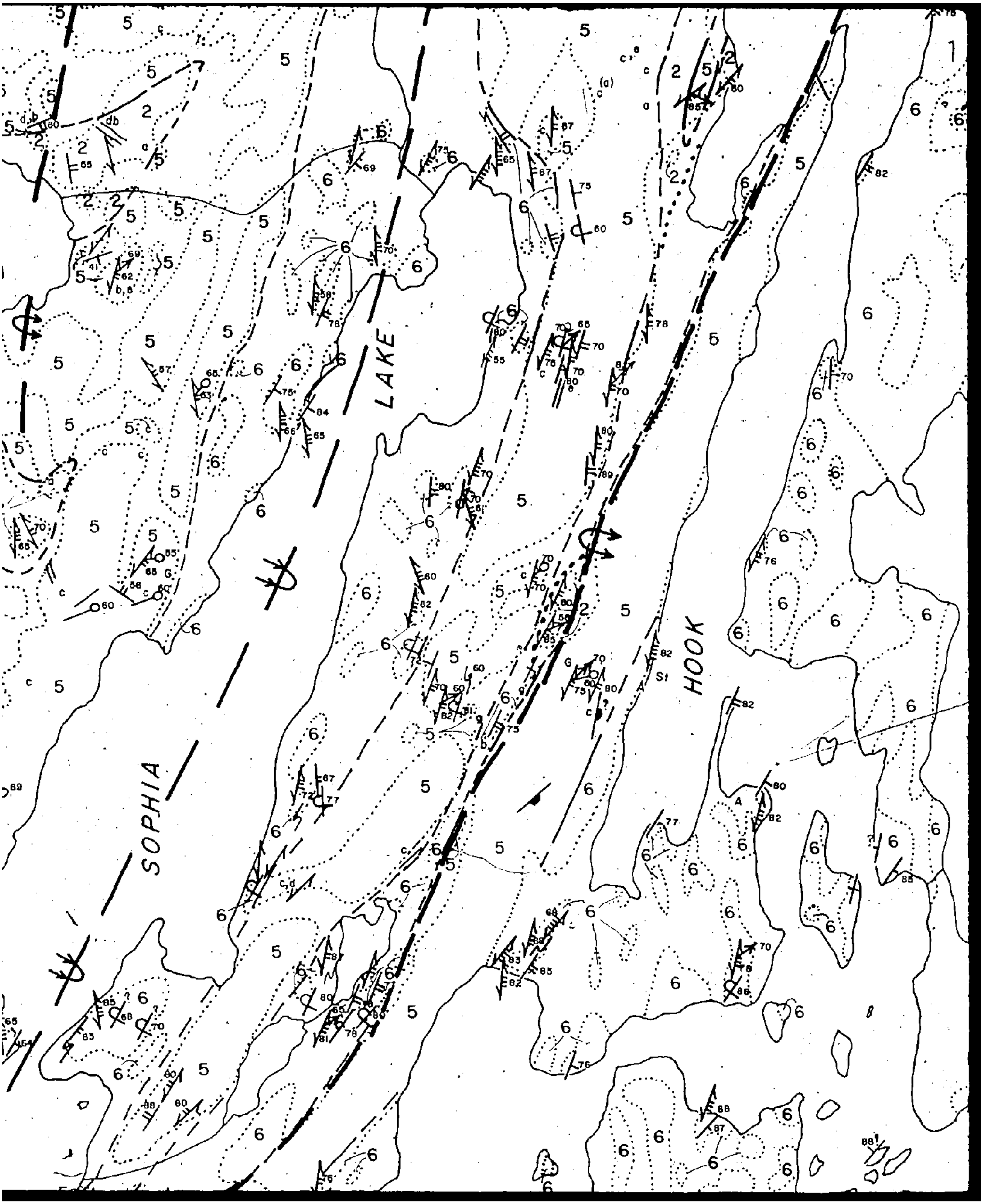
LAKE
SOPHIA
HOOK

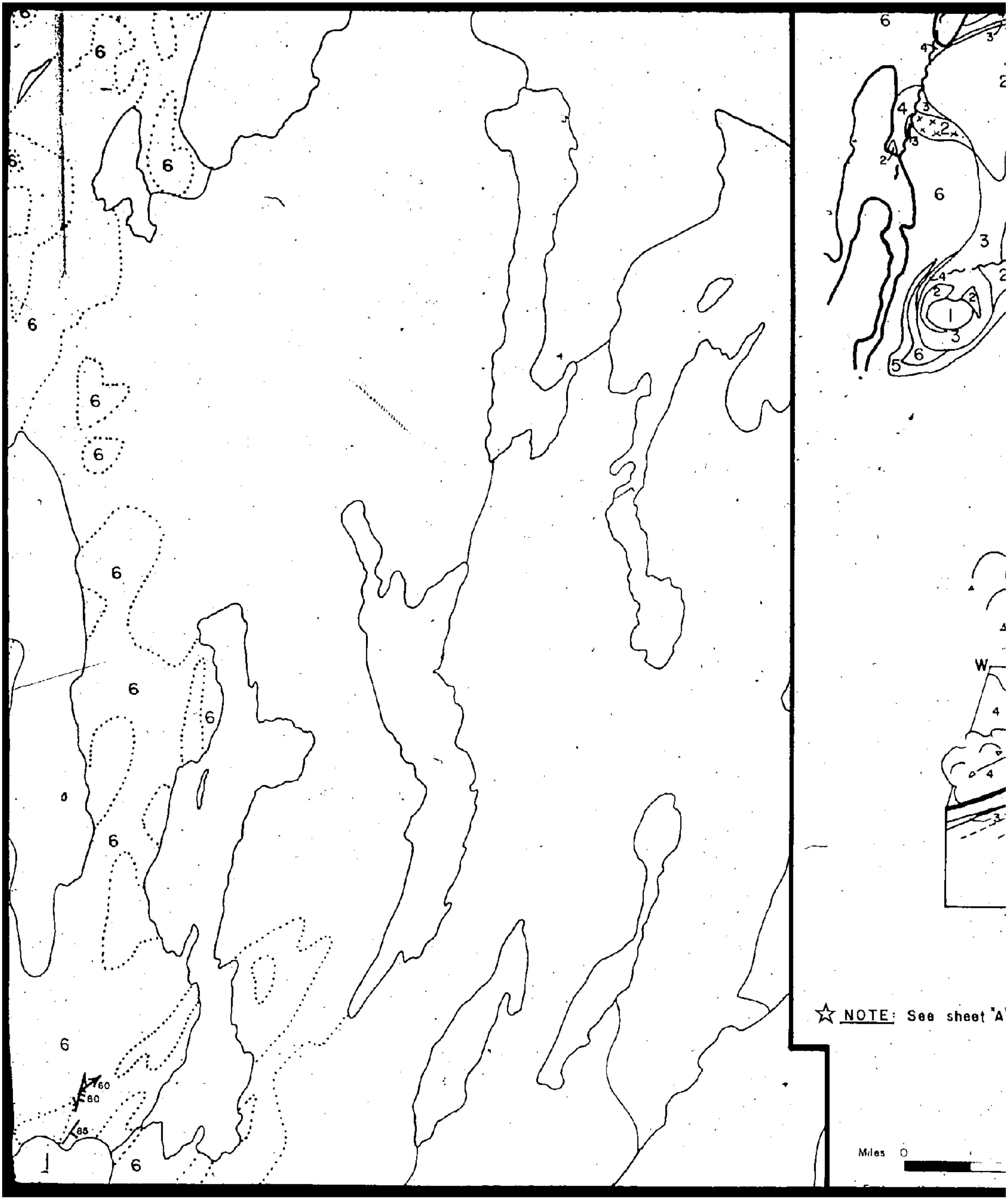

☆ NOTE: See sheet "A"
Miles 0
W

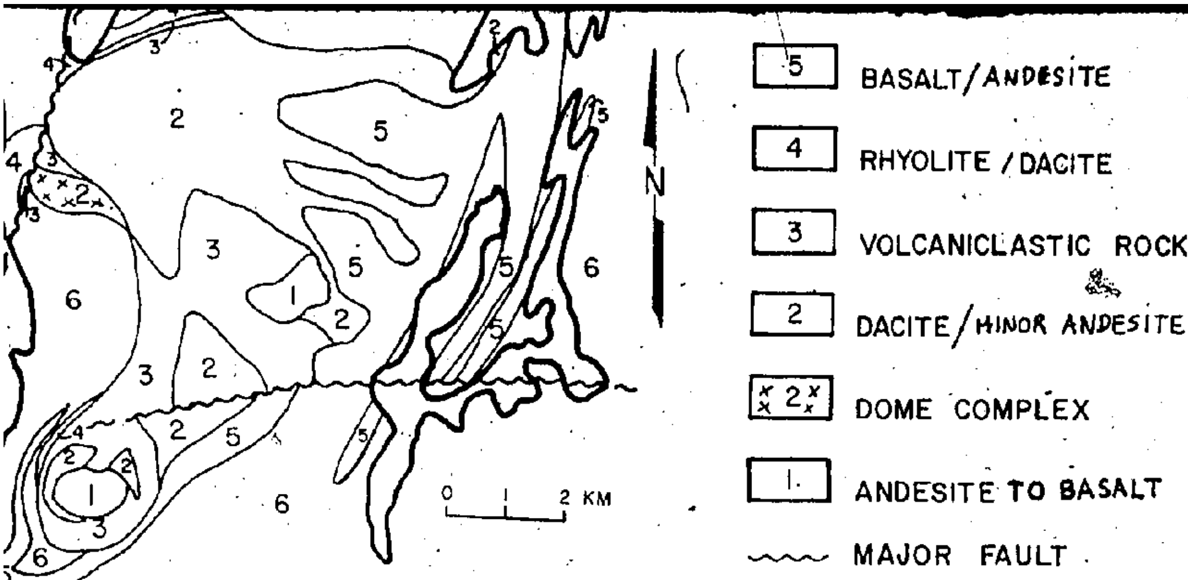


FIGURE : 1

6 of

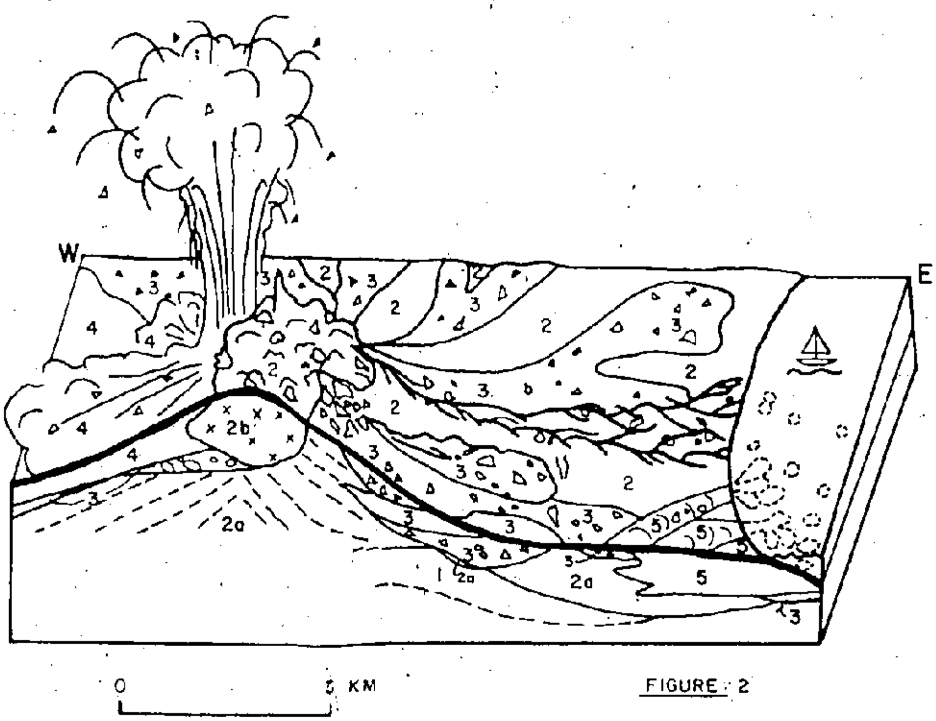


FIGURE : 2

See sheet "A" for main map legend

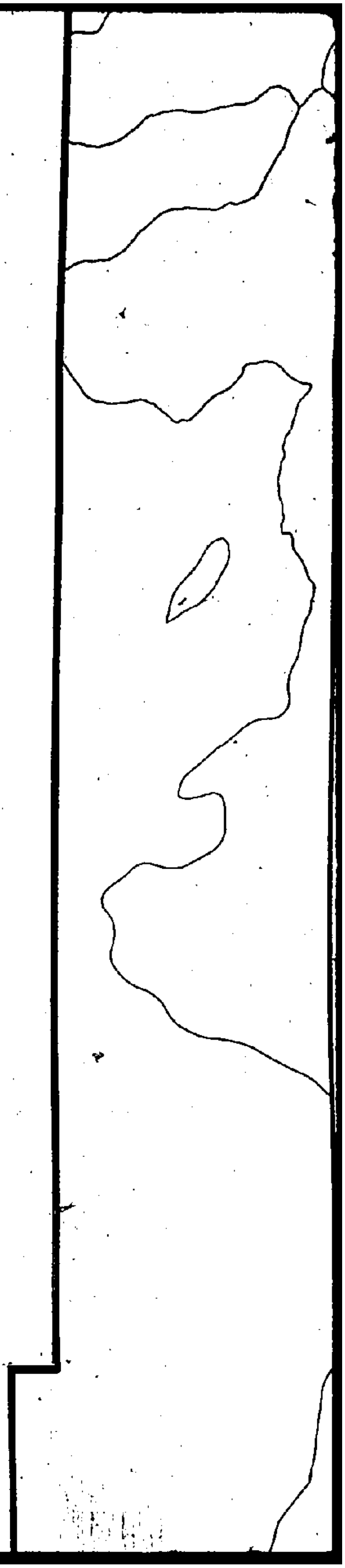

SCALE 1:10,000 (approx.)

0 .3 .4 .5 .6 .7 .8 .9 1

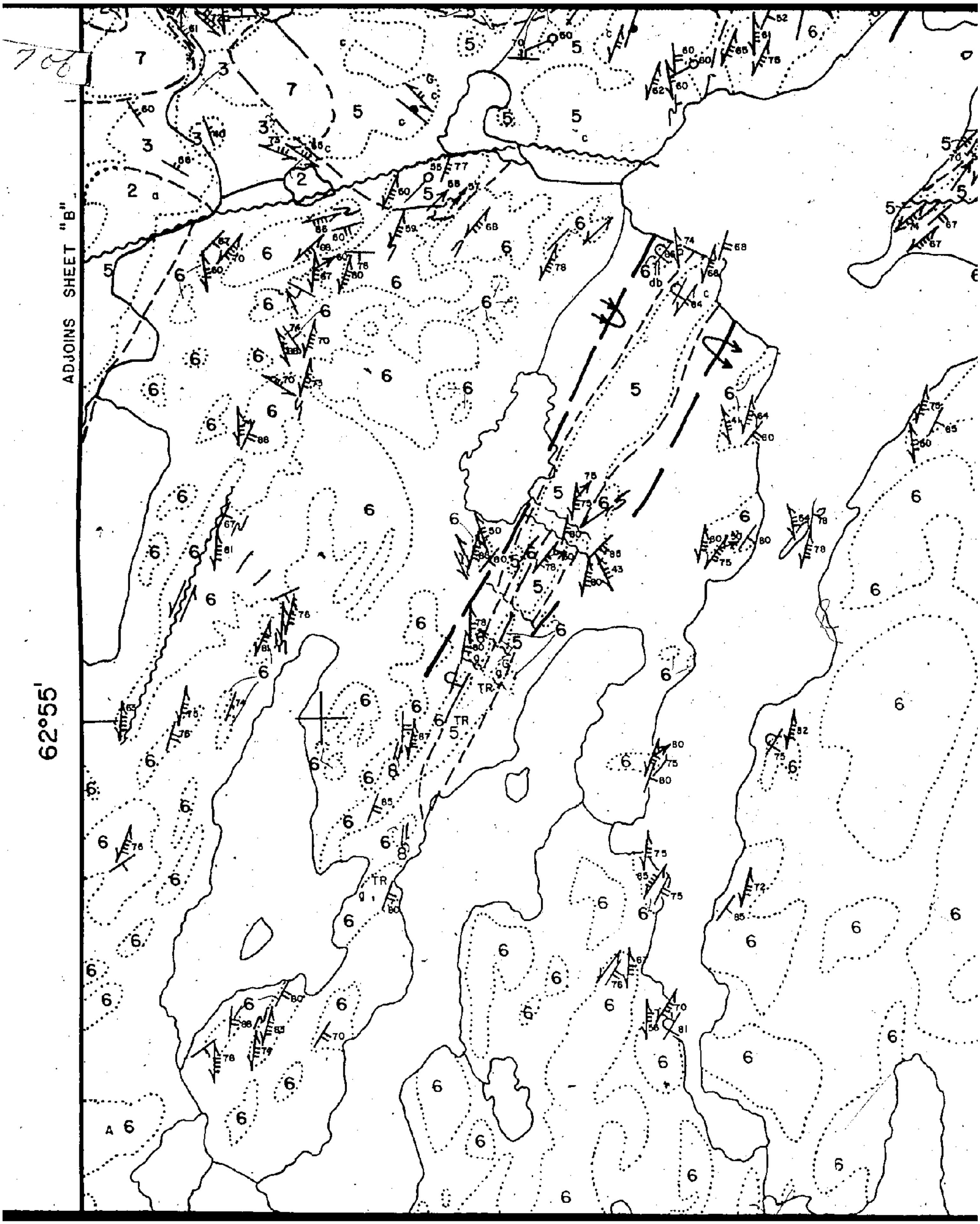
ADJOINS SHEET "B"
62°55'

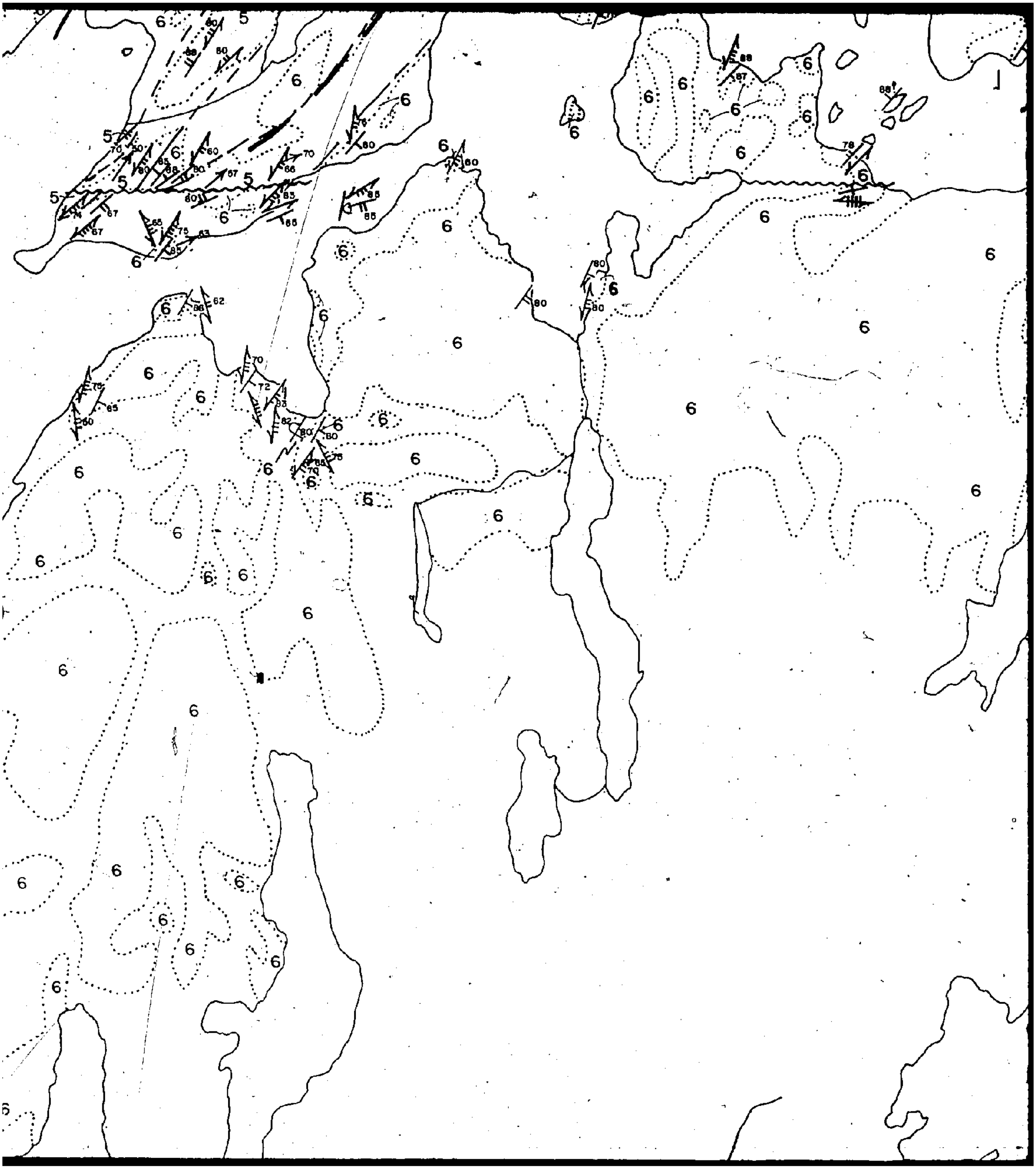

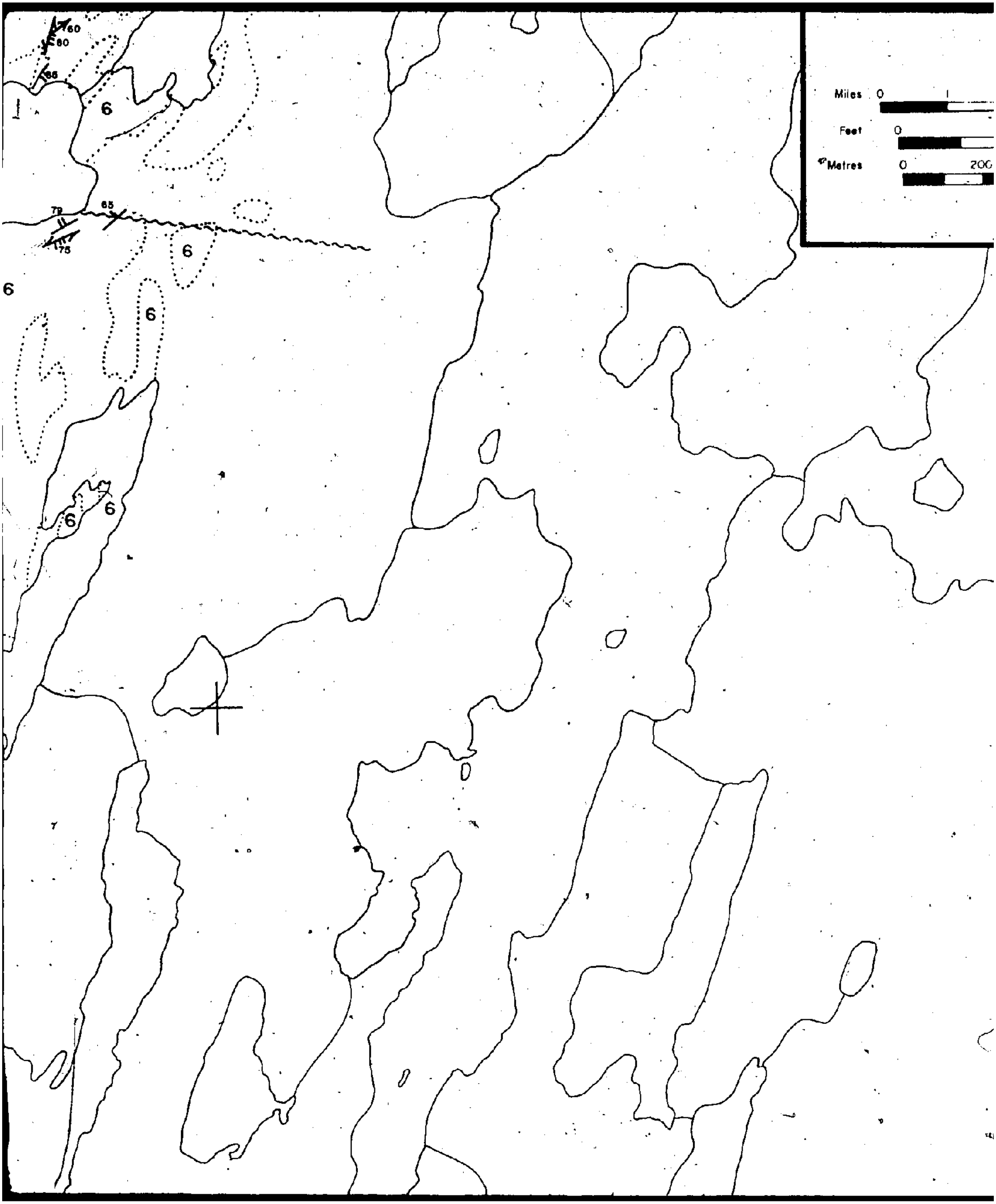

Miles 0 1
Feet 0
Metres 0 200
6
6
6
6
6
6
6
60
80
65
70
65
75

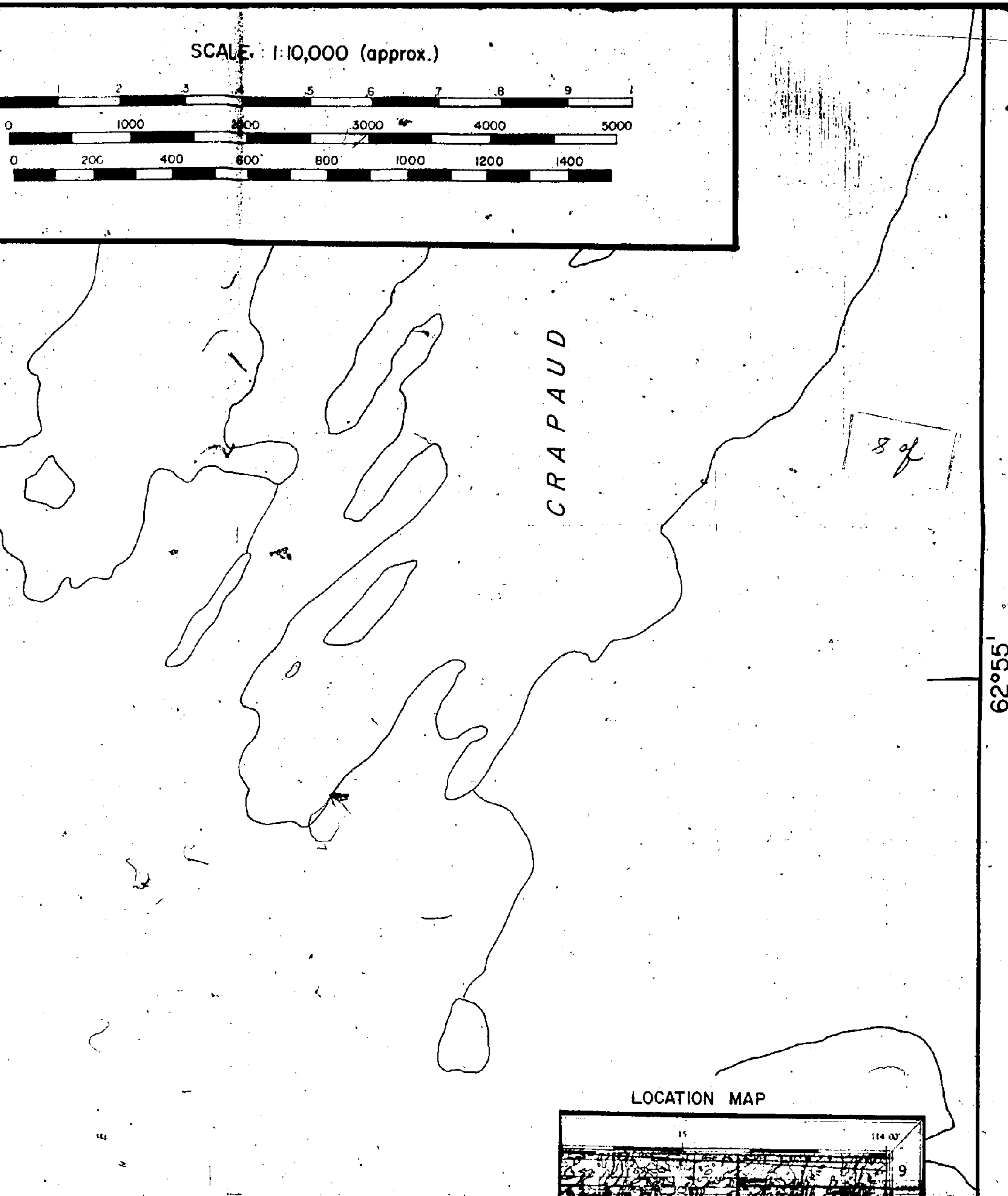
SCALE: 1:10,000 (approx.)
1 2 3 4 5 6 7 8 9 1
0 1000 2000 3000 4000 5000
0 200 400 600 800 1000 1200 1400
CRAPAUD
62°55'
LOCATION MAP
9

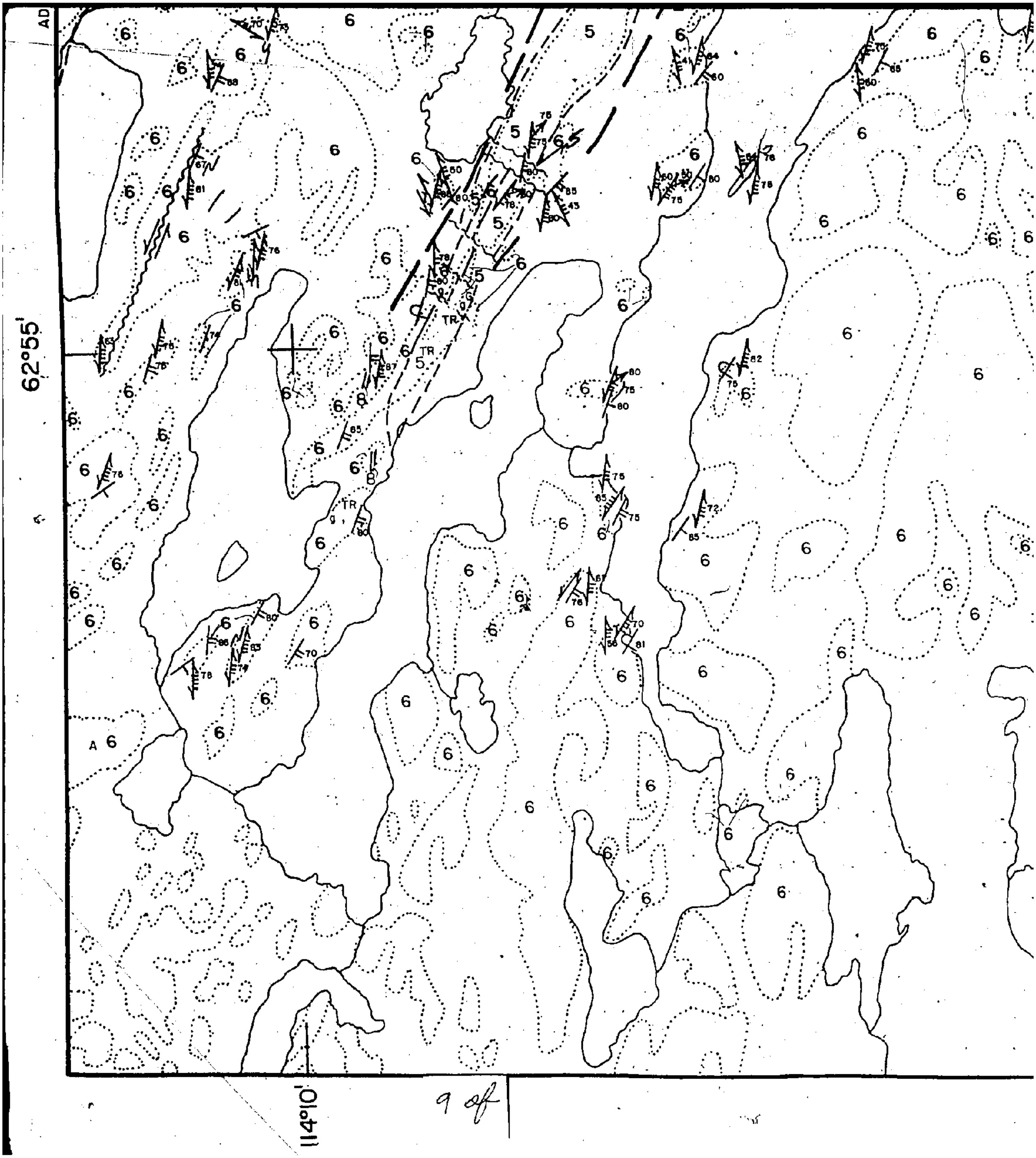

AD
62°55'
114°10'
TR
A
9 of

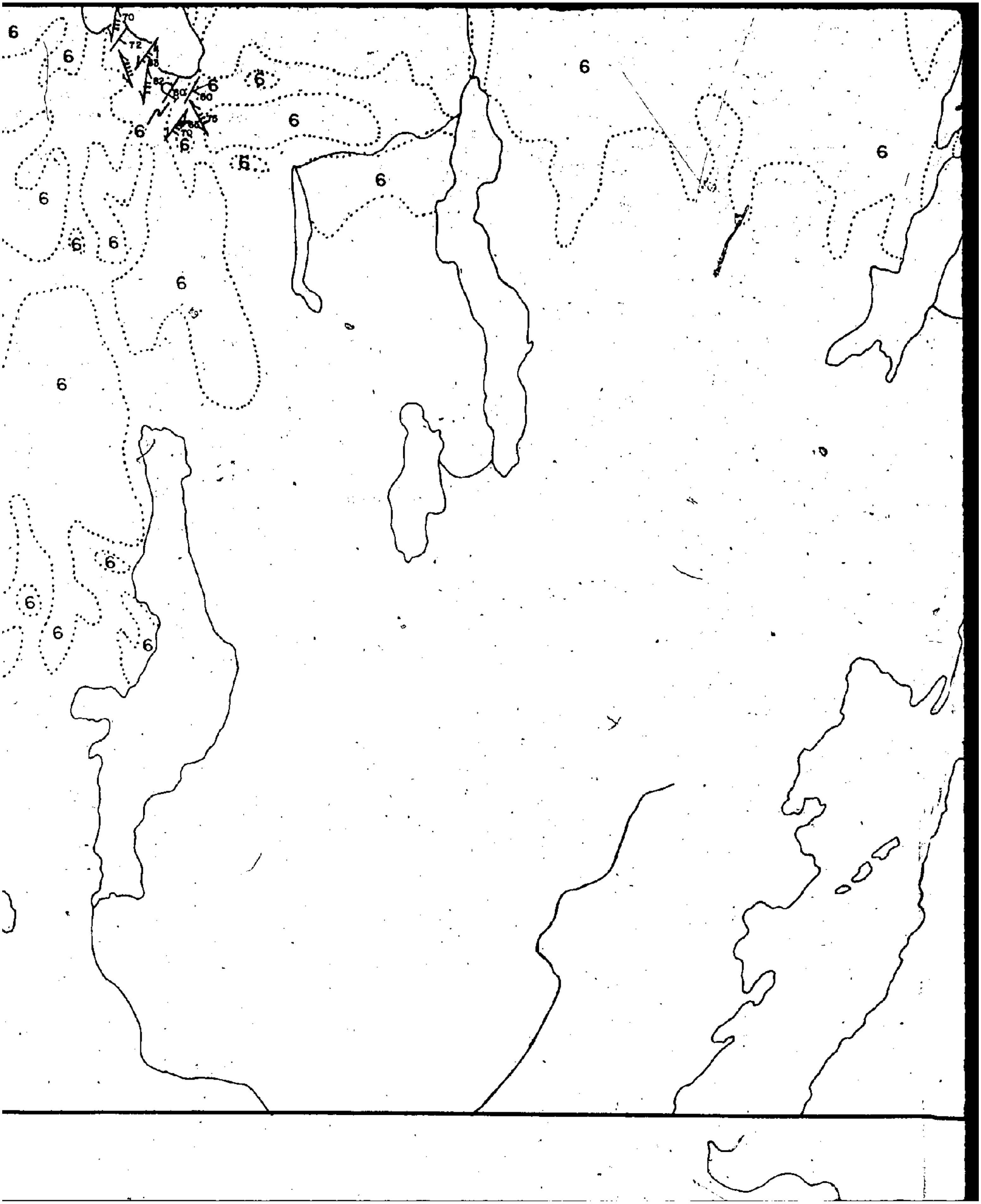
6
6
6
6
6
6
6
6
6
6
6
6
6
6
6
6
6
6
6
6
6
70
72

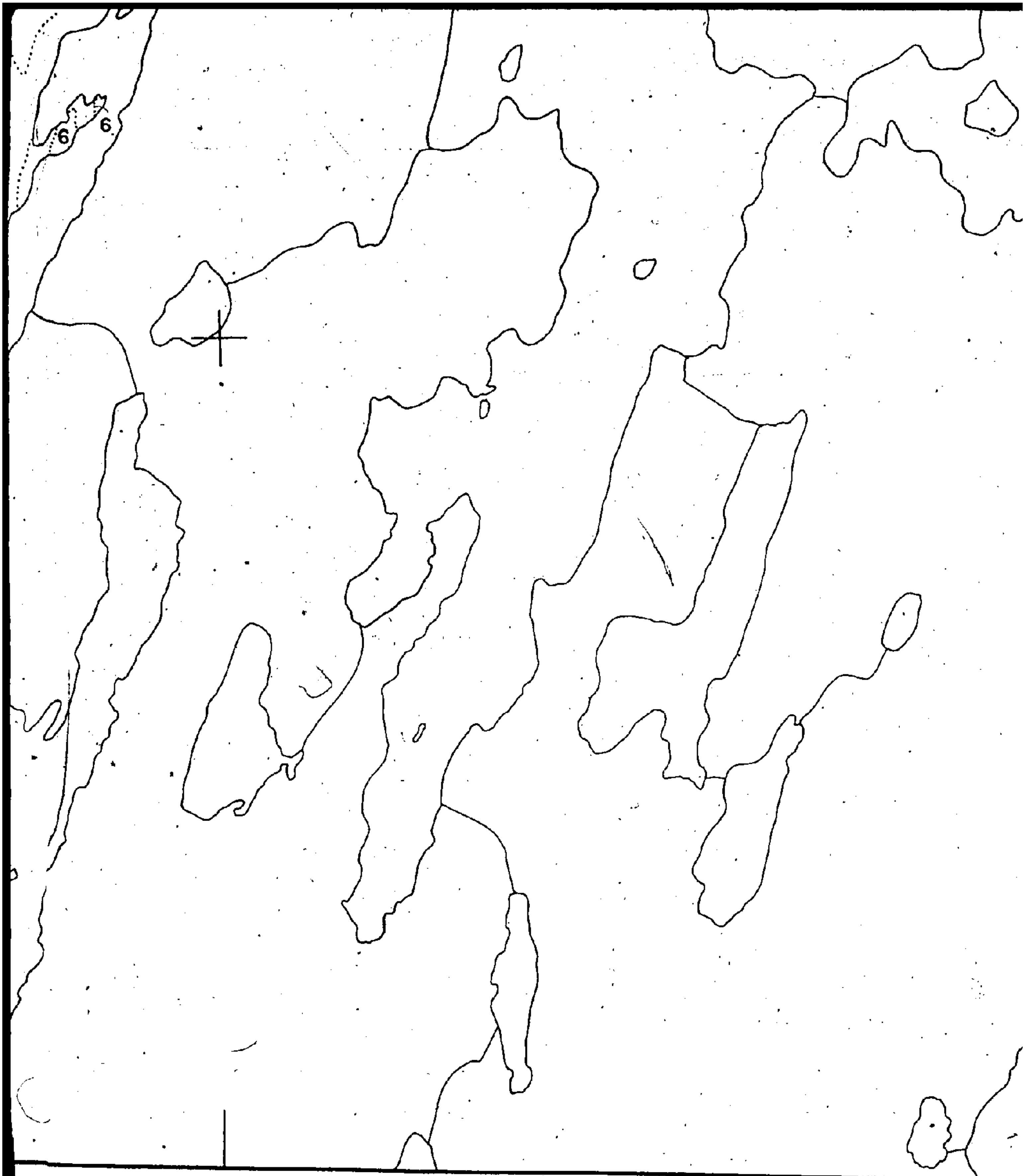


114°05'

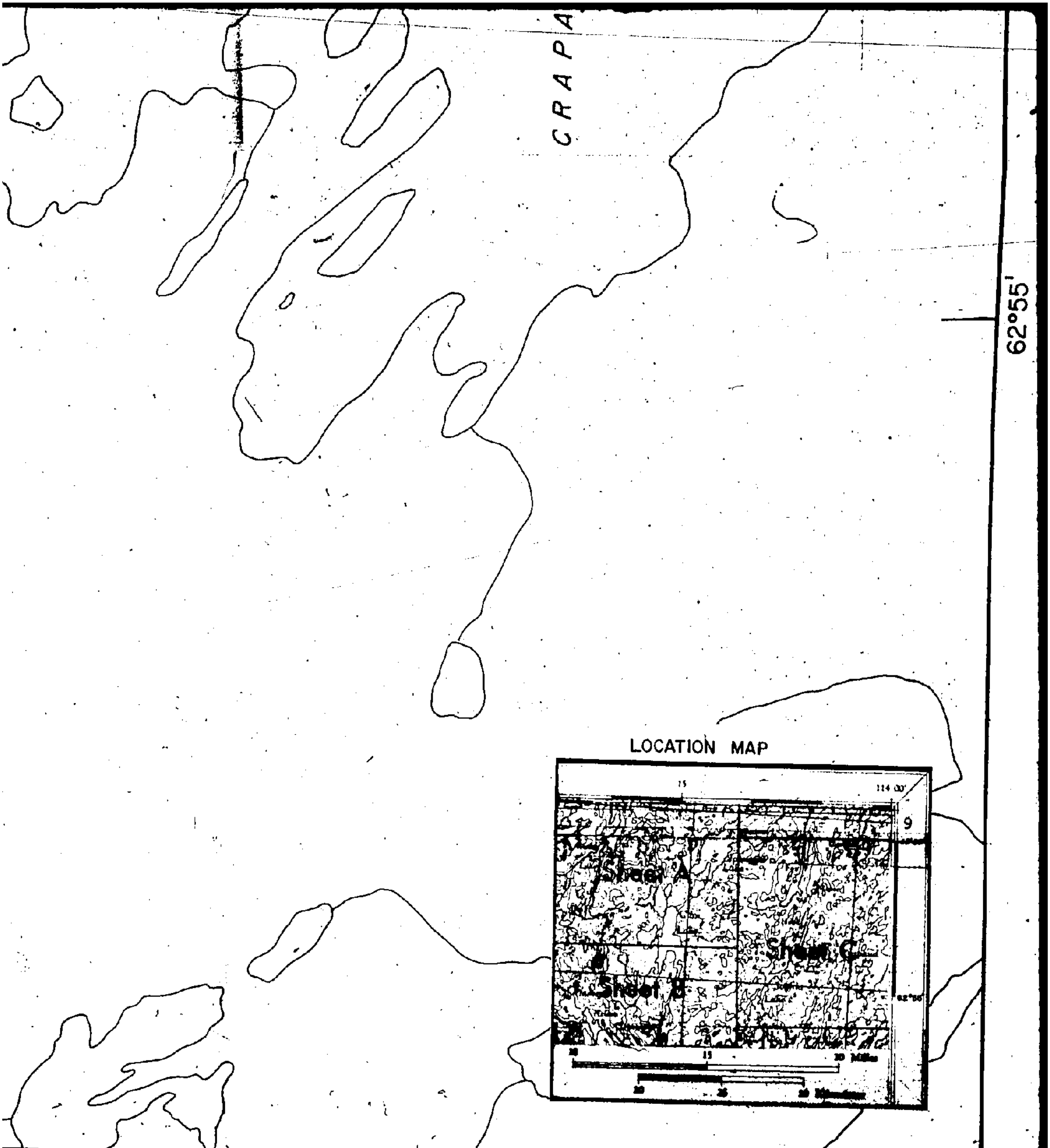


16 June/83 EGS 1983-5 Drafted by D.Valiquette, Drafting Services, for Geology, DIAND.

5.00 ea/15.00 set